



HAL
open science

Age-dependent remodelling of RNP condensates in *Drosophila* neurons

Kavya Vinayan Pushpalatha

► **To cite this version:**

Kavya Vinayan Pushpalatha. Age-dependent remodelling of RNP condensates in *Drosophila* neurons. Molecular biology. Université Côte d'Azur, 2021. English. NNT : 2021COAZ6007 . tel-03593403

HAL Id: tel-03593403

<https://theses.hal.science/tel-03593403>

Submitted on 2 Mar 2022

HAL is a multi-disciplinary open access archive for the deposit and dissemination of scientific research documents, whether they are published or not. The documents may come from teaching and research institutions in France or abroad, or from public or private research centers.

L'archive ouverte pluridisciplinaire **HAL**, est destinée au dépôt et à la diffusion de documents scientifiques de niveau recherche, publiés ou non, émanant des établissements d'enseignement et de recherche français ou étrangers, des laboratoires publics ou privés.

THÈSE DE DOCTORAT

Remodelage des condensats RNP neuronaux au
cours du vieillissement chez la drosophile

Kavya Vinayan PUSHPALATHA

Institut de Biologie Valrose

Equipe « Contrôle post transcriptionnel de la croissance et du guidage axonal »

**Présentée en vue de l'obtention
du grade de docteur en**
Sciences de la vie et de la santé,
Interactions moléculaires et cellulaires
d'Université Côte d'Azur

Dirigée par : Dr. Florence BESSE

Devant le jury, composé de :

Dominique WEIL, PhD, IBPS, Paris, France.

Anne EPHRUSSI, PhD, EMBL, Allemagne.

Arnaud HUBSTENBERGER, PhD, iBV, Nice, France

Simon ALBERTI, PhD, MPI-CBG, Allemagne

Florence BESSE, PhD, iBV, Nice, France

Soutenue le : 22/03/2021



Remodelage des condensats RNP neuronaux au cours du vieillissement chez la drosophile

Jury:

Président du jury

Dominique WEIL, PhD, Institut de biologie Paris-Seine (IBPS), France.

Rapporteurs

Anne EPHRUSSI, PhD, European Molecular Biology Laboratory (EMBL), Allemagne.

Dominique WEIL, PhD, Institut de biologie Paris-Seine (IBPS), France.

Examineurs

Simon ALBERTI, PhD, Max Planck Institute of Molecular Cell Biology and Genetics (MPI-CBG), Allemagne.

Arnaud HUBSTENBERGER, PhD, Institut de Biologie Valrose (iBV), France

Invités

Florence BESSE, PhD, Institut de Biologie Valrose (iBV), France

Remodelage des condensats RNP neuronaux au cours du vieillissement chez la drosophile

Dans la cellule, les molécules d'ARN s'assemblent avec des protéines de liaison aux ARNs pour former des assemblages macromoléculaires très dynamiques appelés granules ribonucléoprotéiques (RNP). Ces assemblages régulent l'expression génique en contrôlant le transport, la stabilité et/ou la traduction des ARNs associés. Des travaux réalisés *in vitro* ont montré que la formation et la composition des granules RNP reposent sur l'établissement de réseaux denses d'interactions établis entre protéines et ARN, ainsi que sur leur stoechiométrie. Comment les propriétés des granules RNP sont régulées en contexte physiologique, et en particulier lors du vieillissement, est cependant actuellement peu connu. Mon projet de thèse visait à répondre à cette question par une étude *in vivo* des granules RNP présents dans les cellules neuronales du cerveau de drosophile.

A cette fin, j'ai analysé dans des cerveaux d'âge croissant des granules RNP caractérisés par la présence de la protéine de liaison aux ARNs Imp/ZBP1 et de la DEAD-box hélicase Me31B/DDX6. Mes travaux ont révélé une augmentation progressive de la condensation de Imp et Me31B en larges granules au cours du vieillissement. Ces granules sont dynamiques et ne co-localisent pas avec des marqueurs d'agrégation, suggérant qu'ils ne correspondent pas à des agrégats protéiques statiques. Remarquablement, la condensation de Imp et Me31B est associée à la perte des granules Me31B+ Imp- observées dans les cerveaux jeunes, et à la coalescence de Me31B et Imp pour former des granules uniques Me31B+ Imp+. De plus, ce processus est accompagné d'une inhibition spécifique de la traduction des ARNs associés aux granules, parmi lesquels *profilin*. Par une analyse fonctionnelle, j'ai mis en évidence qu'une modification de la concentration en Me31B est responsable de la condensation de Me31B dans les cerveaux âgés. Alors qu'une augmentation de la quantité de Me31B est observée au cours du vieillissement, enlever une copie de *me31B* supprime la condensation age-dépendante de ce composant. Etant donné que la condensation de Imp n'est que partiellement affectée dans ce contexte, j'ai réalisé un crible génétique afin d'identifier des régulateurs de ce processus. Ceci m'a permis de montrer que l'activité de la kinase PKA est essentielle d'une part à la condensation de Imp chez les drosophiles âgées, et d'autre part à la répression traductionnelle des ARNs associés aux granules.

En conclusion, mon travail a montré pour la première fois que les propriétés des granules RNP neuronaux sont modifiées au cours du vieillissement, un phénomène qui ne reflète pas une altération générale de l'homéostasie des ARNs, mais plutôt une modulation spécifique de la concentration en composants RNP combinée à l'activité de kinase conservée. Ces résultats démontrent comment les systèmes biologiques peuvent moduler des paramètres clés initialement identifiés dans des contextes *in vitro*, et ouvrent de nouvelles perspectives dans le domaine de la régulation de l'expression génique au cours du vieillissement.

Mots clés : granules RNP, vieillissement, neurones, drosophile, ARN, traduction

Age-dependent remodelling of RNP condensates in *Drosophila* neurons.

Nascent mRNAs complex with RNA binding proteins (RBPs) to form highly dynamic, phase-separated organelles termed ribonucleoprotein (RNP) granules. These macromolecular assemblies can regulate gene expression by controlling the transport, decay and/or translation of associated RNA molecules. As mostly shown *in vitro*, RNP granule assembly and function rely on the interaction networks established by individual components and on their stoichiometry. To date, how the properties of constitutive RNP granules are regulated in different physiological context is unclear. In particular, the impact of physiological aging is unclear. My PhD project aimed at addressing this question by analyzing *in vivo* in long-lived neuronal cells the properties of RNP granules.

To this end, I have analysed in flies of increasing age RNP granules characterized by the presence of the conserved RBP Imp/ZBP1 and DEAD-box RNA helicase Me31B/DDX6. Strikingly, a progressive increase in the condensation of Imp and Me31B into granules was observed upon aging. The large granules observed in aged flies were dynamic, contained *profilin* mRNA, and did not colocalize with Ubiquitin or aggregation markers, suggesting that they do not correspond to static protein aggregates. Increased condensation also associated with the loss of Me31B+ Imp- granules observed in young brains and the collapse of RNP component into a unique class of Me31B+ Imp+ granule. Furthermore, it was accompanied by a specific inhibition of the translation of granule-associated mRNAs, among which the Imp RNA target *profilin*. Through functional analysis, I uncovered that changes in Me31B stoichiometry trigger Me31B condensation in aged flies. While an increase in Me31B protein levels was observed upon aging, decreasing the dosage of Me31B suppressed its age-dependent condensation. As Imp condensation was only partially suppressed in this context, I performed a selective screen to identify regulators of this process. This revealed that downregulating PKA activity by different genetic means both drastically reduced Imp recruitment and prevented the age-dependent translational repression of granule-associated mRNAs.

Taken together, my work thus showed for the first time *in vivo* that the properties of neuronal RNP granules change upon aging, a phenomenon that does not reflect general alterations in RNA homeostasis but rather specific modulation of RNP component stoichiometry and kinase activity. These results demonstrate how biological systems can modulate key parameters initially defined based on *in vitro* framework, and also open new perspectives in the field of age-dependent regulation of gene expression.

Key words: RNP granule, aging, neurons, *Drosophila*, RNA, translation

Contents

Acknowledgements	xiii
List of Figures	xv
List of abbreviations	xvii

Chapter 1. Introduction

1. Ribonucleoprotein (RNP) granule	4
1.1. A collection of RNP granules.....	4
1.1.1. Nuclear RNP granules.....	5
1.1.2. Cytoplasmic RNP granules.....	6
1.2. Cartography of RNP granule content.....	9
1.3. Neuronal RNP or transport granules.....	11
1.3.1. RNA transport and local translation in neurons – an overview.....	11
1.3.2. Identification and molecular composition of neuronal RNP granules.....	14
1.3.3. RNP granule dynamic transport.....	15
1.3.4. RNP granule and translational control.....	16
2. Mechanisms of RNP granule assembly and dynamicity	18
2.1. RNP granules have liquid-like properties	19
2.1.1. Molecules in RNP granules exchange their neighbours rapidly	20
2.1.2. Surface tension dictates the shape of RNP condensates.....	21
2.1.3. RNP granules have definite viscosities.....	22
2.1.4. Material properties of condensates can be modulated in physiological and pathological contexts.....	23
2.2. RNP condensates form through liquid-liquid phase separation (LLPS).....	23
2.2.1. LLPS and concentration.....	25
2.2.2. Nucleation and growth.....	25
2.2.3. Influence of environmental factors.....	26

2.3. Factors affecting RNP component phase separation.....	27
2.3.1. Multivalency.....	27
2.3.2. Chemical modifications on biomolecules.....	30
2.3.3. RNA: protein ratio.....	32
2.3.4. RNA chaperones/helicases.....	33
2.4. Compositional control.....	34
2.4.1. Compositional control based on stoichiometry.....	35
2.4.2. Compositional control based on RNA.....	35
2.5. RNP condensate deregulation and pathologies.....	37
2.5.1. RNP condensates and carcinogenesis.....	37
2.5.2. RNP granules and neurodegeneration.....	38
3. Aging - be past your prime.....	41
3.1. Cellular and molecular hallmarks of aging.....	41
3.2 Changes in gene expression	43
3.3. RNP granules and aging.....	44
4. RNP granules found in <i>Drosophila</i> mushroom body neurons as a paradigm to study the impact of aging on RNP granule properties.....	46
4.1. <i>Drosophila</i> as a model for aging research.....	46
4.2. <i>Drosophila</i> mushroom body: centre of learning and memory.....	47
4.3. IMP: a highly conserved RNA binding protein.....	49
4.3.1. Regulatory functions of IMP on target mRNAs.....	50
4.3.2. IMP regulates various aspects of RNA expression.....	50
4.3.3. dIMP: <i>Drosophila</i> homolog of IMP	51
4.4 Me31B/DDX6: a highly conserved RNA helicase.....	53
4.4.1 DDX RNA helicases	53
4.4.2 Me31B: <i>Drosophila</i> ortholog of DDX6.....	54
4.5. Imp and Me31B/DDX6 in neuronal granules	56
5. Aim of thesis.....	57

Chapter II. Results

6. Summary of results	59
7. Manuscript	62
7.0. Abstract	
7.1. Introduction	
7.2. Results	
7.3. Discussion	
7.4. Materials and methods	
7.5. Figures	
7.6 Supplementary figures	
7.7 Reference	

Chapter III. Discussion

8. Discussion and perspectives	64
8.1. Loss of granule heterogeneity upon aging.....	64
8.2. Is age dependent remodelling a boon or bane?.....	66
8.2.1. Boon- RNP granules as buffering mechanism for stochastic gene expression...66	
8.2.2. Bane- Age dependent memory impairment.....	67
8.3. Global versus gene specific changes in translation upon aging.....	69
9. Conclusion	70

Bibliography

Appendix

1) Review: Local Translation in Axons: When Membraneless RNP Granules Meet Membrane-Bound Organelles

Pushpalatha and Besse, *Frontiers in Molecular Biosciences*, 2019

2) Method chapter- Detecting Stress Granules in *Drosophila* neurons

De Graeve #, Formicola#, Pushpalatha#, Nakamura, Debreuve, Descombes and Besse, submitted.

contributed equally to the work.

Acknowledgements

Successful accomplishment of my Ph.D. Thesis as part of degree fulfilment at UCA is an outcome of the academic setting and research experience I gathered from here and outside in the past four and half years. My journey would have been impossible if not for the long list of people I met *en route*; each of them has been a friend and a teacher at the same time, my sincere thanks to all.

Firstly, I would wish to convey my deepest gratitude to my project supervisor, **Dr. Florence Besse**. Her counsel and patience throughout the period and the confidence she put on me in starting a work from the scratch, and the encouragement she provided while allowing to extend the research independently, has an inevitable role in the completion of this task. I am thankful to her for giving me an opportunity to work under her guidance.

I owe special thanks to **Dr. Arnaud Hubstenberger** and **Dr. Simon Alberti**, my thesis committee members for their kind support, guidance and timely suggestions throughout the project.

I sincerely thank all my lab alumni and current lab members especially **Caroline, Fabienne, Lucile, Jeshlee, Anne-Sophie, Nadia, Marine, Marjorie, Bruna, Lea** for their support, valuable suggestions and encouragement that they have bestowed upon me and also for the lively atmosphere in the lab. Fabienne and Jeshlee, since the day I joined this lab, your continuous support is the one thing that I can always count on. You showed me patience, guided and motivated me whenever the situation arose. Thanks for the wholehearted support throughout this journey. Lucile, I am utterly happy that I met you in my life. You are a real gem, I love our little chat in fly room always, I will forever cherish them in my heart. Caro, I still remember the day when I fell sick and you took my hand without even asking, this is just one of the many instances where your kindness showed through.

Konstanze, because of you my life in France was very smooth, I am in great debt for all the help you provided starting with my VISA application, getting settled in a new country, managing all course works and documentation.

I would wish to thank **PRISM platform** former and current engineers **Magali Mondin, Maeva Gesson, Simon Lachambre, Baptiste Monterroso** and **Sameh Ben-Aicha** for their excellent assistance in imaging. My deepest appreciation goes to the wonderful and strong **Fly community** at iBV for their constant support and fruitful discussions throughout my journey especially

Andrew and **Laurent**. Special mention to **Anita, Olivier, Corinne** and **Brigitte** for their cheerful smile and excellent support.

I am also grateful to the administration of **iBV, UCA, Signalife ANR, FRM** and **LaLigue** for their kind support, both academically and financially. This study was underpinned by the **Labex Signalife** and **Laligue** fellowships.

I extend my earnest gratitude to **Dr. Jishy Varghese, Prof. M.K. Mathew**, and my alma matter **IISER TVM** family for opening the world of scientific research to me. I greatly acknowledge my friends, **Alphy, Ananya, Akshai, Dinil, Naeem, Anamika, Vishnu, Nino, Meng** and my love-my first pet ever “**Soman**”, who were always around me in my path to success. Without their constant support, my research would easily have gone wayward. Ultimately without the love and support from my family, this would have been largely unachievable. I am grateful to my little brother, **Manu** for always being my cheerer. I am forever indebted to my **parents** for believing in me, giving me the wings to chase my dreams and for giving the opportunities and experiences that have made me who I am. And Alphy, what can I say more, you are my pillars, my stress buster, my positivity booster, and a great human I ever met, thank you for being an integral part of my journey.

As being grateful is the biggest form of appreciation and motivation, I also want to thank doctors, nurses, delivery staff, farmers, teachers, researchers, sanitation workers, grocery workers, and emergency services workers, and others who have been constantly assisting in the fight against the current COVID pandemic; Thank you **corona warriors!**

Last but not the least, ***Drosophila melanogaster***, the model organism I worked on, deserves special thanks for being my experimental subject.

List of Figures

Figure 1. Cell cytosol is highly crowded

Figure 2. Schematic representation of an RNP granule

Figure 3. A collection of RNP granule.

Figure 4. Differential localization of RNA in rat hippocampal sections.

Figure 5. Neuronal RNP granule

Figure 6. Artificial and in vitro condensates.

Figure 7. RNP granules behave as liquid-like droplets

Figure 8. RNP granules are dynamic structures

Figure 9. Phase diagram of RNP granule

Figure 10. Multivalency is key for RNP LLPS.

Figure 11. Schematic representation of RNP granule regulation by chemical modifications

Figure 12. A unified model of compositional control in condensates.

Figure 13. Protein aggregates in motor neurons of ALS patients.

Figure 14. ALS-causing mutations accelerated the liquid-to-solid transition of FUS.

Figure 15. Hallmarks of aging

Figure 16. Interacting partners alter the liquid-to-solid transition of FUS ALS-variants.

Figure 17. Drosophila as a model for aging research

Figure 18. Drosophila mushroom body neurons

Figure 19. cAMP/PKA pathway in Drosophila mushroom body neurons.

Figure 20 IMP is a highly conserved RNA binding protein.

Figure 21. Drosophila IMP (dIMP) is cytoplasmic and forms nanometer sized RNP granules.

Figure 22. DDX6/Me31B is a highly conserved RNA helicase

Figure 23. Drosophila Me31B forms cytoplasmic foci.

Figure 24. Model illustrating age-dependent changes in neuronal RNP granule properties

List of Figures and table from Manuscript

Figure 1. Me31B and Imp condensate into larger cytoplasmic granules in aged brains.

Figure 2. Large granules in old flies are dynamic RNP assemblies.

Figure 3. Age-dependent changes in RNP component sorting.

Figure 4. Me31B levels increase upon aging and cause Me31B condensation.

Figure 5. Inactivation of PKA suppresses Imp condensation in aged flies.

Figure 6. Age-dependent decrease in the translation of granule-associated mRNAs.

Figure S1. Clustering of RNP granule components

Figure S2. *me31B*, but not *imp*, is required for nucleation of neuronal RNP granules

Figure S3. Reducing the dosage of *me31B* differentially impacts on Me31B and Imp.

Figure S4. Impact of PKA inactivation of Me31B-containing granule size.

Figure S5. Translation, not RNA stability is modified upon aging.

Figure S6. Imp is phosphorylated on Serines, but its putative PKA phosphorylation sites are dispensable for Imp condensation.

Table S1. List of pathways tested to identify potential regulator of IMP granule remodeling upon aging.

List of Abbreviations

AD	- Alzheimer Disease
ALS	- Amyotrophic Lateral Sclerosis
AMI	-Age related memory impairment
ATP	- Adenosin tri-phosphate
cAMP	- Cyclic AMP
CBs	- Cajal Bodies
CRISPR	- Clustered Regularly Interspaced Short Palindromic Repeats
Csat	- Saturation concentration
Ct	- concentration threshold
eCLIP	- Enhanced Crosslinking and Immunoprecipitation
EM	- Electron Microscopy
FACS	- Fluorescence-activated particle sorting
FRAP	- Fluorescence recovery after photobleaching
FTD	- Frontotemporal dementia
GFP	- Green Fluorescent Protein
HD	- Huntington's disease
iCLIP	- Individual nucleotide resolution UV-cross linking and immunoprecipitation
IDR	- Intrinsically disordered region
IIS	- Insulin/IGFs signalling
KC	-Kenyon cells
KH	- K-homology
LCD	- Low complexity domain
LLPS	- Liquid liquid Phase separation
lncRNA	- Long noncoding RNA
LTM	- Long-Term Memory
MB	- Mushroom Body
miRNA	- Micro RNA
mRNA	- Messenger RNA
MS	-Mass spectrometry
MT	- Microtubule
NB	- Nuclear body
NMDA	- N-Methyl-D-Aspartate
PACAP	- Pituitary adenylate-cyclase-activating polypeptide

PAR-iCLIP	- Photoactivatable ribonucleoside iCLIP
PB	- Processing bodies
PD	- Parkinson's disease
PEG	- Polyethylene glycol
PKA	- Protein Kinase A
PLD	- Prion like domain
PTM	- Posttranslational modification
qRT-PCR	- Quantitative reverse transcription PCR
RBD	- RNA binding domain
RBP	- RNA binding protein
RGC	- Retinal ganglion cell
RNP	- Ribonucleoprotein
ROS	- Reactive oxygen species
RRM	- RNA recognition motif
rRNA	- Ribosomal RNA
scFV	- Single variable fragment
SG	- Stress Granules
Shh	- Sonic Hedgehog
smFISH	- Single molecule fluorescence in situ hybridization
snRNPs	- Small nuclear RNPs
TCA	- Tricarboxylic acid cycle
TIRF	- Total internal reflection fluorescence
TREAT	- 3'-RNA end accumulation during turnover
tRNA	- transfer RNA
UTR	- Untranslated region
V	-Valency

Chapter I

Introduction

Introduction

Cells are the basic structural and functional units of living beings and as such constitute the “building blocks of multicellular organisms”. They must sustain vital functions including structural maintenance, nutrient uptake, or energy production, and carry out more specific functions such as secretion, signal transmission, storage etc. These functions are performed by biochemical reactions that are turned on or off depending on cellular needs and regulated by multiple pathways. These reactions involve biological macromolecules including proteins, nucleic acids and complex sugars that are present in tremendous amounts in cell semifluid cytoplasm, reaching average concentration of 100-450 g/L and physically taking up to 5-40% of the cell volume (Ellis & Minton, 2003) (Figure 1). Such a cellular crowding would be expected to promote unwanted molecular interactions, leading to aberrant cellular processes. Yet, cells constantly perform and orchestrate sub-cellular reactions with high efficiency and exquisite spatio-temporal fidelity, in fraction of seconds. How can they organize functionalities at such a scale of molecular crowdedness?

This is achieved by subcellular compartmentalization and definition of distinct microenvironments enriched in biomolecules specialized in particular functions. Compartmentalization has several advantages for the cell: on one hand, it favours the concentration of components in microenvironment with specific biochemical properties, thus increasing reaction kinetics (Stroberg & Schnell, 2018). On the other hand, it plays an insulating role by segregating molecules and protecting them from calamitous activities like proteolysis, improper covalent modifications, or acidic environment. Compartmentalization has historically been described through the definition of distinct membrane-delimited organelles (*e.g.*, nucleus, mitochondria, golgi bodies, endoplasmic reticulum etc) that appeared in eukaryotic cells in the course of evolution. The lipid membranes ensheathing these organelles act as physical barriers delimiting intra-organelle compartments, the composition of which can be regulated through specific transmembrane transport machineries. More recently, it became clear that not all cellular organelles are delimited by a lipid membrane, and that cellular compartmentalization is also achieved by the condensation of functionally related molecules into membraneless organelles (or biological condensates) (Alberti & Hyman, 2021; Banani et al., 2017). Characteristic features of these macromolecular condensates are their reversible assembly, as well as the dynamic exchange of their components with the surrounding environment. Among those, hundred nanometer- to micron-sized membraneless compartments enriched in proteins and RNAs have been identified in both the cytoplasm and the nucleus and termed ribonucleoprotein (RNP) condensates or granules (Figure 2). Nucleolus was the first membraneless RNP compartment identified (Pederson, 2011). With advances in fluorescent microscopy and super resolution techniques, a

plethora of cytoplasmic RNP granules, including the cytoplasmic P-bodies, stress granules and the cell-specific neuronal or germ cell RNP granules, have later been identified and implicated in the regulation of various post-transcriptional regulatory processes (Anderson & Kedersha, 2006; Buchan, 2014). The nature of these macromolecular assemblies, their cellular functions, and their mode of assembly will be discussed in the following sections.

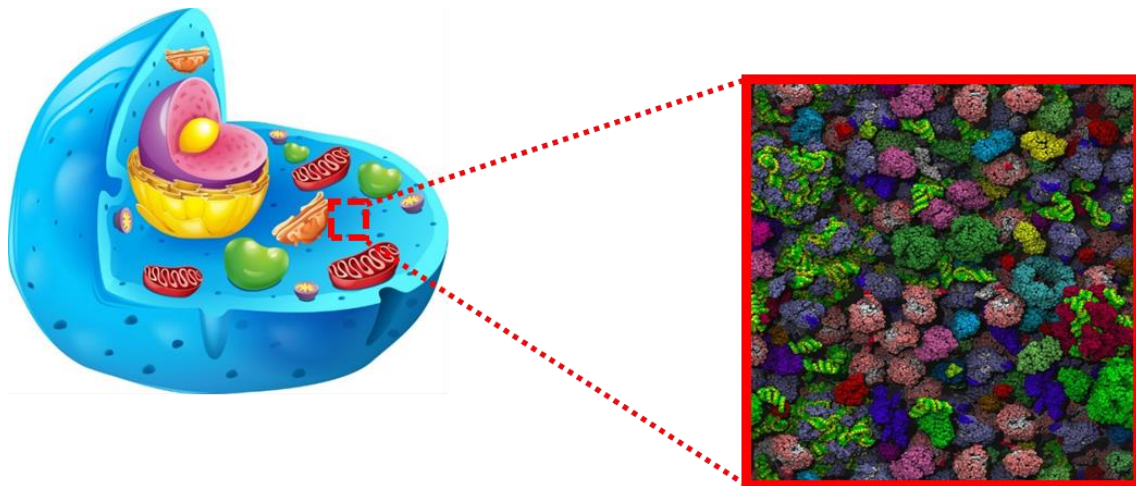


Figure 1: Cell cytosol is highly crowded

A molecular model of the inside of a eukaryotic cell, with a cell cytoplasm tightly packed with proteins and other macromolecules. Image adapted from (McGuffee & Elcock, 2010).

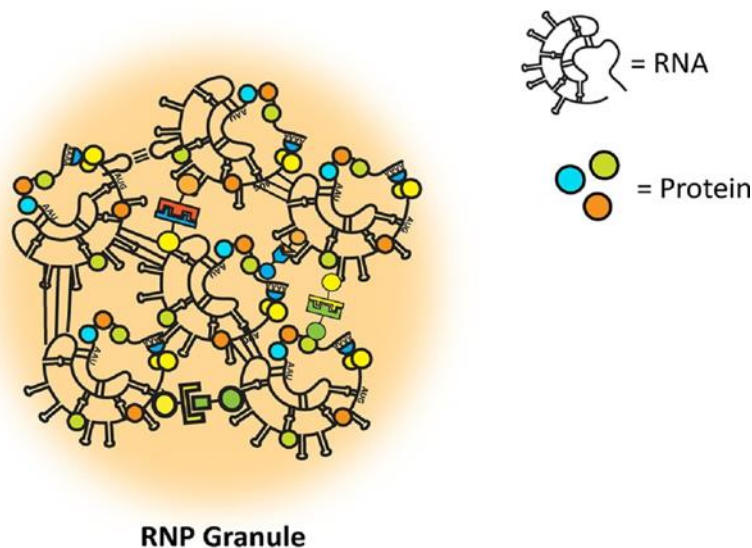


Figure 2: Schematic representation of an RNP granule

RNP granules are membraneless compartments composed of multivalent protein–protein, RNA–RNA, and protein–RNA interactions. Image adapted from (Tauber et al., 2020).

1. Ribonucleoprotein (RNP) granules

1.1. A collection of RNP granules

Extensive research in the field of biological condensates has uncovered distinct types of RNP granules (Figure 3). RNP granules are classified based on their composition, function, subcellular localization, cell of origin, response to stimuli, and dynamicity. A primary distinction based on the subcellular localization classifies RNP granules into two major groups: nuclear and cytoplasmic.

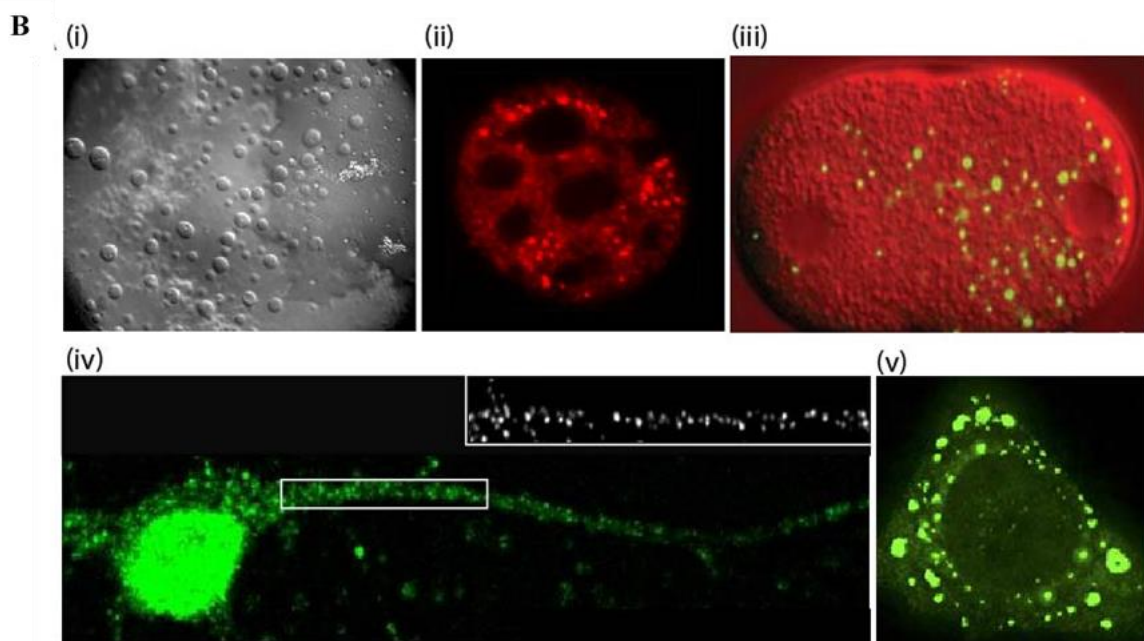
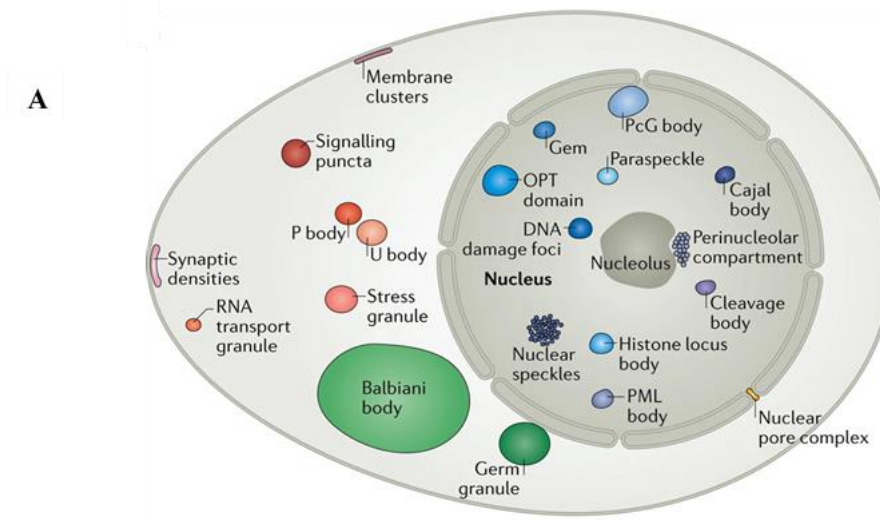


Figure 3: A collection of RNP granule

A. Schematic representation of RNP condensates in the nucleus, cytoplasm and membranes in a hypothetical eukaryotic cell. Nuclear condensates include nucleolus, histone locus body, PML body, Cajal body etc. Cytoplasmic condensates include P body, stress granule, transport granule, germ granule etc. Image adapted from (Banani et al., 2017).

B. RNPs *in vivo/ ex vivo* (i) nucleoli in *Xenopus* oocyte (Brangwynne et al., 2011), (ii) paraspeckles in MEF cells (Spector, 2006), (iii) P granules in *C.elegans* (Brangwynne et al., 2009), (iv) Neuronal RNP granules in rat primary neuronal culture (Gopal et al., 2017), (v) stress granules in HeLa cells (Wheeler et al., 2016).

1.1.1. Nuclear RNP granules

Studies have shown that the nucleoplasm is not homogenous, and that the nucleus is rather organized into various membraneless RNP granules termed nuclear bodies (Handwerger & Gall, 2006; Nunes & Moretti, 2017). Nuclear bodies exhibit a wide spectrum of sizes ranging from hundreds of nanometers for speckles and paraspeckles to several micrometers for nucleoli. The nucleolus is the most prominent nuclear condensate marked by the presence of the marker protein Fibrillarin; it is the site of rRNA biogenesis and ribosome assembly (Boisvert et al., 2007; Lafontaine et al., 2020). Another nuclear body accidentally discovered by Ramon y Cajal in 1903 is the Cajal body (CB). SMN and Coilin protein are prominent markers for CBs. CBs play a pivotal role in assembling and modifying small nuclear ribonucleoprotein particles (snRNPs) which are essential for gene splicing (Sawyer et al., 2016). Nuclear speckles defined by the localization of SRSF1 & 2, and paraspeckles defined by the localization of PSP1, are nuclear bodies found throughout the nucleoplasm, residing in the interchromatin space. They are highly dynamic, regularly recruited to transcription sites. Nuclear speckles work as reservoir of splicing factors (Fox et al., 2018; Galganski et al., 2017). Nuclear bodies thus control various steps of gene expression including transcription and RNA processing. Although left unexplored for a long time after their discovery, intensive research is carried out in the field to understand how these distinct condensates are assembled in the nuclear milieu, how specific proteins are localizing into peculiar membraneless compartments, and what role these dynamic structures play (Strom & Brangwynne, 2019).

1.1.2. Cytoplasmic RNP granules

A variety of either constitutive or stress induced RNP granules have been identified in the cytoplasm of immortalized or differentiated cells. These granules have been implicated in the regulation of various aspects of RNA expression, ranging from RNA translation, localization to degradation, as well as in cellular responses including stress response, or signalling. Drawing a strict boundary to group RNP granules to different classes is not straightforward; many RNP granules share components, they come in contact, and can undergo maturation from one-type to another by recruiting or expelling components (Moser & Fritzler, 2010). Multiple types of cytoplasmic RNP condensates have been described in cells. Some of them are context-, cell-, or organism-specific, while some of those share conserved functions across different phyla. Below, I will be describing only the mainly studied cytoplasmic RNP granules. Neuronal RNP granules will be presented in a dedicated section (section A.3).

P-bodies

P bodies (PBs) have initially been described as assemblies composed primarily of mRNAs in conjunction with proteins involved in translational repression (*e.g.*, Dhh1/RCK/p54), decapping (*e.g.*, Dcp1/Dcp2) and 5'-to-3' mRNA decay (*e.g.*, Xrn1). Beyond these highly common PB-resident molecules, components that are specific to a particular organism or known to be involved in regulating subclasses of mRNAs, have also been identified as PB-components. For example, mammalian PBs include proteins involved in miRNA function and RNA silencing pathway, which are not found in yeast PBs (Liu, Rivas, et al., 2005; Liu, Valencia-Sanchez, et al., 2005). Notably, not all components localized to PBs are essential for their assembly. While Me31B (DDX6), Pat1, and Lsm1 depletion inhibited the formation of PBs in *Drosophila* S2 cells (Eulalio et al., 2007), DDX6 depletion in mammalian cells strongly blocked PB formation, Pat1 depletion had minimal effects (Ayache et al., 2015). These observations indicate that DDX6 could be a key PB assembly factor and that essential components could vary according to the cell-types. RNA, however, appears to be an essential component as PBs are susceptible to RNaseA treatment (Teixeira et al., 2005).

In eukaryotes, mRNA decay is initiated by the removal of 3'-polyA tail by the deadenylase enzyme complex (for example CCR4/NOT complex). Once polyA is truncated, mRNAs are degraded by the 3'-to-5' exonucleases. Alternatively, the 5'-methyl cap is removed on the deadenylated transcripts by decapping proteins like Dcp2, and 5'-to-3' exonucleases like Xrn1 initiate degradation of mRNAs (Houseley & Tollervey, 2009). Strikingly, decapping proteins such as Dcp1/Dcp2, Edc3 and the Lsm1-7 complex, activators of decapping and translational

repressors like Dhh1/RCK/p54, Pat1 and Scd6/RAP55, enzymes like 5' to 3' exonuclease, Xrn1, and the Ccr4/Pop2/Not deadenylase complex were all found to be localized to P-bodies (Parker & Sheth, 2007). Because of their enrichment in components involved in mRNA decapping and degradation, and because P-body size increased when mRNA decapping or degradation was blocked (Andrei et al., 2005; Cougot et al., 2004), P bodies were thus initially hypothesized to be the sites of mRNA decay (Parker & Sheth, 2007; Sheth & Parker, 2003). More recent studies have however challenged this view and shown that P bodies are dispensable for mRNA degradation. E. Izauralde and colleagues, for example, have shown in *Drosophila* S2 cells, that a reporter RNA with the PB-protein GW182 tethered to its 3'UTR got degraded even in cells depleted for Lsm1, Lsm3, or HPat, which had no detectable PBs (Eulalio et al., 2007). Similarly, in yeast defective for P body formation (*edc3Δ lsm4ΔC* mutants), there was no difference in mRNA decay compared to wildtype (Huch & Nissan, 2017). More direct evidence came from a study using the TREAT (3'-RNA end accumulation during turnover) fluorescent reporter to assess mRNA turnover in live with high spatio-temporal resolution (Horvathova et al., 2017). Using the differential signal produced by non-degraded and partially-degraded TREAT reporters, Horvathova et al. showed that mRNA molecules found in PBs were protected against Xrn1-dependent 3' end decay (Horvathova et al., 2017). Transcriptome analysis of mammalian PBs performed by D. Weil and colleagues also reinforced this idea, as truncated RNA products, indicative of decay, were not significantly found in PBs. This study rather indicated that PB targeted mRNAs are translationally repressed (Hubstenberger et al., 2017), suggesting the alternative hypothesis that P bodies are warehouses of translationally repressed mRNAs and inactive mRNA decay enzymes.

Stress Granules

Stress granules (SGs) are cytoplasmic condensates assembled in the cytoplasm of cells exposed to endogenous (hypoxia, pH, redox state) or exogenous (UV irradiation, heat, chemical insult) stressors. Thus, in contrary to other RNP granules, SGs are not constitutive under favourable environments: they are rather assembled within fraction of seconds upon cellular stress and disassembled upon stress release (Guzikowski et al., 2019; Panas et al., 2016) (De Graeve, Formicola, Pushpalatha et al., submitted). SGs comprise translationally stalled mRNAs, RBPs, non-RBPs and components of the 40s ribosomal subunit (Buchan & Parker, 2009; Ivanov et al., 2019). Not all components are “essential” for SG assembly; depleting a subset of RBPs including G3BP1/2 (Kedersha et al., 2016), TIA1 (Gilks et al., 2004), UBAP2 (Cirillo et al., 2020; Markmiller et al., 2018), HDAC6 (Kwon et al., 2007), PRRC, and CSDE1 (Youn et al., 2018) abrogated SG assembly. RNA is also an essential component of SGs as trapping mRNAs in polysome by adding cycloheximide (Buchan et al., 2008) or emetine (Kedersha et al., 2000) blocks SG assembly whereas inducing mRNA release from polysomes by adding puromycin triggers SG assembly (Kedersha et al., 2000). SG assembly follows translational arrest during

stress, which is associated with polysome disassembly and increase in cytoplasmic free mRNA (Panas et al., 2016), suggesting that polysome-free mRNAs could be the rate-limiting factors for SG assembly in cells.

SGs may also have functions independent of storage of translationally repressed RNAs. SGs were proposed to serve as a “bounce back” mechanism for cells to recover quickly after the stress subsides, without needing to produce new protein and RNA molecules. Such a mechanism could be seen during quick re-entry of cell cycle regulator Cdc19 protein into cell cycle after cessation of stress; Cdc19 protein is recruited to SGs in yeast during stress, preventing its degradation (Saad et al., 2017). Surprisingly, indeed, Chao and colleagues have recently shown through single molecule live-imaging that not all the transcripts localized to SGs are translationally silent. ATF4 transcripts, for example, were translated in the SGs formed during arsenite-stress in HeLa cells (Mateju et al., 2020). Furthermore, formation of SGs was also proposed to modulate signalling pathways, as illustrated by the sequestration of the kinase TORC1 in SGs during heat stress and the subsequent block of TORC1 signaling and eventually cell death (Takahara & Maeda, 2012).

Germ granules

Metschnikoff (1865) had an interesting observation of dark stained granules at one pole of *Miastor metraloas* (fly) larvae (Metschnikoff, 1865). Subsequently, these “polar granules” were shown to be the sites of primordial germ cell differentiation in a wide variety of insects. These early observations led to the identification of a broad class of RNP granules called germ granules in both invertebrate and vertebrate models including *D. melanogaster* (polar granules), *C. elegans* (P granules), *Xenopus* (germinal granules), and mammals (nuages) (Sengupta & Boag, 2012). Germ granules are loaded with maternal mRNAs and proteins implicated in translational control; they time the translation of maternal mRNAs to specify germ cell fate in early embryos (Leatherman & Jongens, 2003; Lehmann, 2016). How does germ granules regulate translation? About 95% of protein expression in eukaryotes depend on cap-dependent translation and in this mode of translation, binding of 40S ribosomal subunit to 5'-end depends on the formation of initiation complex (eIF4A/E/G) (Parsyan et al., 2011; Sonenberg & Hinnebusch, 2009). First step during translation initiation is the binding of eIF4E to 5'-cap of mRNA, which is then bound by eIF4G. Many eIF4E-binding proteins (4E-BPs) compete with eIF4G and block its binding to eIF4E. 4E-BPs block the formation of translation initiation complex and hence association of 40S ribosomal subunit (Peter et al., 2015). 4E-BPs are known to be regulators of germ granule formation, for example, Cup, a 4E-BP, is a component of *Drosophila* germ granules and is essential for the localization and translational repression of *nanos* and *oskar* mRNAs (Mahowald, 2001). Mutations in *cup* result in premature translation of repressed mRNAs in oocytes (Nakamura et al., 2004).

Together, it has emerged that cytoplasmic RNP granules are enriched in translationally repressed mRNAs. To which extent they contribute to translational repression is still under debate, as most studies performed so far relied on mutants or cells depleted for RNP components, thus potentially affecting functions inside and outside granules.

1.2. Cartography of RNP granule content

A main feature of RNP granules is their enrichment in proteins and RNA (Anderson & Kedersha, 2006). Protein components of RNP granules have been identified principally using three methods. The first relies on a candidate- or serendipity-based approach by following the localization of fluorescently labelled proteins using confocal microscopy. The other two rely on a more systematic analysis of RNP granule proteome. In the second approach, RNP granules are purified from cell lysates, through differential centrifugation followed by immunoprecipitation (Fritzsche et al., 2013; Jain et al., 2016) or fluorescence-activated particle sorting (FAPS), a method in which cell lysates enriched in fluorescently labelled RNP condensates are sorted using fluorescence activated cell sorting (Hubstenberger et al., 2017). The proteome of granule-enriched fractions is then assessed using mass spectrometry (MS), a technique that identifies and quantifies molecules based on their mass-to-charge ratio. The third approach consists in proximity labeling (BioID or APEX labeling), in which a RNP component (bait) is fused to an enzymatic domain (Biotin ligase or ascorbate peroxidase), leading to the tagging of proteins in close contact with the bait (in the range of tens of nanometers) with biotin (Rhee et al., 2013; Youn et al., 2018). After proximity labelling, biotin-labelled proteins are isolated using streptavidin beads and identified using MS. Although the exact stoichiometry of individual granules is still unclear, these studies have revealed that up to hundreds of proteins can associate with a given class of RNP granules. For example, yeast and mammalian P bodies (PBs) were shown to contain more than 50 and 100 proteins, respectively (Hubstenberger et al., 2017; Youn et al., 2018). In another example, interactome of two distinct neuronal RNP granules identified by Kiebler and colleagues, had less than 100 protein components (Fritzsche et al., 2013). RNP granule protein composition depends on the type and context and a common line cannot be drawn for protein composition of RNP granules. For example, RNA binding proteins, translational repressors, RNA helicases are found as common interactors in the proteome analyses of SGs and PBs. Certain protein families show granule-type specific interaction as in case of ribosomal proteins and translation initiation factors that localize to stress granules and are depleted from P bodies, conversely, mRNA decapping and decay factors are enriched in PBs and are absent in SGs (Ivanov et al., 2019).

Not only proteins but also RNA molecules are enriched in RNP granules (Corbet & Parker, 2019). Here also, different approaches have been used to identify the transcriptome of RNP granules. These include candidate-based approaches using single molecule fluorescence *in situ*

hybridization (smFISH) (Raj et al., 2008) or quantitative PCR (qRT PCR) on purified granules (Namkoong et al., 2018). Systematic approaches such as RNA-seq after RNP granule isolation have also provided an account of the RNA species enriched in RNP granules (Hubstenberger et al., 2017; Khong et al., 2017). These studies have indicated that mRNA molecules are major components of different RNP granules, for example, RNA fractions in mammalian SGs and in mammalian PBs are 80% and 89% mRNAs respectively (Hubstenberger et al., 2017; Khong et al., 2017). Like protein components, RNA repertoire of distinct RNP granules also exhibit certain level of specificity. For example, both 18s and 28s rRNA were depleted from mammalian PBs whereas 18s rRNA was identified in the transcriptome of arsenite-induced mammalian SGs (Hubstenberger et al., 2017). Some RNP granules localize specific RNA molecules, for example, multiple copies of long non-coding *NEAT1* RNA is shown to localize in nuclear paraspeckles (Clemson et al., 2009). These approaches also uncovered RNAs as major stakeholders in RNP granules as, for example, one-fifth of the total cytoplasmic transcripts and one-third of total coding transcripts were selectively enriched in mammalian PBs (Hubstenberger et al., 2017). Such a large repertoire of RNA localization to RNP granules led to search for general sequence elements that could be involved in RNP targeting. Recent studies from the Parker lab suggested that RNAs enrich in SGs with poor specificity, mainly based on their length and poor translation (Khong et al., 2017; Matheny et al., 2021). RNA-seq performed on FAPS-purified PBs, in contrast, showed that most of the RNA molecules enriched in PBs are targets of granule-associated RBPs, suggesting that they may be recruited as RNP complexes (Hubstenberger et al., 2017). Furthermore, work from Wang and colleagues, aimed at identifying the RNA interactome of yeast PBs, has shown that the 3'UTRs in PB-target transcripts are necessary, but not sufficient for PB-targeting. Indeed, endogenous PB mRNAs whose 3'UTR was replaced with that of a non-related RNA failed to localize to PBs but fusing 3'UTR from PB-target mRNA to a non-PB associated RNA did not localize it to yeast PBs (C. Wang et al., 2018). Interestingly, PB-enriched mRNAs were shown to also have a bias in composition and be AU-rich, a feature associated with limited translation yield (Courel et al., 2019). This, however, was not true for the SG-rich RNA fraction. Together, these studies could not find a common zipcode for RNA targeting to RNP granules and rather suggested that granule-enrichment depends on context-specific RNA-protein interactions, sequence elements on RNAs and/or translation activity.

1.3. Neuronal RNP or transport granules

Neuronal RNP granules, also known as neuronal transport granules, represent another cell type-specific class of RNP granules. These macromolecular assemblies can be of various sizes but are generally of the order of hundreds of nanometers (De Graeve & Besse, 2018). They are found in neuronal progenitors as well as developing and mature neuronal cells and have been involved in the transport and translational control of RNA molecules along axons, and dendrites (Formicola et al., 2019; Kiebler & Bassell, 2006). Their characteristics will be discussed in more details below.

1.3.1. RNA transport and local translation in neurons – an overview

Neurons are highly polarized cells; they have long projections, posing a unique challenge to regulate processes happening at long distances from the cell body and nucleus. Targeting of mRNAs to specific neuron subcellular domains, coupled to the onsite translation of localized mRNAs, has emerged as a mechanism employed by neurons to rapidly generate local protein concentrations in response to stimuli. Historical pioneer *in situ* hybridization experiments have revealed the specific targeting of transcripts to axons and/or dendrites. Matus and colleagues, for example, have shown in rat cerebral cortex that mRNAs encoding MAP2 (a dendrite-specific microtubule binding protein) preferentially localize to dendrites, while *tubulin* mRNAs were found exclusively in cell bodies (Garner et al., 1988) (Figure 4A). Furthermore, *β-actin* mRNA was shown to be preferentially sorted into processes and growth cones in cultured neurons (Bassell et al., 1998) (Figure 4B). More recent transcriptomic studies performed on hippocampal sections (Ainsley et al., 2014; Cajigas et al., 2012; Nakayama et al., 2017) and *in vitro* differentiated neurons (Taliaferro et al., 2016; Zappulo et al., 2017) extended this view, demonstrating the existence of pools of up to thousands of mRNAs enriched in neurites. Consistent with a functional role of RNA subcellular targeting, mRNAs identified in these studies as neurite-enriched encoded proteins involved in synaptic functions including neurotransmitter secretion, synaptic vesicle transport, synaptic plasticity, and ion channel clustering etc. Furthermore, as revealed by a recent proteomic analysis combined with ribosome profiling (ribosome-seq), a highly significant correlation between ribosome-bound RNA fraction and protein localization was observed, indicating that the majority of the neurite proteome is locally translated (Zappulo et al., 2017). What roles do targeted RNA localization and local protein synthesis play in neuronal function and development?

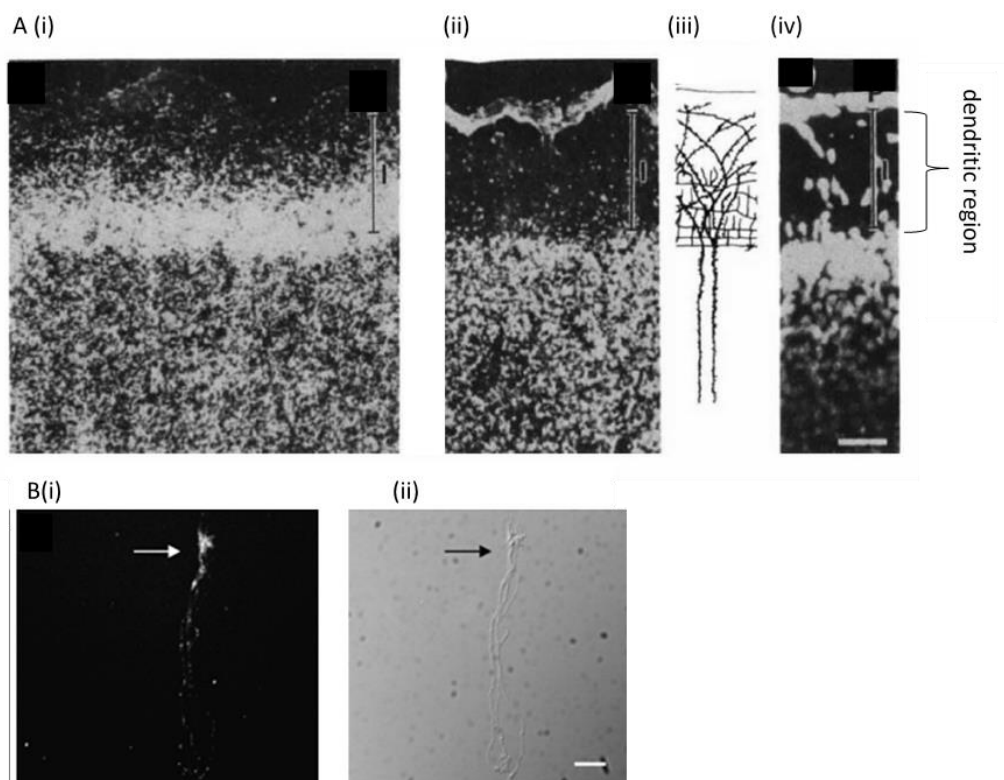


Figure 4: Differential localization of RNA in rat hippocampal sections

A. *MAP2* mRNA is localized to dendrites and *tubulin* mRNA is found in cell bodies in developing rat cortex. (i) *MAP2* mRNA (ii) *tubulin* mRNA (iii) scheme of location of dendrites (iv) Location of cell bodies using nuclear dye. **B.** (i) β -*actin* mRNA is present in axonal growth cone of cultured cortical neurons, (ii) DIC image of axon growth cone. Images are adapted from (Bassell et al., 1998; Garner et al., 1988).

Local translation of transported mRNAs has been shown to be important for various aspects of axonal functions ranging from axon pathfinding and branching during development to axon maintenance, repair or synaptic activity in adult (Campbell & Holt, 2001; Hafner et al., 2019; Jung et al., 2012; Shigeoka et al., 2013). Interestingly, Shigeoka et al. showed that higher number of axonally translated mRNAs are found in developing retinal ganglion cell (RGC) compared to mature neurons (Shigeoka et al., 2016). Furthermore, they uncovered that ribosome-bound mRNAs in embryonic stages code for proteins involved in neurite guidance, morphogenesis and extension, whereas in adult neurons they code for proteins involved in regulation of synaptic transmission or synaptic plasticity. These observations thus suggested first that the axonal RNA content is subjected to developmental regulation and second that modulation of the axonal transcriptome may shape the axonal proteome and adapt it to particular functions.

Local translation in dendrites has been shown to control various aspects of synaptic plasticity, and in particular to be required for establishment of long-term plasticity, the correlate of long-term memory (LTM) (Kang & Schuman, 1996; Martin et al., 1997; Stanton & Sarvey, 1984; Sutton &

Schuman, 2006). Consistent with this idea, RNA binding proteins involved in the translational repression of synaptically-localized mRNAs have been involved in learning and memory functions (Sudhakaran & Ramaswami, 2017). A recent evidence in this line has come from the mouse model; RNG105/Caprin1 is a major component of the neuronal RNP granules found in hippocampal neurons. 1122 mRNAs like *Camk2a*, *Shank2*, *Homer*, *Dlg4*, etc. showed dendritically-enriched localization in case of wildtype hippocampal neurons, whereas in conditional mutants for RNG105, these mRNAs were similarly localized between soma and dendrites (Nakayama et al., 2017).

Neuronal RNP granules, because they have the capacity to package specific RNA molecules together with translational regulators, to be transported to target sites, and to release RNAs through stimuli-specific disassembly (De Graeve & Besse, 2018; Formicola et al., 2019; Holt & Schuman, 2013; Kiebler & Bassell, 2006), appear particularly adapted to spatio-temporally coordinate RNA transport and translation in neuronal cells (Figure 5).

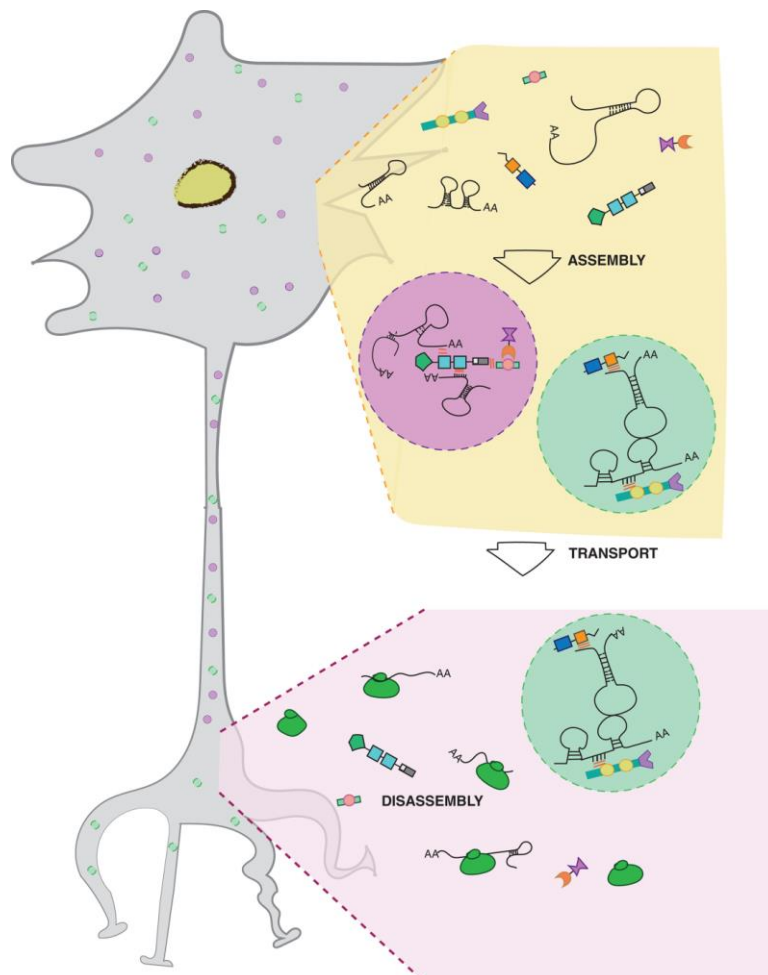


Figure 5: Neuronal RNP granule

RNAs, together with their interactome, form RNP granules in the cell soma, and are transported to dendrites or axons in a translationally dormant state. At their destination, localized RNAs start being translated upon stimuli reception, following RNP granule disassembly. Image adapted from (Formicola et al., 2019).

1.3.2. Identification and molecular composition of neuronal RNP granules

The first evidence for the existence of transport granules in neurons came from the study by Knowles and colleagues, in which endogenous RNA-rich granules visualized using the RNA dye SYTO14 were shown to be transported into neurites of cultured cortical neurons (Knowles et al., 1996). The first demonstration for an RBP to assemble into granules dynamically transported in living neurons came from Kohrmann and colleagues, who expressed a GFP-tagged version of Staufen in rat hippocampal neurons and demonstrated their accumulation in granules exhibiting bidirectional dendritic motion (Kohrmann et al., 1999). Soon after these initial observations, EM analyses on neuronal granules isolated by differential centrifugation from entire brains revealed the membraneless electron-dense nature of these structures (Elvira et al., 2006; Krichevsky & Kosik, 2001). More recently, mass spectrometry analysis on purified granules from both embryonic and adult brain samples revealed a lack of membrane proteins in the isolated fractions, reinforcing the idea that neuronal RNP granules are distinct from membrane-bound organelles (El Fatimy et al., 2016; Fritzsche et al., 2013). These studies also uncovered the protein composition of these assemblages, revealing that they contain ribosomal subunits, translation initiation factors like eIF4E and eIF2 α , and RBPs such as DEAD-box helicases, HuD, G3BP, Sam68, Syncrin, hnRNPA2, ZBP1, FMRP, Staufen, TDP43 etc. (El Fatimy et al., 2016; Kiebler & Bassell, 2006; Singh et al., 2015).

Proteomic analyses of neuronal RNP granules have also shown that not all neuronal RNP granules have the same composition (Fritzsche et al., 2013; Heraud-Farlow et al., 2013). Using density-gradient centrifugation coupled with immunoprecipitation and mass-spectrometry, the Kiebler's lab analysed the content of two distinct populations of RNP granules of rodent brains; one characterized by the presence of Staufen2 (Stau2) and the other by Barentsz (Btz). Remarkably, only a third of the proteins identified were shared between the two granule types. mRNA also showed differential localization; for example, *Arc* mRNA was found in Btz-granules while *CaMKII α* was preferentially enriched in Stau2-granules (Fritzsche et al., 2013). This study thus demonstrated that diverse neuronal RNP granules co-exist within the same neuron, suggesting they may have specific properties and perform distinct functions. Strikingly, neuronal RNP granule composition also appears to vary according to neuronal state. In cultured hippocampal neurons, for example, above 90% of Pur- α -containing granules co-stained for Staufen1 in immature neurons, while only 50% do in mature neurons (Mitsumori et al., 2017). Taken together, it appears that diverse sets of neuronal RNP granules are found in neurons, providing means to respond specifically to ever changing environments.

1.3.3. RNP granule dynamic transport

Live imaging experiments have shown that neuronal RNP granules exhibit bidirectional movements along neurites (Dictenberg et al., 2008; Gopal et al., 2017). These studies have further revealed that neuronal RNP granules are transported along microtubule (MT) tracks, with velocities in the order of $\mu\text{m/s}$ (Dictenberg et al., 2008; Kanai et al., 2004; Knowles et al., 1996; Medioni et al., 2014). Further supporting that they undergo active transport, MT-associated motor proteins such as kinesin and dynein were isolated as components of neuronal RNP granules and functionally shown to regulate transport properties (Kanai et al., 2004). For example, kinesin motors were found to bind the RNP component FMRP and to mediate the transport of dendritic FMRP granules in cultured primary neurons (Davidovic et al., 2007; Dictenberg et al., 2008). Jeong *et al.* have shown that Stau2-containing RNP granules are transported in a MT-dependent manner, supported by the blockade of their transport upon Kinesin inhibition (Jeong et al., 2007). ZBP1-containing granules were shown to be transported in hippocampal neurons in a KIF5A-dependent manner (Urbanska et al., 2017). Remarkably, recent studies also point to a complementary function for the F-actin cytoskeleton in the transport of RNP granules. For instance, MyosinVa was identified as a co-immunoprecipitated partner of neuronal RNP granules (Calliari et al., 2014; El Fatimy et al., 2016) and shown to be functionally important for the translocation of RNP granules to dendritic spines (Mitsumori et al., 2017; Nalavadi et al., 2012). These lines of evidence suggest that the transport of neuronal RNP granules is tightly coordinated by the activity of motors transporting their cargoes on both microtubule and F-actin tracks.

Interestingly, recent work uncovered that axonally translocating mRNAs are co-trafficked with membrane-bound organelles. In vertebral retinal ganglion neurons, for example, axonal RNAs dynamically co-localize with Rab5-positive early endosomes, or Rab7-positive late endosomes (Cioni et al., 2019; Konopacki et al., 2016). In cultured rat cortical neurons, TDP43-containing granules are co-transported with LAMP1 positive lysosomes through a hooking process involving ANXA11, an adaptor molecule linking RNP granules and lysosomes (Liao et al., 2019). The increasing link between mRNA localization and membrane-bound organelles has led to an emerging school of thought in which neuronal RNP granules may hitch a ride on various membrane delimited organelles including mitochondria, lysosomes, vesicles etc. (Pushpalatha & Besse, 2019).

Neuronal RNP granules are not constantly under motion, but also display pauses and docking behaviour. Recent studies have shown that RNP granule docking behaviour may have functional significance; RNP granules containing β -actin mRNA were found to be docked at the sites of new branch points in *Xenopus* retinal ganglion cell (RGC) axon terminals (Wong et al., 2017). Interestingly, acute inhibition of translation disrupted axon branching, pointing to a link between

docking of RNA granules at branch points, local translation, and branch formation. In other studies, *Arc* mRNA or FMRP-containing granules were found to be docked preferentially at the base of dendritic spines (Dynes & Steward, 2012; El Fatimy et al., 2016). These observations suggest that neuronal cells could exploit docking of transported RNP granules to elicit translational response to locally changing environments.

1.3.4. RNP granule and translational control

Different lines of evidence have suggested that the translation of mRNAs found in neuronal RNP granules is largely repressed. These include the specific absence of tRNAs, failure to incorporate radioactive amino acids (Krichevsky & Kosik, 2001), and enrichment in translational repressors (Barbee et al., 2006; Fritzsche et al., 2013).

Recent advances in imaging techniques have enabled the spatio-temporal visualization of single RNA molecule translation in living cells (Bauer et al., 2017). Among those, the SunTag technique, in which arrays of SunTag sequences are fused N-terminally to the coding sequence of an mRNA of interest and recognized by a co-expressed single chain antibody (scFV nanobody) fused to super folder GFP (scFV-sfGFP), thus producing bright fluorescent foci at sites of translation (Yan et al., 2016). Using the SunTag tool, *Wu et al.* showed that translation of RNA is spatially modulated in neurons, with ~40% of RNAs translated at proximal dendrites, while only ~10% at distal dendrites, indicating that mRNAs are translationally repressed in dendritic terminals (Wu et al., 2016). More research should now be carried out to investigate translational repression and local translation in living neurons in order to investigate to which extend mRNAs transported in neuronal RNP granules are translationally silent.

How are mRNA molecules translationally repressed in neuronal RNP granules and how do they get de-repressed? RBPs found in neuronal RNP granule proteome include RNA helicases such as DEAD box proteins, and translational repressors such as FMRP, hnRNPs or miRNA pathway components (El Fatimy et al., 2016; Elvira et al., 2006; Fritzsche et al., 2013). These conserved proteins have been shown to repress translation of their target mRNAs through different mechanisms (Pimentel & Boccaccio, 2014). Mechanism of translation repression of target mRNAs by neuronal RNP granules is still under debate. One line of evidence suggests that translational silencing occur at the level of elongation. This is supported by the presence of repressor proteins like FMRP (Darnell et al., 2011; El Fatimy et al., 2016), leading to the accumulation of stalled ribosomes. Around 66% of binding sites for FMRP on target transcripts was on coding sequence and FMRP was found in heavy fraction after *in vitro* ribosome run off experiment, indicating that FMRP blocks translation at elongation step (Darnell et al., 2011). Furthermore, ribopuromycylation, an immunofluorescent technique to visualize polysomes, coupled with ribosome runoff experiment in cultured neurons showed that most neurite-localized

polysomes were resistant to runoff, suggesting that they are stalled at elongation step (Graber et al., 2013). This is in contrary to the alternative proposal that neuronal RNP granules suppress translation by blocking initiation (Besse & Ephrussi, 2008; Klann & Dever, 2004). This is supported by the observation that nuclearly-loaded factors bound on nascent transcripts that are usually released upon first round of translation were found in immunoprecipitated neuronal RNP granules (Fritzsche et al., 2013). Another evidence in this line is the presence of factors like ZBP1, that block translation initiation by preventing 60S joining through binding to target RNA 3'UTR, as components of neuronal RNP granules (Huttelmaier et al., 2005). While such disparities still remain to be resolved, these conflicting results might further illustrate the diversity of neuronal RNP granules (De Graeve & Besse, 2018; Pimentel & Boccaccio, 2014).

How is translation of localized neuronal mRNAs de-repressed in response to specific stimuli? Release of mRNAs from dense granules or “unmasking” has been suggested to represent a mechanism by which translation repression would be relieved through recruitment of active translation machineries (Buxbaum et al., 2014; De Graeve & Besse, 2018). Consistent with this model, Zipcode binding protein 1 (ZBP1), which binds to *β-actin* mRNA to promote its translocation along neurites and its translational repression, gets phosphorylated by the Src kinase upon reaching cell periphery. This phosphorylation decreases the affinity of ZBP1 binding to *β-actin*, thus inducing its release from translation repression (Huttelmaier et al., 2005). This model has also been validated *in vivo* in commissural neurons where *β-actin* is locally translated in response to Sonic hedgehog (Shh) signaling. It was found that Shh signaling induces ZBP1 phosphorylation and that expressing a non-phosphorylatable allele of ZBP1 impedes both local *β-actin* translation and axon turning in response to Shh (Lepelletier et al., 2017). These studies, however, did not show a direct link between granule disassembly and translation regulation. A more direct evidence for translational derepression upon granule disassembly came from the study of Smaug1-foci (S-foci) in cultured hippocampal neurons. Mammalian Smaug1 acts as a translational repressor, forms S-foci at postsynapses of hippocampal neurons. Neuronal activation by NMDA receptor induced reversible disassembly of S-foci, release of localized mRNAs such as *camkIIa* and translation activation of these mRNAs (Baez et al., 2011).

Neuronal RNP granules are micron-sized membraneless organelles which are dynamically responding to environmental cues. To understand how they are regulated, it is thus absolutely essential to understand how these organelles are assembled and disassembled, and how they perform their functions *in cellulo*. Recently, interdisciplinary approaches have been used to tackle these questions, showing that liquid-liquid phase separation (LLPS) may be a unifying mechanism driving RNP assembly. An overview of the mechanisms underlying RNP granule assembly will be discussed in the next section (Section 2).

2. Mechanisms of RNP granule assembly and dynamicity

RNP granules exist as separate entities in the cramped cytoplasm, though they are not delimited by a definite lipid membrane. How do these assemblies concentrate relevant components, and maintain their integrity and functions, while dynamically exchanging components with the cytoplasm?

Different model systems have been developed to probe the biophysical properties of RNP condensates, ranging from *in vitro* reconstituted condensates assembled using purified proteins and/or synthetic or purified endogenous RNA and, *ex vivo* granules formed in cultured cell lines and neurons, to endogenous granules formed *in vivo* in organisms such as *C. elegans*, *Drosophila*, *Xenopus* etc (Figure 3B, Figure 6). *In vitro* studies give the opportunity to have strict control over the concentration, composition, pH, salt, molecular crowding and stoichiometry of components, thus enabling quantitative analyses and reducing the number of variables to be considered. *In vitro* studies, however, lack the potential to phenocopy physiological conditions and to recapitulate the complexity of endogenous granule composition, which can only be achieved in *ex vivo* or *in vivo* cellular systems. Brangwynne and colleagues have recently developed an optogenetic tool to address this drawback; they used domains that interact upon light induction to initiate condensation of proteins of interest inside cells (optodroplets) (Shin et al., 2017). Optodroplets enable a precise control of granule nucleation in a cellular environment; even if nucleation of condensation is artificial, recruitment of partner molecules is not. Thus, integrated approaches combining disciplines of biology, chemistry, physics and computation have provided a conceptual framework defining liquid-liquid phase separation (LLPS) as the molecular principle driving the formation and coexistence of RNP granule as distinct phases within the cytoplasm (see 2.2 and Figure 7).

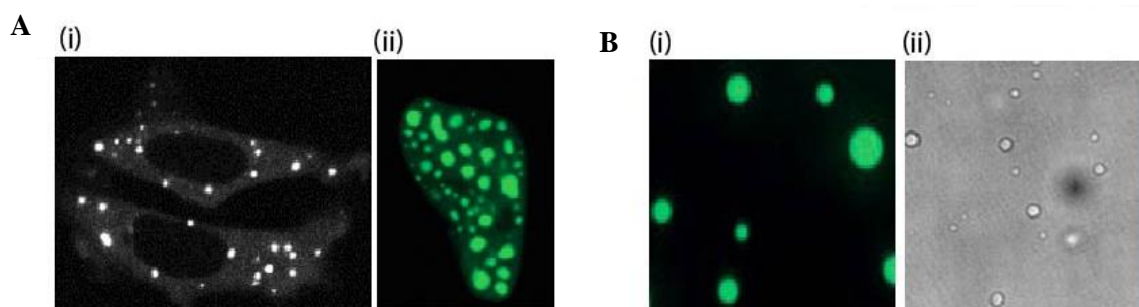


Figure 6: Artificial and *in vitro* condensates

A. Artificial condensates in cells (i) ArtiG-chimeric FFM (Garcia-Jove Navarro et al., 2019), (ii) photo-activated FUS Corelet-expressing HEK293 cells (Bracha et al., 2018). **B.** *In vitro* droplets of (i) purified human FUS-GFP (Patel et al., 2015), (ii) purified RNA from yeast (Van Treeck et al., 2018).

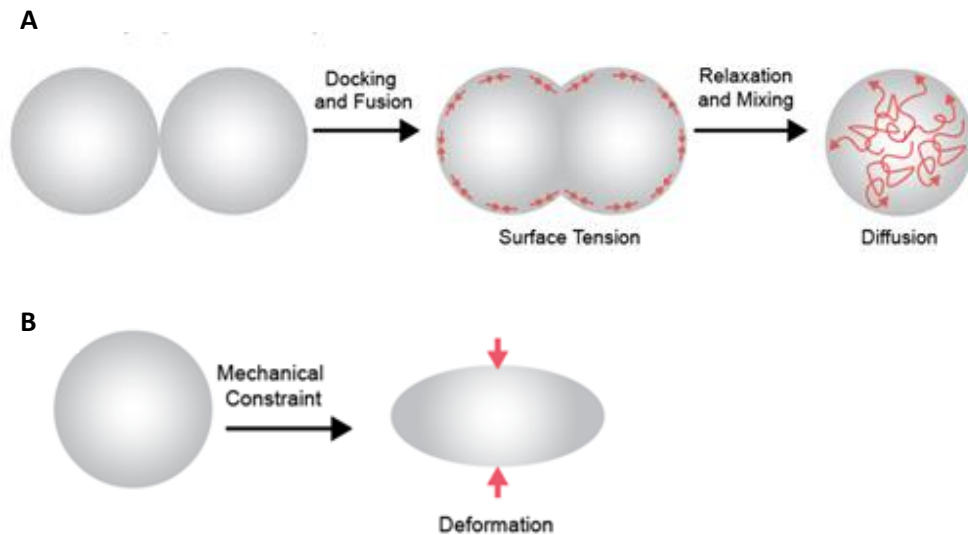


Figure 7: RNP granules behave as liquid-like droplets

A. RNP granules are generally spherical in shape, thus reducing surface tension. RNP granules can dock, fuse and relax back to spheres to reduce surface tension. Molecules inside RNP granules exchange neighbours rapidly. **B.** Due to viscoelastic properties, RNP granules deform upon applied shear stress. Image adapted from (Adekunle & Hubstenberger, 2020).

2.1. RNP granules have liquid-like properties

Recent *in vitro* and *in vivo* studies have converged to demonstrate that RNP granules exhibit properties of liquid-like droplets. First, in contrast to solid entities where molecules maintain their neighborhood for long periods of time, they tend to have a higher degree of freedom and exchange their neighbors rapidly (see 2.1.1). Second, they tend to minimize their surface (and number of molecules) in contact with their surroundings, indicating that surface tension dictates their shape. (see 2.1.2). Third, they deform upon mechanical shear stress, owing to their viscoelastic properties (see 2.1.3).

Handwerger *et al.* in 2005 showed that the nuclear membraneless structure, Cajal bodies, are semifluid objects suspended in semifluid nucleoplasm (Handwerger *et al.*, 2005). Since then, the stable existence of such dynamic structures, with diffusion rates ranging from seconds to minutes, baffled scientists. A seminal discovery was made in the Hyman lab, where P granules in the germ cells of *C.elegans* embryos were found to be liquid-like and have the characteristics of structured formed through liquid-liquid phase separation (LLPS) (Brangwynne *et al.*, 2009). Since then, other membraneless compartments like nucleoli (Brangwynne *et al.*, 2011), DNA damage repair foci (Altmeyer *et al.*, 2015; Patel *et al.*, 2015), stress granules (Kedersha *et al.*, 2005; Molliex *et al.*, 2015) and neuronal transport granules (Andrusiak *et al.*, 2019; Gopal *et al.*, 2017) have been shown to also exhibit liquid-like properties.

2.1.1. Molecules in RNP granules exchange their neighbours rapidly

Constituent molecules of RNP granules are highly dynamic and undergo turnover on timescales ranging from seconds to minutes. Fluorescence recovery after photobleaching (FRAP) analysis has been used for decades as gold-standard for probing turnover of biomolecules (Axelrod et al., 1976) and has been used to measure the dynamicity of molecules in RNP condensates (Figure 8). Whole granule-FRAP analyses have shown that many of these condensates, including SGs, nuclear bodies, and neuronal RNP granules, dynamically exchange materials with their surrounding cytoplasm (Gopal et al., 2017; Kedersha et al., 2005; Weidtkamp-Peters et al., 2008). Not just proteins, *in vitro* purified protein-free RNA molecules alone were shown to self-assemble into RNA droplets and to display dynamic molecular turnover (Jain & Vale, 2017; Van Treeck & Parker, 2018; Van Treeck et al., 2018; Zhang et al., 2015). Remarkably, distinct populations of molecules with varying dynamicity have been identified in the same granule. G3BP, for example, showed very fast and complete recovery (100% within 30s) in Arsenite (As)-induced stress granules in COS cells, while PABP showed partial (45% within 30s) and FAST poor recovery (12.5 % within 30s) (Kedersha et al., 2005). Similarly, *Putnam et al.* assessed the dynamics of different components of P granules in *C.elegans* embryo; PGL-1, PGL-3, GLH-1 and LAF-1 showed higher exchange rates, while MEG-3 showed slow dynamics (Putnam et al., 2019). Dynamicity of RNP components can also vary depending on the cell type. *Cougot et al.* had shown that the same protein component exhibits different turnover rates depending on cell type; Dcp1a had a 90% immobile fraction in granules found in cultured hypothalamic neurons while only 20% in HeLa cells (Cougot et al., 2008). Differential interaction strengths between molecules and cell-type specific interactome could account for the divergent dynamicity observed for RNP granule components.

Molecules are also dynamically exchanging within RNP granules. A method to monitor dynamicity of components within a granule is intra-granule FRAP, where a small region of the granule is bleached, and fluorescence recovery is monitored (Figure 8B). Since the bleached region does not contact the cytosol directly, most of the molecular diffusion will be happening within the granule (Bakthavachalu et al., 2018; Hubstenberger et al., 2013). Intra-granule FRAP has been used to assess the diffusion of components within *in vitro* assembled granules (Burke et al., 2015). A disadvantage of intra-granule FRAP is that it can be done only on large RNP granules. Another tool to assess the molecular dynamicity within granules was half-bleach. As first demonstrated in *C.elegans* embryo, bleaching half of a single P granule with a targeted laser resulted in a significant recovery of signal intensity in the bleached region together with a concomitant decrease of the signal in the unbleached region, indicating that molecules rearrange in these granules with a diffusion coefficient of $1\mu\text{m}^2/\text{s}$ (Brangwynne et al., 2009). Half-bleach of TDP43 RNP granules was used by *Gopal et al.* to identify two distinct populations of TDP43

granules in cultured rat neurons; granules found in mid-axons had higher recovery rate compared to the ones found in proximal axons (Gopal et al., 2017). Above examples show that RNP granule components exchange within and with the surrounding dilute phase of granules; each component having characteristic rates of diffusion.

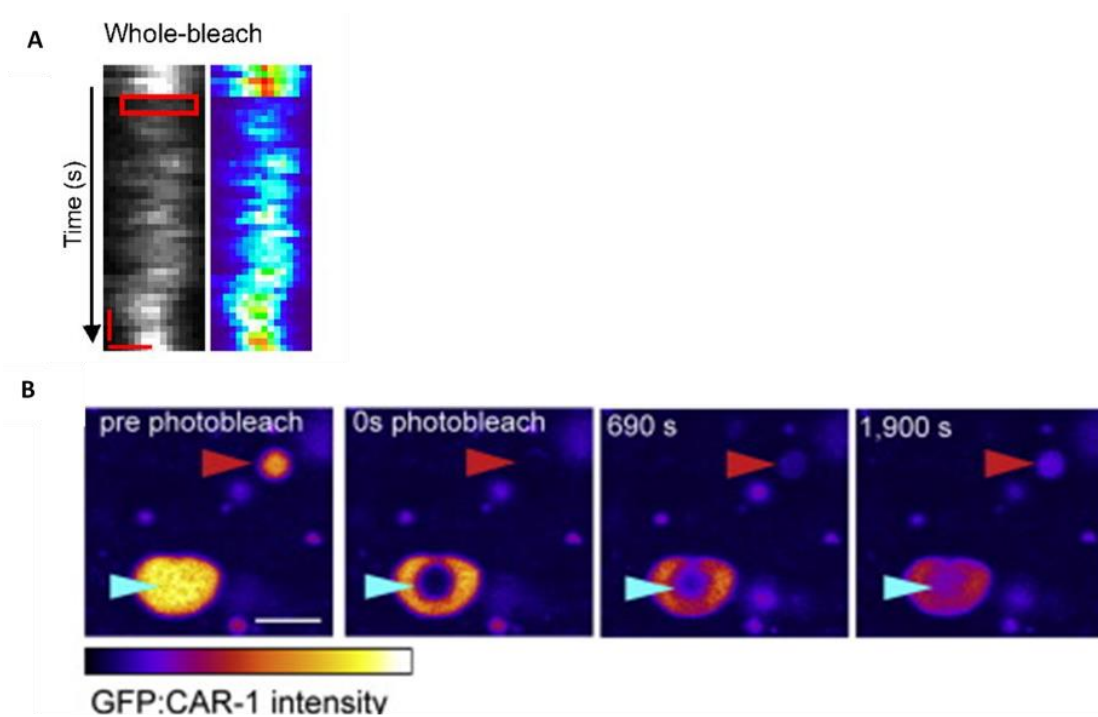


Figure 8: RNP granules are dynamic structures

A. Whole granule bleach of neuronal RNP granule TDP-43 showed rapid recovery suggesting that there is active exchange of TDP-43 molecules between granule and cytoplasm (Gopal et al., 2017). **B.** Fluorescence recovery upon intra-granule bleach of P bodies in *C.elegans* shows inside granule also, molecules rearrange and they are dynamic. Image adapted from (Hubstenberger et al., 2013).

2.1.2. Surface tension dictates the shape of RNP condensates

RNP granules are generally spherical in shape, which is a typical characteristic of liquid droplets. This has been demonstrated in *in vitro* systems, where assembled protein condensates of purified FUS (Patel et al., 2015), LAF1 (Elbaum-Garfinkle et al., 2015) or hnRNPA1 (Molliex et al., 2015) assume spherical shape during condensation. Purified RNA molecules alone can also self-assemble into spherical droplets (Tauber et al., 2020; Van Treeck et al., 2018). In cells, stress granules (Lin et al., 2015; Tourriere et al., 2003), P bodies (Kedersha et al., 2005), germ granules (Brangwynne et al., 2009; Mahowald, 1962; Updike & Strome, 2009), nucleoli (Brangwynne et al., 2011), or neuronal granules (Baez et al., 2011; Gopal et al., 2017) were also described to exhibit circularity indices close to 1.

Another implication of surface tension is that smaller RNP granules of similar type, when in contact, should fuse with characteristic relaxation times to form larger granules, similar to rain drops on windshield. Indeed, coalescence of smaller drops to a large one minimizes surface area, and is thus energetically favourable (Jens Eggers, 1999). *In vitro* assembled condensates containing purified FUS low complexity domain (Burke et al., 2015) or DDX3 RNA helicase LAF-1 (Elbaum-Garfinkle et al., 2015) underwent fusion events. *In vivo*, one of the first observations was that of P granules undergoing fusion in *C.elegans* embryos (Brangwynne et al., 2009). Later, Brangwynne et al. also showed that compression of dissected *Xenopus* oocyte nucleus under a coverslip induces nucleoli to fuse one another, relaxing back to spherical shape at the end of fusion (Brangwynne et al., 2011). TIRF microscopy of neuronal TDP43 RNP granules showed that these granules also fuse and relax to form spherical droplets. Fusion occurs at rates in the range of milliseconds to seconds (Gopal et al., 2017), thus faster than yeast P bodies that fuse and relax in a timeframe of seconds (Kroschwald et al., 2015). This disparity may be accounted for by differences in initial surface tensions, as higher surface tension increases fusion kinetics.

2.1.3. RNP granules have definite viscosities

RNP granules deform in response to shear forces, that are unbalanced forces generated when part of a material (which could be liquid) is pushed in one direction while the other part is pushed in opposite direction. As first shown in *C.elegans* germline, applying shear stress on P granules resulted in their significant deformation (Brangwynne et al., 2009). As another example, *ex vivo* isolated TIAR-2 granules from *C.elegans* mechanosensory neurons also showed dripping-like deformation under shear flows (Andrusiak et al., 2019). Furthermore, near-TIRF live imaging of TDP43 RNP granules in cultured rat neuronal axons showed that TDP43 granules undergoing fast transport, in contrast to motile membrane-bound organelles like mitochondria, underwent significant shape deformation, exhibiting elongated morphology (aspect ratio ~ 1.79) compared to static granules with an aspect ratio ~ 1 (Gopal et al., 2017).

Although RNP granules undergo deformation in response to shear stress, they tend to resist deformation in function of their viscosity. Viscosity of fluids can be conceptualized as the frictional resistance between two adjacent layers of fluids, when they flow. As measured in Swiss 3T3 fibroblasts, cytoplasmic viscosity is comparable to that of water (1.2-1.4 times higher), consistent with the fact that water constitutes 80% of cytosol (Fushimi & Verkman, 1991). Viscosity of *C.elegans* P granules has been estimated from component diffusion coefficient and it is approximately 1 Pa.s (Brangwynne et al., 2009), which is 1000-fold more than water, similar to that of glycerol or colloids. Viscosity of *Xenopus* oocyte nucleoli, measured from the characteristic fusion times, is approximately 1000 Pa.s, which is comparable to that of thick honey

(Brangwynne et al., 2011). TDP43-containing axonally transported RNP granules found in cultured rat neurons have an estimated viscosity of ~ 0.1 Pa.s, which is only 100-fold than that of water (Gopal et al., 2017). Above data suggests that each type of RNP granules can have distinct viscosities; for example, granules that function for storage like P granules or nucleoli are more viscous than motile neuronal granules. Surface tension and viscosity dictated by the molecular interactions thus plays a key role in defining the material properties of RNP granules.

2.1.4. Material properties of RNP condensates can be modulated in physiological and pathological contexts

In living cells, the physical properties of RNP granules have been shown to be modulated in response to the cellular environment. For example, TDP43 granules found in the proximal axon of rat neurons are more solid-like with less recovery after FRAP, while granules found in the mid axon are more liquid-like, deforming upon fast transport (Gopal et al., 2017). Similarly, Dcp1a localized to P-body like structures found in cultured rat hippocampal neurons exhibited a strong increase in their mobile fraction after synaptic activation (Cougot et al., 2008).

Transitioning into solid-like structures has been observed in different instances and characterized by a loss of granule typical spherical shape. Stable solid aggregates of purified FUS protein were shown to acquire stellar shapes *in vitro* (Patel et al., 2015). *In vivo*, inactivation of the *cgh-1* RBP in *C.elegans* gonad induced the transition of normally dynamic and round grP-bodies (grPBs) to solid entities with a square sheet morphology (Hubstenberger et al., 2013). Furthermore, less dynamic TDP43-granules found in the proximal region of rat primary cortical neuron axons have irregular shapes compared to the dynamic and spherical mid-axon localized TDP43-granules (Gopal et al., 2017). Together, the above examples suggest that granule properties can be modulated on-the-fly in response to environmental changes, raising the question of how these dynamic condensates are assembled and regulated. Both theoretical and experimental lines of evidence have established that liquid-liquid phase separation (LLPS) may be a key process driving formation of RNP condensates.

2.2. RNP condensates form through liquid-liquid phase separation (LLPS)

Cytoplasm or nucleoplasm are semi-fluid in nature. If a cell is pricked, cytoplasm oozes out. How could then two liquid phases coexist, when they can rapidly diffuse and mix? Co-existence of liquids as separate phases is not rare, for example colloids, oil-in-water emulsion etc. In case of oil-in-water emulsion, oil molecules are hydrophobic; they tend to bind to other oil molecules than to water molecules. Spontaneous phase separation of liquids is driven by these differential interactions of constituent molecules which counteract the natural entropy driven tendency to mix.

The first mention of phase separation in a biological system dates to 1946 in a fundamental study by Ehrenberg, in which he described the nucleolus as a coacervate, *i.e.* “a separated phase out of a concentrated solution” (Ehrenberg, 1946). The first experimental insight into the mechanisms driving formation of such coacervates was given by the Hyman lab, which suggested that P granules form through liquid-liquid phase separation (LLPS) (Brangwynne et al., 2009). In this physicochemical process, solutions of saturated biological macromolecules undergo spontaneous separation to form a dense phase enriched in granule components and a coexisting dilute phase consisting in the cytoplasm (or nucleoplasm).

Studying LLPS requires a knowledge of which parameters control the demixing of components from solution. Phase diagrams are used to demonstrate the effects of selected state variables (concentration, temperature, salt, pH etc.) on the existence of different phases (Figure 9). They are generated by systematically altering two conditions (*e.g.*, pH and concentration), and checking if two phases co-exist or not. A new phase emerges when the preferential interaction networks dominate the entropy-driven diffusion of molecules. *In vitro* phase separation assays using purified proteins or RNAs have been performed to study the effects of specific variables on the LLPS reaction underlying RNP condensate formation, keeping all other variables constant (Boeynaems, S. *et al.*, 2018, Trends in Cell Biology). These studies have highlighted the importance on one hand of intrinsic factors such as concentration of protein/RNA components, self-organizing domains or motifs, post-translational modifications, valences etc. and on the other hand of extrinsic environmental parameters such as pH, ionic strength, temperature etc. (see below).

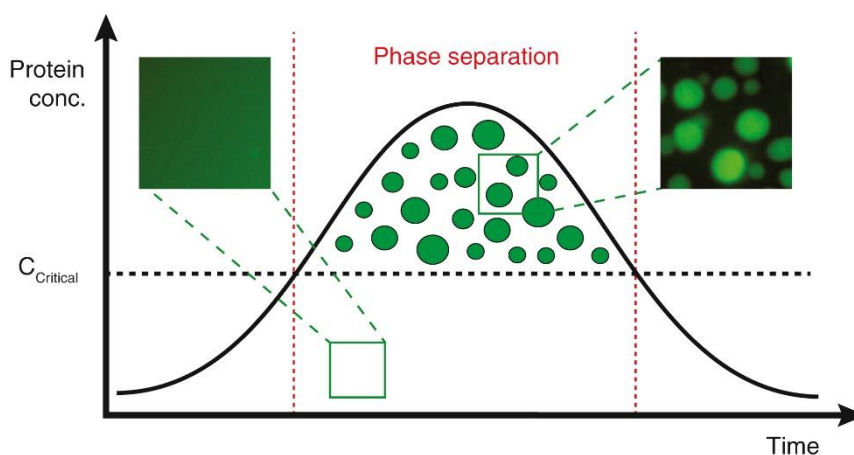


Figure 9: Phase diagram of RNP granule

The proteins that are usually diffused in cells/*in vitro* can demix and form droplets when their concentration is above a critical concentration. They can exist as dense liquid droplets in dilute diffused state. Purified GFP-tagged FUS (a prion-like domain-containing RNA-binding protein) phase separates and forms droplets *in vitro* (inset). Image adapted from (Alberti, 2017).

2.2.1. LLPS and concentration

LLPS is a function of component concentration. Phase separation occurs only when the concentration of phase-separating moiety is above a critical threshold concentration (C_t) (Li et al., 2012; Molliex et al., 2015; Nott et al., 2015). For example, *in vitro* purified LAF1 (a component of P granules in *C.elegans*) stayed diffuse at a concentration below 800nM at physiological salinity, but readily formed condensates when the protein concentration was increased beyond 800nM (Elbaum-Garfinkle et al., 2015). Notably, addition of molecular crowding agents like polyethylene glycol (PEG) can artificially increase the local concentration of RNP components, inducing their phase separation. For example, purified FUS protein was diffuse at a concentration of 10 μ M (slightly above measured physiological concentration) but formed spherical granules in presence of molecular crowding agents like 10% PEG (Patel et al., 2015). Purified RNA itself can phase separate into liquid-like condensates when reaching a critical concentration (Jain & Vale, 2017; Langdon et al., 2018). Addition of positively charged polyamines like spermine and spermidine to initially diffused total yeast RNA was shown to produce RNA condensates (Van Treeck et al., 2018).

Concentration-dependent condensation was also observed *in cellulo* in U2OS cells. Using fluorescent correlation spectroscopy, Sanders *et al.* showed that low concentrations of G3BP1 (0-0.6 μ M) failed to support SG formation while concentrations exceeding \sim 0.6 μ M, permitted the assembly of micron-sized SGs upon stress (Sanders et al., 2020). Another strong evidence for the dependency of LLPS on concentration came from the study from Weber and Brangwynne in which they have shown that nucleolar size directly scales during embryonic development with cell size. Nucleolar size however has an inverse relation to the cell volume when cell size is increased using RNAi in embryos of the same stage because nucleolar material supplied by mother is diluted upon increasing cell size. This shows that nucleolar size depends on the concentration of maternally loaded nucleolar components (Weber & Brangwynne, 2015). Notably, the concentration-dependency of RNP granule assembly shows how crucial it is to express RNP components at endogenous levels in a physiological context to probe for RNP granule assembly and function.

2.2.2. Nucleation and growth

Dependency of phase separation on concentration is not linear, rather is a step-function; until the system reaches a C_t , the components stay mixed. When the system surpasses C_t , it can spontaneously demix to form coexisting distinct phases (Figure 9). Formation of RNP granules can itself be thought of as a two-step process: the first being the spontaneous “birth” of new granules (also known as nucleation), and the second being the growth of these nucleation centres. How cellular RNP condensates are nucleated remains largely elusive. A recent study has shown

that UBAP2L nucleates stress granules in cells under any kind of stress and acts upstream of another core protein G3BP1/2 (Cirillo et al., 2020). Nevertheless, *in vitro* experiments showed that not all protein components belonging to the same RNP granule have equivalent critical concentration at which they initiate condensation. For instance, PGL3, MEG3, and LAF1 are components of P-granules found in *C.elegans* with different C_i s for *in vitro* condensation: PGL3 and MEG3 was measured to be 0.5 μ M (Saha et al., 2016; Smith et al., 2016), while LAF1 was as low as 800nM (Elbaum-Garfinkle et al., 2015). These differences in threshold concentrations for components of RNP granules hint that the protein with lowest C_i could initiate the nucleation event, recruiting components that have higher C_i . This could also mean that the rate limiting step for a cell to regulate condensation is by keeping a checkpoint on the RNP granule component with lowest C_i . Apart from protein molecules acting as nucleators, there is mounting evidence that RNA can also nucleate RNP condensation. For example, mRNAs freed upon translational arrest during cellular stress were shown to act as seed for the assembly of SGs (Boundedjah et al., 2014). Another case of RNA acting as a nucleator is during nucleolar assembly. Nucleoli form near rRNA transcription sites (Karpen et al., 1988) and when rRNA was transcribed from an ectopic locus on the chromosome, a nucleolus-like condensate was found at that location (Oakes et al., 2006). Positional information of nucleolar assembly is lost when rRNA transcription is inhibited or ribosomal DNA is deleted (Berry et al., 2015; Falahati et al., 2016), having nucleoli at arbitrary positions. Once the process of condensation is nucleated, RNP granules can then grow in size by coalescence. During this step, small condensates can come in contact and fuse to form larger granules, a process driven either by simple diffusion or by molecular motors. Thus, nucleation and growth thus determine when and where a cell assembles a particular condensate.

2.2.3. Influence of environmental factors

Concentration-dependent LLPS of proteins can also be regulated, either positively or negatively, by environmental factors such as pH, salinity, or temperature. Increasing salt concentration, for example, can help masking charge-based repulsive interactions, such as those induced by the negative charges on RNA phosphate backbones. As illustrated, by *Van Treeck et al.*, isolated total yeast RNA can readily undergo LLPS and further form stable ‘RNA tangles’ with increasing salt concentration (Van Treeck et al., 2018). Similarly, any molecule that can reduce charge repulsion, like polyamines or spermidine, also can cause RNA condensation (Aumiller et al., 2016; Van Treeck et al., 2018). Stabilization of charge-based interactions by salt also holds true for proteins. *Boeynaems et al.* found that under high salt conditions, poly GR and PR peptides formed fractal-like structures that were resistant to thermal denaturation (Boeynaems et al., 2019). An opposite effect is predicted for protein-protein interactions and has been observed with *in vitro* assembled granules formed from IDRs of RBPs. These IDRs tend to phase separate in low salt conditions while high salt disassembles them (Lin et al., 2015).

From a thermodynamic viewpoint, increasing temperature can dissolve RNP granules. This was tested using *in vitro* assembled DDX4 granules and showed that there is a negative correlation between temperature and phase separation for DDX4 (Nott et al., 2015).

pH can have a broader effect on LLPS of proteins and RNA as it affects the nature of protein interactions by changing the protonation of charged residues. Both the strength and geometry of electrostatic interactions are modified by changing pH, thus creating new interaction spaces. Changes in pH can also confer conformational changes to proteins and RNAs, providing new interacting domains or masking already existing ones. Extreme pH changes even can result in denaturation of the components, which is of less interest in LLPS of RNP granule formation. pH-dependence of LLPS was well-demonstrated for the formation of *in vitro* assembled TDP43-IDR droplets; at physiological neutral pH, LLPS was observed even in the absence of salt but as the pH decreased, higher salt concentration was required for the TDP43-IDR to phase separate (Babinchak et al., 2019). Similar study was made on the LLPS of *in vitro* purified low complexity (LC) domains, LC1 and LC2 of the RNA-associated protein U1-70K. Both U1-70K LC1 and LC2 required higher concentrations at alkaline pH to phase separate, to the extent they underwent LLPS at acidic pH, suggesting that low pH promoted their phase separation probably due to the increased availability of protons (Xue et al., 2019). Above examples therefore reinforce the fact that pH can indeed restructure the electrostatic interaction space of components undergoing LLPS. They also highlight that phase diagrams provide insight on factors affecting phase separation *in vitro* and on physiological conditions that may induce phase separation in living systems.

2.3. Factors affecting RNP component phase separation

LLPS of protein and RNA molecules does not rely solely on environmental factors, but also heavily depends on composition and component properties. As revealed over the past years, RNP granule assembly results from the self-assembly of components as a culmination of protein-protein, RNA-protein and RNA-RNA interactions that constitute dynamic network of interactions and determine the properties and function of each RNP granule.

2.3.1. Multivalency

Multivalency is key for the scaffold proteins to readily undergo LLPS. Valency is the term used to define the number of independent interaction sites a molecule exhibit. A ground-breaking and pioneer discovery on the essentiality of multivalency was made using Polypyrimidine-tract binding protein (PTB). PTB has four RNA binding motifs (RRM1-4) (Sawicka et al., 2008) and mixing PTB together with RNA oligonucleotide caused demixing of PTB to form condensates (Li et al., 2012). This observation indicates that multivalent interactions in intracellular systems may drive LLPS. An analogy driven from the patchy-colloid theory (Bianchi et al., 2011) suggests

that a system of interacting particles (particles can be protein, RNA, or a complex in case of RNP condensates) can undergo phase separation only if each particle has enough number of binding sites for other particles. A particle with no interacting sites is termed as a bystander (valency, $v=0$), a particle with one interaction site ($v=1$) is named as a cap, with two interaction sites ($v=2$) as a bridge and a particle with more than two interacting sites ($v \geq 3$) is known as a node (Figure 10).

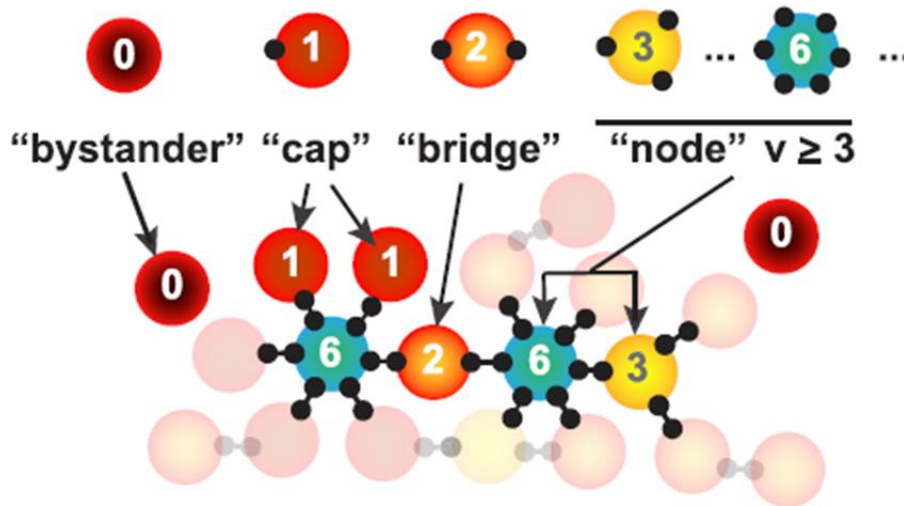


Figure 10: Multivalency is key for RNP LLPS

Valency (v) refers to number of possible interactions of a protein/RNA/complex. $v = 0$ can be considered as a bystander which does not interact with any particles, $v = 1$ (referred to as a cap), interacts with just one component and can restrict further interaction of the complex, $v = 2$ acts like bridge, $v > 2$ (referred to as a node) can interact with multiple components. According to the theory of patchy colloids, increased valency favours LLPS by extending interaction networks. Image adapted from (Sanders et al., 2020).

The role played by each type of component has been tested by *Sanders et al.* using SGs in U2OS cells as a paradigm (Sanders et al., 2020). The importance of G3BP valency was tested by replacing the dimerization domain (NTF2) of this scaffold protein with a synthetic oligomerization domain (FKBP), which failed to support SG formation. This led the authors to reason that the NTF2 domain contains more than a dimerization sequence, thus providing node properties to G3BP. Indeed, NTF2 was shown to recruit UBAP2L, which is also required for SG formation. Another interesting hypothesis that was tested in this study is that the presence of caps can interfere with granule condensation by disrupting the underlying interaction network. Indeed, over-expression of USP10, the only G3BP-interacting partner without an RNA binding domain, led to inhibition of SG formation, suggesting that USP10 acts as cap interfering with the capacity of G3BP to establish multivalent interactions required for condensate nucleation.

Within RNP condensates, multivalency can be conferred mainly by four types of interactions: protein-protein interaction through structured domains, protein-protein interaction through intrinsically disordered regions (IDRs), RNA-protein interaction and RNA-RNA interaction. Many RBPs have structured domains that can bind to RNA, including KH, RRM, zinc-finger etc. Individual interactions between these structured domains are strong and are of covalent or and/or ionic in nature. Another module for protein-protein interaction is intrinsically disordered regions (IDRs), also known as low complexity domains (LCDs). IDRs are peptide sequences without a stable tertiary structure and often exhibit flexible conformations (Oldfield & Dunker, 2014). Some IDRs show highly biased amino acid compositions characterized by an enrichment of particular residues like polyglycine, polyserine etc. Proteins with IDRs are not rare in eukaryotic proteome as 30% of proteins contain regions without any specific 3D structure (Malinowska et al., 2013) and interestingly, RBPs are enriched with IDRs (Castello et al., 2012; Kato et al., 2012). In solution, IDRs do not have stereospecific interactions as they stay unfolded, but a number of them were shown to act as “molecular stickers” mediating weak, promiscuous IDR-IDR interactions. Purified IDRs of FUS, Lsm4, hnRNPA1, and Pub1 have been shown to undergo LLPS in a concentration-dependent fashion (Lin et al., 2015). These weak and promiscuous interactions between IDRs are indeed essential for the liquidity of RNP granules (J. Wang et al., 2018). But recent evidence suggests that projecting IDRs alone as drivers of RNP granule assembly could be misleading. Even though *in vitro* purified IDRs can undergo LLPS on their own, most of them do so in a protein and salt concentration regime far from *in cellulo* concentrations, suggesting that IDRs alone cannot account for the LLPS of proteins (Franzmann & Alberti, 2019). A recent extensive mutagenic approach on the FUS family of proteins showed that heterotypic interaction between IDRs and RNA binding domains (RBDs) in the same or partner proteins drives their condensation (J. Wang et al., 2018).

RBPs can have multiple binding sites for RNA and RNA molecules indeed can have multiple binding sites for corresponding RBP, adding up to the total valency. For example, *in vitro* purified Whi3 protein found in *Ashbya* forms RNP granule upon addition of associated *CLN3* mRNA even at high salt and low protein concentrations while Whi3 alone fails to form granules; Whi3 has an RRM domain that is essential for granule formation and *CLN3* mRNA has five Whi3 binding sites (Lee et al., 2015; Zhang et al., 2015), suggesting that multivalency conferred by RNA binding drives the condensation of Whi3 even at high salt concentration. Taken together, multivalent interactions between proteins and RNA molecules play a crucial role in establishing a well-linked network, driving LLPS of protein and RNA in solution.

2.3.2. Chemical modifications on biomolecules

By modulating the charge, hydrophobicity, steric properties, flexibility etc. of polypeptide chains, post-translational modifications (PTMs) can dramatically alter the physical and chemical characteristics of proteins. Thus, an emerging theme in LLPS of RBPs is, that PTMs can directly regulate RNP granule assembly by enhancing or weakening the interactions between proteins and/or RNAs, thereby directly affecting the multivalency of RNP granule components (Figure 11). Proteins can be modified in a few different ways, by the addition of functional groups including methyl (-CH₃), acetyl (-COOH), phospho groups (Hofweber & Dormann, 2019; Rhoads, Monahan, Yee, & Shewmaker, 2018) or by addition of peptide moieties like SUMOylation (Khayachi et al., 2018) etc.

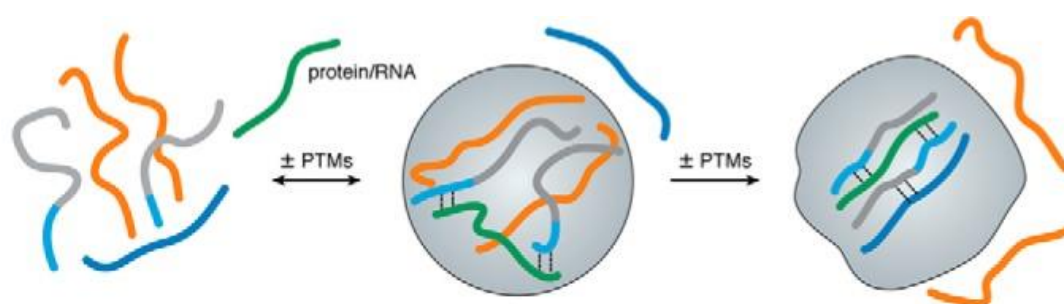


Figure 11: Schematic representation of RNP granule regulation by chemical modifications

PTMs can either enhance or reduce the interaction between RNP components and modulate RNP granule assembly and properties. Image adapted from (Hofweber & Dormann, 2019).

Phosphorylation is the most frequent PTM of proteins (St-Denis & Gingras, 2012), that occurs by the addition of a phosphate moiety to Serine, Threonine or Tyrosine residues. Phosphorylation acts as a rapid and reversible switch mechanism bi-directionally controlled by kinases, that add phosphate group, and phosphatases, that remove them. Phosphorylation introduces two negative charges to the modified amino acid sidechain, thereby providing possibilities for both intra- and inter-molecular charge-based electrostatic interactions. Phosphorylation generally tends to inhibit LLPS of proteins. For example, *in vitro* purified FUS low complexity domain (LCD) undergoes phase separation, a process inhibited through phosphorylation by DNA-dependent protein kinase (DNA-PK) (Monahan et al., 2017; Rhoads, Monahan, Yee, Leung, et al., 2018). There is mounting evidence for regulation of RNP granules via phosphorylation *in vivo*. Dual specificity tyrosine phosphorylation-regulated kinase 3 (DYRK3) was shown to get recruited to SGs in HeLa cells and to promote SG dissolution (Wippich et al., 2013). In addition to its role as a “switch-mechanism”, phosphorylation can be a determinant of subcompartment formation. When mixed with the phosphorylated C-terminal IDR of FMRP (pFMRP_{IDR}) and *sc1* RNA *in vitro*, CAPRIN1

IDR was shown to form a distinct subcompartment containing RNA inside a shell of pFMRP. In contrast, Tyrosine phosphorylated CAPRIN1 IDR (pYCAPRIN) formed a uniform miscible phase after addition of *sc1* RNA, showing that phosphorylation of RNP components can generate distinct subcompartments (Kim et al., 2019). Phosphorylation is thus an essential switch mechanism that regulates RNP granule assembly, disassembly, and/or compartmentalization.

Another common modification on RNP granule components is Arginine (Arg) methylation. Members of protein arginine methyl transferase (PRMT) family were shown to methylate Arg residues located in RGG/RG motifs (Bedford & Clarke, 2009), that are essential for phase separation of FUS (Qamar et al., 2018) and Ddx4 (Nott et al., 2015). *Nott et al.* have shown that the N-terminal RGG-rich domain of Ddx4 (Ddx^{N1}) undergoes phase separation *in vitro* and that dimethylation on Arg by co-expression of PRMT1 and Ddx^{N1} in *E. coli* destabilizes droplets (Nott et al., 2015). In 2018, *Hofweber et al.* showed that *in vitro* methylated FUS exhibits significantly reduced LLPS and shows enhanced dynamics upon half-bleach FRAP compared to unmethylated FUS (Hofweber et al., 2018). In another study, hypomethylated FUS (hypoFUS) purified from insect cells treated with AdOx (a global inhibitor of methylation) formed larger number of droplets and had reduced sphericity, compared to normal FUS (Qamar et al., 2018). In HeLa cells, suppression of SGs upon Arg-dimethylation of G3BP1 was observed, while inhibition of PRMT1 or PRMT5 reduced the levels of methylated G3BP1 and elevated the number of SGs (Tsai et al., 2016). Furthermore, UBAP2L methylation inhibited SG formation (Huang et al., 2020). Above examples show that Arg-methylation acts to solubilize the RNP granules. Conversely, methylation could also positively affect LLPS of RNP components, for example, RAP55A, a member of Scd6/Lsm14 family, is a dimethylated protein whose localization to P bodies is dependent on methylation (Matsumoto et al., 2012). Another example in this line is the finding that symmetrically dimethylated RGG domain of Lsm4 is shown to be essential for P body formation and PRMT5 depletion reduced Lsm4 methylation and P body formation (Arribas-Layton et al., 2016). Arg-methylation is thought to be a more stable PTM than phosphorylation, hence it less likely act as a rapid switch to operate spontaneously upon environmental changes.

LLPS of proteins *in vivo* is a culmination of interaction between different PTMs. Such combinatorial effects are seen, for instance, for G3BP1, it has been proposed that demethylation together with dephosphorylation promotes SG assembly (Reineke et al., 2018; Tsai et al., 2017). Interestingly, acetylation on Lys-321 of Tau has an inhibitory effect on Ser-324 phosphorylation, which promotes Tau aggregation (Carlomagno et al., 2017). Another PTM that is tightly interlinked to phosphorylation is O-GlcNAcylation, which adds O-linked N-acetylglucosamine (O-GlcNAc) moieties to Ser/Thr residues. *Wang et al.* has shown that loss of O-GlcNAcylation in forebrain neurons causes accumulation of hyperphosphorylated Tau and Tau aggregates and induces progressive neurodegeneration (Wang et al., 2016).

Chemical modifications are not just restricted to RNP-resident proteins. Methylation, for example, is a common modification on nucleic acids and N⁶-methyl adenosine (m⁶A) has been shown to be a prominent modification found in mRNAs (Cao et al., 2016). Recently, *Ries et al.* showed that polymethylated mRNA, but no single methylated mRNAs, can enhance the phase separation of cytoplasmic m⁶A-binding proteins YTHDF1, YTHDF2 and YTHDF3 in mammalian cells (Ries et al., 2019).

Together, the above examples showcase the impact of chemical modifications of RNP component condensation. By regulating the valency of RNP components, PTMs can act as switches to respond spontaneously to environmental changes. Recent developments in the field of proteomics will allow researchers to identify more PTMs in RNP components, thus shedding light onto the regulation of RNP granule assembly and dynamics.

2.3.3. RNA:protein ratio

Though proteins can phase separate *in vitro*, presence of RNA helps to reduce the concentration threshold required for LLPS (Drino & Schaefer, 2018). This is consistent with studies identifying RNA as an essential component of RNP granule assembly in cells. As shown by *Teixeira et al.*, for example, P-body assembly in yeast is sensitive to both RNase treatment and cycloheximide treatment, that traps RNA in ribosomes, abolishes P-body formation (Teixeira et al., 2005). RNA can also act as a scaffold for RNP assembly. *NEAT1 lncRNA*, for example, is required in HeLa cells for the assembly of paraspeckles, a type of nuclear RNP granules (Zhang et al., 2013). Furthermore, isolated SG cores were shown to be highly resistant to high salt, a condition known to destabilize protein-protein interactions (Jain et al., 2016), leading to the observation that purified yeast total RNA can undergo LLPS, forming droplets that recruit known SG transcriptomes (Van Treeck et al., 2018). RNA has also been shown to regulate the size and structure of RNP granules. In a seminal study by Zoher and colleagues, engineered artificial granules (artiGs) were created in HeLa cells using ferritin 24-mer self-assembling nanocage. The ratio between RNA and protein was shown to affect the physical properties of these artiGs; when bound to higher amounts of RNA, artiGs were smaller in size and present in large number, while lesser RNA/protein ratio resulted in small number of large granules (Garcia-Jove Navarro et al., 2019). This could be due to the net negative charge imparted by RNA molecules that inhibit coalescence of granules. While the above examples point to a role of RNA in promoting phase separation, a ground-breaking observation made by Alberti and colleagues suggests that RNA can buffer the phase behaviour of prion-like RBPs at high concentration. They have shown that a low RNA/protein ratio can lead to LLPS of proteins like FUS, TDP43, hnRNPA1, while a higher ratio prevents granule formation *in vitro* (Maharana et al., 2018). Taken together, the above lines of

evidence suggest that RNA/protein ratio could be a major determinant in assembly of RNP by modulating molecular interactions.

2.3.4. RNA chaperones/helicases

Given the propensity of RNA to self-assemble (Van Treeck & Parker, 2018; Van Treeck et al., 2018), cells must keep a check on RNA cis- and trans-interactions. RNA helicases are a group of RNA chaperones; they ensure proper folding of RNA molecules into native conformations and unwind long-lived misfolds to assist in their accurate re-folding. The unwinding activity of RNA helicases depends on ATP binding and hydrolysis (Jankowsky, 2011). Strikingly, RNA helicases, especially DEAD-box helicases, are found to be integral part of RNP condensates *in vivo* (Fu, 2020). For example, SGs recruit RNA helicases such as Ded1/DDX3, eIF4A/DDX2, RHAU (Chalupnikova et al., 2008; Jain et al., 2016; Markmiller et al., 2018), PBs recruit Dhh1/DDX6, Ded1p (Anderson & Kedersha, 2006; Beckham et al., 2008), germ granules recruit RNA helicase Vasa (Gustafson & Wessel, 2010) and neuronal transport granules contain DDX1, Ded1/DDX3, and Dhh1/DDX6 (Kanai et al., 2004; Miller et al., 2009).

RNA helicases have conserved domains/ motifs for RNA-binding (e.g. RecA domain), ATP binding and hydrolysis, and helicase domains like DEAD-box. Both genetic and pharmacological studies have shown that helicase activity is necessary for RNP condensate turnover. Using Hippuristanol (Hipp), a drug that specifically inhibits the helicase activity of eIF4A, Tauber and co-workers showed that eIF4A normally limit the recruitment of RNA to SGs and SG formation in U2OS cells upon arsenite-stress (Tauber et al., 2020). In yeast, K. Weis and colleagues have shown that Dhh1 mutants for helicase activity (Dhh1^{DQAD}) had reduced recovery after FRAP compared to control and triggered the formation of constitutive PBs, indicating that helicase activity and ATP hydrolysis is necessary for Dhh1 dynamicity and disassembly of PBs *in vivo* (Mugler et al., 2016). Similar was the case for yeast Ded1 and *C.elegans* GLH-1 helicases. Helicase mutants for yeast Ded1 RNA helicase also form constitutive SGs even in the absence of a stressor (Hilliker et al., 2011). DQAD mutation in *C.elegans* GLH-1 caused persisting P-granules in germ cells that, unlike wildtype P-granules, did not disassemble during the pseudocleavage stage of the embryo (Chen et al., 2020). These examples show that RNA helicases regulate the turnover and disassembly of RNP condensates *via* their ATPase cycle. grPBs assembled in arrested oocytes of *C.elegans* are liquid-like compartments, which become solid and less dynamic with square-sheet morphology upon RNAi-mediated knockdown of *cgh-1* (DDX6) RNA helicase (Hubstenberger et al., 2013).

RNA helicases also play a crucial role as nucleating factors for RNP condensates. Dhh1 is required for PB formation, as yeast cells mutant for *dhh1* (*dhh1Δ*), or expressing a Dhh1 variant mutants for ATP binding or RNA binding, fail to assemble PB (Mugler et al., 2016). Similarly,

DDX3 was shown to be necessary for assembly of SGs in HeLa cells after sorbitol treatment, as shRNA-mediated knockdown of DDX3 impairs SG assembly, whereas overexpression led to spontaneous assembly of SG in the absence of a stressor (Shih et al., 2012).

DEAD-box helicases, both *in vitro* and *in vivo*, exhibit preferential binding to target RNA and /or unwinding of specific structures (Chen et al., 2018; Ribeiro de Almeida et al., 2018). This means that RNA helicases could mediate the condensation of particular RNA molecules to a specific condensate and modulate the multiphase coexistence mediated by RNA interactions. In support of this, pharmacological inhibition of eIF4A helicase activity increased the docking frequency of PBs on SGs (Kedersha et al., 2005; Tauber et al., 2020). RNA helicases also could mediate the transfer of RNA molecules between distinct RNP condensates. As an evidence, *in vitro* purified yeast Dhh1, together with target RNA, formed distinct condensates that did not mix with droplets composed of Ded1 (a SG component helicase). Addition of Dhh1 helicase activator, however, dissolved the Dhh1 condensates, releasing labelled RNA that was taken up by Ded1 condensates (Hondele et al., 2019). Taken together, RNA helicases are proteins that can directly regulate the assembly, dynamics, and disassembly of RNP condensates, principally through altering RNA interactions.

2.4. Compositional control

Individual RNP condensates though heterogeneous, have a define composition, accommodating up to tens to hundreds of protein molecules and often RNAs. Composition of RNP condensates is not static, they are modulated on-the-fly; some components are constitutive, while others are dynamically added depending on the stimuli and cellular environment. Furthermore, only a small fraction is essential for the assembly and integrity of these structures. This led to the distinction of biomolecules into two groups: “scaffolds” and “clients” (Ditlev et al., 2018). Scaffolds are indispensable for granule integrity as deletion or depletion of these components decreases the size and/or number of granules. For example, PML is a scaffold for PML nuclear body (NB) as knocking out PML abolishes NB formation (Ishov et al., 1999; Zhong et al., 2000). Similarly, G3BP is an essential component of stress granules, as knocking out G3BP abolishes SG formation upon arsenite-induced stress (Bley et al., 2015; Guillen-Boixet et al., 2020; Matsuki et al., 2013; Sanders et al., 2020). DDX6 and LSM14A are essential for P-body formation in HEK293 cells, as P-body formation is abrogated in DDX6 or LSM14A knockout cells (Ayache et al., 2015). In contrast to scaffolds, client molecules are dispensable for the formation of RNP granules and are recruited *via* their interaction with the scaffold(s) (Ditlev et al., 2018; Lin et al., 2006). PML nuclear body proteins Sp100 and BLM are examples of client proteins; depletion of either of them does not affect PML nuclear body formation (Weidtkamp-Peters et al., 2008). Using FRAP, it has been shown that clients tend to exhibit higher turnover rates than scaffolds and that interactions

among scaffold components are more stable than transient client-scaffold interactions (Dundr et al., 2004; Weidtkamp-Peters et al., 2008; Xing et al., 2020).

2.4.1. Compositional control based on stoichiometry

The composition of RNP granules has been shown to be regulated by the stoichiometry of scaffold proteins in the core. Using *in vitro* assembled polySUMO-polySIM, polySH3-polyPRM and PTB-polyUCUCU condensates, it was shown that clients partition into RNP condensates, when their corresponding scaffold is present in stoichiometric excess (Banani et al., 2016). For example, when polySIM was in excess, GFP-SUMO was preferentially enriched in the polySUMO-polySIM condensates, whereas when polySUMO was in excess, an opposite trend was observed, with enrichment of GFP-SIM in the condensed phase. Stoichiometry of core components could also drive multiphase coexistence. For example, SGs are sometimes seen docked with P bodies (PBs) upon stress (Kedersha et al., 2005; Stoecklin & Kedersha, 2013). An increase in concentration of shared components between two distinct RNP granules can result in fusion of these otherwise coexisting granules. UBAP2L is a SG component that can interact with DDX6, a helicase present in both SGs and PBs. Overexpression of UBAP2L in G3BP1/2 KO cells resulted in collapse of several SG- and PB-components into a single miscible phase, whereas overexpression of SG-specific G3BP1 together with PB-specific DCP1A favored decoupling of SGs from PBs (Sanders et al., 2020). These studies indicate that RNP granule formation might be driven by the assembly of stable core/scaffold, over which the transient client molecules interact to fine tune the scaffold-scaffold bond networks.

2.4.2. Compositional control based on RNA

The role of RNA in the regulation of molecular condensate composition has only recently started to emerge. The Gladfelter lab recently showed that the secondary structure of RNA molecules determines their base pairing, and this essentially determines their incorporation into RNP condensates (Langdon et al., 2018). Whi3 in *Ashbya* fungi forms RNP condensates that contain RNA molecules and both Whi3 and associated RNA can undergo phase separation *in vitro* (Zhang et al., 2015). Strikingly, Whi3 forms RNP condensates with distinct composition within the same cell at different locations. While the Whi3 condensates found at growing tips contain *BNII* and *SPA2* mRNAs, the perinuclear Whi3 condensates instead recruit *CLN3* mRNA. *In vitro*, *SPA2* RNA readily incorporates into pre-formed *BNII*-Whi3 condensates, however *CLN3* is largely excluded from *BNII*-Whi3 condensates. When mixed together, *CLN3* competed with *BNII* for Whi3 and formed distinct *CLN3*-Whi3 condensates. Differential sorting was recapitulated when using RNA only, as *CLN3* formed condensates with itself, whereas *BNII* and *SPA2* co-assembled into distinct condensates. These results indicate that RNA-RNA interactions determine the composition of resulting RNP condensates (Langdon et al., 2018). They further showed that the

specificity of RNA recruitment is encoded in the secondary structure of RNA molecules, as *CLN3* transcripts with altered secondary structure lost their specific behavior and readily incorporated into *BNI1*-Whi3 condensates. It remains to be determined whether this RNA-RNA interaction-mediated composition control is a universal principle applying to other types of RNP condensates.

These studies have led to an emerging unified model for compositional control of RNP condensates (Figure 12). Protein and RNA scaffolds interact via their protein:RNA interactions (mediated by specific modular RBDs and RBD binding elements on RNA) to nucleate RNP condensation. Protein scaffolds can further interact using modular domains and IDRs. The resulting condensate can then recruit client proteins and/or RNAs depending on their molecular features. A client protein with a compatible modular domain for interaction with protein scaffold, multivalent RBD for interaction with RNA scaffold, and IDR with specific sequence will partition readily into the condensate whereas clients with monovalent RBDs or incompatible IDRs are excluded from the condensates. RNA clients can be recruited depending on their interactions to RNA scaffolds mediated by their secondary structure and base pairing and on their interactions to protein scaffolds through multivalent RBDs. This unified model thus provides a theoretical framework for understanding how RNP condensate composition is determined and dynamically regulated.

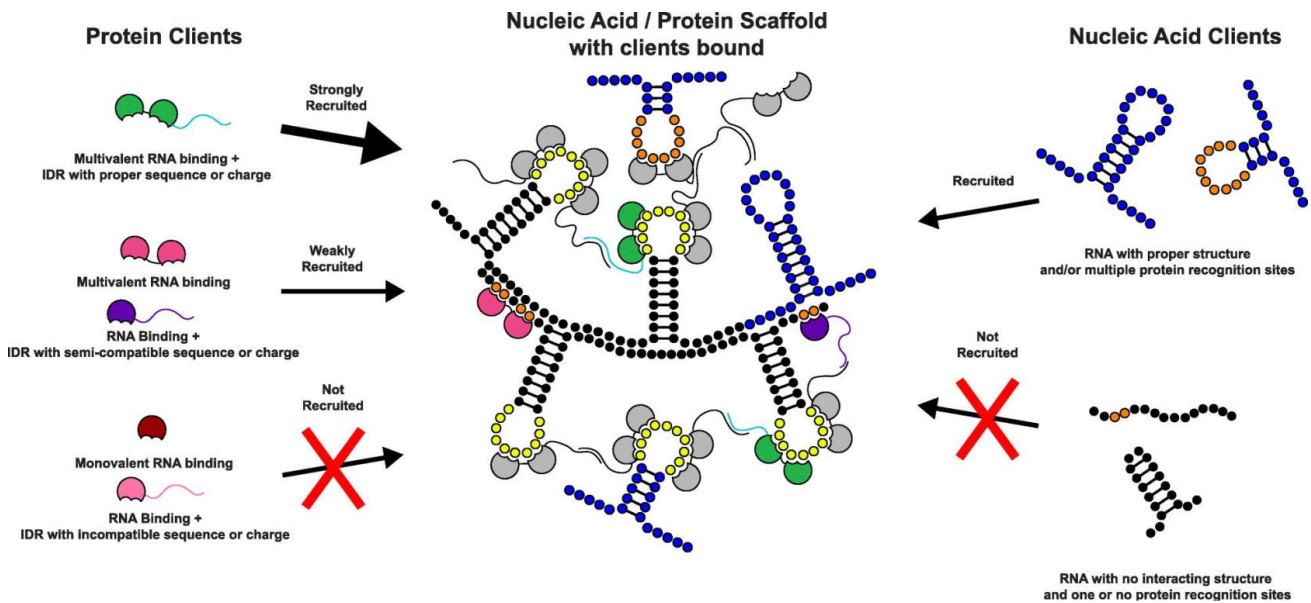


Figure 12: A unified model of compositional control in condensates

A representative condensate formed by a “scaffold” fused to an IDR (black), and an RNA scaffold with multiple RBD binding elements (yellow). “Client” protein recruitment depends on the number of RBDs and the sequence of IDR. Clients with incompatible RBDs or IDRs are excluded from the condensate. Client RNA molecules are recruited based on secondary structure and valency of RBD binding elements. RNA clients with no interacting secondary structure or without appropriate RBD binding elements are not recruited. Image adapted from (Ditlev et al., 2018).

2.5. RNP condensate deregulation and pathologies

RNP granules are highly dynamic, constantly exchanging components with their surrounding environment. The modalities used to create a dynamic entity, in particular the establishment of flexible and transient interactions mediated by IDRs or LCDs, however come with a trade-off: IDRs are susceptible to aberrant interactions and are highly prone to aggregation. The main features that make RNP condensates breeding grounds for aggregates are: first, their formation depends on multivalent interactions, that is, dense network of interactions (Clifford et al., 2015), second, protein components use IDRs that are characterized by the presence of high polar or ionic amino acids, and low overall hydrophobicity, for maintaining weak interactions (King et al., 2012; Malinowska et al., 2013), third, they are highly concentrated in condensates, for example, studies with *in vitro* RNP condensates have shown that the concentration can be 100-fold higher compared to the surrounding (Molliex et al., 2015; Patel et al., 2015), fourth, RNP condensates are highly sensitive to fluctuation in pH, temperature, salinity, concentration etc. Accumulation of pathological aggregates enriched in RNP components but with altered dynamic properties has emerged as a common feature of degenerative diseases, particularly neurodegenerative diseases. Furthermore, research in recent years have causally linked alterations in RNP granule components with various pathologies (Kapeli et al., 2017; Ramaswami et al., 2013; Taylor et al., 2016), leading to a model where loss of RNP granule dynamicity and aggregate formation may drive pathogenesis. Whether RNP aggregates are a cause or a consequence of pathogenesis is however still debated.

2.5.1. RNP condensates and carcinogenesis

As epigenetic modulators of gene expression (altering gene expression without directly modifying the genetic code), RNP condensates play a key role in maintaining cellular homeostasis. Loss of their dynamicity, function, and localization has been implicated in pathogenesis. There is growing evidence for aberrant phase separation of proteins involved in transcriptional regulation, oncogenic substrate degradation, genomic stability and signalling pathways during carcinogenesis (Jiang et al., 2020). For example, p53, a tumour suppressor protein, was shown to be recruited to nuclear bodies like PML upon stress, a process triggering its transcriptional activation (Guo et al., 2000). Furthermore, p53 was recently shown to undergo phase separation *in vitro* (Kamagata et al., 2020). Remarkably, p53 assembled at pH 7 into liquid-like condensates that were able to bind dsDNA target whereas p53 formed aggregates at pH 5.5 that showed reduced affinity for dsDNA target. These aggregates are reminiscent of the amyloid-like fibrils formed by tumour-associated

mutants of p53 with perturbed tumour-suppressive role (Higashimoto et al., 2006; Wilcken et al., 2012).

Accumulation of RNP components into pathological aggregates is also a common feature of samples from patients suffering from neurodegenerative disorders (Figure 13) (Mori et al., 2008; Taylor et al., 2002). As explained in more details below, research in recent years has shed light on the link between mutant RNP components and neurodegenerative diseases (Kapeli et al., 2017; Ramaswami et al., 2013; Taylor et al., 2016).

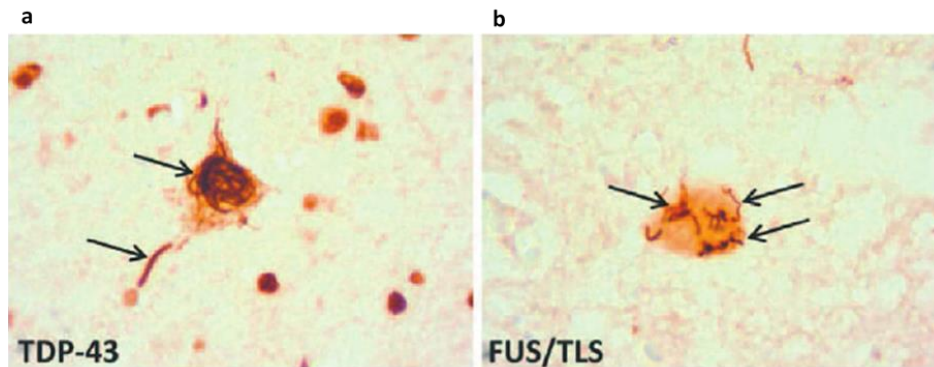


Figure 13: Protein aggregates in motor neurons of ALS patients.

Arrows point to aggregates found in ALS patient-derived samples stained for TDP43 (a) and FUS (b). Image adapted from (Droppelmann et al., 2014).

2.5.2. RNP granules and neurodegeneration

Neurons have a particular need to control RNP condensate dynamic properties. First, since they are terminally differentiated, dissipation of aggregates during cell division is not an option; they must rely on cellular degradation machinery to clear aggregates. Second, due to their elaborate architecture, they highly depend on long-distance transport of RNA and local RNA translation (see section 1.3). Lastly, they are excitable and hence consume a lot of ATP, which is involved in the maintenance of RNP granule properties in different ways. As explained in section 2.3.4, indeed, ATP-dependent RNA helicase activity maintains dynamicity and disassembly of RNP condensates. Furthermore, recent studies have suggested that ATP can act as a hydrotope at intracellular concentrations, *i.e.*, a compound that dissolves hydrophobic molecules in aqueous solution (Patel et al., 2017). Thus, an increased demand for ATP in neuronal cells could elevate the propensity of aggregation.

Neurodegenerative diseases are characterized by the progressive loss of motor ability and cognition; for example, cognitive deficit is a key feature of Alzheimer's (AD), frontotemporal dementia (FTD), motor deficits are seen in patients with amyotrophic lateral sclerosis (ALS),

Huntington's (HD) and Parkinson's disease (PD). Although a direct cause-consequence relation remains elusive, cytosolic, or nuclear aggregates have become a common theme in this field. Examples include cytosolic aggregates of Tau in AD, of RBPs such as TDP-43 or FUS in ALS and FTD, and poly-glutamine (polyQ) aggregates in HD. Although rare, mutations in familial cases often occur in genes coding for proteins with high aggregation propensity. Similar proteins are identified in aggregates of sporadic cases too, pointing to a common mechanism causing neurodegenerative diseases (Gan et al., 2018). Interestingly, recent research has shown that SGs, that are normally transient structures formed during cellular stress, may persist upon chronic stress, thus acting as crucibles for aggregation of disease-associated biomolecules (Advani & Ivanov, 2020; Wolozin & Ivanov, 2019).

Past five years of research have shown that aberrant phase separation could drive the formation of pathological aggregates. Several neurodegenerative disease-causing mutations have been reported in protein components and RNA of RNP granules, that can cause aberrant phase transitions. Fused in sarcoma (FUS) is an RBP enriched in the nucleus, that plays a vital role in regulating transcription, splicing and DNA repair (Wang et al., 2013). Mutations in FUS were found in patients suffering from ALS and rarely frontotemporal lobar degeneration (FTLD) (Deng et al., 2014; Woulfe et al., 2010). *In vitro*, purified FUS was shown to produce observable liquid-like droplets when kept for 8 hours, whereas FUS protein with patient-derived mutations formed fibrillar aggregates within this 8-hour window. These aggregates showed almost zero recovery in FRAP assays, indicating an absence of exchange with surrounding molecules (Figure 14) (Patel et al., 2015). George-Hyslop and colleagues further showed that mutant FUS aggregates can trap other RNP components such as SMN and STAU1, and when expressed in cultured neurons, reduced the synthesis of new proteins in axons and terminals (Murakami et al., 2015). hnRNPA1 is an RBP enriched in SGs. Mutations in the IDR of hnRNPA1 are associated with ALS and multisystem proteinopathy, a dominantly inherited degenerative disorder that results in wastage of muscles and degeneration of CNS ((Kim et al., 2013). *In vitro* purified hnRNPA1 and ALS-mutant hnRNPA1 both undergo LLPS in an IDR-dependent manner. However, formation of Thioflavin-T-positive fibrils indicative of a more solid-like state was accelerated in mutant compared to wildtype context (Molliex et al., 2015). TIA1 (T cell-restricted intracellular antigen-1) is another prominent SG component (Kedersha et al., 2000), in the IDR of which mutations linked to familial cases of ALS and ALS/FTD were found (Mackenzie et al., 2017). *In vitro* condensates formed by ALS mutant TIA1 showed reduced internal molecular mobility as shown by FRAP. Furthermore, expressing ALS-variant of TIA1 *in cellulo* dampened SG disassembly after stress (Mackenzie et al., 2017). Thus, the above examples show that many proteins implicated in ALS/FTD are related to SGs, raising the hypothesis that SGs may act as the precursors to aberrant phase-separated aggregates found in disease conditions. A more direct link

between degeneration and SGs came from a pivotal study performed by Taylor lab. In this study, an optically inducible system driving SG assembly (optodroplet) was used in human iPSC-derived neurons, revealing that chronic optoSGs were cytotoxic and that RBPs like TIA1 and TDP43 were progressively recruited into these condensates, reminiscent of ALS/FTD pathology evolution (Zhang et al., 2019).

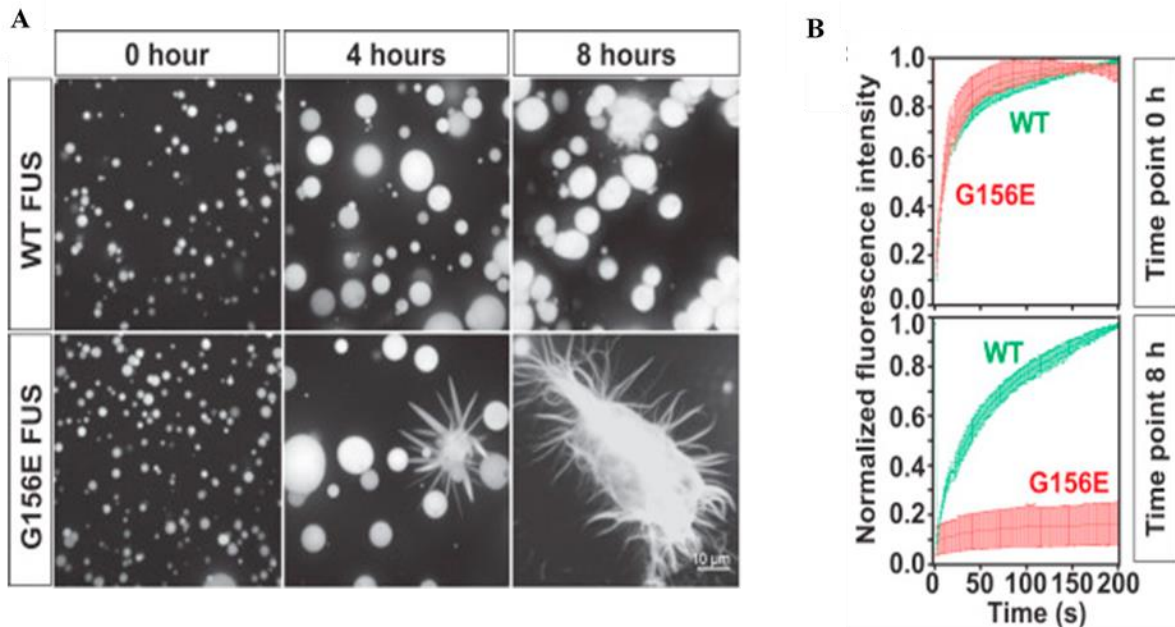


Figure 14: ALS-causing mutations accelerated the liquid-to-solid transition of FUS.

A. Representative images showing *in vitro* aging of FUS WT and FUS mutant. **B.** Plots showing recovery of fluorescence after photobleaching between WT (green) and mutant (red) FUS at two time points (0h and 8h). Image adapted from (Patel et al., 2015).

In the examples given above, mutations were located in the IDRs, RBDs or other crucial domains, thus altering interactions with RNP components and driving aberrant phase separations. Mutations were also found on localization signals of RNP components causing mislocalization to an ectopic location, change in solubility and aberrant LLPS. ALS-associated mutations in the FUS nuclear localization signal (NLS), for example, lead to its altered localization to the cytoplasm (Dormann et al., 2010). These changes have been speculated to induce liquid-to-solid transition of FUS condensates for two main reasons: i- RNA weakens and buffers the interaction strength of RNP components and is much more concentrated in the nucleus than in the cytoplasm (Maharana et al., 2018) and ii- an increase in cytoplasmic FUS concentration itself may favour liquid-to-solid transition (Patel et al., 2015).

Not just mutations, inappropriate chemical modifications of RNP components could also drive aberrant phase transitions associated with neurodegenerative disorders (Hofweber & Dormann,

2019). For example, in healthy human samples, RGG/RG-rich IDRs of FUS have arginine methylation (Rappsilber et al., 2003), whereas they are unmethylated or monomethylated in patient-derived samples (Dormann et al., 2012; Suarez-Calvet et al., 2016). Both *in vitro* and *in cellulo* studies have shown that loss of methylation reduces the dynamics of FUS condensates, potentially due to increased cation- π interactions between arginine and aromatic residues (Hofweber et al., 2018; Qamar et al., 2018).

Albeit the fact that these disease-causing conditions may arise right from childhood, these degenerative disorders usually show a late onset. Such aberrant phase transitions are rarely observed in young cells, meaning that aging is associated with a failure to keep a check on aggregate-formation and loss of dynamicity (Alberti et al., 2017).

3. Aging - be past your prime

Aging is an inevitable and irreversible progressive decline in fitness of cells, organs, or organisms. Aging is recognised as a primary risk factor for many disorders including, cancers, metabolic disorders, neurodegeneration, and cardiovascular diseases (Johnson et al., 2015; Niccoli & Partridge, 2012). The likelihood of diseases does not increase with age simply because of time-dependent accumulation of somatic mutations. Rather, recent work has shown that aging-associated physiological and molecular changes could lead to the development of disorders (Aunan et al., 2017; de Magalhaes, 2013; Ramaswami et al., 2013), even though the relationship between aging signatures and their relative contributions to the process of aging still remains elusive. To date, a widely accepted concept is that the progressive accumulation of cellular damage could be a causative agent for aging (Gems & Partridge, 2013; Kirkwood, 2005). Indeed, homeostatic mechanisms are progressively deteriorated in aging cells, resulting in impaired repair and unhealthy state.

3.1. Cellular and molecular hallmarks of aging.

The major recognized hallmarks of aging cells include genomic instability, telomere attrition, epigenetic alterations, loss of proteostasis, mitochondrial dysfunction, cellular senescence, disrupted nutrient sensing, exhaustion of stem cell niche, and altered intercellular signalling (Figure 15) (Lopez-Otin et al., 2013). As describing them all is beyond the scope of this manuscript, I am illustrating below few with conserved underlying mechanisms and potential relevance to RNP granule homeostasis.

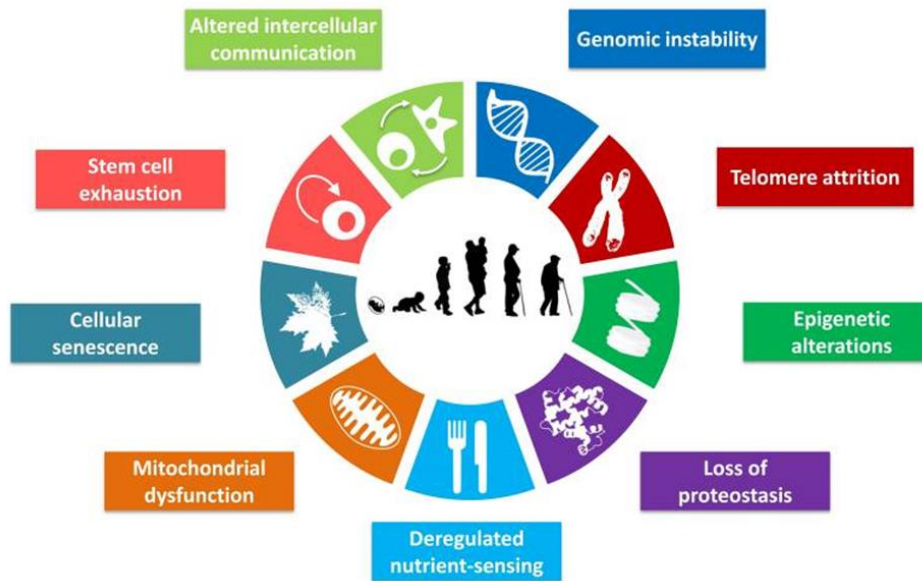


Figure 15: Hallmarks of aging

Recognized hallmarks of aging include genomic instability, telomere attrition, epigenetic alterations, loss of proteostasis, altered metabolism, mitochondrial dysfunction, cellular death, stem cell exhaustion, and altered cell-cell communication. Image adapted from (Lopez-Otin et al., 2013).

Insulin and IGF1 signalling (IIS) is a major pathway involved in cellular nutrient sensing. Remarkably, IIS has evolutionary conserved functions in controlling aging (Fontana et al., 2010; Kenyon, 2010). Mutations that repress the activity of receptors of IIS or downstream effectors such as mTOR, and AKT, have all been shown to be associated with longevity (Barzilai et al., 2012; Demontis & Perrimon, 2010; Kenyon, 2010). This is conferred by dephosphorylation and nuclear import of the prosurvival transcription factor FOXO, resulting in transcriptional activation of genes involved in resistance to stress and stem cell maintenance (Martins et al., 2016).

Reduction in protein quality control is another major hallmark of aging cells. Protein aggregates are key features of aging cells (David et al., 2010; Reis-Rodrigues et al., 2012; Walther et al., 2015). A reduction in the activity of autophagy and ubiquitin proteasome machineries is associated with aging (Lipinski et al., 2010; Rubinsztein et al., 2011; Tomaru et al., 2012). Murine and mouse mutants for autophagy related gene *atg7* have shorter lifespan and display neurodegenerative disorders (Hara et al., 2006; Juhasz et al., 2007; Komatsu et al., 2006). Reinforcing autophagic machineries in old cells can rescue aging, for instance, an extra copy of the autophagy receptor LAMP2a improved the hepatic function with aging in transgenic mice models (Zhang & Cuervo, 2008). Furthermore, Liu et al. showed that EGF signalling can activate ubiquitin protease system in *C. elegans* to improve lifespan (Liu et al., 2011). Last, chaperones,

when overexpressed in flies and *C. elegans*, were shown to increase the lifespan of these organisms (Morrow et al., 2004; Walker & Lithgow, 2003).

Studies in mammalian models have shown that *mitochondrial dysfunction* can accelerate aging (Trifunovic et al., 2004; Vermulst et al., 2008) and may thus be considered as a cause of cellular aging. Mitochondrial dysfunction translates into a decreased efficiency of the respiratory transport chain with aging, resulting in leakage of electrons and reduced ATP synthesis (Green et al., 2011). Furthermore, it is coupled with increased levels of *reactive oxygen species (ROS)* which cause oxidative damage on biomolecules and were proposed to be causative agent for aging (Santos et al., 2018).

3.2 Changes in gene expression

Healthy young cells maintain a balance of both transcription and translation, which is lost in aged cells. Development of state-of-the-art techniques including RNA seq, ribosome profiling (Ribo-seq), microfluidics, mass spectrometry etc. have allowed researchers to analyse transcriptomes, and proteomes from model organisms of different age groups.

Transcriptomic studies

Transcriptomics studies performed in different tissues and different organisms have shown that, although variability increases with age, gene expression is globally not widely misregulated during aging (Ori et al., 2015; Stegeman & Weake, 2017). However, as observed in both *Drosophila* and human brain samples, specific sets of genes show transcriptional changes upon aging, as illustrated by the upregulation of immune response gene expression, and the decline in genes involved in synaptic transmission and plasticity (Ham & Lee, 2020; Pacifico et al., 2018). Consistent with this, studying transcriptomes using RNA-seq approaches across different species of *Drosophila* with varying lifespans pointed to a potential role for regulation of gene expression in extending their life span (Ma et al., 2018). These studies indicate a general trend that within a single cell type or tissue, only minimal set of genes show transcriptional changes with age, arguing against the idea of global, widespread misregulation of gene expression during aging (Ori et al., 2015; Stegeman & Weake, 2017).

How age-dependent changes in RNA levels are mediated is still largely unclear, although epigenetic alterations may play a key role. Increased histone H4K20 trimethylation, or H3K4 trimethylation, for example, were identified as epigenetic marker for aging (Han & Brunet, 2012). Furthermore, deacetylases of the Sirtuin family were recently identified as a class of epigenetic modulators that control longevity in mouse models (Kanfi et al., 2012; Mostoslavsky et al., 2006).

Proteomic studies

Proteomic studies based on quantitative mass spectrometry have been performed to assess global changes in protein levels in aging tissues. These studies revealed that although overall protein levels tend to be lower in aged samples, most proteins did not exhibit significant changes in their expression levels (Brown et al., 2018; Ori et al., 2015). In fact, aging was associated with increased fluctuations in protein amount and changes in the amount of restricted sets of proteins. Work performed in aging *Drosophila* heads, for example, showed that proteins involved in oxidative phosphorylation, and TCA cycle accumulate to higher level in aged flies, while proteasomal and ribosomal proteins showed age-dependent reduction in level (Brown et al., 2018). Furthermore, aging rat brain showed reduced expression of proteins involved in Calcium response, signal transduction, and ion channels, aging rat liver in contrary showed altered expression of proteins in metabolic pathways (Ori et al., 2015).

As changes in protein levels can result from changes in translation or proteostasis. Ribo-seq experiments were performed to detect ribosome-protected mRNAs, *i.e.*, mRNAs undergoing translation in samples of different age (Ingolia et al., 2009). Remarkably, these experiments have revealed that regulation of translation extensively contribute to the changes in expression levels observed upon aging. Part of these changes may be due to a reduction in the level of translation machinery components, as reduction in concentration of elongation and initiation factors, and aminoacylated tRNAs were reported in aging organisms (Anisimova et al., 2018; Anisimova et al., 2020).

Thus, increased variability of protein levels is a common feature of aging tissues, indicating a deregulated transcriptional and translational program. To date, the contribution of RNP granules to derailed cellular homeostasis remains elusive.

3.3. RNP granules and aging

Very few studies have addressed age-dependent changes in RNP granules and their functional significance. *In vitro* work has shown that assembled condensates transition from a liquid to a more solid-like state through a phenomenon termed “*in vitro aging*”. Indeed, *In vitro* purified RNP granule components such as FUS, hnRNPA1, Whi3, and other purified IDR-containing protein fractions were shown to undergo LLPS to form dynamic liquid droplets that transition over time into less dynamic entities with poor capacity to fuse (Feric et al., 2016; Ingolia et al., 2009; Lin et al., 2015; Molliex et al., 2015; Patel et al., 2015; Xiang et al., 2015; Zhang et al., 2015). Interestingly, addition of RNP components that co-assemble into condensates can either slow down or accelerate the process. For example, *in vitro* aging of the ALS-associated FUS

(P525L) variant was shown to be effectively prevented or reduced by the addition of hnRNPA1, EWSR1 or TAF15 (Figure 16) (Marrone et al., 2019).

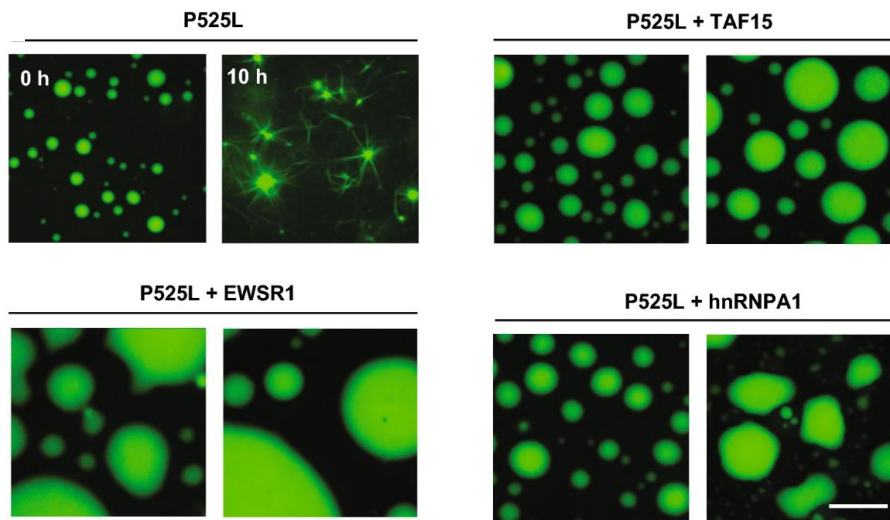


Figure 16: Interacting partners alter the liquid-to-solid transition of FUS ALS-variants.

The presence of FUS-interacting proteins such as TAF15, EWSR1, and hnRNPA1 inhibits the *in vitro* aging of FUS mutant. Image adapted from (Marrone et al., 2019).

A key observation made by *Rousakis et al.* in *C. elegans* showed how P-bodies respond to aging *in vivo*. Age-dependent accumulation of P-bodies was observed in *C. elegans* and this accumulation was suggested to have a protective role in aging worms as mutants for the PB component *dcap1* had shorter lifespan (Rousakis et al., 2014). Della and colleagues showed that two SG components, PAB-1 and TIAR-2, form solid-like aggregates as the *C.elegans* age and that worms with higher number of aggregates displayed reduced fitness. Remarkably, the solid-like properties of SGs in old worms could be reversed by blocking insulin signalling as shown in Insulin receptor (*daf2*) mutants (Lechler et al., 2017). However, the underlying cellular mechanisms as well as the consequences on gene expression have not been addressed.

To date, the link between aging and granule homeostasis is thus largely underappreciated and the following questions remain open: How do the age-dependent change in the composition of the cellular milieu affect the assembly and composition of RNP granules? What are the molecular mechanisms and pathway that regulate age-dependent changes in RNP granules, independently of disease state? What are the consequences of these changes on the translation of granule-associated mRNAs?

These questions are particularly relevant for neurons which heavily rely on local translation and mRNA transport, and in which age-related degeneration is linked to accumulation of abnormal RNP granules.

4. RNP granules found in *Drosophila* mushroom body neurons as a paradigm to study the impact of aging on RNP granule properties

To understand the effects of aging on the composition, material properties and functions of neuronal RNP granules, I sought to use RNP granules found in the mushroom body (MB) γ -neurons of *Drosophila* CNS as a paradigm.

4.1. *Drosophila* as a model for aging research

As multicellular organisms, invertebrate models offer the possibility to not only study cell autonomous effects of aging, but also to understand how intra-tissue and inter-organ communication impact on aging. A main advantage of these models is their relatively short life spans compared to their vertebrate counterparts. *C.elegans*, for instance, live approximately 3 weeks, *Drosophila* around 2 months, while African killifish lives for 6-8 months, mice and rats for approximately 3 years. Evolutionary conservation between pathways involved in aging is an added advantage to work in invertebrate systems. 77% of age-related genes in humans, indeed, are expressed in equivalent fly tissue (Figure 17) (Piper & Partridge, 2018). Functional conservation has also been shown, as mutants in conserved components of the Insulin pathways, for example, were shown to exhibit long life expectancy from worms (Friedman & Johnson, 1988), flies (Clancy et al., 2001; Tatar et al., 2001), mice (Holzenberger et al., 2003) to even humans (Anselmi et al., 2009).

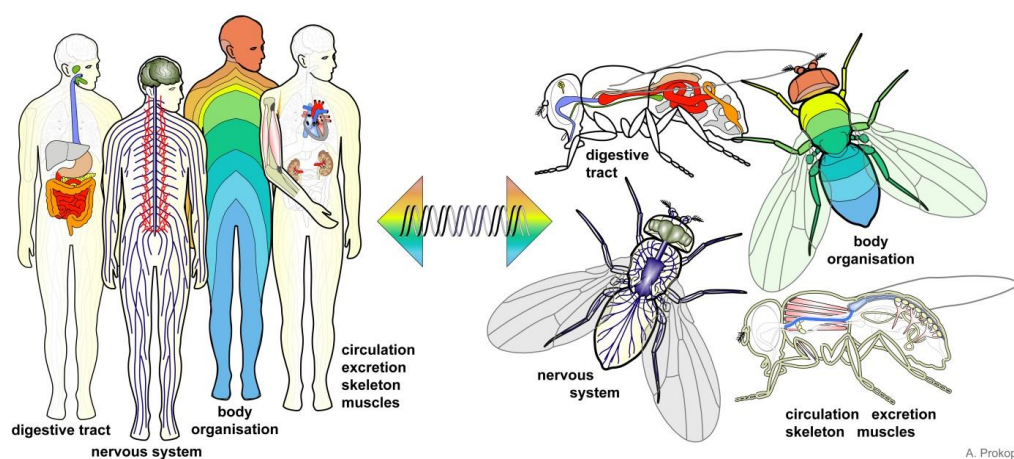


Figure 17: *Drosophila* as a model for aging research

Aging-related molecular pathways are highly conserved between flies and humans. For almost all organs in humans, flies have analogous counterparts that show age-dependent deterioration. Thus, flies can shed light onto the age-associated pathways in a multicellular, multiorgan context.

Image adapted from droso4schools.wordpress.com.

Drosophila appears as a model particularly suited for aging research. Collections of genetic tools including mutants, clone generation, two-component gene expression systems like Gal4/UAS or LexA/LexAOP, CRISPR reagents for genome editing are available for research (Del Valle Rodríguez et al., 2012), which has paved the way to a strong understanding of the genetic bases of aging. Furthermore, physiological parameters such as changes in fat and protein synthesis, stress resistance, reproductive capacity, physical activity, immunity, neuronal functions and behaviour can be used to monitor aging-related functional decline.

4.2 *Drosophila* mushroom body: centre for learning and memory

Mushroom bodies (MBs) or *corpora pedunculata* in insects are bilateral structures specialised in learning and memory and have thus been compared to the mammalian hippocampus (Akmal et al., 2006; Heisenberg, 2003). In *Drosophila*, each MB is composed of 2,500 neurons (also known as Kenyon cells, KCs), making them prominent structures of the fly brain neuropil (dense network of interwoven neurons) (Figure 18) (Heisenberg, 2003; Ito & Hotta, 1992). From dorsal to ventral, they consist of a shell of Kenyon cell bodies followed first by the cup-shaped calyx (composed of KC dendrites), then by the peduncle and finally by two orthogonal lobes composed of KC axons pointing vertically and medially (Figure 18). MBs host three distinct populations of neurons, whose formation is developmentally timed, namely γ , α'/β' , and α/β (Lee et al., 1999). γ -neurons in *Drosophila* undergo extensive remodelling during metamorphosis (Yu & Schuldiner, 2014), characterized by the pruning of larval axons followed the regrowth of adult axons; a process that depends on the transport of neuronal RNP granules (Medioni et al., 2014; Vijayakumar et al., 2019).

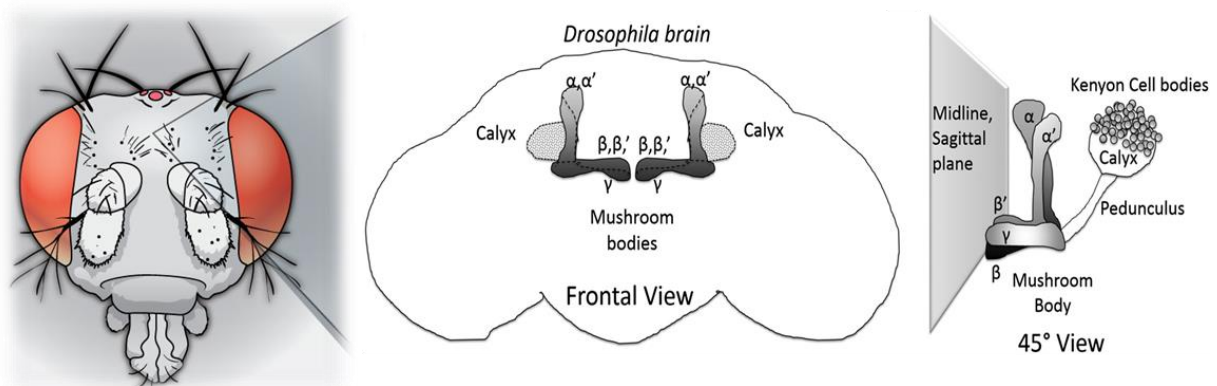


Figure 18: *Drosophila* mushroom body neurons

Mushroom bodies (MBs) are a pair of neuropils (dense network of interwoven neurons) found in the central brain of flies, each of which composed of 2,500 neurons (also known as Kenryon cells, KCs). MBs host three distinct types of neuronal populations, namely γ , α'/β' , and α/β . In a dorsal to ventral view, MBs consist of a shell of KC cell bodies followed by a cup-shaped calyx (group of dendrites), a peduncle and finally two orthogonally pointing lobes (vertical and medial). Images are adapted from (Dubnau, 2012; Schmidt & Sheeley, 2015).

Drosophila MBs were shown to be necessary for eliciting olfactory memory (McGuire et al., 2001). As demonstrated by pioneer experiments, indeed, flies lacking >90% of KCs were defective in displaying odour-dependent memory, while evoking normal response to naïve attractive or repulsive odours (Heisenberg et al., 1985). Through extensive studies using mutants and transgenic flies, a link between intracellular cAMP signalling and olfactory memory has been established in *Drosophila* (Figure 19) (DeZazzo & Tully, 1995), and later shown to have conserved function in learning and memory (Abel & Nguyen, 2008). Several genes of this pathway including cAMP phosphodiesterase (*dunce*) (Nighorn et al., 1991), adenylyl cyclase (*rutabaga*) (Levin et al., 1992), and cAMP-dependent kinase PKA (Drain et al., 1991) are preferentially expressed in MBs (Han et al., 1992) and required for olfactory memory (Davis, 2005). Furthermore, *amnesiac*, a gene homologous to the mammalian pituitary adenylate cyclase-activating peptide (PACAP), is required for activation of PKA in MBs, as well as for a specific form of mid-term olfactory memory termed *amnesiac*-dependent memory (Turrel et al., 2020). Interestingly, aging was shown to induce a specific decline in *amnesiac*-dependent memory (referred to as age-related memory impairment (AMI)) (Tamura et al., 2003), a phenotype suppressed by reducing the dosage of the PKA catalytic subunit *DCO* (Yamazaki et al., 2007). Thus, the cAMP pathway is essential in MB neurons for intact cognition, and tightly regulating its activity can counteract age-dependent memory deficits.

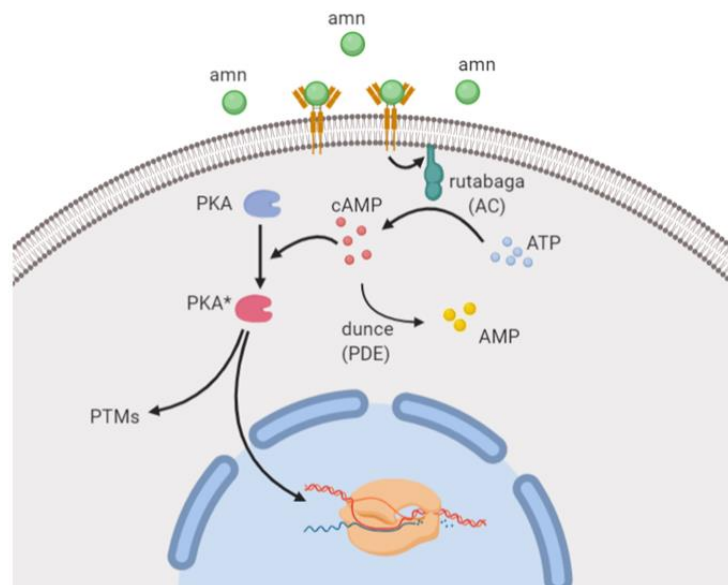


Figure 19: cAMP/PKA pathway in *Drosophila* mushroom body neurons

cAMP is a product of the cyclization reaction of ATP by the adenylyl cyclase, Rutabaga. The phospho diesterase Dunce is an enzyme that cleaves the ester bond in cAMP, producing AMP and maintaining the balance between production and removal of cAMP. cAMP is a major secondary messenger in cells. In MB neurons, cAMP activates PKA. Active PKA in turn can phosphorylate CREB to initiate transcription or phosphorylate several cytoplasmic target proteins. Amnesiac is homologous to the mammalian pituitary adenylate cyclase-activating peptide (PACAP) and is required for activation of PKA in MBs.

4.3. IMP: a highly conserved RNA binding protein

The VICKZ (acronym for the founding protein members) family of proteins is composed of highly conserved RBPs including human IGFII mRNA binding proteins (IGF2BP 1-3 or IMP 1-3), mouse *c-myc* coding region instability determinant binding protein CRD-BP, *Xenopus* Vg1RBP/Vera, chicken ZBP1, and *Drosophila* IMP (Degrauwe et al., 2016) (Figure 20A). Human IMP1 is orthologous to chicken ZBP1 with 95% identity (Ross et al., 1997), and the mouse CRD-BP with 99% identity (Doyle et al., 1998). IMP3 is orthologous to *Xenopus* Vg1RBP with 83% identity (Deshler et al., 1998; Havin et al., 1998). Invertebrate IMP homologues have also been identified in *Drosophila* (Nielsen et al., 2000) and *C.elegans* (accession #T23837). These proteins have six highly conserved RNA binding domains (two RRM and four KH domains) organized into 3 tandems (RRM1-2; KH1-2; KH3-4) (Figure 20B).

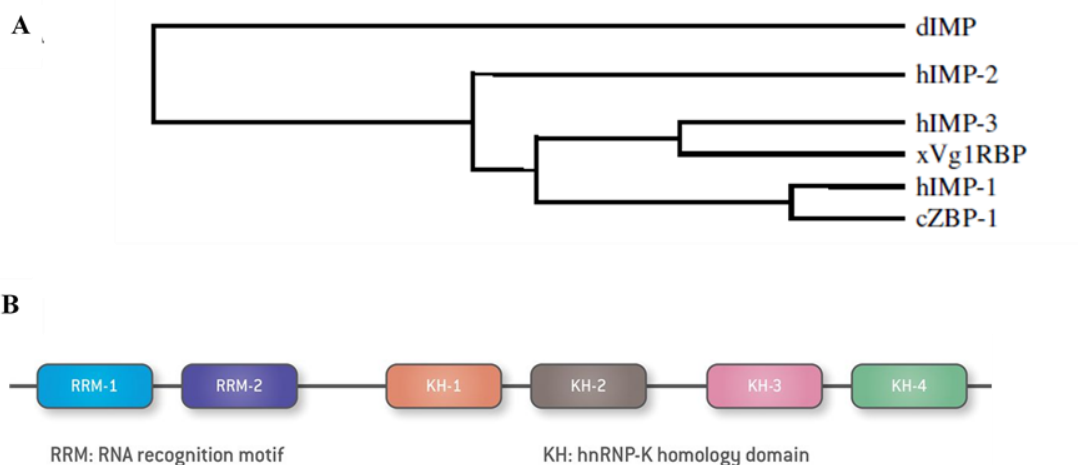


Figure 20: IMP is a highly conserved RNA binding protein

A. Unrooted dendrogram showing the evolutionary conservation of IMP in metazoans (Nielsen et al., 2000). **B.** Schematic representation of conserved RNA binding domains in IMP. Vertebrate IMP proteins have two N-terminal RNA recognition motifs (RRM-1 and RRM-2), followed by four K-homology domains (KH1-4) at the C-terminus. Image adapted from (Degrauwe et al., 2016).

IMP proteins play key roles in development and disease. IGF2BP1 knock-out mice, for example, have been shown to exhibit a high perinatal lethality accompanied by defective growth and impaired intestine development (Hansen et al., 2015). In *Drosophila*, *imp* is an essential gene whose loss of function is associated with larval lethality (Munro et al., 2006). Different physiological functions have been attributed to Imp proteins, mainly studied ones including functions in polarized cell migration and growth as well as functions in maintenance of stem cell

fate. In *Xenopus*, depletion of Vg1RBP resulted in impaired migration of neural tube roof plate cells and defective neural crest migration (Yaniv et al., 2003). In the developing nervous system, commissural axons in mouse mutants for ZBP1 exhibited guidance defects, entering ectopic locations in the ventral spinal cord (Lepelletier et al., 2017). Imp/ZBP1 function is also important for axonal regrowth in both developmental and adult context. Imp is required for the developmentally-controlled axon regrowth occurring during *Drosophila* CNS remodelling (Medioni et al., 2014). In adult sensory neurons, ZBP1 dosage modulate regrowth after axon severing (Donnelly et al., 2011). Imp has also been shown to have conserved functions in the control of stem cell renewal, in particular in the regulation of temporal changes in stem cell properties (Degrauwe et al., 2016). In *Drosophila*, for example, Imp governs the production of varied neuronal fates (Liu et al., 2015) and the decommissioning of neural stem cells (Yang et al., 2017). It also controls their growth and proliferation (Samuels et al., 2020). In human, IMP1 was shown to influence neural stem cell fates (Conway et al., 2016; Degrauwe et al., 2016). IMP1 expression is also upregulated in various types of cancer cells and is associated with poor prognosis in patients (Gu et al., 2004).

4.3.1. Regulatory functions of IMP on target mRNAs

IMP RNA interactome

IMP proteins show predominantly cytoplasmic localization (Wachter et al., 2013) and are known to bind target mRNAs with high affinity. Transcriptome-wide approaches using RIP-seq, UV-cross-linking and immunoprecipitation (iCLIP), photoactivatable ribonucleoside-iCLIP (PAR-iCLIP), and enhanced CLIP (eCLIP) have identified thousands IMP target RNAs in different model systems (Conway et al., 2016; Hansen et al., 2015; Huang et al., 2018; Jonson et al., 2007). Consistent with this, 1% of the HEK293 cell transcriptomes is represented in the IMP1 RNP granules (Jonson et al., 2007). As revealed by both transcriptomic analyses and RNA-specific studies, IMP proteins predominantly bind to *cis*-acting sequence elements, and 3'UTRs in particular. Human IMP1, for example, binds *H19* RNA *via* its 3'UTR (Runge et al., 2000), ZBP1 binds *β -actin* mRNA *via* its 3'UTR (Ross et al., 1997) so does Vg1RBP bind to *Vg1* mRNA (Doyle et al., 1998). RNA binding is primarily mediated by Imp KH domains whereas vertebrate RRM might contribute to the stabilization of RNA-protein complex (Nielsen et al., 2004; Wachter et al., 2013).

4.3.2. IMP regulates various aspects of RNA expression

Depending on cell types and/or RNA targets, IMP has been shown to regulate different aspects of RNA fate, ranging from control of RNA localization and translation to control of stability.

IMP binding inhibits translation of target RNAs

Binding of hIMP1 to IGF-II mRNA inhibits its translation (Nielsen et al., 1999). *β-actin* transcripts are translationally silent when bound by ZBP1 as shown in cultured neurons (Huttelmaier et al., 2005). Translational repression could partially be achieved by excluding translation initiation factors and ribosomal subunits, for example, IMP1 interactome in HEK293 cells indicate the absence of key initiation factors and 60 S ribosomes (Jonson et al., 2007).

IMP binding promotes the transport of RNA molecules

In chicken, ZBP1 was shown to bind a 54-nucleotide zipcode in the 3'UTR of *β-actin* mRNA (Ross et al., 1997), resulting in the transport of transcripts to regions of polarized cell growth in fibroblasts (Farina et al., 2003) and neurons (Huttelmaier et al., 2005; Tiruchinapalli et al., 2003). Consistent with their role in mRNA transport, IMP and orthologs were shown to associate with cytoskeletal motor proteins such as Kinesins, MyoVa etc., thus likely helping in transporting RNP granules by hooking RNA complexes to intracellular transport machineries (Calliari et al., 2014; Urbanska et al., 2017).

IMP binding stabilizes bound RNA molecules

Apart from functions in transport and local translation, association of mRNA with IMP can also be important for the stabilization of RNAs, as shown for *c-myc*, *βTrCP1*, and *CD44* mRNAs binding to murine CRD-BP (Lemm & Ross, 2002; Noubissi et al., 2006; Vikesaa et al., 2006). In case of *c-myc*, mRNA stabilization is mediated by CRD-BP through inhibition of mRNA degradation by polysome-associated endonucleases (Sparanese & Lee, 2007). IMP has also been proposed to regulate RNA stability by blocking miRNA function. IMP3 RNP complexes, for example, contain *let-7* miRNA targets and IMP3 overexpression showed a general upregulation of miRNA-regulated transcripts (Jonson et al., 2014). This observation suggested that IMP3 RNP granules act as safehouses for mRNAs against miRNA silencing.

4.3.3. dIMP: *Drosophila* homolog of IMP

The *Drosophila* genome hosts only one gene coding for IMP, dImp (Nielsen et al., 2000). dIMP lacks the two RRM RBDs found in its vertebrate homologs but shows 47% sequence conservation in the region coding the four conserved KH domains (KH1-4) (Nielsen et al., 2000). dIMP has an intrinsically disordered glutamine-rich C-terminal tail (or PLD), which is absent in vertebrate IMP (Vijayakumar et al., 2019) (Figure 21A). In flies, like in vertebrates, dIMP has a biphasic expression, with the initial maternally deposited pool of *dImp* mRNA being degraded at the end of embryonic stage 4, followed by a re-expression of *dImp* in developing CNS (Nielsen et al., 2000). dIMP is cytoplasmic and is recruited into RNP granules found in germ cells, neurons and S2R cells (Figure 21B-D). One of the first evidence for dIMP forming RNP granules in neurons came from the study by Medioni and colleagues, in which they showed that dIMP is present in

RNP granules colocalizing with *profilin* mRNA (Medioni et al., 2014). Notably, dIMP granules are found in MB neurons not just during development but are also present throughout adult life. To date, the regulation of dIMP granules in aging brains and their potential functions are however still unclear.

To identify dIMP RNA targets, Hansen and colleagues performed iCLIP-seq in S2R cells, revealing that dIMP binds to a vast repertoire of mRNAs. dIMP binding sites were enriched in the 3'UTRs on these mRNAs, and GO analysis showed that several of these mRNAs were coding for F-actin regulators including *profilin* (*chickadee*), *cdc42*, or *moe* (Hansen et al., 2015). In concordance with these data, RNP immunoprecipitation and sequencing (RIP seq) performed on larval brain lysates led to the identification of more than 300 mRNA targets for dIMP (Samuels et al., 2020).

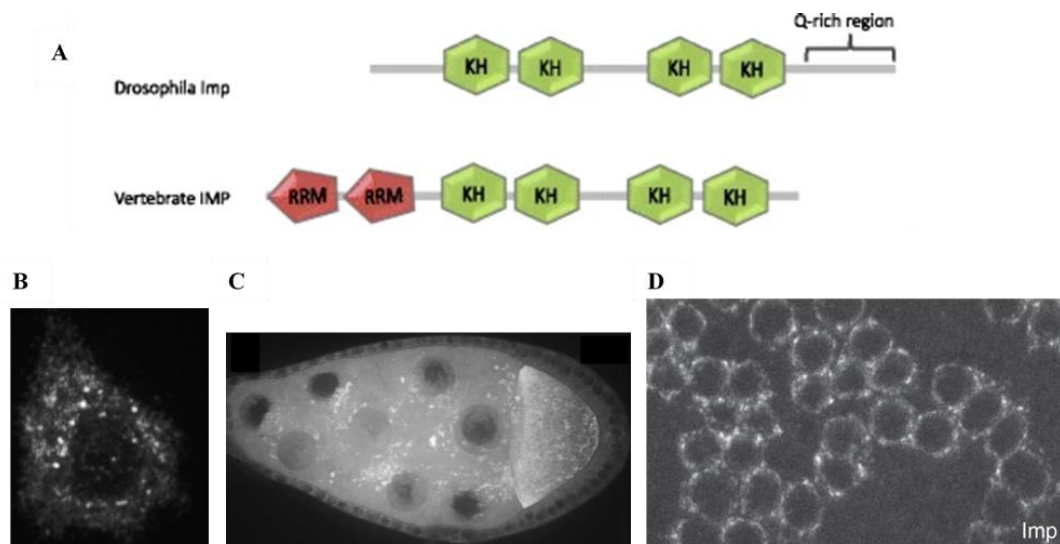


Figure 21: *Drosophila* IMP (dIMP) is cytoplasmic and forms nanometer sized RNP granules

A. Schematic representation of dIMP and comparison to vertebrate homologs. dIMP contains the four conserved KH-domains but lacks the N-ter RRM domains found in the vertebrate protein. It also has an additional Q-rich region (Prion-like domain) in its C-ter (Hansen et al., 2015).

B-D. dIMP distribution is cytoplasmic and forms cytoplasmic foci. Representative examples of dIMP granules found in S2R cells (**B**) (Hansen et al., 2015), oocyte (**C**) (Boylan et al., 2008), and MB neurons (**D**) (Vijayakumar et al., 2019).

4.4 Me31B/DDX6: a highly conserved RNA helicase

4.4.1 DDX RNA helicases

DEAD-box protein 6 (DDX6) belongs to the highly conserved DDX RNA helicase protein family found in organisms ranging from viruses or bacteria to humans (Ostareck et al., 2014) (Figure 22). Human DDX6 is 63.9% identical to yeast Dhh1p, 69.2% to *C.elegans* CGH-1, 67.5% to *Drosophila* Me31B, 94.4% to *Xenopus* Xp54, and 97.7% to mouse mRCK (Ostareck et al., 2014). Proteins belonging to DDX RNA helicase family share nine highly conserved motifs involved in ATPase and helicase activities (Linder et al., 1989; Tanner et al., 2003). Among those, motif-II, composed of Asp-Glu-Ala-Asp (D-E-A-D), gave its name to the protein. Together, these conserved motifs showed very little variation throughout evolution. DEAD box confers DDX6 with its ATPase activity while other motifs are necessary for ATP binding and hydrolysis, and for RNA binding (Linder, 2006). Since their discovery, more than 500 proteins were found to have the signature motifs of DDX family, making them key components of life (Silverman et al., 2003).

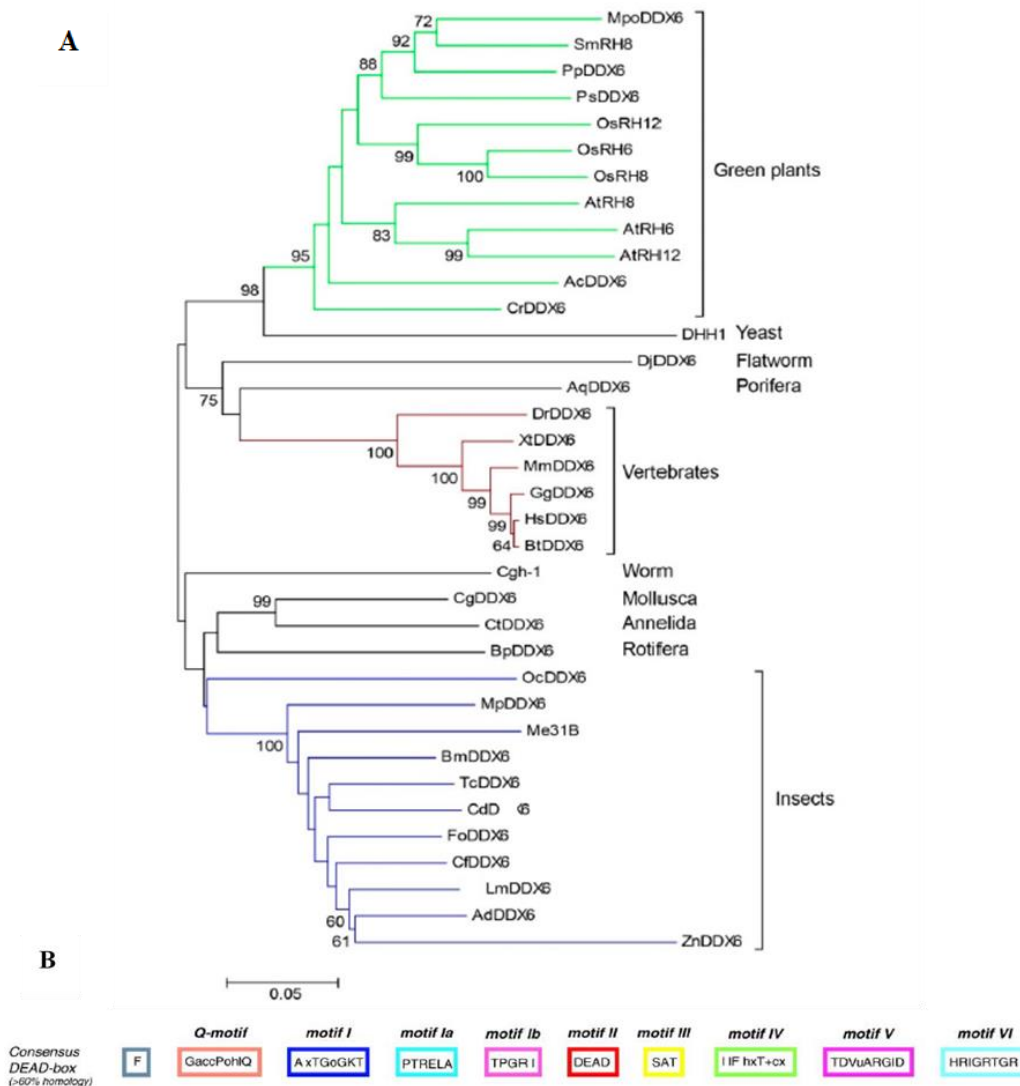


Figure 22: DDX6/Me31B is a highly conserved RNA helicase

A. Phylogenetic tree for DDX6 showing the extend of evolutionary conservation across different phyla. Image adapted from (Wang et al., 2021). **B.** Conserved motifs in the DEAD-box and related family of RNA helicases. Image adapted from (Cordin et al., 2006).

DDX family members work as RNA helicases or RNAPases. Rather than being processive helicases, DEAD-box proteins may take up the role of RNA “chaperones”, ensuring proper RNA structure through local RNA unwinding, or of RNAPases by tuning RNA–protein interactions (Fairman et al., 2004; Jankowsky et al., 2001; Schwer, 2001). DDX RNA helicases were shown to regulate every facet of RNA metabolism including transcription, splicing, transport, translation, and decay. For example, 15 out of 25 DDXs in yeast are shown to regulate ribosome biogenesis (Rocak & Linder, 2004); DDX20/DP103 are transcriptional repressors in mammalian cells (Gillian & Svaren, 2004; Yan et al., 2003); human DDX3 was shown to be necessary for translation initiation (Lee et al., 2008). DDX6 proteins, including yeast Dhh1p (Tseng-Rogenski et al., 2003) have been identified as core PB components (Hubstenberger et al., 2017). In *C.elegans*, CGH-1 containing granules termed P-granules and storage bodies were identified as warehouses of translationally silent mRNAs (Boag et al., 2008).

4.4.2 Me31B: *Drosophila* ortholog of DDX6

Drosophila genome has only a single gene homologous to DDX6, expressed from the chromosomal locus 31B, namely Me31B (de Valoir et al., 1991). Like its vertebrate homologs, Me31B has a conserved ATP binding site and RNA helicase domain (Figure 23A). Me31B was shown to be recruited into RNP granules found in germ cells and in neurons (Figure 23B-D) (Hillebrand et al., 2010; Nakamura et al., 2001). During oogenesis, Me31B localizes in cytoplasmic RNP granules and silences the translation of transported mRNAs *osk* and *BicD*, as evidenced by fluorescence *in situ* hybridization (FISH) and immunostaining (Nakamura et al., 2001). An *in vivo* proteome analysis of *Drosophila* germ granules identified binding partners of Me31B including the RNA regulatory proteins like Cup, Tral, Edc3, and motor proteins such as Klc, and Khc (DeHaan et al., 2017). Furthermore, functional studies have shown that the translation repression of Me31B is mediated through a factor called Cup, to which Me31B interacts *via* the adaptor Trailer hitch (Tral) (Nakamura et al., 2004; Tritschler et al., 2008). Cup competes with eIF4G for binding to cap-bound eIF4E, thus preventing the recruitment of translation initiation factors (Kinkelin et al., 2012; Nelson et al., 2004).

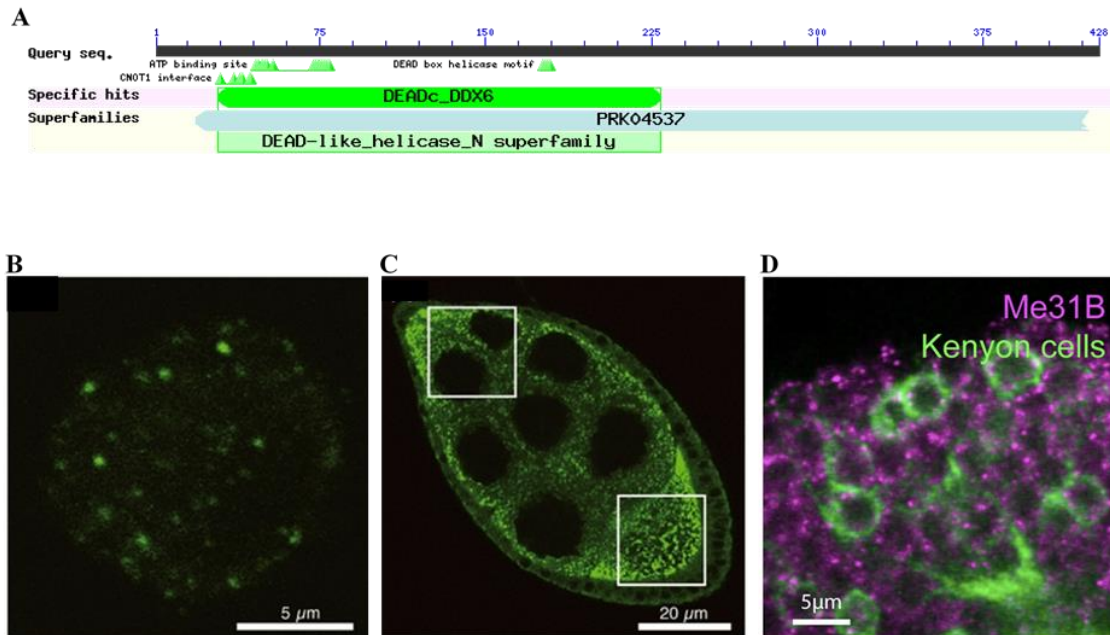


Figure 23: *Drosophila* Me31B forms cytoplasmic foci.

A. Schematic representation of conserved ATP-binding site and DEAD-box helicase domain in *Drosophila* Me31B (rendering using NCBI conserved domain search).

B-D. Me31B is cytoplasmic and assembles into RNP granules. Representative examples of Me31B granules found in S2R cells (**B**) (Kato & Nakamura, 2012), oocytes (**C**) (Kato & Nakamura, 2012), and MB neurons (**D**) (Hillebrand et al., 2010).

Me31B in *Drosophila* has also been involved in RNA decay. Me31B interacts with the decapping complex *via* the adaptor proteins CNOT1, EDC3, and HPat (Pat1) (Chen et al., 2014; Haas et al., 2010; Jonas & Izaurralde, 2013). In addition, Tral can directly interact with the decapping complex protein Dcp1, thus in the absence of Cup, Me31B can initiate decay pathway (Tritschler et al., 2008). Thus, Me31B can generally be considered as a repressor, whose repressive mode depends on biological context and partners. For example, it was shown that Me31B forms complex with eIF4E, Cup, Tral, and PABP during oogenesis and early embryonic stage, silencing translation of target mRNAs. During maternal-to-zygotic transition (MZT), the abundance of eIF4E, Cup, and Tral fall, triggering the degradation of Me31B- bound mRNAs (Wang et al., 2017).

4.5. Imp and Me31B/DDX6 in neuronal granules

Both dIMP/ZBP1 and Me31B/DDX6 accumulate in neuronal RNP granules in vertebrates and invertebrates. In vertebrates, ZBP1 has long been identified as a major component of neuronal RNP granules containing β -actin and transported to axons (Donnelly et al., 2011; Leung et al., 2006; Zhang et al., 2001) and dendrites (Huttelmaier et al., 2005; Tiruchinapalli et al., 2003; Urbanska et al., 2017). In *Drosophila*, dIMP localizes in granules that are transported to the axons of MB γ -neurons along MT tracks in a developmentally regulated manner, from metamorphosis onwards (Medioni et al., 2014). This process requires the function of dIMP PLD (Vijayakumar et al., 2019).

Vertebrate DDX6 was found to localize in punctated structures in the dendrites of cultured hippocampal neurons (Miller et al., 2009; Zeitelhofer et al., 2008). These granules were not homogenous as only a subset contained the Dcp1 protein (Miller et al., 2009). In *Drosophila*, Me31B was found to co-localize with Staufen- and FMRP-containing granules found in cultured motor neurons (Barbee et al., 2006) and to localize in postsynaptic foci in MB and projection neurons (Hillebrand et al., 2010).

Remarkably, the regulation and function of dIMP and Me31B-containing RNP granules has been mainly studied in developmental contexts. Although these granules are found in neurons throughout adult life, little is known about the changes they may undergo upon aging or their physiological role in a healthy aging organism.

5. Aim of thesis

Previous studies have shown that the material properties of RNP granules are highly sensitive to biomolecular composition. Physico-chemical properties of cells vary with time and how RNP granules respond in a physiological cellular aging context remains largely unexplored. The main objectives of my thesis were:

i) to understand how neuronal RNP granules are affected by aging in vivo

To address the effects of aging on neuronal RNP granules, I sorted to analyse the properties of *Drosophila* RNP granules characterized by the presence of IMP and Me31B in two age groups of flies, young (2-days) and old (35-39 days, past mid-age). I chose the RBP IMP, and the DEAD-box helicase Me31B as markers of neuronal RNP granules because they are highly conserved RBPs abundant in neurons, known to form RNP granules in the soma of *Drosophila* MB neurons. To monitor the changes in material properties of these RNP granules, I imaged them combining high-resolution imaging with quantitative analysis.

ii) to assess whether age-associated changes in neuronal RNP granules alter the expression of target mRNAs,

To this end, I monitored the translation of reporter RNAs associating (or not) with neuronal RNP granules. I particularly studied the translation of *profilin*, a direct RNA target of Imp bound through its 3'UTR (Medioni et al., 2014)

iii) to identify the aging-related molecular pathways that are responsible for neuronal RNP granule remodelling.

To identify the molecular pathways involved in aging-dependent RNP granule remodelling, I performed a candidate-based RNAi screen testing for the function pathways known from the literature to regulate aging or be deregulated upon aging.

Chapter II

Results

6. Summary of results

Neuronal RNP granules progressively remodel upon aging and their associated mRNAs get translationally silenced.

To understand how neuronal RNP component composition is regulated in a physiological context, I sought to monitor the impact of aging on neuronal RNP granules. I first analysed the subcellular distribution of two conserved components of neuronal RNP granules, IMP and Me31B, in *Drosophila* flies of different ages: 2 days post eclosion (young) and 35-39 days post eclosion (old). A progressive increase in the condensation of IMP and Me31B into granules was observed upon aging. Whereas IMP was preferentially cytoplasmic in young neurons, it relocates into granules in old cells. Me31B localized in numerous small granules in young cells and in larger less numerous ones as age increased. Notably, the large condensates observed in old neurons do not correspond to static protein aggregates; first these granules did not colocalize with aggregation markers such as p62 or Ubiquitin, second, the granule components exhibited similar recovery rates in both young and old cells when assessed using FRAP. Furthermore, age-dependent condensation of RNP components in neurons is not a general trend as RNA binding proteins such as PABP or Rin did not show any difference in distribution.

To assess the functional impact of age-dependent RNP granule remodelling on mRNA expression, I analysed the translation profiles of *profilin*, which is a target mRNA of IMP, in young and old neurons. Using inducible reporters in which the coding sequence of EGFP was fused to the 3'UTR of *profilin*, or to a non related 3'UTR (*sv40*), I could demonstrate that *profilin* translation decreases upon aging. This result is in accordance with the observed reduction in endogenous Profilin protein, but not RNA, expression. Notably, the translation of reporters depleted from granules (EGFP-*camkII* 3'UTR and EGFP-*eIF4E* 3'UTR) did not decrease upon aging, whereas the translation of another granule-enriched mRNA, *cofilin*, did. Thus, these results revealed that age-dependent remodelling of neuronal RNP granules is associated with an increased translational repression of associated mRNAs.

Age-dependent remodeling of neuronal RNP granules associates with reduced sorting specificity and depends on Me31B stoichiometry.

High resolution imaging of neuronal RNP granules revealed that age-dependent condensation of Imp and Me31B was also associated with a loss of granule population heterogeneity. While two populations of Me31B⁺ granules were observed in young neurons (Me31B⁺IMP⁻ and Me31B⁺IMP⁺), the majority of Me31B⁺ granules found in old neurons contained IMP. To understand the contributions of IMP and Me31B in age-dependent remodelling of neuronal RNP granules, I inactivated both genes after eclosion *via* dsRNA-mediated knockdown. Interestingly, *me31b* knockdown blocked the assembly of IMP into RNP granules, without altering overall IMP protein levels. The converse was not true, as *imp* inactivation did not affect Me31B recruitment to RNP granules. These data suggested that Me31B behaves as a nucleator whose concentration may regulate the assembly and composition of RNP granules. Consistent with this model, I found that Me31B protein concentration increases upon aging. By genetically reducing the dosage of *me31b* using deletion mutants, I further showed that age-dependent remodelling of Me31B granules is suppressed in this context.

Remarkably, IMP recruitment into granules was only partially affected upon reducing the dosage of Me31B and translational repression of reporters was not affected, indicating the existence of an additional regulatory pathway regulating these processes.

PKA signalling acts as an additional regulatory pathway regulating IMP recruitment and translational repression.

Through a candidate RNAi screen, I identified the PKA pathway as a regulator of age-dependent neuronal RNP granule condensation. Blocking this pathway by expressing a kinase dead variant of the PKA catalytic subunit, or dsRNA targeting the PKA catalytic subunit, strongly suppressed age-dependent condensation of IMP. This however only mildly affected Me31B condensation, indicating that PKA differentially regulates the behaviour of distinct RNP granule components. Still, inhibiting PKA induced the translational derepression of IMP target mRNAs in aged brains, indicating that the recruitment of IMP into condensates may mediate translational repression.

Taken together, my results uncovered that IMP/Me31B neuronal RNP granules undergo extensive remodelling upon aging. Such an age-dependent RNP granule remodelling is associated with the translational repression of target mRNAs. The compositional changes observed during aging depends on the stoichiometry of the core protein Me31B. Furthermore, PKA pathway acts an additional regulatory layer that promotes the recruitment of IMP and its target RNAs to neuronal RNP granules and translational repression (Figure 24).

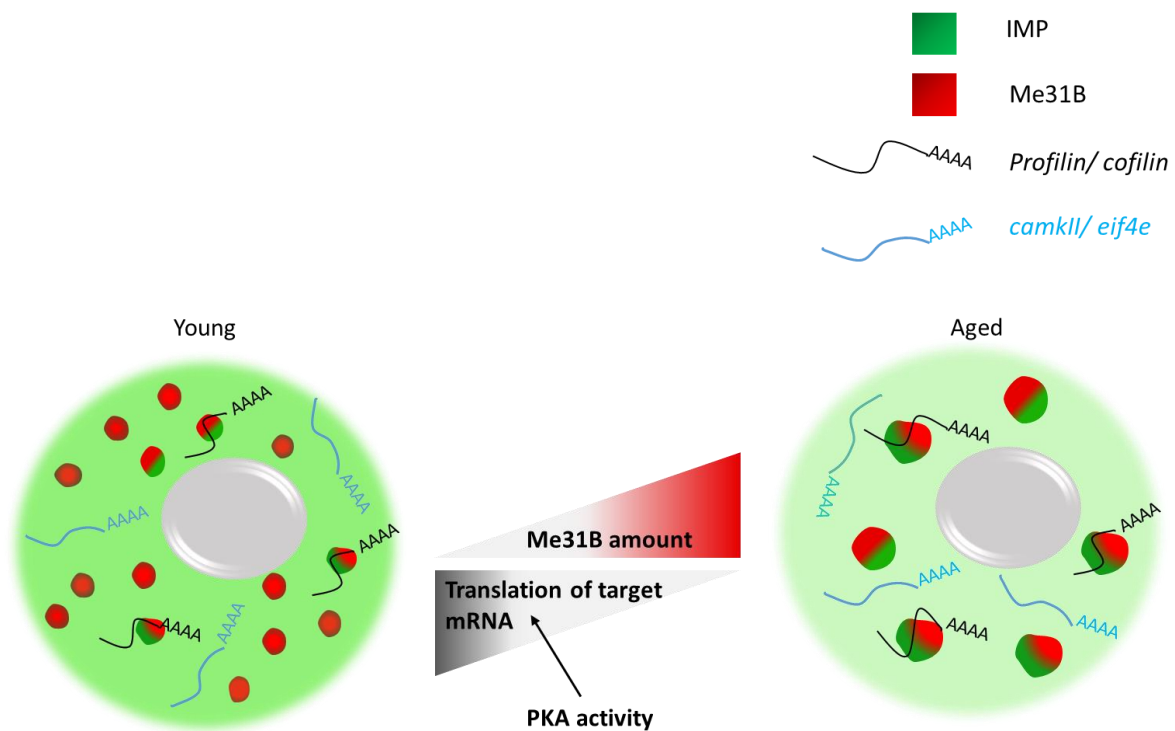


Figure 24: Model illustrating age-dependent changes in neuronal RNP granule properties

IMP/Me31B RNP components RNP granules extensively remodel to form large granules in aged *Drosophila* brains. Age-associated condensation of Me31B and Imp is accompanied by a reduced specificity of sorting: while two populations of Me31B+ granules are observed in young neurons (Me31B+IMP- and Me31B+IMP+), the majority of Me31B+ granules found in old neurons contain IMP. Increased condensation is also associated with the specific translational silencing of granule-associated mRNAs (*e.g. profilin*). Functionally, two main factors regulate the observed age-dependent changes: increased stoichiometry of the DEAD-box helicase Me31B promotes the coalescence of smaller granules and loss of heterogeneity, and PKA kinase activity regulates IMP recruitment and translational repression.

These results are presented in more detailed in the following research article.

7. Manuscript

Increased helicase dosage and PKA induce the coalescence of RNP components in aging *Drosophila* brains

Kavya Vinayan Pushpalatha¹, Fabienne De Graeve¹, Akira Nakamura² and Florence Besse^{1,3}

1: Université Côte d'Azur, CNRS, Inserm, Institut de Biologie Valrose, Nice, France

2: Department of Germline Development, Institute of Molecular Embryology and Genetics, and Graduate School of Pharmaceutical Sciences, Kumamoto University, Kumamoto, Japan

3: correspondence: Florence.BESSE@univ-cotedazur.fr

7. Manuscript

Increased helicase dosage and PKA induce the coalescence of RNP components in aging *Drosophila* brains

Kavya Vinayan Pushpalatha¹, Fabienne De Graeve¹, Akira Nakamura² and Florence Besse^{1,3}

1: Université Côte d'Azur, CNRS, Inserm, Institut de Biologie Valrose, Nice, France

2: Department of Germline Development, Institute of Molecular Embryology and Genetics, and Graduate School of Pharmaceutical Sciences, Kumamoto University, Kumamoto, Japan

3: correspondence: Florence.BESSE@univ-cotedazur.fr

7.0. Abstract (125 words max)

Cytoplasmic RNP condensates enriched in mRNAs and proteins are found in various cell types and associated with both buffering and regulatory functions. While a clear link has been established between accumulation of aberrant RNP aggregates and progression of aging-related neurodegenerative diseases, the impact of physiological aging on neuronal RNP condensates has never been explored. Here, we uncovered that RNP components progressively coalesce into large and less diverse condensates in the aging *Drosophila* brain. Increased coalescence reflects specific changes in the levels of the conserved RNP scaffold Me31B/DDX6 and requires PKA kinase activity. Furthermore, increased recruitment of specific mRNAs to RNP condensates is associated with their translation repression, identifying cytoplasmic RNA-protein condensation as a novel post-transcriptional mechanism underlying age-dependent changes in gene expression.

7.1. Introduction

Formation of membrane-less condensates enriched in functionally related biological molecules has recently emerged as a major principle enabling dynamic cell compartmentalization (Alberti 2017b). Because they can rapidly, selectively and reversibly concentrate molecules, biological condensates are very effective in both buffering intracellular fluctuations and flexibly regulating molecular reactions in response to physiological or environmental changes (Alberti 2017b; Banani et al. 2017; Shin and Brangwynne 2017). Ribonucleoprotein (RNP) condensates (or granules) are defined by their enrichment in RNA molecules and regulatory proteins such as RNA binding proteins or RNA helicases. They have been observed in the cytoplasm of a variety of species and cell types (Voronina et al. 2011; Buchan 2014; De Graeve and Besse 2018; Formicola et al. 2019; Trcek and Lehmann 2019; Cohan and Pappu 2020; Riggs et al. 2020), and linked to functions ranging from RNA storage and decay to spatiotemporal control of RNA translation and localization (Decker and Parker 2012; Buchan 2014; Wang et al. 2018; Formicola et al. 2019; Riback and Brangwynne 2020).

Extensive recent work has been performed to unravel the molecular principles underlying RNP condensate assembly and dynamic regulation. Studies performed in *in vitro* reconstituted systems, on one hand, have revealed that purified RNAs and/or proteins condensate into droplets through liquid-liquid phase separation, a process critically dependent on both component concentration and the establishment of dense networks of protein-protein and protein-RNA interactions (Alberti 2017a; Mittag and Parker 2018; Protter et al. 2018; Van Treeck and Parker 2018). Studies performed in living cells, on the other hand, have shown that cytoplasmic RNP condensates exhibit in normal conditions properties expected from liquid-like entities, including high component turnover as well as inter-condensate fusion and mixing of components (Brangwynne et al. 2009; Hyman et al. 2014; Kroschwald et al. 2015 ; Patel et al. 2015; Gopal et al. 2017; Shin and Brangwynne 2017).

As further revealed by proteomic and transcriptomic analyses, endogenous RNP condensates have a complex composition characterized by the presence of up to dozens of

proteins and RNA molecules (Fritzsche et al. 2013; Jain et al. 2016; Hubstenberger et al. 2017; Khong et al. 2017; Markmiller et al. 2018; Youn et al. 2019). These molecules are not all functionally equivalent: while a limited number of resident molecules, referred to as scaffolds, are required for the nucleation of RNP condensates, others, termed clients, are dispensable and recruited in a context-dependent manner (Banani et al. 2016; Ditlev et al. 2018). Interestingly, systematic comparison of RNP granule content has also revealed that distinct RNP entities contain both unique and shared components. In neuronal cells, collections of RNP granules with both distinct and overlapping composition have been identified through high-resolution imaging (Cougot et al. 2008; Mikl et al. 2011; De Graeve and Besse 2018; Formicola et al. 2019) (De Graeve, Formicola, Pushpalatha et al., method chapter submitted) or biochemical purification (Fritzsche et al. 2013). Together, these studies thus raise the following questions: how is the molecular specificity of each condensate encoded? how is the differential recruitment of RNP components regulated in different physiological contexts? Frameworks have recently been proposed to explain both the nucleation of multicomponent condensates and the differential sorting of their constituents (Langdon et al. 2018; Kim et al. 2019; Sanders et al. 2020). In these frameworks, competition between RNA and protein interaction networks is a key driver of differential sorting, such that increasing the dosage of highly interconnected components can trigger the miscibility of initially distinct entities. Post-translational modifications of RNP components also play a key role, by either promoting or inhibiting the differential recruitment of client molecules through changes in affinity and/or valency of interactions (Hofweber and Dormann 2018; Kim et al. 2019; Snead and Gladfelter 2019; Gerbich et al. 2020). Whether and how these principles are integrated *in vivo* for the regulation of constitutive RNP condensates, and whether they are used in biological systems to modulate RNP granule assembly and composition in response to physiological stimuli has however remained largely unclear.

We addressed this question by analyzing the properties of neuronal RNP granules during the aging process. Although various studies have correlated the progression of age-related neurodegenerative diseases with the accumulation of RNP aggregates with aberrant stability and/or composition (Li et al. 2013; Ramaswami et al. 2013; Bowden and Dormann 2016), these

studies mostly used mutant variants and/or analyzed advanced disease stages and thus did not address the impact of physiological aging on RNP condensates. Here, we show in *Drosophila* brains that cytoplasmic RNP components progressively condensate into large granules distinct from pathological aggregates upon aging. Increased condensation is accompanied by a decreased specificity of RNP granule component sorting. Combining quantitative imaging and genetics, we further uncovered that age-dependent coalescence of RNP components is regulated by two main factors: an increase in the stoichiometry of the conserved DEAD-box helicase Me31B/DDX-6/Rck1 and activity of the conserved kinase PKA. These two regulatory processes differentially act on RNP components as Me31B dosage mainly influences Me31B condensation while PKA mainly impacts of Imp condensation. Finally, we demonstrate using translational reporters that age-dependent remodeling of RNP granules associates with increased repression of granule-associated mRNA translation. Together, this work clearly illustrates how biological systems can physiologically regulate the main parameters underlying condensate assembly and composition to regulate the fate of associated mRNAs. This study also provides the first functional demonstration that aging, independently of associated diseases, impacts on the *in vivo* properties and function of constitutive RNP condensates, opening new perspectives on the regulation of gene expression in the context of aging brains.

7.2. Results

Increased condensation of neuronal RNP components upon aging

To monitor the impact of physiological aging on neuronal RNP granule properties, we first analyzed the subcellular distribution of granule markers in *Drosophila* brains of two different ages that we subsequently refer to as “young” and “aged” respectively: 2-days post-eclosion (*i.e.* right after the extensive neuronal maturation occurring upon eclosion) and 35-39 days post-eclosion (*i.e.* at about mid-life, before significant drop in viability). The DEAD-box helicase Me31B/DDX-6/Rck-1 and the RBP Imp/ZBP-1/IGF2BP were chosen as markers, as both are conserved RNA-associated proteins known to localize to RNA-containing granules in vertebrate and invertebrate neurons (Tiruchinapalli et al. 2003; Leung et al. 2006; Miller et al. 2009;

Hillebrand et al. 2010; Vijayakumar et al. 2019; Tang et al. 2020). In *Drosophila*, Me31B-positive and Imp-positive cytoplasmic RNP granules have previously been described in the soma of Mushroom Body γ neurons, a population of neurons essential for learning and memory functions (Keene and Waddell 2007; Keleman et al. 2007; Akalal et al. 2010; Hillebrand et al. 2010; Vijayakumar et al. 2019). In young brains, indeed, we observed that endogenous Me31B and Imp accumulate into numerous small cytoplasmic punctate structures (Figure 1A,C), a distribution recapitulated in Me31B-GFP and GFP-Imp knock-in lines (Figure 1E,G). Remarkably, these two proteins displayed very different partitioning properties at this stage. Me31B was mostly found in granules (Figure 1A,E), exhibiting a high partition coefficient calculated as the intensity ratio between the granule-associated and the soluble cytoplasmic pools (Figure 1K). In contrast, a significant fraction of Imp also localized diffusively throughout the cytoplasm (Figure 1C,G), as illustrated by the lower partition coefficient (Figure 1K). In aged brains, a dramatic re-localization of Me31B and Imp was observed, manifested by an increased clustering of these proteins into large granules (Figure 1B,D,F,H,L). Condensation of RNP components was characterized by a significant increase in the partition coefficient of both Me31B and Imp (Figure 1N), and was particularly visible for Imp whose diffuse cytoplasmic signal strongly decreased (Figure 1D,H). It also translated into a decreased number of Me31B-containing granules (Figure 1M), and a concomitant increase in the number of Imp-containing granules detectable over the cytoplasm (Supplementary Figure S1A and Figure 4E). To determine if the observed re-localization reflected an abrupt, or rather a more gradual change in RNP component distribution, we next analyzed brains at three additional time points after eclosion: 10 days, 20-23 days and 50-52 days. As shown in Figure 1O and Supplementary Figure S1A, a gradual and continuous clustering of Imp was observed from 2 days to 50 days post-eclosion, arguing against a sudden switch in behavior.

To then test if the re-distribution of Me31B and Imp observed upon aging reflects a general trend, we analyzed the localization of other conserved neuronal granule components including Trailer-hitch/Lsm-14 (Tral), HPat1 and Staufen (Stau) (Kohrmann et al. 1999 ; Cougot et al. 2008; Zeitelhofer et al. 2008). As observed for Me31B and Imp, these proteins clustered into larger cytoplasmic granules upon aging (Supplementary Figure S1B-G). Clustering,

however, was not observed for stress granule components such as Rin (Figure 1I,J) or PABP (Supplementary Figure S1H,I), indicating first that not all RNA binding proteins tend to cluster upon aging, and second that large granules do not correspond to entities forming in response to increasing stress.

The large neuronal RNP granules observed in aged brains do not correspond to static protein aggregates.

Protein aggregates have been observed in brains of aged animals and human patients in response to altered proteostasis (Lord et al. 2020). To determine if the large granules observed in aged brains correspond to dysfunctional protein aggregates, we first performed co-localization experiments using antibodies recognizing p62/Ref(2)P and Ubiquitin, both known to accumulate in protein aggregates forming in aged flies (Nezis et al. 2008). As shown in Figure 2A and B, p62⁺ and Ubiquitin⁺ aggregates were visible in aged brains, but did not co-localize with the large Imp-positive granules found at this age. To further ensure that these granules contain RNA, we performed smFISH experiments with probes recognizing *profilin* mRNA, that we previously identified as a direct target of Imp (Medioni et al. 2014). As shown in Figure 2C-C'' (arrowheads), *profilin* transcripts could be found in large Imp-positive granules in aged brains, further indicating that these entities correspond to *bona fide* neuronal RNP granules.

In *in vitro* reconstituted systems, RNP droplets mature over time into less dynamic entities (Patel et al. 2015; Alberti and Hyman 2016; Conicella et al. 2016). To test if *in vivo* physiological aging is associated with changes in the turnover of RNP granule components, we performed FRAP experiments on intact young and aged brains and compared fluorescent signal recovery upon bleaching Me31B-GFP⁺ or GFP-Imp⁺ granules. Remarkably, the two RNP components exhibited very different recovery rates, with Me31B-GFP signal exhibiting a near complete recovery within few seconds and GFP-Imp signal exhibiting only partial (~40%) recovery after dozens of seconds (Figure 2D) (Vijayakumar et al. 2019). Similar recovery was however observed for each protein in young and aged brains, indicating that the dynamic turnover of granule-associated proteins is not impacted by aging.

Age-dependent condensation of RNP components is linked to decreased sorting specificity.

Previous biochemical and imaging studies have shown that collections of RNP granules with partially overlapping, but distinct composition are typically observed in neuronal cells (De Graeve and Besse 2018; Formicola et al. 2019). In young MB γ neurons, indeed, Me31B is found in two types of granules: Me31B⁺ Imp⁺ (white arrowheads in Figure 3A-A'') and Me31B⁺ Imp⁻ (blue arrowheads in Figure 3A-A'') granules. To determine if the formation of large granules observed in aged flies results from the coalescence of components initially sorted into distinct entities, we analyzed the proportion of both types of granules in young and aged brains. As shown in Figure 3C, a more than 2-fold increase in the proportion of Me31B⁺ Imp⁺ granules was observed upon aging, such that most Me31B-positive granules contained Imp in aged brains (Figure 3B-B''). Remarkably, high-resolution imaging of Imp⁺ Me31B⁺ granules in fixed (Figure 3D) as well as living (Movie 1) brains revealed that Imp and Me31B do not homogeneously mix, but rather segregate into distinct subdomains within neuronal RNP condensates. Together, these results thus indicate that Me31B concentrates upon aging into larger neuronal RNP granules that recruit Imp to form multiphase entities. This process is accompanied by the loss of Me31B⁺ Imp⁻ granules and thus reflects alterations in RNP component sorting specificity.

Age-dependent increase in Me31B levels induces the condensation of Me31B

To understand the relative contribution of Me31B and Imp in RNP component condensation and coalescence, we inactivated each gene through adult-specific RNAi. Remarkably, inactivating *me31B* prevented the assembly of Imp-containing granules without affecting Imp overall protein levels (Supplementary Figure S2A,B,D,E). Conversely, inactivating *imp* did not impact on Me31B⁺ granule assembly (Supplementary Figure S2C), consistent with a model in which Imp protein behaves as a client molecule recruited to granules by the scaffold protein Me31B. As the formation and composition of condensates is known to critically depend on the concentration of scaffolds (Banani et al. 2016 ; Ditlev et al. 2018), we then investigated whether age-dependent RNP granule remodeling may be linked to changes in Me31B dosage. We

first measured Me31B protein levels in MB γ neurons of young and aged brains. As shown in Figure 4A, a 1.5-fold increase in Me31B levels, but not in Imp levels, was observed upon aging. To further test if reducing the dosage of Me31B would suppress the age-dependent condensation of neuronal RNP components, we genetically removed a copy of *me31B* using two previously described deletions (*me31B Δ 1* and *me31B Δ 2*; (Nakamura et al. 2001)). Remarkably, this suppressed the age-dependent condensation of Me31B, as both the number (Figure 4D) and the size (Supplementary Figure S3A) of Me31B-positive granules found in aged *me31B Δ 1/+* and *me31B Δ 2/+* brains were similar to that of young control brains. Reducing the dosage of *me31B*, however, only partially decreased the age-dependent condensation of Imp, as illustrated by the still elevated number of Imp⁺ granules detected in aged *me31B Δ 1/+* and *me31B Δ 2/+* brains (Figure 4E) and the moderate decrease in Imp partition coefficient (Supplementary Figure S3B). Such a differential behavior of Imp and Me31B translated into partial, but not complete, suppression of their coalescence into common condensates (Figure 4F). Together, these results demonstrate that the concentration of the limiting nucleator protein Me31B increases upon physiological aging, which triggers the condensation of Me31B and partially contributes to the condensation of Imp and its recruitment to Me31B-containing granules.

PKA is required for the condensation of Imp in aged-flies.

Having shown that Me31B dosage only partially impacts on Imp condensation and coalescence, we sought to identify pathways that may regulate this process. To this end, we performed a selective screen in which we modulated the activity of conserved pathways known to either be impacted by aging, or contribute to aging. RNAi or dominant negative constructs were expressed specifically in adult MB neurons to avoid developmental contributions, and the subcellular distribution of Imp analyzed in aged flies. Strikingly, altering most of the pathways tested did not have a significant impact on Imp condensation (Table S1). However, inhibiting the activity of the cAMP-dependent kinase PKA *via* expression of a catalytic-dead variant prevented the condensation of Imp into large granules (Figure 5B,D). Similar results were observed when

expressing either dsRNA targeting PKA catalytic domain or when RNAi-inactivating *amnesiac*, a gene known to produce a peptide positively activating PKA in MB neurons (Figure 5C,D) (Turrel et al. 2020). As shown in Figure 5E and Supplementary Figure S4A, however, PKA inactivation only mildly impacted on the condensation of Me31B, suggesting that PKA differentially modulates the behavior of RNP components. By blocking the condensation of Imp, PKA inactivation also inhibited the coalescence of Imp and Me31B into common granules, as illustrated by the decrease in the proportion of Me31B⁺ Imp⁺ granules (Figure 5F). Together, these results demonstrate that the activity of PKA is required for the condensation of Imp into detectable granules in aged brains.

Age-dependent condensation of RNP components associates with increased translational repression of granule-associated mRNAs.

Neuronal RNP granules are enriched in translational repressors and thought to contain translationally-repressed mRNAs (Krichevsky and Kosik 2001; Fritzsche et al. 2013; El Fatimy et al. 2016; De Graeve and Besse 2018). Thus, to determine if the increased condensation of Imp and Me31B and their coalescence into large granules may impact on the expression of associated mRNAs, we expressed inducible translational reporters generated by fusing the coding sequence of EGFP to the 3'UTR of Imp RNA target *profilin*. SV40 3'UTR was used as a negative control, and GFP protein levels were quantified in both young and aged brains. Remarkably, a significant decrease in GFP expression was observed for *profilin* reporter, but not for the *SV40* control, in aged brains (Figure 5A-E). As measured by quantification of *gfp* smFISH signals (Supplementary Figure S5A), decreased GFP expression did not correlate with decreased *gfp* RNA levels, confirming that it reflects variations in the translation of *profilin* reporter. Notably, a similar decrease in the levels of endogenous Profilin protein, but not of *profilin* mRNA, was observed (Supplementary Figures S5B,C). Thus, these results suggest that age-dependent partitioning of Imp into large granules is associated with an increased translational repression of its target mRNAs.

To extend our study to other neuronal RNAs shown to undergo 3'UTR-dependent regulation (Mayford et al. 1996; Piper et al. 2006; Moon et al. 2009; Topisirovic et al. 2009 ; Bellon et al. 2017), we analyzed the translation of three other reporters: GFP-*camk2* 3'UTR, GFP-*eiF4e* 3'UTR and GFP-*cofilin* 3'UTR. While the translation of GFP-*camk2* 3'UTR and GFP-*eiF4e* 3'UTR did not decrease upon aging, increased repression was observed for the GFP-*cofilin* 3'UTR transcripts (Figure 6F). To test whether age-dependent decrease in translation levels correlated with recruitment to RNP granules, we performed for each reporter line smFISH experiments using *gfp* probes. These experiments were performed in mTomato-Me31B-expressing flies, enabling quantitative assessment of the fraction of Me31B+ granules containing *gfp* reporter RNAs. Remarkably, a significant association with Me31B+ granules was observed only for GFP-*profilin* 3'UTR and GFP-*cofilin* 3'UTR transcripts (Figure 6G), further suggesting that partitioning of RNAs into dense condensates enriched in Imp and Me31B inhibits their translation.

PKA, but not Me31B dosage, are essential for age-dependent translational repression

To determine the relative contribution of Me31B and Imp condensation in the translational repression of granule-associated mRNAs, we first sought to analyze the translation of GFP-*profilin* 3'UTR upon removal of one copy of *me31B*. Strikingly, the age-dependent decrease in GFP-*profilin* 3'UTR translation was not altered in *me31BΔ1/+* and *me31BΔ2/+* brains (Supplementary Figure S3C), indicating that Me31B condensation itself is not sufficient to repress GFP-*profilin* 3'UTR translation. To then test the impact of Imp condensation, we monitored GFP levels in flies co-expressing GFP-*profilin* 3'UTR reporter RNAs and the catalytic-dead PKA dominant negative. As shown in Figure 5G, this led to a strong de-repression of *profilin* translation in aged flies, suggesting that PKA-dependent Imp condensation might be a key determinant underlying granule-associated mRNA translation.

7.3. Discussion

Increased scaffold concentration and PKA-dependent phosphorylation are required for condensation and coalescence of RNP components in aging brains.

Our functional analysis has revealed that Me31B, in contrast to Imp, is required for the assembly of neuronal RNP granules and thus qualifies as a “core” or “scaffold” component. Furthermore, we have shown on one hand that Me31B levels increase upon aging, and on the other hand that genetically reducing the dosage of Me31B largely inhibits both age-dependent condensation of Me31B and increased coalescence of Me31B and Imp. Such an Me31B level-dependent collapse of initially distinct Me31B⁺ Imp⁺ and Me31B⁺ Imp⁻ granules is consistent with a model in which components common to distinct neuronal RNP granules may establish overlapping networks of interactions that compete for the recruitment of granule-specific clients. Together, these results not only validate frameworks proposed based on artificial manipulations of component concentrations *in vitro* or in cells (Sanders et al. 2020), but also illustrates how biological systems can efficiently modulate RNP condensate properties and composition through subtle physiological changes in RNP component stoichiometry. Remarkably, increasing the dosage of Me31B through addition of an extra copy of *me31B* in young flies is not sufficient to trigger “aging-like” condensation (K.P and F.B., data not shown), suggesting that additional factors contribute to the age-dependent remodeling of neuronal RNP granules. These may include increased levels of other yet to be discovered nucleating factors with limiting concentration in young flies, or age-dependent changes in the valency or binding affinities of critical RNP components. Consistent with this idea, our work as revealed that PKA-dependent phosphorylation events are key for the condensation of Imp in aged flies. Whether PKA activity itself is modulated upon aging is an open question. Although previous work has suggested that both expression levels and activity of PKA do not vary in the aging *Drosophila* brain (Yamazaki et al. 2007), this analysis was performed on entire brain lysates and thus did not address potential population-specific differences. In light of recent work showing that neuronal activity modulates Rck1/DDX6

RNP granules in maturing neurons (K. Bauer and M. Kiebler, personal communication), and given that PKA is activated by neuronal activity (Dunn et al. 2006), an interesting possibility is that establishment of specific activation pattern in response to accumulating experience may participate to the observed long-term changes in neuronal RNP granule properties.

PKA activity is required for condensation of Imp in aged flies

Our genetic analysis has uncovered that blocking the catalytic activity of PKA prevents the condensation of the RNP component Imp in aged flies. A role for PKA in RNP condensate regulation has previously been described for yeast P-body. In this system, however, ectopic activation of PKA prevented the assembly of P-bodies upon glucose starvation while pharmacological inhibition of PKA triggered the condensation of P-body components in glucose-replete conditions (Ramachandran et al. 2011). Such a regulatory role was shown to be mediated by phosphorylation of the scaffold protein Pat1, a critical phospho-target of PKA whose capacity to recruit components such as the helicase Dhh1 and to nucleate P-body assembly is inhibited by phosphorylation (Ramachandran et al. 2011 ; Sachdev et al. 2019). Although *Drosophila* Pat1 localizes to neuronal RNP granules (Supplementary Figure S1D), it is unlikely to represent a target of PKA in *Drosophila* brain, as no PKA consensus site ((R/K)(R/K)XS/T) are found in the fly protein. Furthermore, our functional analysis rather predicts that phosphorylation of PKA targets promotes condensation of RNP components in neurons. Interestingly, Imp contains putative PKA phosphorylation sites and that is phosphorylated on Ser in *Drosophila* brains (Supplementary Figure S6A). Mutating three putative PKA phosphorylation sites into Ala to generate a GFP-Imp-S58A-S98A-T349A phosphomutant form expressed from the endogenous locus, however, did not impact on the condensation of Imp in aged flies (Supplementary S6B), indicating that PKA acts through phosphorylation of other sites or other targets. Given the differential effect of PKA inactivation on Imp and Me31B, this target is likely not a core regulator of RNP assembly but rather another RNP component involved in the recruitment of client molecules such as Imp. Whether PKA is recruited to neuronal RNP granules to modulate the phosphorylation of their components in response to physiological stimuli remains to be

investigated, but this might represent a relevant possibility as PKA catalytic subunits were found to accumulate in P-bodies in yeast (Tudisca et al. 2010).

Regulation of the neuronal translome upon aging

Aging has long been associated with alterations in gene expression and proteostasis (Anisimova et al. 2018). However, the relative contribution of transcriptional, post-transcriptional and post-translational changes to age-dependent modifications in protein content has only recently started to be explored through the systematic integration of RNA-seq, Ribo-seq and advanced mass-spectrometry analyses. Unexpectedly, analyses performed in the rat brain have revealed that the fraction of transcripts and proteins that are significantly up- or down-regulated upon aging is in fact relatively small (<10%) (Walther and Mann 2011 ; Wood et al. 2013; Ori et al. 2015; Stegeman and Weake 2017). Changes in the translational output of specific sets of genes, however, could be observed independently of changes in original RNA levels (Ori et al. 2015). This work thus indicated that the translation efficiency of specific transcripts is modulated upon aging, though mechanisms yet to be discovered. Consistent with this, our analysis of translation reporters did not reveal a general decrease in translation efficiency over time, but rather transcript-specific responses. Remarkably, RNAs enriched in RNP granules exhibited a specific regulatory profile characterized by an age-dependent decrease in translation. Furthermore, increased translational repression of the Imp RNA target *profilin* could be reverted upon inactivation of PKA and concomitant loss of Imp condensation, suggesting that recruitment of RNAs to RNP condensates enriched in the translational repressor Imp (Huttelmaier et al. 2005) might play a key role in this process. As revealed by recent *in vitro* assays, assembly of condensates enriched in neuronal RBP with repressor functions may inhibit translation in different ways: by segregating away the translational machinery and generating a micro-environment enriched in translational repressors (Tsang et al. 2019), and/or by favoring deadenylation through enhancement of the catalytic activity of the CCR4/NOT complex (Kim et al. 2019). Although new tools would be required to address this question *in vivo* in neurons, our previous immunostaining experiments using antibodies recognizing Rpl32, a component of the ribosomal 60S unit, suggested that ribosomes are not present in, and thus likely excluded from, Imp-containing neuronal RNP granules

(Vijayakumar et al. 2019). Together, our results thus raise the hypothesis that targeting of RNA species to RNP granules hosting translational repressors may represent a mechanism employed by neurons to regulate the translation of specific sets of transcripts upon aging.

7.4. Materials and Methods

Drosophila stocks and genetics

Fly crosses were performed on standard media and raised at 25°C unless specified. For aging experiments, flies were transferred to fresh media every 3 days until reaching the age of 35-39 days. For screening of pathways involved in Imp clustering and PKA inactivation, adult-specific inactivation was carried out using a tubulin-Gal80^{ts}; OK107-Gal4 line. Specifically, flies were raised at 18°C until eclosion, transferred to 29°C to allow transgene expression, and aged to 30 days.

The following fly stocks were used in this study: GFP-Imp protein-trap line #G080 (Medioni et al. 2014); Me31B::EGFP and Me31B::mTomato knock-in lines (Formicola et al., under revision); *w*; *me31B*Δ1 FRT40A/CyO and *w*; *me31B*Δ2 FRT40A/CyO (Nakamura et al. 2001) ; UAS-*me31B* RNAi (BDSC #33675); UAS-*imp* RNAi (BDSC #34977); UAS-PKA C1 K75A(PKA catalytic dead subunit; BDSC #35557); UAS-PKA C1 RNAi (BDSC#31277); UAS-*amn* RNAi (BDSC #25797); UAS-*amn* RNAi (VDRC #5606).

UAS-EGFP 3'UTR reporter lines (*sv40 3'UTR*, *profilin 3'UTR*, *cofilin 3'UTR*, *eiF4 3'UTR* and *camkII 3'UTR*) were described in (Formicola et al., under revision) and expressed in MB neurons using OK107 Gal4.

The mcherry-Rin knock-in lines were generated using the CRISPR/Cas9 technology, as described in (Kina et al. 2019).

Preparation of *Drosophila* brains for imaging

Immunostaining

Brains were dissected in cold PBS1X for 1 hour and fixed in 4% formaldehyde for 30 minutes. After fixation, brains were washed thrice in 0.1% PBS/Triton-X (PBT). Brains were then blocked overnight in PBT supplemented with 1% BSA and incubated with the following primary antibodies: rabbit α -Imp (1:1000, Medioni et al., 2014); rat α -Imp (1:1,000, Medioni et al., 2014); rabbit α -Me31B (1:3000, gift from C. Lim); mouse α -Me31B (1:3000, gift from Nakamura); rabbit α -HPat1 (1:1000, gift from A. Nakamura), rabbit α -Tral (1:1000, gift from A. Nakamura), rat α -Staufen (1:1000, gift from A. Ephrussi); rabbit α -GFP (rabbit, 1:1,000; Molecular Probes, A-11122), mouse α -Profilin (1:100, DSHB); rabbit α -p62 (1:1,000, gift from Gabor Juhasz); mouse α -Ubiquitin (1:500, gift from Gabor Juhasz), rabbit α -PABP (1:1500, gift from C. Lim). After incubation in primary antibodies, brains were washed thrice in PBT 0.1% and incubated with α -rabbit or α -mouse or α -rat secondary antibodies (1:1000 dilution) conjugated with Alexa Fluor 568/488/647 for 2 hours at room temperature or overnight at 4°C. Fixed and stained brain samples were mounted in vectashield (Vector Laboratories) medium.

Detection of endogenous fluorescent signals

For the detection of endogenous GFP signals, flies were dissected in cold PBS1X, and fixed in 4% formaldehyde for 30 minutes. Fixed samples were then washed thrice with 0.1% PBT and directly mounted in vectashield (Vector Laboratories) medium.

Single molecule fluorescent *in situ* hybridization (smFISH)

Drosophila brains were dissected in cold RNase-free PBS for 1 hour. Dissected brains were then fixed in 4% formaldehyde in PBS for 1 hour at 4°C and rinsed twice with PBS. Brains were dehydrated overnight in 70% ethanol and rinsed the day after in wash buffer (10% formamide in 2x SSC) for 5 minutes at room temperature. Brains were then incubated overnight, at 45°C, and under agitation, with Quasar® Stellaris® Probes in 100 μ L hybridization buffer (100 mg/mL

dextran sulfate, 10% formamide in 2x SSC). After hybridization, brains were washed for 30 minutes in pre-warmed wash buffer under agitation, at 45°C. This step was followed by a further 5 minute-wash in 2x SSC at RT and by mounting in vectashield (Vector Laboratories) medium. The following probe sets were used: *chic* 570 stellaris probes (2µl-12.5uM) ; 2) *egfp* 670 stellaris probes (1µl -12.5uM) ; 3) *egfp* 570 stellaris probes (0.5µl -25uM)

Image Acquisition

Brain samples were imaged using a LSM880 confocal equipped with a airy scan module and a 63X 1.4 NA oil objective. Images were taken with a 0.04 µm pixel size and were processed with the automatic Airy Scan processing module of Zen (strength 6.0).

For analysis of EGFP-3'UTR reporters, freshly mounted samples were imaged using a Zeiss LSM 780 confocal microscope equipped with a GaAsP spectral detector and a Plan Apo 63X 1.4 NA oil objective.

Fluorescence recovery after photobleaching (FRAP)

G080-GFP-Imp or Me31B::EGFP brains were dissected in Schneider's medium. Dissected brains were mounted in polylysinated Lab-Tek chambers as described in (Medioni et al. 2015), with the difference that hormones were not added to the imaging medium. FRAP experiments were performed on a Nikon microscope coupled with a Yokogawa spinning head and an Andor EM-CCD camera. Imaging was performed using a Plan Apo 100X oil 1.2 NA objective and a 488 laser line. The metamorph software was used to acquire images (1 image every 0.24 s) and to bleach the samples. Samples were bleached with a 488nm laser, using the point laser method. A maximum of 10 granules were bleached per brain.

Fluorescence signals were measured using the following procedure. First, images were aligned using the stack shuffling plugin of ImageJ. To measure granule intensity over time, granule positions were marked manually and an ROI (3*3 pixel) was saved for each granule in the ROI manager. ROI mean fluorescence intensities were then calculated using the multimeasure option

of ImageJ ROI manager. A double normalization was applied to intensity values, which consisted in bleach correction followed by normalization to pre-bleach intensities..

Live imaging

Brains of 5-day old flies were dissected in cold Schneider's medium. Dissected brains were mounted in polylysinated Lab-Tek chambers. Once properly oriented (dorsal side of the brain towards the objective), brains were stabilized using a metal ring as described in Medioni *et al.*, 2015. Movies were acquired on an inverted Zeiss LSM880 confocal microscope equipped with an airy scan module and a 63X 1.4 NA oil objective. Images were acquired every 10 seconds for 15 minutes, with a pixel size of 0.028 μm .

Image Analysis

RNP granule detection

ROIs containing 6-7 cells were cropped from single z slices and processed *via* the following steps: 1) resizing to a factor of 1 using the Laplacian Pyramid plugin on ImageJ, 2) rescaling to enhance contrast and to keep 0.01% pixels saturated, and 3) converting 32bit images to 16bit in order to change float numbers to integer values. Granules were detected using the Small Particle Detection (SPaDe) algorithm described in (<https://raweb.inria.fr/rapportsactivite/RA2016/morpheme/uid13.html>) (De Graeve et al. 2019). Cutoff size for granules was set to 4 pixels and thresholds used for detection of Imp granules, Me31B granules, *GFP* RNA were 0.62, 0.42 and 0.22 respectively. Number, size and masks of detected objects were recovered

Measurement of partition coefficients

Partition coefficients were defined for each granule as the ratio between the maximal intensity of Me31B or Imp signal in SPaDE-generated masks to the manually calculated average cytoplasmic signal intensity.

Colocalization

Masks of granules generated by SPADE were converted to binary images using ImageJ. Colocalization was measured with the JACoP plugin of ImageJ, using binarized images corresponding to different channels and the centroid-Mask method. Ratio of colocalizing spots to total number of spots was calculated. Fold changes were calculated by normalizing the data to the young conditions.

Reporter quantification

Maximal intensity projection of Z stacks was performed and 2 ROIs were selected per brain. The mean GFP intensity was calculated for each ROI and normalized to the average of respective controls.

Total amount of protein

2 ROIs containing 6-7 cells were selected from each brain and mean intensity calculated for each ROI. Data were normalized to values of respective controls.

Immuno-precipitations

Fly heads were snap frozen in liquid nitrogen and lysed using micro pestles in RIPA buffer (0.1% sodium deoxycholate, 1% triton x100, 0.1% SDS, 150mM NaCl, 50mM TRIS pH 7.00) supplemented with Halt™ Protease Inhibitor Cocktail 1:100 (Thermofisher, #78429). Lysates were incubated under agitation at 4°C for 30 minutes, then centrifuged at 2,000 rpm for 10 minutes at 4°C to remove tissue debris. Supernatants were collected and incubated with equilibrated ChromoTek GFP-Trap® beads (ChromoTek, gt-10, #70112001A) for 2 hours at 4°C. Beads were washed three times 30 minutes in RIPA buffer, resuspended in 25 µl 2X SDS loading buffer, and incubated at 95°C for 5 minutes for elution and denaturation.

Input and bound protein fractions were subjected to electrophoresis and blotted to PVDF membrane. Membranes were then blocked with 4% BSA for 1 hour at room temperature prior to antibody addition. The following primary antibodies were used: rabbit anti-GFP (1:2,500; Torrey Pines); rabbit anti-phospho serine (3ug/mL; ABCAM) and mouse anti-phospho serine (1:200; Sigma).

RT-QPCR

RNA was isolated from fly head lysates using Trizol (Invitrogen) and used as template for reverse-transcription reaction performed with Superscript III (Invitrogen) and Oligo(dT). 1% of the RT product was then PCR-amplified through QPCR, using the following couples of optimized primers: *qPCRrpl7_fwd*: 5'-CGTGCGGGAGCTGATCTAC-3' / *qPCRrpl7_rev*: 5'-GCGCTGGCGGTTATGCT-3'; *rp49_fwd*: 5'-CTTCATCCGCCACCA-3' / *rp49_rev*: 5'-CTTCATCCGCCACCA-3'; *profilin_fwd*: 5'-CTGCATGAAGACAACACAAGC-3' / *profilin_rev*: 5'-CAAGTTTCTCTACCACGGAAGC-3'.

Statistical Analysis

All data were plotted and statistically analyzed using Graphpad Prism 8. As stated in the corresponding figure legends, student t-tests were performed for comparison of two conditions, while one-way ANOVA with multiple comparison tests were used to compare several samples. Graphs are represented as SuperPlots (Lord et al. 2020).

Acknowledgements

This study was supported by the CNRS, as well as grants from the ANR (ANR-15-CE12-0016 and ANR-20-CE16-) and the Fondation pour la Recherche Médicale (Equipe FRM; grant #DEQ20180339161) to F.B. Part of this work was also supported by the Joint Usage/Research Center for Developmental Medicine, IMEG, Kumamoto University. K.P. was supported by a fellowship from the LABEX SIGNALIFE program (#ANR – 11 – LABX – 0028 – 01) and a one year- La Ligue contre le cancer fellowship. We thank the iBV PRISM Imaging facility for use of their microscopes and support (especially B. Monterroso), and L. Palin for excellent technical assistance. We are grateful to members of the Besse group for discussion and advise. We thank XX for critical reading of the manuscript. We are grateful to the Bloomington Drosophila Stock Center and the Developmental Studies Hybridoma Bank for reagents.

7.5. Figures

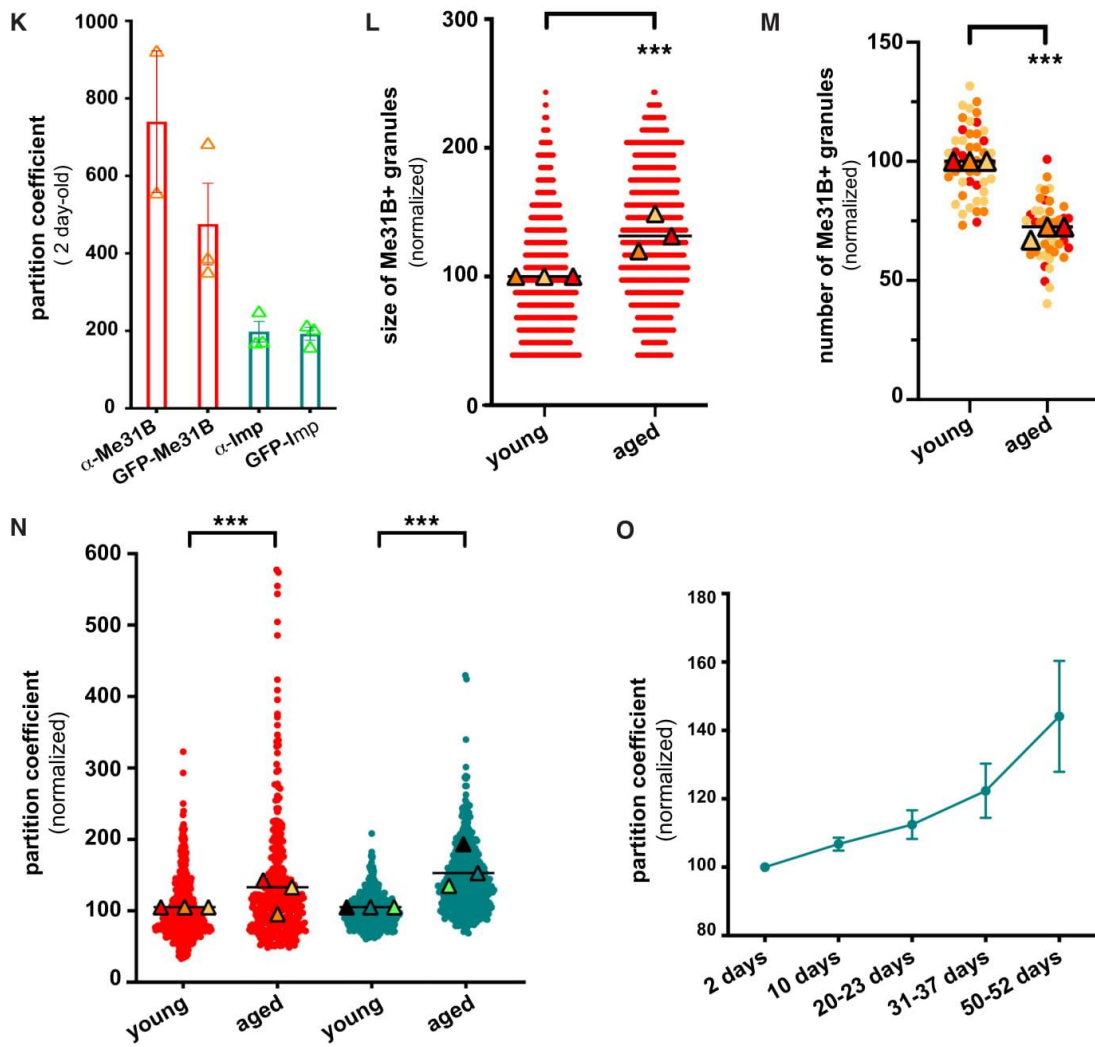
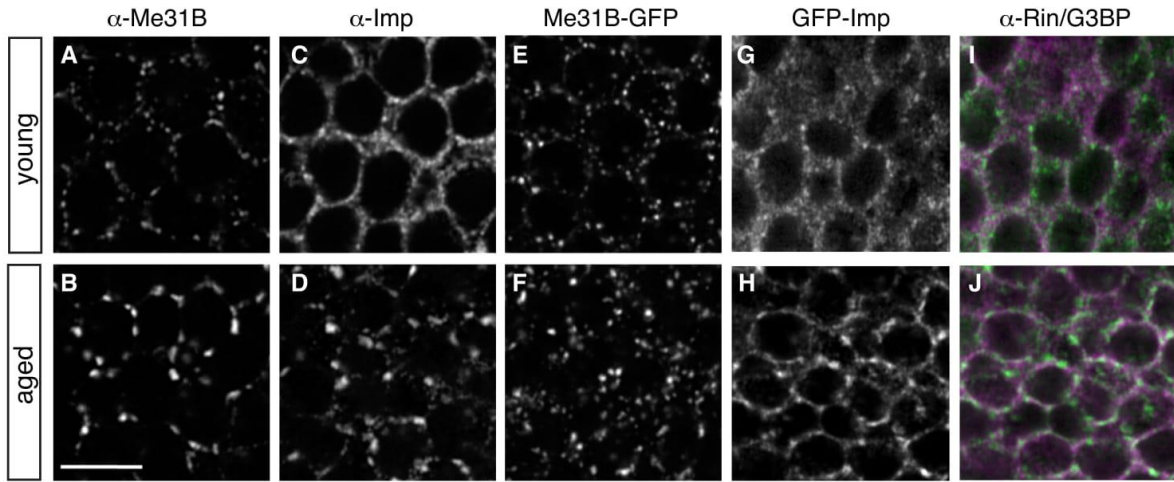


Figure 1. Me31B and Imp condensate into larger cytoplasmic granules in aged brains.

(A-J) Cell bodies of MB \square neurons imaged from 2 day- (A,C,E,G,I; young), or 37-38 day- (B,D,F,H,J; aged) old brains. Brains were stained with anti-Me31B (A,B) or anti-Imp (C,D) antibodies. Me31B-GFP (E,F), GFP-Imp (grey in G,H and green in I,J) and Rin-mcherry (magenta in I,J) were expressed at endogenous levels, from knock-in insertions. Single confocal sections are shown. Note that nuclei (dark discs) occupy most of MB \square neuron soma, and thus that the cytoplasmic signal is restricted to the cell periphery. Scale bar: 5 \square m. (K) Mean granular:cytoplasmic intensity ratio in brains of 2 day-old flies. Each data point represents the mean value obtained for a given replicate. At least 10 fields were analyzed per replicate. Two to three independent experiments were quantified per condition. (L) Normalized size of Me31B-containing granules in MB \square neurons of 2 day- (young) and 37-38 day- (aged) old brains. (M) Normalized numbers of Me31B-containing granules (per surface area) in MB \square neurons of 2 day- (young) and 37-38 day- (aged) old brains. In L and M, individual data points were collected from brains immuno-stained with anti-Me31B antibodies and normalized to the young condition. Three replicates were performed and the mean value of each replicate is indicated as a symbol (triangle). In L, the distribution of granule sizes is shown for one replicate only. In M, data points were color-coded based on the experimental replicate they belong to. (N) Partition coefficients of Me31B (red) and Imp (green) in 2 day- (young) and 37-38 day- (aged) old brains. Partition coefficients were estimated by dividing the maximal intensity of Me31B or Imp signal in individual RNP granules to the intensity of the cytoplasmic diffuse pool (see Materials and Methods), and calculated for each granule detected in the imaged fields. Three replicates were performed and the mean value of each replicate is indicated as a symbol (triangle). The distribution of individual granule partition coefficients is shown for one replicate only. (O) Mean partition coefficients of Imp upon gradual aging. Each data point represents the average of mean values obtained from three independent replicates. Three replicates were performed; errors bars correspond to s.e.m. ***, $P < 0.001$ (unpaired t-test on individual data points in L,M and N).

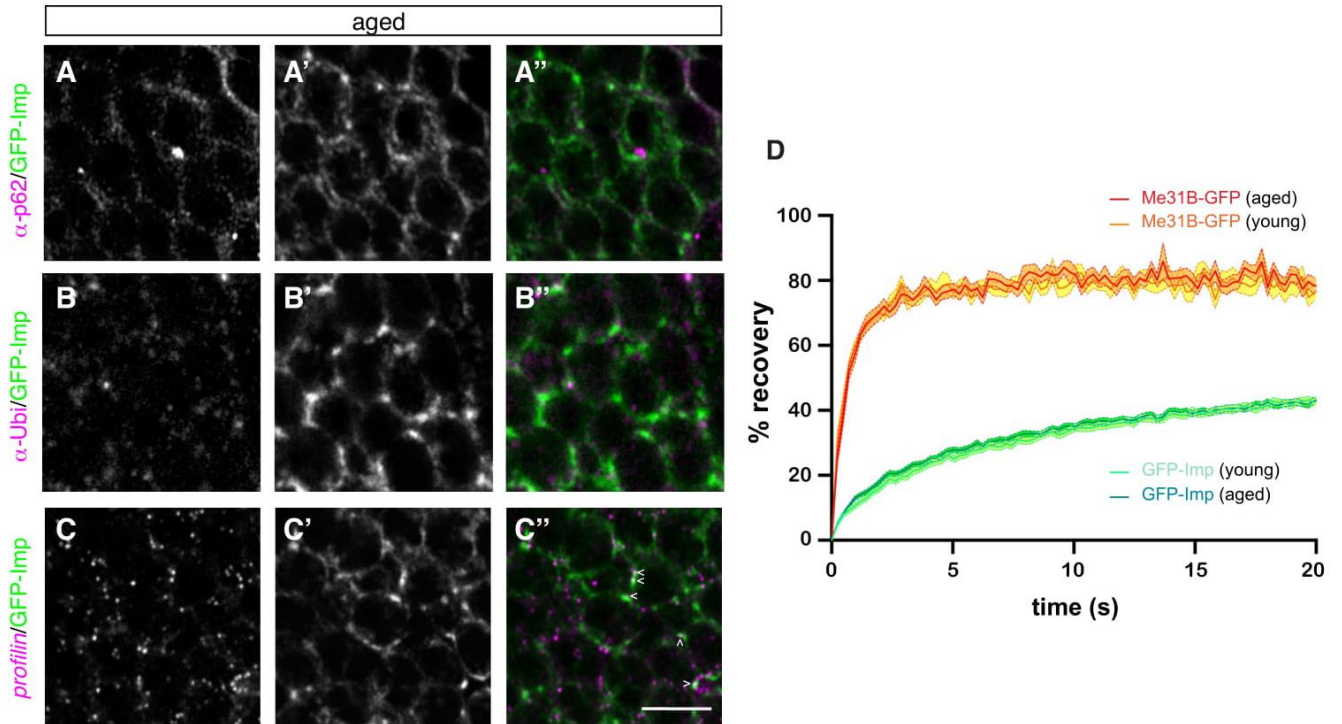


Figure 2. Large granules in old flies are dynamic RNP assemblies.

(A-C) Cell bodies of MB \square neurons imaged from 37-38 day-old (aged) brains. GFP-Imp-expressing brains were stained with anti-p62 (A, magenta in A'') antibodies, anti-Ubiquitin (B, magenta in B'') antibodies, or *profilin* smFISH probes (C, magenta in C''). GFP-Imp distribution is shown in white in green in A'-C' and green in A''-C''. Arrowheads in C'' point to large granules containing *profilin* mRNA. Scale bar: 5 \square m. (D) Average FRAP curves obtained after photobleaching of GFP-Imp-positive (green) or Me31B-GFP-positive (red-orange) granules from 2 day- (young) or 38 day- (old) old brain explants. At least 90 granules from at least 9 brains were analyzed per condition. Error bars (fill areas) represent s.e.m.

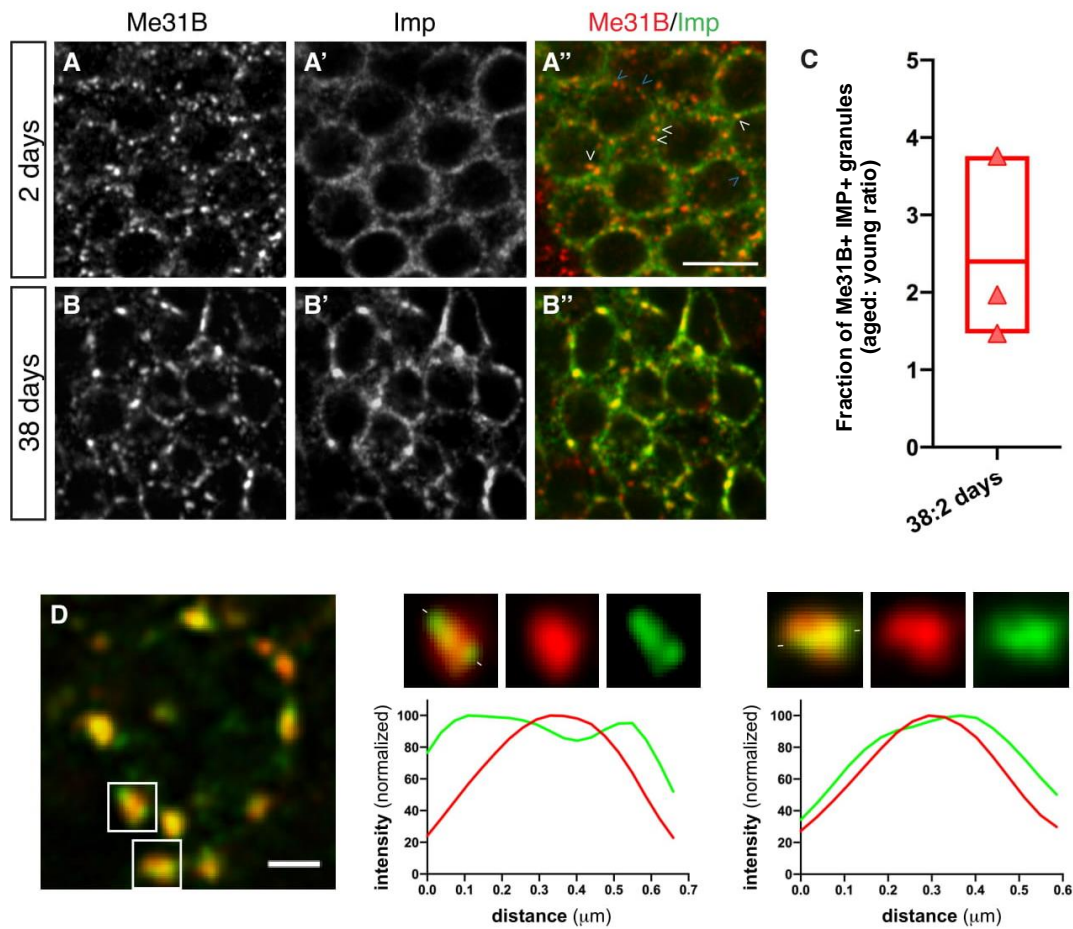


Figure 3. Age-dependent changes in RNP component sorting.

(A,B) Cell bodies of MB γ neurons imaged from 2 day- (A, young) or 37-38 day- (B, aged) old brains. GFP-Imp- (grey in A',B' and green in the overlay) expressing brains were stained with anti-Me31B antibodies (grey in A,B; red in the overlay). The white arrowheads point to some Me31B+ Imp+ granules while the blue ones point to some Me31B+ Imp- granules. (C) Fold increase in the number of Me31B+ granules containing Imp. The fraction of Me31B+ granules containing Imp was estimated using the JACoP plugin of Fiji (see Materials and Method), and fold changes calculated as the ratio of 38 day-old vs 2 day-old values. The error bar represents s.e.m. (D) Left: cell body of a 38 day-old MB γ neuron expressing GFP-Imp (green) and stained with anti-Me31B antibodies (red). Scale bar: 1 μ m. Magnifications of the boxed areas 1 and 2 are shown in the middle and right panels respectively. Intensity profiles of GFP-Imp (green) and Me31B (red) measured along the line marked by white segments are shown below.

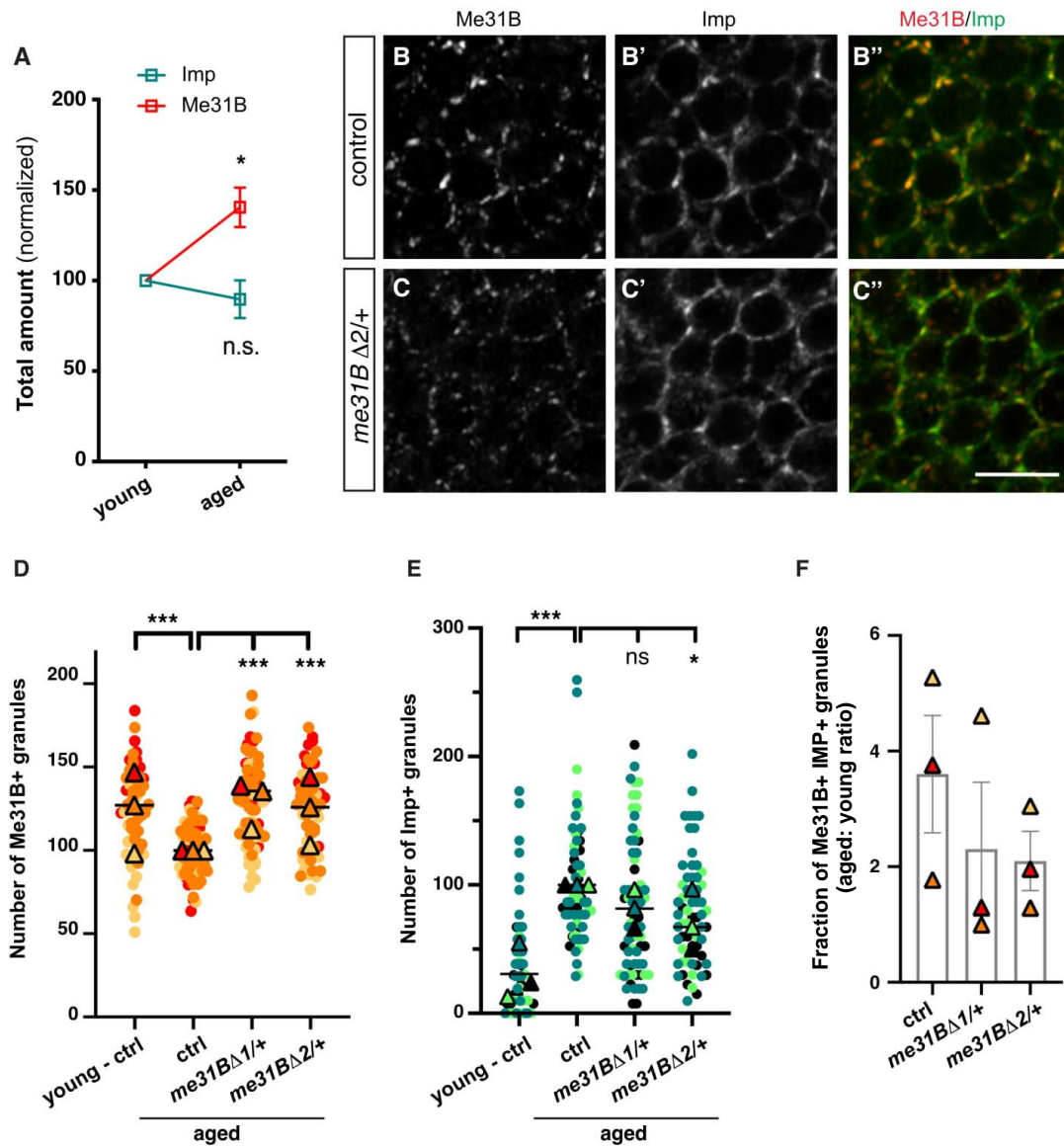


Figure 4. Me31B levels increase upon aging and cause Me31B condensation.

(A) Imp and Me31B levels measured from confocal images of 2 day- (young) and 37-40 day- (aged) old MB γ neurons. Each data point represents the mean value obtained for a given replicate. Three independent experiments were quantified per condition. At least 10 fields were imaged per replicate and per condition. *, $P < 0.05$ (Mann-Whitney test). (B,C) Cell bodies of control (B) and *me31BΔ2/+* (C) MB γ neurons from 37-38 day-old brains stained with anti-Me31B (B, red in B'') and anti-Imp (B', green in B''). Scale bar: 5 μ m. (D,E) Numbers of Me31B-positive (D) and Imp-positive (E) granules (per surface area; normalized to 37 day-old controls). Three replicates were performed and the mean value of each replicate is indicated as a symbol (triangle). Data points were color-coded based on the experimental replicate they belong to. At least 10 fields were imaged per condition. *, $P < 0.05$; ***, $P < 0.001$ (one-way ANOVA test with Sidak's multiple comparison tests). n.s. stands for not significant. (F) Fold increase in the number of Me31B+

Imp+ granules. The fraction of Me31B+ granules containing Imp was estimated using the JACoP plugin of Fiji (see Materials and Method), and fold changes calculated as the ratio of 38 day-old vs 2 day-old values. The error bars represent s.e.m.

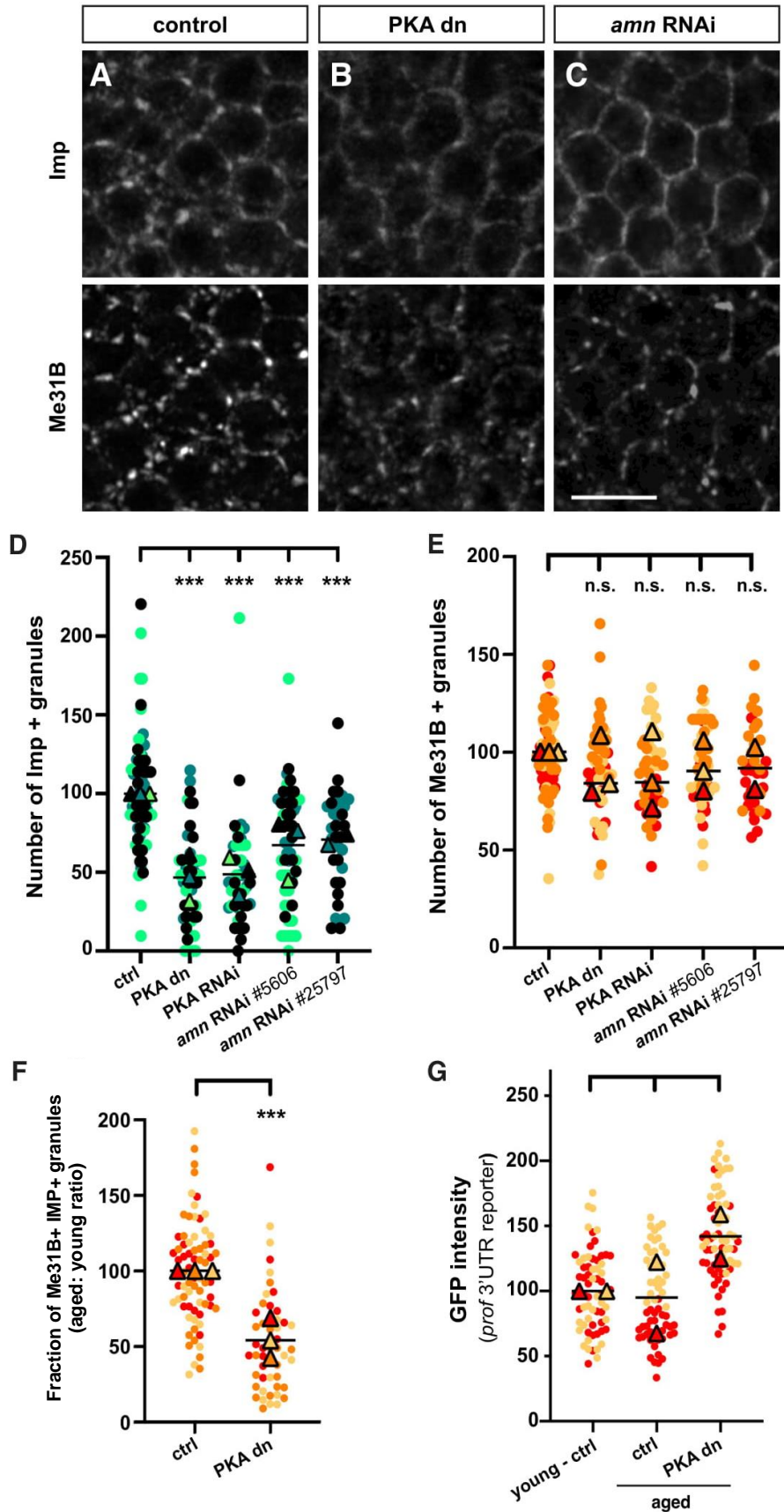


Figure 5. Inactivation of PKA suppresses Imp condensation in aged flies.

(A-C) Cell bodies of MB γ neurons imaged from 30 day-old (aged) control brains (A), brains expressing a kinase dead PKA catalytic subunit (B), or brains expressing *amn* RNAi (C). Scale bar: 5 μ m. (D,E) Normalized numbers of Imp-positive (D) and Me31B-positive (E) granules (per surface area) in 30 day-old (aged) control brains (left) and brains with reduced PKA activity. PKA dn stands for PKA dominant negative and corresponds to expression of a kinase dead variant. At least 10 fields were imaged per condition. (F) Normalized number of Me31B+ granules containing Imp, as estimated using the JACoP plugin of Fiji (see Materials and Method). At least 14 fields were imaged per condition. (G) GFP signal intensities measured from brains expressing EGFP-*profilin* 3'UTR together with either a neutral luciferase construct (controls) or a kinase dead PKA variant (PKA dn). At least 14 fields were imaged per condition. In D-G, three replicates were performed and the mean value of each replicate is indicated as a symbol (triangle). Data points were color-coded based on the experimental replicate they belong to. ***, $P < 0.001$ (one-way ANOVA test with Sidak's multiple comparison tests in D,E,G; unpaired t-test in F). n.s. stands for not significant.

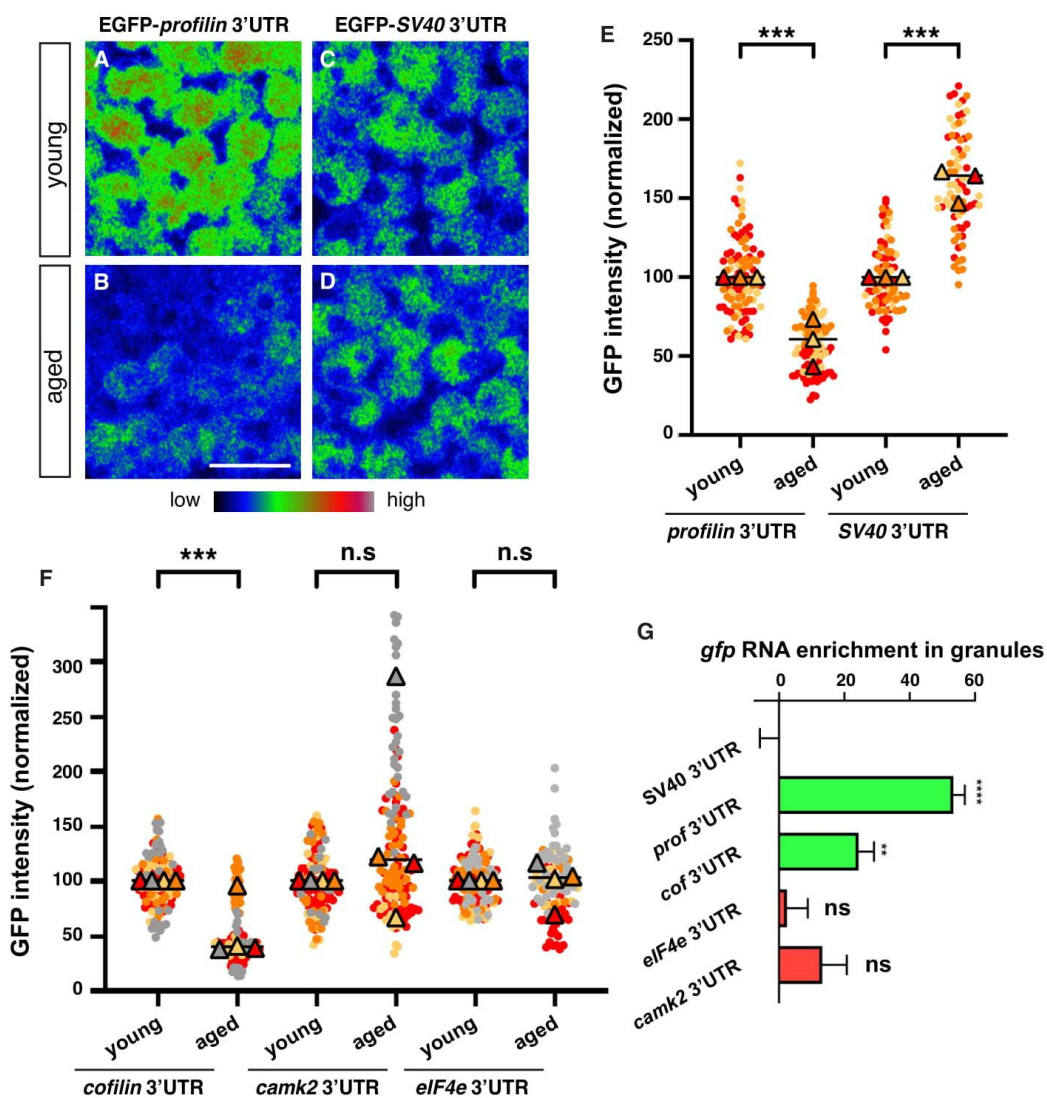


Figure 6. Age-dependent decrease in the translation of granule-associated mRNAs.

(A-D) Cell bodies of MB γ neurons expressing EGFP-*profilin* 3'UTR (A,B) or EGFP-*SV40* 3'UTR (C,D) transcripts in 2 day- (A,C; young) or 37-38 day- (B,D; aged) old brains. Images were color-coded using the Rainbow RGB visualization mode of Fiji. Scale bar: 5 μ m. (E) GFP signal intensities measured from 2 day- (young) and 37-40 day- (aged) old brains expressing EGFP-*profilin* 3'UTR (left) or EGFP-*SV40* 3'UTR (right). (F) Distributions of GFP signal intensities measured from 2 day- (young) and 37-40 day- (aged) old brains expressing EGFP-*cofilin* 3'UTR (left), EGFP-*camk2* 3'UTR (middle) and EGFP-*eIF4e* 3'UTR (right). In E,F, values were normalized to 2 day-old flies. Four replicates were performed and the mean value of each replicate is indicated as a symbol (triangle). Data points were color-coded based on the experimental replicate they belong to. At least 12 fields were imaged per condition. ***, $P < 0.001$ (one-way ANOVA test with Sidak's multiple comparison tests, performed on individual data points). n.s. stands for not significant. For the *camk2* 3'UTR reporter, eight outlier data were omitted from the graph (although they were considered to calculate the mean of the corresponding replicate and to perform statistical tests). Complete genotype: UAS-EGFP-3'UTR/+; OK107-Gal4/+. (G) Fraction of Me31B+ granules containing *gfp*-3'UTR reporter RNA. For each reporter, the number of Me31B-mTomato+ granules containing smFISH *gfp* RNA spots was evaluated using the JACoP plugin of Fiji (see Materials and Method). Numbers were then normalized to the values found with the SV40 3'UTR control reporter. **, $P < 0.01$; ***, $P < 0.001$ (one-way ANOVA test with Sidak's multiple comparison tests). n.s. stands for not significant.

7.6. Supplementary Figures

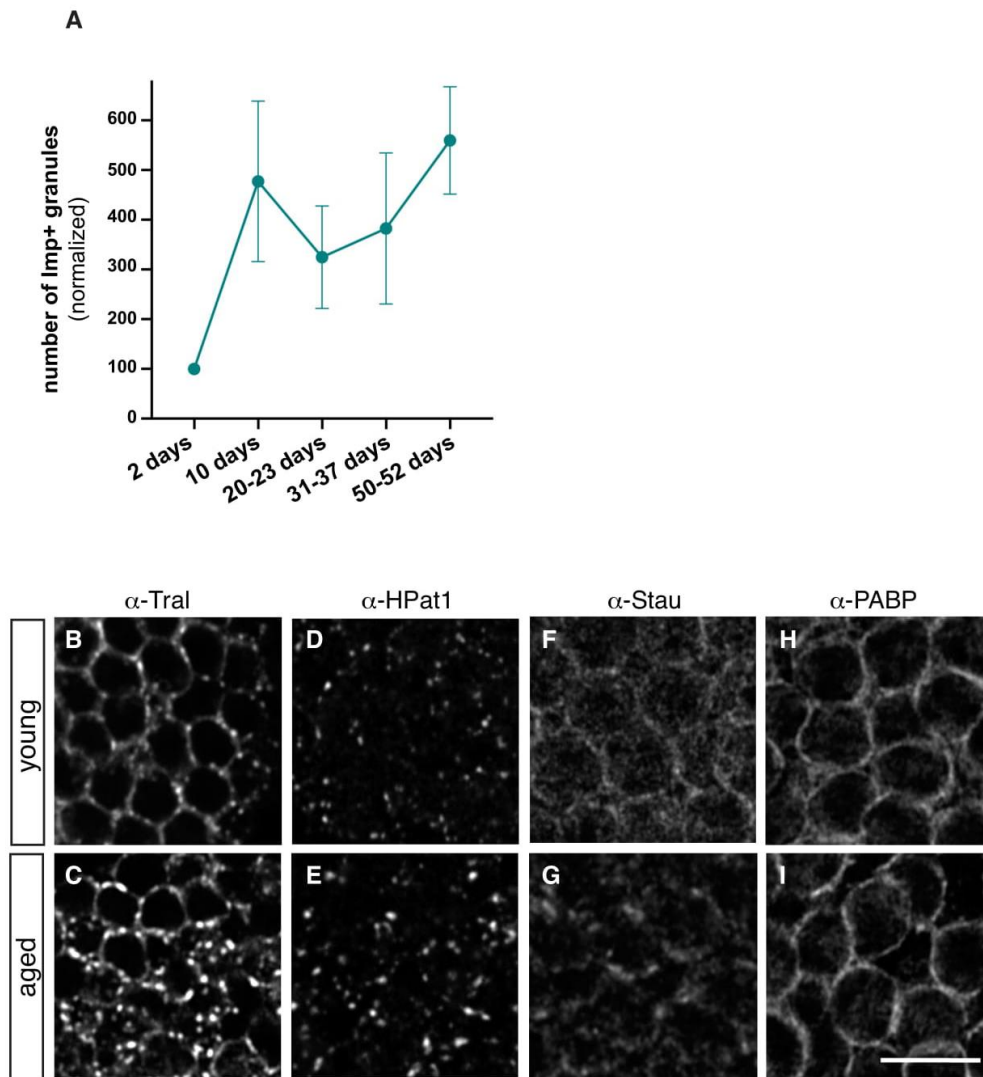


Figure S1. Clustering of RNP granule components – related to Figure 1

(A) Mean number of Imp-containing granules upon gradual aging (per surface area, normalized to 2 days). Three replicates were performed per condition. At least 15 samples were analyzed per condition. Error bars represent s.e.m. (B-I) Cell bodies of MB γ neurons imaged from 2 day- (“young”; B,D,F,H), or 37-38 day- (“aged”; C,E,G,I) old brains. Brains were stained with anti-Tral (B,C), anti-HPat1 (D,E), anti-Stau (F,G) or anti-PABP (H,I) antibodies. Scale bar: 5 μ m.

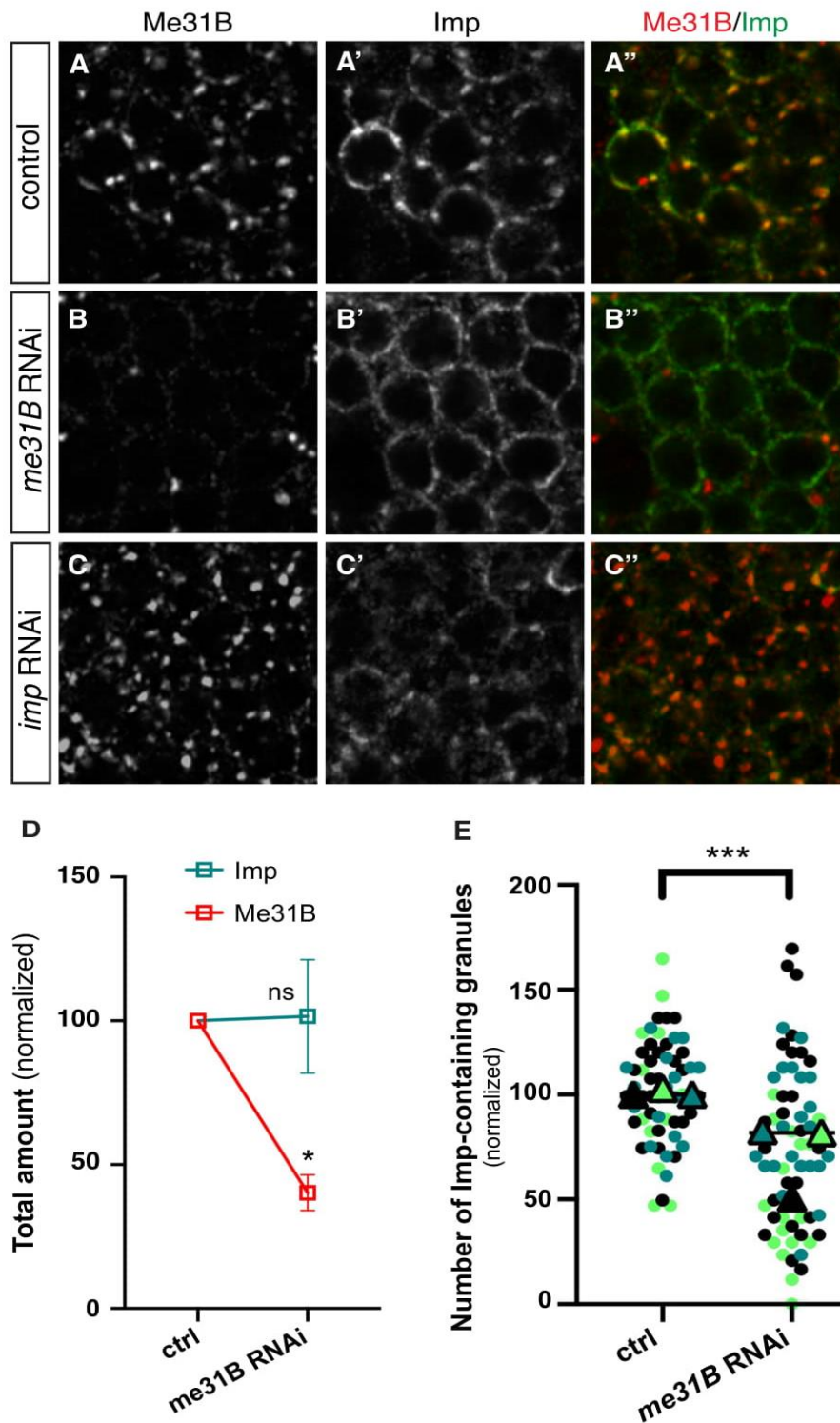


Figure S2. *me31B*, but not *imp*, is required for nucleation of neuronal RNP granules *related to Figure 3*

(A-C) Cell bodies of GFP-*Imp*-expressing MB γ neurons stained with anti-*Me31B* (A-C; red in A''-C'') and anti-*Imp* (A'-C'; green in A''-C'') antibodies. Cell bodies shown in B and C were subjected to *me31B* and *imp* RNAi respectively. Scale bar: 5 μ m. (D) Total amount of *Imp* (green)

and Me31B (red) in MB γ neurons from control and *me31B* RNAi brains. Data were normalized to the control values. Each data point represents the mean value obtained in four independent replicates. Error bars represent s.e.m. *, $P < 0.05$ (Mann Whitney test on replicate means). (E) Number of Imp⁺ granules (per surface area, normalized) in control and *me31B* RNAi conditions. Three replicates were performed and the mean value of each replicate is indicated as a symbol (triangle). Data points were color-coded based on the experimental replicate they belong to. At least 12 fields were imaged per condition. ***, $P < 0.001$ (unpaired t-test). n.s. stands for not significant. Complete genotype: UAS-*me31B*-RNAi (or UAS-*imp*-RNAi)/tub-Gal80ts;OK107-Gal4/+.

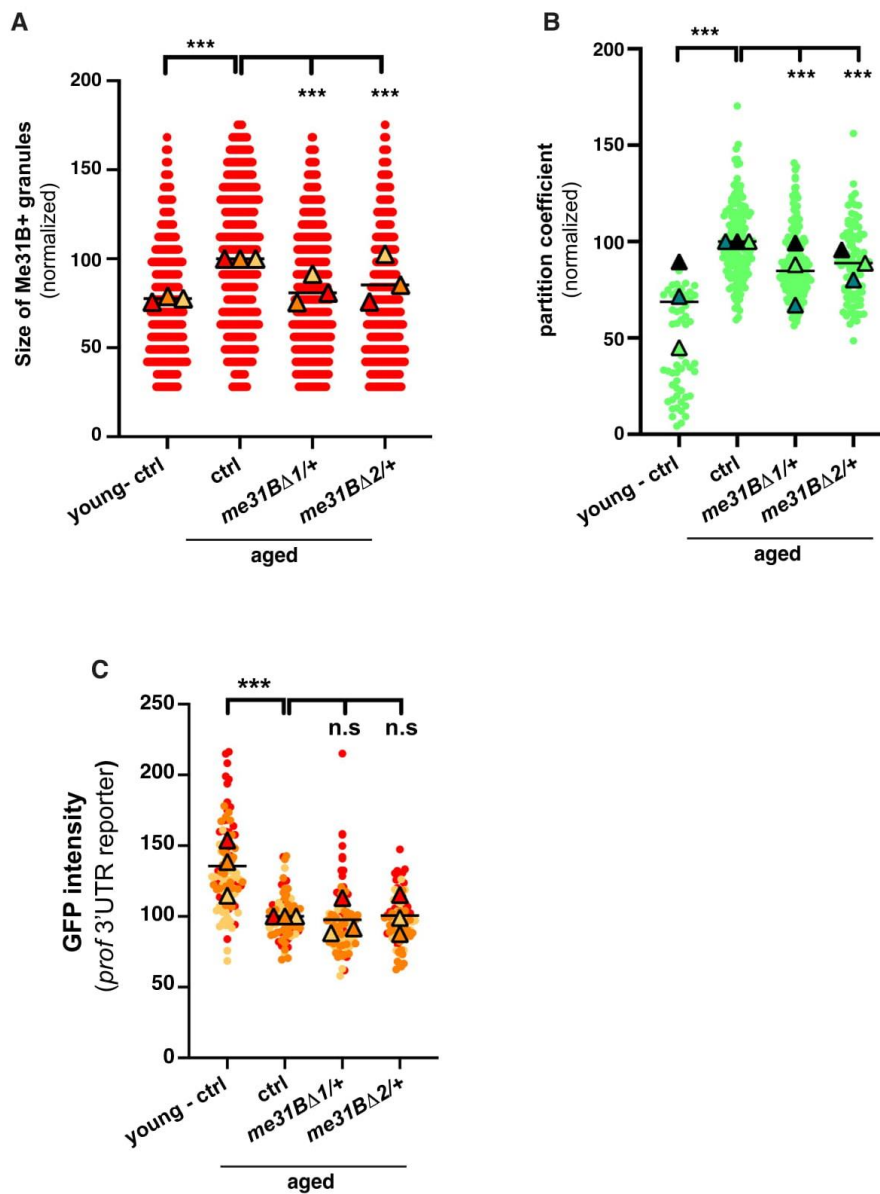


Figure S3. Reducing the dosage of *me31B* differentially impacts on Me31B and Imp – related to Figure 4

(A) Size of Me31B-containing granules in control (ctrl) and heterozygous (*me31BΔ1/+* or *me31BΔ2/+*) brains from 2 day- (young) or 37-40 day- (aged) flies. Values were normalized to the aged control condition. Three replicates were performed and the mean value of each replicate is indicated as a symbol (triangle). The distribution of granule sizes is shown for one replicate only. (B) Distributions of Imp partition coefficients. Partition coefficients were estimated by dividing the maximal intensity of Me31B signal in individual RNP granules to the intensity of the cytoplasmic diffuse pool (see Materials and Methods), and calculated for each granule detected in the imaged fields. Three replicates were performed and the mean value of each replicate is indicated as a symbol (triangle). The distribution of individual granule partition coefficients is shown for one replicate only. (C) GFP signal intensities measured from brains expressing EGFP-*profilin* 3'UTR. At least 16 fields were imaged per condition. Three replicates were performed and the mean value of each replicate is indicated as a symbol (triangle). Data points were color-coded based on the experimental replicate they belong to. ***, $P < 0.001$ (one-way ANOVA test with Sidak's multiple comparison tests, performed on individual data points). n.s. stands for not significant.

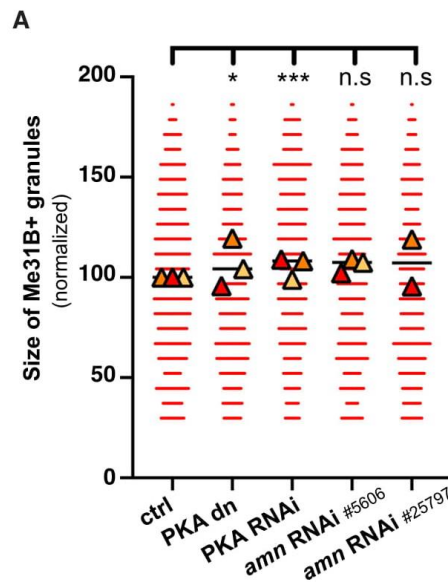


Figure S4. Impact of PKA inactivation of Me31B-containing granule size – related to Figure 5

(A) Size of Me31B-containing granules in control (ctrl) and heterozygous (*me31BΔ1/+* or *me31BΔ2/+*) brains from 2 day- (young) or 37-40 day- (aged) flies. Values were normalized to the control condition. Three replicates were performed and the mean value of each replicate is

indicated as a symbol (triangle). The distribution of granule sizes is shown for one replicate only. *, $P < 0.05$; ***, $P < 0.001$ (one-way ANOVA test with Sidak's multiple comparison tests, performed on individual data points). n.s. stands for not significant.

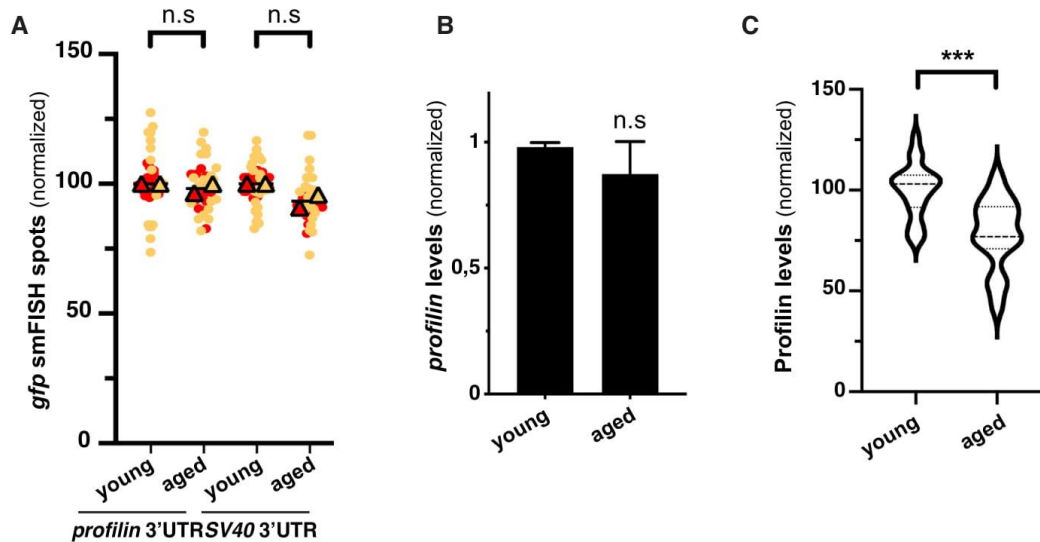


Figure S5. Translation, not RNA stability is modified upon aging – related to Figure 6

(A) Numbers of *gfp* smFISH spots (per surface area) in 2 day- (young) and 37-40 day- (aged) brains expressing EGFP-*profilin* (left) or SV40 (right) 3'UTR reporters. Values were normalized to the young condition. Two replicates were performed and the mean value of each replicate is indicated as a symbol (triangle). Data points were color-coded based on the experimental replicate they belong to. (B) Endogenous *profilin* RNA levels. RNA levels were quantified by quantitative RT-PCR and normalized to those of *rp49* and *rpl7*. n.s. stands for not significant. (C) Normalized *Profilin* protein levels measured after immunostaining on 2 day (young) or 37-38 (aged) day-old *Drosophila* brains. ***, $P < 0.001$ (Mann Whitney test).

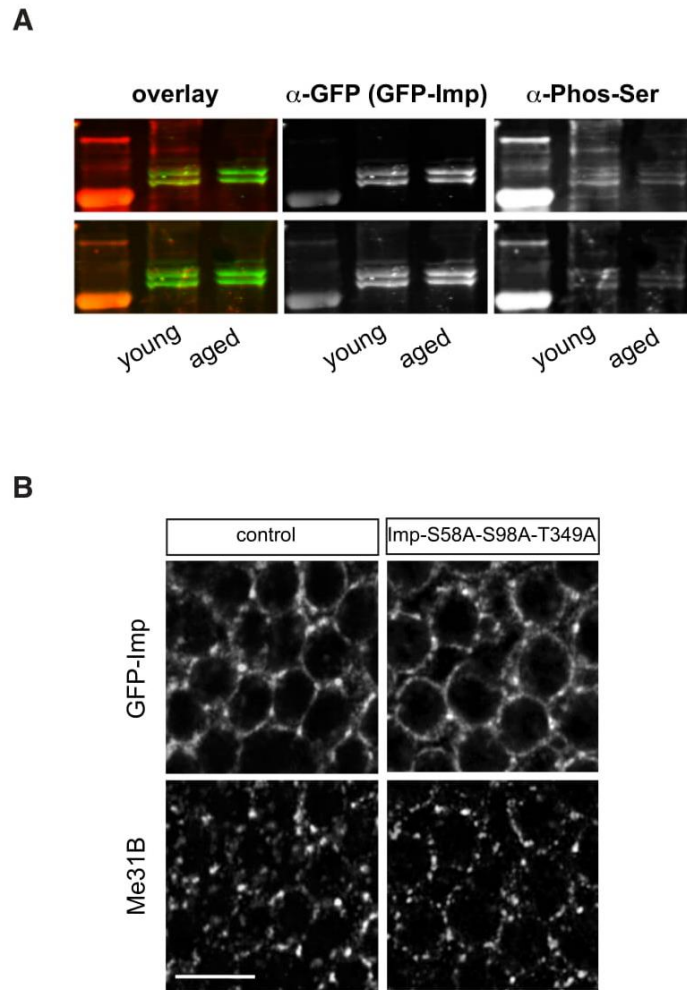


Figure S6. Imp is phosphorylated on Serines, but its putative PKA phosphorylation sites are dispensable for Imp condensation.

(A) Western-Blot performed on fractions recovered after immuno-precipitation of GFP-Imp proteins from GFP-Imp-G080 head lysates. Head lysates were prepared from 2 day-old (young) or 37-40 day- old (aged) flies. Two different anti-phos-Ser antibodies were used for the Western-Blot: a mouse anti-Phos-Ser (Sigma #P3430; upper panel) and a rabbit anti-Phos-Ser (Abcam #ab9332; lower panel). Both revealed bands co-localizing with the GFP-Imp ones. (B) Cell bodies of MB γ neurons from 37-40 day-old control GFP-Imp-G080 (left) and mutant GFP-Imp--S58A-S98A-T349A (right) brains. Imp condensed to a similar degree in both conditions. Scale bar: 5 μ m.

Table S1. List of lines tested in the selective screen for modifiers of Imp clustering						
Pathway	Gene	Construct	Stock reference	Source	Modification of Imp condensation in aged flies ?	
ROS	Sod1	UAS-Sod1.RNAi	24491	BDSC	no	
		UAS-Sod1	33605	BDSC	no	
		UAS-Sod1 RNAi	36804	BDSC	no	
		UAS-Sod2 RNAi	25969	BDSC	no	
Sod and catalase	Catalase	UAS cat/cyo; UAS sod/tm		Bolan Laura	no	
		UAS-Cat.A	24621		no	
chaperones	hsp 22	UAS hsp22 RNAi (GD)	v43632	VDRG	no	
		UAS hsp22	20055	BDSC	no	
		UAS_Hsc70wt	5846	BDSC	no	
Autophagy	Atg1	yw,hsflp;UASatg1		Neufeld Thomas	no	
Insulin pathway	InR	UAS InR DN	8251	BDSC	no	
		UAS InR CA	8263	BDSC	no	
Aging-related genes	sirt2	UAS sirt2 RNAi	31613	BDSC	no	
		UAS sirt1 RNAi	53697	BDSC	no	
	sirt1	UAS sirt1 (low expression)	44217	BDSC	no	
		UAS sirt1 (high expression)	44216	BDSC	no	
	Methusellah	UAS mth	64194	BDSC	no	
		mth mutant	27896	BDSC	no	
mth RNAi		27495	BDSC	no		
Methyl transferase	Methyl transferase	mth RNAi	67829	BDSC	no	
		UAS Mettl3 RNAi	41590	BDSC	no	
Mitochondrial function	surf1	UAS surf1 RNAi	51783	BDSC	no	
		UAS surf1 RNAi	51783	BDSC	no	
	TFAM	UAS TFAM RNAi	26744	BDSC	no	
		UAS TFAM RNAi	57742	BDSC	no	
	dj1-β	UAS dj1-β	33604	BDSC	no	

Table S1. List of pathways tested to identify potential regulator of IMP granule remodeling upon aging.

7.7. References

- Akalal DB, Yu D, Davis RL. 2010. A late-phase, long-term memory trace forms in the γ neurons of *Drosophila* mushroom bodies after olfactory classical conditioning. *J Neurosci* **30**: 16699-16708.
- Alberti S. 2017a. Phase separation in biology. *Curr Biol* **27**: R1097-R1102.
- . 2017b. The wisdom of crowds: regulating cell function through condensed states of living matter. *J Cell Sci* **130**: 2789-2796.
- Alberti S, Hyman AA. 2016. Are aberrant phase transitions a driver of cellular aging? *Bioessays* **38**: 959-968.
- Anisimova AS, Alexandrov AI, Makarova NE, Gladyshev VN, Dmitriev SE. 2018. Protein synthesis and quality control in aging. *Aging* **10**: 4269-4288.
- Banani SF, Lee HO, Hyman AA, Rosen MK. 2017. Biomolecular condensates: organizers of cellular biochemistry. *Nat Rev Mol Cell Biol* **18**: 285-298.
- Banani SF, Rice AM, Peeples WB, Lin Y, Jain S, Parker R, Rosen MK. 2016. Compositional Control of Phase-Separated Cellular Bodies. *Cell* **166**: 651-663.
- Bellon A, Iyer A, Bridi S, Lee FCY, Ovando-Vázquez C, Corradi E, Longhi S, Rocuzzo M, Strohbuecker S, Naik S et al. 2017. miR-182 Regulates Slit2-Mediated Axon Guidance by Modulating the Local Translation of a Specific mRNA. *Cell Rep* **18**: 1171-1186.
- Bowden HA, Dormann D. 2016. Altered mRNP granule dynamics in FTLD pathogenesis. *J Neurochem* **138 Suppl 1**: 112-133.
- Brangwynne CP, Eckmann CR, Courson DS, Rybarska A, Hoege C, Gharakhani J, Jülicher F, Hyman AA. 2009. Germline P granules are liquid droplets that localize by controlled dissolution/condensation. *Science (New York, NY)* **324**: 1729-1732.
- Buchan JR. 2014. mRNP granules. Assembly, function, and connections with disease. *RNA Biol* **11**: 1019-1030.
- Cohan MC, Pappu RV. 2020. Making the Case for Disordered Proteins and Biomolecular Condensates in Bacteria. *Trends Biochem Sci*.
- Conicella AE, Zerze GH, Mittal J, Fawzi NL. 2016. ALS Mutations Disrupt Phase Separation Mediated by α -Helical Structure in the TDP-43 Low-Complexity C-Terminal Domain. *Structure (London, England : 1993)* **24**: 1537-1549.
- Cougot N, Bhattacharyya SN, Tapia-Arancibia L, Bordonne R, Filipowicz W, Bertrand E, Rage F. 2008. Dendrites of mammalian neurons contain specialized P-body-like structures that respond to neuronal activation. *J Neurosci* **28**: 13793-13804.
- De Graeve F, Besse F. 2018. Neuronal RNP granules: from physiological to pathological assemblies. *Biol Chem* **399**: 623-635.
- De Graeve F, Debreuve E, Rahmoun S, Ecsedi S, Bahri A, Hubstenberger A, Descombes X, Besse F. 2019. Detecting and quantifying stress granules in tissues of multicellular organisms with the Obj.MPP analysis tool. *Traffic*.
- Decker CJ, Parker R. 2012. P-bodies and stress granules: possible roles in the control of translation and mRNA degradation. *Cold Spring Harb Perspect Biol* **4**: a012286.
- Ditlev JA, Case LB, Rosen MK. 2018. Who's In and Who's Out-Compositional Control of Biomolecular Condensates. *J Mol Biol* **430**: 4666-4684.
- Dunn TA, Wang CT, Colicos MA, Zaccolo M, DiPilato LM, Zhang J, Tsien RY, Feller MB. 2006. Imaging of cAMP levels and protein kinase A activity reveals that retinal waves drive oscillations in second-messenger cascades. *J Neurosci* **26**: 12807-12815.
- El Fatimy R, Davidovic L, Tremblay S, Jaglin X, Dury A, Robert C, De Koninck P, Khandjian EW. 2016. Tracking the Fragile X Mental Retardation Protein in a Highly Ordered Neuronal RiboNucleoParticles Population: A Link between Stalled Polyribosomes and RNA Granules. *PLoS Genet* **12**: e1006192.

- Formicola N, Vijayakumar J, Besse F. 2019. Neuronal ribonucleoprotein granules: Dynamic sensors of localized signals. *Traffic* **20**: 639-649.
- Fritzsche R, Karra D, Bennett KL, Ang FY, Heraud-Farlow JE, Tolino M, Doyle M, Bauer KE, Thomas S, Panyavsky M et al. 2013. Interactome of two diverse RNA granules links mRNA localization to translational repression in neurons. *Cell Rep* **5**: 1749-1762.
- Gerbich TM, McLaughlin GA, Cassidy K, Gerber S, Adalsteinsson D, Gladfelter AS. 2020. Phosphoregulation provides specificity to biomolecular condensates in the cell cycle and cell polarity. *The Journal of cell biology* **219**.
- Gopal PP, Nirschl JJ, Klinman E, Holzbaur EL. 2017. Amyotrophic lateral sclerosis-linked mutations increase the viscosity of liquid-like TDP-43 RNP granules in neurons. *Proc Natl Acad Sci U S A* **114**: E2466-E2475.
- Hillebrand J, Pan K, Kokaram A, Barbee S, Parker R, Ramaswami M. 2010. The Me31B DEAD-Box Helicase Localizes to Postsynaptic Foci and Regulates Expression of a CaMKII Reporter mRNA in Dendrites of Drosophila Olfactory Projection Neurons. *Front Neural Circuits* **4**: 121.
- Hofweber M, Dormann D. 2018. Friend or foe - post-translational modifications as regulators of phase separation and RNP granule dynamics. *J Biol Chem* **294**: 7137-7150.
- Hubstenberger A, Courel M, Bénard M, Souquere S, Ernoult-Lange M, Chouaib R, Yi Z, Morlot JB, Munier A, Fradet M et al. 2017. P-Body Purification Reveals the Condensation of Repressed mRNA Regulons. *Molecular cell* **68**: 144-157.e145.
- Huttelmaier S, Zenklusen D, Lederer M, Dichtenberg J, Lorenz M, Meng X, Bassell GJ, Condeelis J, Singer RH. 2005. Spatial regulation of beta-actin translation by Src-dependent phosphorylation of ZBP1. *Nature* **438**: 512-515.
- Hyman AA, Weber CA, Jülicher F. 2014. Liquid-liquid phase separation in biology. *Annual review of cell and developmental biology* **30**: 39-58.
- Jain S, Wheeler JR, Walters RW, Agrawal A, Barsic A, Parker R. 2016. ATPase-Modulated Stress Granules Contain a Diverse Proteome and Substructure. *Cell* **164**: 487-498.
- Keene AC, Waddell S. 2007. Drosophila olfactory memory: single genes to complex neural circuits. *Nature reviews Neuroscience* **8**: 341-354.
- Keleman K, Krüttner S, Alenius M, Dickson BJ. 2007. Function of the Drosophila CPEB protein Orb2 in long-term courtship memory. *Nature neuroscience* **10**: 1587-1593.
- Khong A, Matheny T, Jain S, Mitchell SF, Wheeler JR, Parker R. 2017. The Stress Granule Transcriptome Reveals Principles of mRNA Accumulation in Stress Granules. *Molecular cell* **68**: 808-820.e805.
- Kim TH, Tsang B, Vernon RM, Sonenberg N, Kay LE, Forman-Kay JD. 2019. Phospho-dependent phase separation of FMRP and CAPRIN1 recapitulates regulation of translation and deadenylation. *Science (New York, NY)* **365**: 825-829.
- Kina H, Yoshitani T, Hanyu-Nakamura K, Nakamura A. 2019. Rapid and efficient generation of GFP-knocked-in Drosophila by the CRISPR-Cas9-mediated genome editing. *Development, Growth and Differentiation* **61**: 265-275.
- Kohrmann M, Luo M, Kaether C, DesGroseillers L, Dotti CG, Kiebler MA. 1999. Microtubule-dependent recruitment of Staufen-green fluorescent protein into large RNA-containing granules and subsequent dendritic transport in living hippocampal neurons. *Mol Biol Cell* **10**: 2945-2953.
- Krichevsky AM, Kosik KS. 2001. Neuronal RNA granules: a link between RNA localization and stimulation-dependent translation. *Neuron* **32**: 683-696.
- Kroschwald S, Maharana S, Mateju D, Malinowska L, Nüske E, Poser I, Richter D, Alberti S. 2015. Promiscuous interactions and protein disaggregases determine the material state of stress-inducible RNP granules. *eLife* **4**: e06807.
- Langdon EM, Qiu Y, Ghanbari Niaki A, McLaughlin GA, Weidmann CA, Gerbich TM, Smith JA, Crutchley JM, Termini CM, Weeks KM et al. 2018. mRNA structure determines specificity of a polyQ-driven phase separation. *Science (New York, NY)* **360**: 922-927.

- Leung KM, van Horck FP, Lin AC, Allison R, Standart N, Holt CE. 2006. Asymmetrical beta-actin mRNA translation in growth cones mediates attractive turning to netrin-1. *Nature neuroscience* **9**: 1247-1256.
- Li YR, King OD, Shorter J, Gitler AD. 2013. Stress granules as crucibles of ALS pathogenesis. *The Journal of cell biology* **201**: 361-372.
- Lord SJ, Velle KB, Mullins RD, Fritz-Laylin LK. 2020. SuperPlots: Communicating reproducibility and variability in cell biology. *The Journal of cell biology* **219**.
- Markmiller S, Soltanieh S, Server KL, Mak R, Jin W, Fang MY, Luo EC, Krach F, Yang D, Sen A et al. 2018. Context-Dependent and Disease-Specific Diversity in Protein Interactions within Stress Granules. *Cell* **172**: 590-604.e513.
- Mayford M, Baranes D, Podsypanina K, Kandel ER. 1996. The 3'-untranslated region of CaMKII alpha is a cis-acting signal for the localization and translation of mRNA in dendrites. *Proc Natl Acad Sci U S A* **93**: 13250-13255.
- Medioni C, Ephrussi A, Besse F. 2015. Live imaging of axonal transport in Drosophila pupal brain explants. *Nat Protoc* **10**: 574-584.
- Medioni C, Ramialison M, Ephrussi A, Besse F. 2014. Imp promotes axonal remodeling by regulating profilin mRNA during brain development. *Curr Biol* **24**: 793-800.
- Mikl M, Vendra G, Kiebler MA. 2011. Independent localization of MAP2, CaMKIIalpha and beta-actin RNAs in low copy numbers. *EMBO Rep* **12**: 1077-1084.
- Miller LC, Blandford V, McAdam R, Sanchez-Carbente MR, Badeaux F, DesGroseillers L, Sossin WS. 2009. Combinations of DEAD box proteins distinguish distinct types of RNA: protein complexes in neurons. *Molecular and cellular neurosciences* **40**: 485-495.
- Mittag T, Parker R. 2018. Multiple Modes of Protein-Protein Interactions Promote RNP Granule Assembly. *J Mol Biol* **430**: 4636-4649.
- Moon IS, Cho SJ, Seog DH, Walikonis R. 2009. Neuronal activation increases the density of eukaryotic translation initiation factor 4E mRNA clusters in dendrites of cultured hippocampal neurons. *Experimental & molecular medicine* **41**: 601-610.
- Nakamura A, Amikura R, Hanyu K, Kobayashi S. 2001. Me31B silences translation of oocyte-localizing RNAs through the formation of cytoplasmic RNP complex during Drosophila oogenesis. *Development* **128**: 3233-3242.
- Nezis IP, Simonsen A, Sagona AP, Finley K, Gaumer S, Contamine D, Rusten TE, Stenmark H, Brech A. 2008. Ref(2)P, the Drosophila melanogaster homologue of mammalian p62, is required for the formation of protein aggregates in adult brain. *The Journal of cell biology* **180**: 1065-1071.
- Ori A, Toyama BH, Harris MS, Bock T, Iskar M, Bork P, Ingolia NT, Hetzer MW, Beck M. 2015. Integrated Transcriptome and Proteome Analyses Reveal Organ-Specific Proteome Deterioration in Old Rats. *Cell systems* **1**: 224-237.
- Patel A, Lee HO, Jawerth L, Maharana S, Jahnle M, Hein MY, Stoyanov S, Mahamid J, Saha S, Franzmann TM et al. 2015. A Liquid-to-Solid Phase Transition of the ALS Protein FUS Accelerated by Disease Mutation. *Cell* **162**: 1066-1077.
- Piper M, Anderson R, Dwivedy A, Weinl C, van Horck F, Leung KM, Cogill E, Holt C. 2006. Signaling mechanisms underlying Slit2-induced collapse of Xenopus retinal growth cones. *Neuron* **49**: 215-228.
- Protter DSW, Rao BS, Van Treeck B, Lin Y, Mizoue L, Rosen MK, Parker R. 2018. Intrinsically Disordered Regions Can Contribute Promiscuous Interactions to RNP Granule Assembly. *Cell Rep* **22**: 1401-1412.
- Ramachandran V, Shah KH, Herman PK. 2011. The cAMP-dependent protein kinase signaling pathway is a key regulator of P body foci formation. *Molecular cell* **43**: 973-981.
- Ramaswami M, Taylor JP, Parker R. 2013. Altered ribostasis: RNA-protein granules in degenerative disorders. *Cell* **154**: 727-736.
- Riback JA, Brangwynne CP. 2020. Can phase separation buffer cellular noise? *Science (New York, NY)* **367**: 364-365.

- Riggs CL, Kedersha N, Ivanov P, Anderson P. 2020. Mammalian stress granules and P bodies at a glance. *J Cell Sci* **133**.
- Sachdev R, Hondele M, Linsenmeier M, Vallotton P, Mugler CF, Arosio P, Weis K. 2019. Pat1 promotes processing body assembly by enhancing the phase separation of the DEAD-box ATPase Dhh1 and RNA. *eLife* **8**.
- Sanders DW, Kedersha N, Lee DSW, Strom AR, Drake V, Riback JA, Bracha D, Eeftens JM, Iwanicki A, Wang A et al. 2020. Competing Protein-RNA Interaction Networks Control Multiphase Intracellular Organization. *Cell* **181**: 306-324 e328.
- Shin Y, Brangwynne CP. 2017. Liquid phase condensation in cell physiology and disease. *Science (New York, NY)* **357**.
- Snead WT, Gladfelter AS. 2019. The Control Centers of Biomolecular Phase Separation: How Membrane Surfaces, PTMs, and Active Processes Regulate Condensation. *Molecular cell* **76**: 295-305.
- Stegeman R, Weake VM. 2017. Transcriptional Signatures of Aging. *J Mol Biol* **429**: 2427-2437.
- Tang NH, Kim KW, Xu S, Blazie SM, Yee BA, Yeo GW, Jin Y, Chisholm AD. 2020. The mRNA Decay Factor CAR-1/LSM14 Regulates Axon Regeneration via Mitochondrial Calcium Dynamics. *Curr Biol* **30**: 865-876.e867.
- Tiruchinapalli DM, Oleynikov Y, Kelic S, Shenoy SM, Hartley A, Stanton PK, Singer RH, Bassell GJ. 2003. Activity-dependent trafficking and dynamic localization of zipcode binding protein 1 and beta-actin mRNA in dendrites and spines of hippocampal neurons. *J Neurosci* **23**: 3251-3261.
- Topisirovic I, Siddiqui N, Orolicki S, Skrabanek LA, Tremblay M, Hoang T, Borden KL. 2009. Stability of eukaryotic translation initiation factor 4E mRNA is regulated by HuR, and this activity is dysregulated in cancer. *Molecular and cellular biology* **29**: 1152-1162.
- Trcek T, Lehmann R. 2019. Germ granules in Drosophila. *Traffic* **20**: 650-660.
- Tsang B, Arsenaault J, Vernon RM, Lin H, Sonenberg N, Wang LY, Bah A, Forman-Kay JD. 2019. Phosphoregulated FMRP phase separation models activity-dependent translation through bidirectional control of mRNA granule formation. *Proc Natl Acad Sci U S A*.
- Tudisca V, Recouvreux V, Moreno S, Boy-Marcotte E, Jacquet M, Portela P. 2010. Differential localization to cytoplasm, nucleus or P-bodies of yeast PKA subunits under different growth conditions. *European journal of cell biology* **89**: 339-348.
- Turrel O, Rabah Y, Plaçaïs PY, Goguel V, Preat T. 2020. Drosophila Middle-Term Memory: Amnesiac is Required for PKA Activation in the Mushroom Bodies, a Function Modulated by Neprilysin 1. *J Neurosci* **40**: 4219-4229.
- Van Treeck B, Parker R. 2018. Emerging Roles for Intermolecular RNA-RNA Interactions in RNP Assemblies. *Cell* **174**: 791-802.
- Vijayakumar J, Perrois C, Heim M, Bousset L, Alberti S, Besse F. 2019. The prion-like domain of Drosophila Imp promotes axonal transport of RNP granules in vivo. *Nat Commun* **10**: 2593.
- Voronina E, Seydoux G, Sassone-Corsi P, Nagamori I. 2011. RNA granules in germ cells. *Cold Spring Harb Perspect Biol* **3**.
- Walther DM, Mann M. 2011. Accurate quantification of more than 4000 mouse tissue proteins reveals minimal proteome changes during aging. *Molecular & cellular proteomics : MCP* **10**: M110.004523.
- Wang C, Schmich F, Srivatsa S, Weidner J, Beerenwinkel N, Spang A. 2018. Context-dependent deposition and regulation of mRNAs in P-bodies. *eLife* **7**.
- Wood SH, Craig T, Li Y, Merry B, de Magalhães JP. 2013. Whole transcriptome sequencing of the aging rat brain reveals dynamic RNA changes in the dark matter of the genome. *Age (Dordrecht, Netherlands)* **35**: 763-776.
- Yamazaki D, Horiuchi J, Nakagami Y, Nagano S, Tamura T, Saitoe M. 2007. The Drosophila DCO mutation suppresses age-related memory impairment without affecting lifespan. *Nature neuroscience* **10**: 478-484.
- Youn JY, Dyakov BJA, Zhang J, Knight JDR, Vernon RM, Forman-Kay JD, Gingras AC. 2019. Properties of Stress Granule and P-Body Proteomes. *Molecular cell* **76**: 286-294.

Zeitelhofer M, Karra D, Macchi P, Tolino M, Thomas S, Schwarz M, Kiebler M, Dahm R. 2008. Dynamic interaction between P-bodies and transport ribonucleoprotein particles in dendrites of mature hippocampal neurons. *J Neurosci* **28**: 7555-7562.

Chapter III

Discussion

8. Discussion and perspectives

8.1. Loss of granule heterogeneity upon aging

Multiplexing analyses to identify the composition of purified neuronal RNP granules have shown that multiple types of RNP granules can be present in the same cell, having partial overlapping content. For instance, two distinct RNP granules isolated from rat brain lysates and characterized by the presence of Staufen2 or Barentz shared only one-third of their protein components. Characterization of the RNA content of these two granules did not show any significant overlap, indicating that neuronal RNP granules are very heterogeneous in composition (Fritzsche et al., 2013; Heraud-Farlow et al., 2013). Interestingly, neuronal RNP granule composition can change with time, for example, during differentiation or in response to activity. Such a process is seen during the maturation of cultured hippocampal neurons; 90% Pur- α granules found in immature neurons contain Staufen1 as an interacting partner, whereas this proportion reduces to 50% in mature neurons (Mitsumori et al., 2017). Another example is the KCl-induced neuronal depolarization, which was shown to trigger the association of FMRP, Staufen, and TDP43 in common RNP granules (Wang et al., 2008). These studies thus suggested that the collection of distinct neuronal RNP granules and their compositional modulation may be employed by neuronal cells to respond to changing environment and needs. How is then the sorting and composition specificity of neuronal RNP granules regulated during cellular processes? One recently proposed model for compositional control is the “scaffold-client model”: scaffold molecules form a core onto which specific client molecules are dynamically and differentially recruited depending on cellular contexts (Banani et al., 2016).

My work, using *Drosophila* neuronal RNP granules as a paradigm, demonstrated that RNP component sorting and granule composition are modulated upon aging. In young cells, two distinct populations of Me31B⁺ neuronal RNP granules were identified: IMP⁻Me31B⁺ and IMP⁺Me31B⁺. Upon aging, the number of IMP⁻Me31B⁺ granules decreased, such that the majority of Me31B⁺ granules became double positive for Me31B and IMP. This age-dependent increase in the coalescence of Me31B and Imp is an outcome of increased Me31B protein expression. First, there was almost a 1.5-fold increase in Me31B expression upon aging and second, genetically reducing the levels of Me31B in old brains significantly suppressed the loss of Me31B⁺ Imp⁻ granules. This observation is in accordance with the framework developed *in vitro* by Sanders *et al.* to explain the compositional control of RNP condensates. In this model, competition for shared molecules controls the composition of phase separated entities and their coexistence in cells. Increasing the concentration of a shared component leads to increased

miscibility of initially distinct phases to form a more homogenous phase (Sanders et al., 2020). Me31B is an RNA helicase belonging to the DEAD-box helicase family that has been shown to establish multiple interactions. Me31B interacts using its C-ter RecA-like domain with protein partners like EDC3 and Tral through their FDF motifs and to Hpat on its conserved N-ter sequence. Interestingly, each of these proteins compete for binding to Me31B and their interactions are mutually exclusive (Haas et al., 2010; Tritschler et al., 2009; Tritschler et al., 2008). Me31B can also bind multiple granule-associated mRNAs, as shown in the *Drosophila* germline where it is associating with *oskar* (Nakamura et al., 2001), *nanos* (Gotze et al., 2017), and *pgc* (Flora et al., 2018). Orthologs of Me31B were also shown to undergo oligomerization in the presence of RNA, as observed in the case of the *Xenopus* Xp54, further increasing their valency (Minshall & Standart, 2004). Thus, Me31B has the properties expected from a shared multivalent node in the Sanders et al. model. Notably, a mere increase in the stoichiometry of the common node Me31B was insufficient to trigger the collapse of granules *in vivo*, as increasing the dosage of Me31B in young brains did not induce increased condensation. This indicates an additional regulatory layer which might involve chemical modification of constituent molecules. Chemical modifications on protein/RNA molecules, indeed, can alter the valency of RNP constituents by modifying their binding affinity or binding partners (Snead & Gladfelter, 2019). Consistent with this idea, blocking PKA activity inhibits the recruitment of the client molecule IMP into RNP granules upon aging.

Interestingly, high resolution confocal imaging of IMP⁺Me31B⁺ granules revealed that the two components did not completely mix, but rather segregated into different granule subdomains, in both young and old brains. Similar microphases have already been observed for SGs when following the behaviour of three SG components: G3BP1, UBAP2L and FXR1. G3BP1 does not interact directly with FXR1, UBAP2L acts as a linker between G3BP1 and FXR1. When the ratio of G3BP1:FXR1 concentration was low, these two proteins compete for their common linker, thus occupying distinct microphases within the same granule. A high G3BP1:FXR1 concentration ratio induced the formation of a homogenous phase-separated condensate (Sanders et al., 2020). Such a mechanism involving competition for a linker molecule might also be regulating multiphase coexistence within IMP/Me31B granules. In our study, blocking PKA activity specifically inhibited IMP localization to RNP granules upon aging, without altering overall Me31B granule remodelling. This could indicate the presence of a yet-to-be identified competitor for IMP to bind Me31B. PKA mediated phosphorylation of this competitor would reduce its affinity for Me31B, thus enabling IMP-Me31B interaction. Blocking the PKA-dependent phosphorylation of this molecule would increase its affinity for Me31B and exclude IMP from granules.

Identification of the phospho-substrate(s) of PKA is now key and can be achieved using a commercially available antibody directed against PKA phospho-target sites (α -PKA-phospho-substrate RRXS*/T*). Two approaches can be envisaged: i) a candidate-based approach in which the protein fraction immuno-precipitated from head lysates with this antibody would be used for western blot using antibodies for known RNP granule components; ii) a more systematic approach in which two consecutive immunoprecipitations would be performed (immunoprecipitation of IMP followed by immunoprecipitation using PKA phospho-substrate antibody) and Mass Spectrometry used to shed light onto the PKA-phosphorylated components of the IMP interactome.

8.2. Is age-dependent RNP remodelling a boon or bane?

The large IMP/Me31B granules observed in aged MB neurons are not aggregates, as they do not stain for ubiquitination and still dynamically exchange materials with their surroundings. Furthermore, the observed age-dependent changes do not appear to result from a general alteration of RNA homeostasis, as i)- not all RBPs present in neurons showed age-dependent changes, and ii)- most of the longevity-inducing pathways tested (IIS, oxidative stress etc.) did not impact on age-dependent RNP condensation. Said so, it would be interesting to determine the physiological impact of age-dependent neuronal RNP granule remodelling.

8.2.1. Boon – RNP granules as buffering mechanism for stochastic gene expression

In biological systems, biochemical reactions exhibit inherent stochastic nature or noise. Such noises indeed introduce fluctuations in RNA and protein production, which is detrimental for a cell, negatively impacting the biosynthesis, organization, growth and replication. Noisy gene expression is not rare, as cell populations derived from a single lineage, reared under same environmental conditions, display variable amounts of gene expression (Symmons & Raj, 2016). Multiplexing analyses of proteomes and transcriptomes of aging tissue at single cell-resolution have indicated that gene expression shows huge cell-to-cell variability with progressing age (He et al., 2020). Compartmentalization has been proposed to buffer stochastic variations and recent evidence suggests that phase separation of biological macromolecules to form RNP granules may contribute to this process (Riback & Brangwynne, 2020; Stoeger et al., 2016). A theoretical framework for noise reduction by LLPS has been proposed by Klosin *et al.* for a system with single phase-separating component (Klosin et al., 2020). A phase-separating component starts forming condensates when the concentration reaches a threshold (C_{sat}). A further increase in concentration primarily changes size and number of condensates, keeping the dilute-phase concentration stable. Interestingly, phase separated organelles in cells are often multicomponent and multicomponent phase separation often does not have a fixed C_{sat} (Riback et al., 2020). How

do multicomponent phase-separated compartments buffer biomolecular concentration in cells? *Klosin et al.* addressed this issue using phase separation of the NPM1, protein found in granule component (GC) of nucleolus. They observed that the presence of the nucleolar GC reduces variations in NPM1 protein concentration in the nucleoplasm. Dissolution of the nucleolar GC during mitosis increased the noise of NPM1 protein levels in nucleoplasm (Klosin et al., 2020), indicating that multicomponent membraneless organelles buffer biomolecular expression in cells.

In our study, we could observe an increase in the size of Me31B granules with an age-dependent increase in Me31B amount. Whether such a change in Me31B upon aging corresponds to a buffering mechanism remains to be assessed. Theoretical frameworks mentioned above consider phase separation as a passive mechanism to buffer increasing component concentration. In living cells, this might not be straightforward as cells imply additional regulatory layers on phase separation mediated *via* for instance post translational modifications on proteins. Indeed, my results have indicated that increasing Me31B expression in young cells was not sufficient to induce Me31B condensation to larger granules.

8.2.2. Bane - age-dependent memory impairment (AMI)

PKA/cAMP signalling plays a central role in regulating memory formation in metazoans (Abel & Nguyen, 2008; Kandel, 2012). In *Drosophila*, the PKA pathway has been shown to be essential for learning and memory. First, components of the PKA pathway, including PKA, are preferentially expressed in MB neurons (Han et al., 1992; Nighorn et al., 1991; Skoulakis et al., 1993). As revealed by recent transcriptomic analysis of isolated MB nuclei, cAMP/PKA pathway components showed specific upregulation after memory induction (Jones et al., 2018). Second, mutants for components of this pathway elicit memory deficits (Margulies et al., 2005). Overexpressing PKA (Drain et al., 1991; Yamazaki et al., 2007), or decreasing PKA activity by mutations in its catalytic subunit, impair memory (Li et al., 1996; Skoulakis et al., 1993), indicating that learning and memory in *Drosophila* MB neurons is highly sensitive to PKA expression levels and activity. Whether PKA expression and/or activity varies in these cell type upon aging remains to be clarified. Previous work has shown that PKA expression and activity do not globally change with age, but these analyses were carried out in entire fly head lysates, thus masking potential cell-type differences (Yamazaki et al., 2007). Furthermore, previous studies have shown that age-dependent alterations in PKA activity are not homogenous throughout the brain tissue. In rat brain, for instance, there is reduction in PKA activity in the hippocampus with advancing age, whereas PKA activity in prefrontal cortex increases upon aging as indicated by increased levels of its phosphotarget CREB (Ramos et al., 2003). Variations in PKA activity may even be restricted to specific subcellular compartments within *Drosophila* MB neurons. Treatment with forskolin, an activator of the adenylyl cyclase enzyme that increases cAMP levels and thus activates PKA, was indeed shown to induce a dynamic range of PKA

activity in dendrites but not in cell bodies (Gervasi et al., 2010). Such a differential response to a uniformly applied activator indicates the existence of functional compartmentalization within the MBs for cAMP/PKA signalling. Measuring PKA activity in specific cell populations and in subcellular regions upon aging is thus required to understand how aging-dependent modulations of PKA activity affect molecular interactions and functions. Expressing reporters such as the Foster energy resonance transfer (FRET)-based, AKAR2 (Gervasi et al., 2010) or the PKA-phosphorylation induced LLPS reporter, SPARK (Sears & Broadie, 2020), in MB neurons can be utilised to measure PKA activity with advancing age.

Metazoans display cognitive decline associated with advanced chronological age; a process known as age-dependent memory impairment (AMI) (Gallagher, 1997). As shown using the olfactory conditioning assay, *Drosophila* also display AMI, characterized by ~35-40% reduction in mid-term memory (Yamazaki & Saitoe, 2008). Remarkably, this form of AMI was shown to depend on the PKA pathway, as it was suppressed in mutants for *amnesiac* and *dc0* (*pka catalytic subunit c1*) (Tamura et al., 2003; Yamazaki et al., 2007), or in flies that have reduced PKA catalytic activity (Yamazaki et al., 2010). To date, the mechanisms downstream of the PKA pathway regulating AMI are still unknown. Interestingly, our study has unravelled a novel role for PKA activity in MB neurons in age-dependent condensation of RNP components and translational repression. Blocking PKA activity by expressing a dominant negative allele of PKA, or by knocking down *pka* or the PKA activator *amnesiac* through RNAi, inhibited IMP condensation into the neuronal RNP granules found in old brains and led to translational derepression. Furthermore, recent results from our lab supports the idea that IMP is essential for memory in *Drosophila*, as IMP deficient flies display long-term memory deficits upon courtship conditioning (B. De Queiroz, unpublished results). These results thus raise the hypothesis that age-induced remodelling of IMP-positive neuronal RNP granules reduces the translation of associated mRNAs, leading to AMI. iCLIP data from *Drosophila* S2R cell lysate identified Imp mRNA targets related to neuronal development and differentiation in the IMP interactome (Hansen, H T, et al, Genome Biology, 2015), however a comprehensive analysis of RNA molecules bound by IMP granules in neurons is still lacking. It would be interesting to analyze the RNA content of IMP/Me31B granules in young and old MB neurons to identify different interacting RNA molecules. Although RIP-seq experiments to identify Imp-bound mRNAs from head lysates has been optimized (M. Heim and F. Besse), purification of intact granules has not. This could be achieved using density-gradient centrifugation or FAPS.

Since cells utilize RNP granules as platforms for regulating gene expression and signalling, neuronal IMP/Me31B RNP granule modulation by PKA pathway could be a potential mechanism driving AMI. Identifying potential phosphorylation targets of PKA would then allow one to address whether PKA phosphorylation of granule components result in AMI. Indeed, memory

assays could be performed using PKA non-phosphorylatable mutants of granule components to test this hypothesis. Such a study could unveil a novel and potentially conserved axis of regulation involving the PKA pathway, neuronal RNP granules and AMI.

8.3. Global versus gene-specific changes in translation upon aging

Integrating genomics and proteomics approaches coupling RNA-seq, Ribo-seq and peptide mass spectrometry has become a common theme in aging research, enabling a precise assessment of gene expression changes in tissues and organs (He et al., 2020). Surprisingly, these studies have shown that globally, only subtle variations in gene and protein expression are observed upon aging, and that these variations are less important than variations between different aging tissues. For instance, integrated genomics and proteomics studies performed on aging rat tissues have shown that the vast majority (>90%) of genes and proteins exhibit stable expression in tissues across aging (Jiang et al., 2001; Lee et al., 2000; Ori et al., 2015). Similarly, the majority of proteins found in *Drosophila* postmitotic tissues showed minor or unaltered levels of expression with increasing age (Yang et al., 2019). Cell or tissue-specific upregulation or downregulation of specific pathway components are however observed upon aging. For instance, in aging fly heads, proteins involved in oxidative phosphorylation, and TCA cycle increases, while proteasomal and ribosomal proteins showed age-dependent reduction (Brown et al., 2018). Furthermore, a comparison of proteomes between old rat liver and brain samples showed that a downregulation of proteins involved in Calcium response, signal transduction, and ion channels occurs in brain, whereas in liver proteins involved in metabolic pathways are rather downregulated (Ori et al., 2015). Cells maintain their specific repertoire of proteins by regulating different mechanisms ranging from transcription and translation to localization, PTM, or degradation. Which mechanisms are modulated/altered upon aging to regulate specific sets of proteins appears to depend on tissue type. For example, analysis of aging rat tissues has shown that 15% of transcripts in brain are regulated at the level of translation compared to 2% in liver (Ori et al., 2015). How cell and tissue-specific variations in gene and protein expression are molecularly regulated upon aging still remains unexplored. Our study led to propose a mechanism by which cells can regulate translation of specific transcripts during aging. Expression of translational reporters in neurons did not exhibit a general trend of translation reduction, rather reporters that were specifically enriched in IMP/Me31B RNP granules exhibited an age-dependent translational repression. We also show that age-dependent translational repression of these target mRNAs can be derepressed by blocking PKA activity in aging neurons, suggesting that RNA enrichment in RNP granules hosting translational repressors could be a potential regulated mechanism employed by neurons to regulate specific gene and protein expression during aging.

9. Conclusion

In conclusion, my work has shown that in a physiological context like aging, stoichiometry of scaffold molecules regulates the sorting specificity and component composition of phase-separated RNP granules. I also showed that, in addition to scaffold concentration, multiple regulatory layers are imposed by cells to regulate the recruitment of client molecules. Assembly and control of phase-separated organelles is a way cells can elicit quick and tuneable response to changing environment. In this study, we provide evidence that neuronal cells remodel their RNP granule repertoire in order to reduce the translation of particular mRNA molecules, which is mediated by cAMP/PKA pathway.

There are still interesting questions that are now open for research. For example, whether RNP granule compositional control as a function of stoichiometry holds true in other physiological contexts like neuronal activation, development, etc. remains to be addressed. Furthermore, my work uncovered that the dynamic nature of IMP and Me31B in granules is preserved upon aging, a result contradicting to the prevailing notion that aging increases aggregation propensity. What are the molecular mechanisms that cells employ to counteract aggregation of RNP granules upon aging thus remains to be investigated? Also, we observed a reduction in the heterogeneity of types of RNP granules in neuronal cells upon aging. What can we infer from this reduced heterogeneity? My work emphasizes the necessity to look at condensate formation with a physiological context lens.

Bibliography

- Abel, T., & Nguyen, P. V. (2008). Regulation of hippocampus-dependent memory by cyclic AMP-dependent protein kinase. *Prog Brain Res*, *169*, 97-115. [https://doi.org/10.1016/S0079-6123\(07\)00006-4](https://doi.org/10.1016/S0079-6123(07)00006-4)
- Adekunle, D. A., & Hubstenberger, A. (2020). The multiscale and multiphase organization of the transcriptome. *Emerg Top Life Sci*, *4*(3), 265-280. <https://doi.org/10.1042/ETLS20190187>
- Advani, V. M., & Ivanov, P. (2020). Stress granule subtypes: an emerging link to neurodegeneration. *Cell Mol Life Sci*, *77*(23), 4827-4845. <https://doi.org/10.1007/s00018-020-03565-0>
- Ainsley, J. A., Drane, L., Jacobs, J., Kittelberger, K. A., & Reijmers, L. G. (2014). Functionally diverse dendritic mRNAs rapidly associate with ribosomes following a novel experience. *Nat Commun*, *5*, 4510. <https://doi.org/10.1038/ncomms5510>
- Akalal, D. B., Wilson, C. F., Zong, L., Tanaka, N. K., Ito, K., & Davis, R. L. (2006). Roles for *Drosophila* mushroom body neurons in olfactory learning and memory. *Learn Mem*, *13*(5), 659-668. <https://doi.org/10.1101/lm.221206>
- Alberti, S. (2017). Phase separation in biology. *Curr Biol*, *27*(20), R1097-R1102. <https://doi.org/10.1016/j.cub.2017.08.069>
- Alberti, S., & Hyman, A. A. (2021). Biomolecular condensates at the nexus of cellular stress, protein aggregation disease and ageing. *Nat Rev Mol Cell Biol*. <https://doi.org/10.1038/s41580-020-00326-6>
- Alberti, S., Mateju, D., Mediani, L., & Carra, S. (2017). Granulostasis: Protein Quality Control of RNP Granules. *Front Mol Neurosci*, *10*, 84. <https://doi.org/10.3389/fnmol.2017.00084>
- Altmeyer, M., Neelsen, K. J., Teloni, F., Pozdnyakova, I., Pellegrino, S., Grofte, M., Rask, M. D., Streicher, W., Jungmichel, S., Nielsen, M. L., & Lukas, J. (2015). Liquid demixing of intrinsically disordered proteins is seeded by poly(ADP-ribose). *Nat Commun*, *6*, 8088. <https://doi.org/10.1038/ncomms9088>
- Anderson, P., & Kedersha, N. (2006). RNA granules. *J Cell Biol*, *172*(6), 803-808. <https://doi.org/10.1083/jcb.200512082>
- Andrei, M. A., Ingelfinger, D., Heintzmann, R., Achsel, T., Rivera-Pomar, R., & Luhrmann, R. (2005). A role for eIF4E and eIF4E-transporter in targeting mRNPs to mammalian processing bodies. *RNA*, *11*(5), 717-727. <https://doi.org/10.1261/rna.2340405>
- Andrusiak, M. G., Sharifnia, P., Lyu, X., Wang, Z., Dickey, A. M., Wu, Z., Chisholm, A. D., & Jin, Y. (2019). Inhibition of Axon Regeneration by Liquid-like TIAR-2 Granules. *Neuron*, *104*(2), 290-304 e298. <https://doi.org/10.1016/j.neuron.2019.07.004>
- Anisimova, A. S., Alexandrov, A. I., Makarova, N. E., Gladyshev, V. N., & Dmitriev, S. E. (2018). Protein synthesis and quality control in aging. *Aging (Albany NY)*, *10*(12), 4269-4288. <https://doi.org/10.18632/aging.101721>
- Anisimova, A. S., Meerson, M. B., Geraschenko, M. V., Kulakovskiy, I. V., Dmitriev, S. E., & Gladyshev, V. N. (2020). Multifaceted deregulation of gene expression and protein synthesis with age. *Proc Natl Acad Sci U S A*, *117*(27), 15581-15590. <https://doi.org/10.1073/pnas.2001788117>
- Anselmi, C. V., Malovini, A., Roncarati, R., Novelli, V., Villa, F., Condorelli, G., Bellazzi, R., & Puca, A. A. (2009). Association of the FOXO3A locus with extreme longevity in a southern Italian centenarian study. *Rejuvenation Res*, *12*(2), 95-104. <https://doi.org/10.1089/rej.2008.0827>
- Arribas-Layton, M., Dennis, J., Bennett, E. J., Damgaard, C. K., & Lykke-Andersen, J. (2016). The C-Terminal RGG Domain of Human Lsm4 Promotes Processing Body Formation Stimulated by Arginine Dimethylation. *Mol Cell Biol*, *36*(17), 2226-2235. <https://doi.org/10.1128/MCB.01102-15>
- Aumiller, W. M., Jr., Pir Cakmak, F., Davis, B. W., & Keating, C. D. (2016). RNA-Based Coacervates as a Model for Membraneless Organelles: Formation, Properties, and Interfacial Liposome Assembly. *Langmuir*, *32*(39), 10042-10053. <https://doi.org/10.1021/acs.langmuir.6b02499>
- Aunan, J. R., Cho, W. C., & Soreide, K. (2017). The Biology of Aging and Cancer: A Brief Overview of Shared and Divergent Molecular Hallmarks. *Aging Dis*, *8*(5), 628-642. <https://doi.org/10.14336/AD.2017.0103>
- Axelrod, D., Koppel, D. E., Schlessinger, J., Elson, E., & Webb, W. W. (1976). Mobility measurement by analysis of fluorescence photobleaching recovery kinetics. *Biophys J*, *16*(9), 1055-1069. [https://doi.org/10.1016/S0006-3495\(76\)85755-4](https://doi.org/10.1016/S0006-3495(76)85755-4)
- Ayache, J., Benard, M., Ernoult-Lange, M., Minshall, N., Standart, N., Kress, M., & Weil, D. (2015). P-body assembly requires DDX6 repression complexes rather than decay or Ataxin2/2L complexes. *Mol Biol Cell*, *26*(14), 2579-2595. <https://doi.org/10.1091/mbc.E15-03-0136>

- Babinchak, W. M., Haider, R., Dumm, B. K., Sarkar, P., Surewicz, K., Choi, J. K., & Surewicz, W. K. (2019). The role of liquid-liquid phase separation in aggregation of the TDP-43 low-complexity domain. *J Biol Chem*, 294(16), 6306-6317. <https://doi.org/10.1074/jbc.RA118.007222>
- Baez, M. V., Luchelli, L., Maschi, D., Habif, M., Pascual, M., Thomas, M. G., & Boccaccio, G. L. (2011). Smaug1 mRNA-silencing foci respond to NMDA and modulate synapse formation. *J Cell Biol*, 195(7), 1141-1157. <https://doi.org/10.1083/jcb.201108159>
- Bakthavachalu, B., Huelsmeier, J., Sudhakaran, I. P., Hillebrand, J., Singh, A., Petrauskas, A., Thiagarajan, D., Sankaranarayanan, M., Mizoue, L., Anderson, E. N., Pandey, U. B., Ross, E., VijayRaghavan, K., Parker, R., & Ramaswami, M. (2018). RNP-Granule Assembly via Ataxin-2 Disordered Domains Is Required for Long-Term Memory and Neurodegeneration. *Neuron*, 98(4), 754-766 e754. <https://doi.org/10.1016/j.neuron.2018.04.032>
- Banani, S. F., Lee, H. O., Hyman, A. A., & Rosen, M. K. (2017). Biomolecular condensates: organizers of cellular biochemistry. *Nat Rev Mol Cell Biol*, 18(5), 285-298. <https://doi.org/10.1038/nrm.2017.7>
- Banani, S. F., Rice, A. M., Peeples, W. B., Lin, Y., Jain, S., Parker, R., & Rosen, M. K. (2016). Compositional Control of Phase-Separated Cellular Bodies. *Cell*, 166(3), 651-663. <https://doi.org/10.1016/j.cell.2016.06.010>
- Barbee, S. A., Estes, P. S., Cziko, A. M., Hillebrand, J., Luedeman, R. A., Collier, J. M., Johnson, N., Howlett, I. C., Geng, C., Ueda, R., Brand, A. H., Newbury, S. F., Wilhelm, J. E., Levine, R. B., Nakamura, A., Parker, R., & Ramaswami, M. (2006). Staufen- and FMRP-containing neuronal RNPs are structurally and functionally related to somatic P bodies. *Neuron*, 52(6), 997-1009. <https://doi.org/10.1016/j.neuron.2006.10.028>
- Barzilai, N., Huffman, D. M., Muzumdar, R. H., & Bartke, A. (2012). The critical role of metabolic pathways in aging. *Diabetes*, 61(6), 1315-1322. <https://doi.org/10.2337/db11-1300>
- Bassell, G. J., Zhang, H., Byrd, A. L., Femino, A. M., Singer, R. H., Taneja, K. L., Lifshitz, L. M., Herman, I. M., & Kosik, K. S. (1998). Sorting of beta-actin mRNA and protein to neurites and growth cones in culture. *J Neurosci*, 18(1), 251-265. <https://www.ncbi.nlm.nih.gov/pubmed/9412505>
- Bauer, K. E., Kiebler, M. A., & Segura, I. (2017). Visualizing RNA granule transport and translation in living neurons. *Methods*, 126, 177-185. <https://doi.org/10.1016/j.ymeth.2017.06.013>
- Beckham, C., Hilliker, A., Cziko, A. M., Noueiry, A., Ramaswami, M., & Parker, R. (2008). The DEAD-box RNA helicase Ded1p affects and accumulates in *Saccharomyces cerevisiae* P-bodies. *Mol Biol Cell*, 19(3), 984-993. <https://doi.org/10.1091/mbc.e07-09-0954>
- Bedford, M. T., & Clarke, S. G. (2009). Protein arginine methylation in mammals: who, what, and why. *Mol Cell*, 33(1), 1-13. <https://doi.org/10.1016/j.molcel.2008.12.013>
- Berry, J., Weber, S. C., Vaidya, N., Haataja, M., & Brangwynne, C. P. (2015). RNA transcription modulates phase transition-driven nuclear body assembly. *Proc Natl Acad Sci U S A*, 112(38), E5237-5245. <https://doi.org/10.1073/pnas.1509317112>
- Besse, F., & Ephrussi, A. (2008). Translational control of localized mRNAs: restricting protein synthesis in space and time. *Nat Rev Mol Cell Biol*, 9(12), 971-980. <https://doi.org/10.1038/nrm2548>
- Bianchi, E., Blaak, R., & Likos, C. N. (2011). Patchy colloids: state of the art and perspectives. *Phys Chem Chem Phys*, 13(14), 6397-6410. <https://doi.org/10.1039/c0cp02296a>
- Bley, N., Lederer, M., Pfalz, B., Reinke, C., Fuchs, T., Glass, M., Moller, B., & Huttelmaier, S. (2015). Stress granules are dispensable for mRNA stabilization during cellular stress. *Nucleic Acids Res*, 43(4), e26. <https://doi.org/10.1093/nar/gku1275>
- Boag, P. R., Atalay, A., Robida, S., Reinke, V., & Blackwell, T. K. (2008). Protection of specific maternal messenger RNAs by the P body protein CGH-1 (Dhh1/RCK) during *Caenorhabditis elegans* oogenesis. *J Cell Biol*, 182(3), 543-557. <https://doi.org/10.1083/jcb.200801183>
- Boeynaems, S., Holehouse, A. S., Weinhardt, V., Kovacs, D., Van Lindt, J., Larabell, C., Van Den Bosch, L., Das, R., Tompa, P. S., Pappu, R. V., & Gitler, A. D. (2019). Spontaneous driving forces give rise to protein-RNA condensates with coexisting phases and complex material properties. *Proc Natl Acad Sci U S A*, 116(16), 7889-7898. <https://doi.org/10.1073/pnas.1821038116>
- Boisvert, F. M., van Koningsbruggen, S., Navascues, J., & Lamond, A. I. (2007). The multifunctional nucleolus. *Nat Rev Mol Cell Biol*, 8(7), 574-585. <https://doi.org/10.1038/nrm2184>
- Boundedjah, O., Desforgues, B., Wu, T. D., Pioche-Durieu, C., Marco, S., Hamon, L., Curmi, P. A., Guerquin-Kern, J. L., Pietrement, O., & Pastre, D. (2014). Free mRNA in excess upon polysome dissociation is a scaffold for protein multimerization to form stress granules. *Nucleic Acids Res*, 42(13), 8678-8691. <https://doi.org/10.1093/nar/gku582>
- Boylan, K. L., Mische, S., Li, M., Marques, G., Morin, X., Chia, W., & Hays, T. S. (2008). Motility screen identifies *Drosophila* IGF-II mRNA-binding protein--zipcode-binding protein acting in oogenesis and synaptogenesis. *PLoS Genet*, 4(2), e36. <https://doi.org/10.1371/journal.pgen.0040036>

- Bracha, D., Walls, M. T., Wei, M. T., Zhu, L., Kurian, M., Avalos, J. L., Toettcher, J. E., & Brangwynne, C. P. (2018). Mapping Local and Global Liquid Phase Behavior in Living Cells Using Photo-Oligomerizable Seeds. *Cell*, *175*(6), 1467-1480 e1413. <https://doi.org/10.1016/j.cell.2018.10.048>
- Brangwynne, C. P., Eckmann, C. R., Courson, D. S., Rybarska, A., Hoege, C., Gharakhani, J., Julicher, F., & Hyman, A. A. (2009). Germline P granules are liquid droplets that localize by controlled dissolution/condensation. *Science*, *324*(5935), 1729-1732. <https://doi.org/10.1126/science.1172046>
- Brangwynne, C. P., Mitchison, T. J., & Hyman, A. A. (2011). Active liquid-like behavior of nucleoli determines their size and shape in *Xenopus laevis* oocytes. *Proc Natl Acad Sci U S A*, *108*(11), 4334-4339. <https://doi.org/10.1073/pnas.1017150108>
- Brown, C. J., Kaufman, T., Trinidad, J. C., & Clemmer, D. E. (2018). Proteome changes in the aging *Drosophila melanogaster* head. *Int J Mass Spectrom*, *425*, 36-46. <https://doi.org/10.1016/j.ijms.2018.01.003>
- Buchan, J. R. (2014). mRNP granules. Assembly, function, and connections with disease. *RNA Biol*, *11*(8), 1019-1030. <https://doi.org/10.4161/15476286.2014.972208>
- Buchan, J. R., Muhlrads, D., & Parker, R. (2008). P bodies promote stress granule assembly in *Saccharomyces cerevisiae*. *J Cell Biol*, *183*(3), 441-455. <https://doi.org/10.1083/jcb.200807043>
- Buchan, J. R., & Parker, R. (2009). Eukaryotic stress granules: the ins and outs of translation. *Mol Cell*, *36*(6), 932-941. <https://doi.org/10.1016/j.molcel.2009.11.020>
- Burke, K. A., Janke, A. M., Rhine, C. L., & Fawzi, N. L. (2015). Residue-by-Residue View of In Vitro FUS Granules that Bind the C-Terminal Domain of RNA Polymerase II. *Mol Cell*, *60*(2), 231-241. <https://doi.org/10.1016/j.molcel.2015.09.006>
- Buxbaum, A. R., Wu, B., & Singer, R. H. (2014). Single beta-actin mRNA detection in neurons reveals a mechanism for regulating its translatability. *Science*, *343*(6169), 419-422. <https://doi.org/10.1126/science.1242939>
- Cajigas, I. J., Tushev, G., Will, T. J., tom Dieck, S., Fuerst, N., & Schuman, E. M. (2012). The local transcriptome in the synaptic neuropil revealed by deep sequencing and high-resolution imaging. *Neuron*, *74*(3), 453-466. <https://doi.org/10.1016/j.neuron.2012.02.036>
- Calliari, A., Farias, J., Puppo, A., Canclini, L., Mercer, J. A., Munroe, D., Sotelo, J. R., & Sotelo-Silveira, J. R. (2014). Myosin Va associates with mRNA in ribonucleoprotein particles present in myelinated peripheral axons and in the central nervous system. *Dev Neurobiol*, *74*(3), 382-396. <https://doi.org/10.1002/dneu.22155>
- Campbell, D. S., & Holt, C. E. (2001). Chemotropic responses of retinal growth cones mediated by rapid local protein synthesis and degradation. *Neuron*, *32*(6), 1013-1026. [https://doi.org/10.1016/s0896-6273\(01\)00551-7](https://doi.org/10.1016/s0896-6273(01)00551-7)
- Cao, G., Li, H. B., Yin, Z., & Flavell, R. A. (2016). Recent advances in dynamic m6A RNA modification. *Open Biol*, *6*(4), 160003. <https://doi.org/10.1098/rsob.160003>
- Carlomagno, Y., Chung, D. C., Yue, M., Castanedes-Casey, M., Madden, B. J., Dunmore, J., Tong, J., DeTure, M., Dickson, D. W., Petrucelli, L., & Cook, C. (2017). An acetylation-phosphorylation switch that regulates tau aggregation propensity and function. *J Biol Chem*, *292*(37), 15277-15286. <https://doi.org/10.1074/jbc.M117.794602>
- Castello, A., Fischer, B., Eichelbaum, K., Horos, R., Beckmann, B. M., Strein, C., Davey, N. E., Humphreys, D. T., Preiss, T., Steinmetz, L. M., Krijgsveld, J., & Hentze, M. W. (2012). Insights into RNA biology from an atlas of mammalian mRNA-binding proteins. *Cell*, *149*(6), 1393-1406. <https://doi.org/10.1016/j.cell.2012.04.031>
- Chalupnikova, K., Lattmann, S., Selak, N., Iwamoto, F., Fujiki, Y., & Nagamine, Y. (2008). Recruitment of the RNA helicase RHAU to stress granules via a unique RNA-binding domain. *J Biol Chem*, *283*(50), 35186-35198. <https://doi.org/10.1074/jbc.M804857200>
- Chang, H. R., Munkhjargal, A., Kim, M. J., Park, S. Y., Jung, E., Ryu, J. H., Yang, Y., Lim, J. S., & Kim, Y. (2018). The functional roles of PML nuclear bodies in genome maintenance. *Mutat Res*, *809*, 99-107. <https://doi.org/10.1016/j.mrfmmm.2017.05.002>
- Chen, M. C., Tippiana, R., Demeshkina, N. A., Murat, P., Balasubramanian, S., Myong, S., & Ferred'Amare, A. R. (2018). Structural basis of G-quadruplex unfolding by the DEAH/RHA helicase DHX36. *Nature*, *558*(7710), 465-469. <https://doi.org/10.1038/s41586-018-0209-9>
- Chen, W., Hu, Y., Lang, C. F., Brown, J. S., Schwabach, S., Song, X., Zhang, Y., Munro, E., Bennett, K., Zhang, D., & Lee, H. C. (2020). The Dynamics of P Granule Liquid Droplets Are Regulated by the *Caenorhabditis elegans* Germline RNA Helicase GLH-1 via Its ATP Hydrolysis Cycle. *Genetics*, *215*(2), 421-434. <https://doi.org/10.1534/genetics.120.303052>
- Chen, Y., Boland, A., Kuzuoglu-Ozturk, D., Bawankar, P., Loh, B., Chang, C. T., Weichenrieder, O., & Izaurralde, E. (2014). A DDX6-CNOT1 complex and W-binding pockets in CNOT9 reveal direct

- links between miRNA target recognition and silencing. *Mol Cell*, 54(5), 737-750. <https://doi.org/10.1016/j.molcel.2014.03.034>
- Cioni, J. M., Lin, J. Q., Holtermann, A. V., Koppers, M., Jakobs, M. A. H., Azizi, A., Turner-Bridger, B., Shigeoka, T., Franze, K., Harris, W. A., & Holt, C. E. (2019). Late Endosomes Act as mRNA Translation Platforms and Sustain Mitochondria in Axons. *Cell*, 176(1-2), 56-72 e15. <https://doi.org/10.1016/j.cell.2018.11.030>
- Cirillo, L., Cieren, A., Barbieri, S., Khong, A., Schwager, F., Parker, R., & Gotta, M. (2020). UBAP2L Forms Distinct Cores that Act in Nucleating Stress Granules Upstream of G3BP1. *Curr Biol*, 30(4), 698-707 e696. <https://doi.org/10.1016/j.cub.2019.12.020>
- Clancy, D. J., Gems, D., Harshman, L. G., Oldham, S., Stocker, H., Hafen, E., Leever, S. J., & Partridge, L. (2001). Extension of life-span by loss of CHICO, a Drosophila insulin receptor substrate protein. *Science*, 292(5514), 104-106. <https://doi.org/10.1126/science.1057991>
- Clemson, C. M., Hutchinson, J. N., Sara, S. A., Ensminger, A. W., Fox, A. H., Chess, A., & Lawrence, J. B. (2009). An architectural role for a nuclear noncoding RNA: NEAT1 RNA is essential for the structure of paraspeckles. *Mol Cell*, 33(6), 717-726. <https://doi.org/10.1016/j.molcel.2009.01.026>
- Clifford, Tompa, P., & Rohit. (2015). Polymer physics of intracellular phase transitions. *Nature Physics*, 11(11), 899-904. <https://doi.org/10.1038/nphys3532>
- Conway, A. E., Van Nostrand, E. L., Pratt, G. A., Aigner, S., Wilbert, M. L., Sundararaman, B., Freese, P., Lambert, N. J., Sathe, S., Liang, T. Y., Essex, A., Landais, S., Burge, C. B., Jones, D. L., & Yeo, G. W. (2016). Enhanced CLIP Uncovers IMP Protein-RNA Targets in Human Pluripotent Stem Cells Important for Cell Adhesion and Survival. *Cell Rep*, 15(3), 666-679. <https://doi.org/10.1016/j.celrep.2016.03.052>
- Corbet, G. A., & Parker, R. (2019). RNP Granule Formation: Lessons from P-Bodies and Stress Granules. *Cold Spring Harb Symp Quant Biol*, 84, 203-215. <https://doi.org/10.1101/sqb.2019.84.040329>
- Cordin, O., Banroques, J., Tanner, N. K., & Linder, P. (2006). The DEAD-box protein family of RNA helicases. *Gene*, 367, 17-37. <https://doi.org/10.1016/j.gene.2005.10.019>
- Cougot, N., Babajko, S., & Seraphin, B. (2004). Cytoplasmic foci are sites of mRNA decay in human cells. *J Cell Biol*, 165(1), 31-40. <https://doi.org/10.1083/jcb.200309008>
- Cougot, N., Bhattacharyya, S. N., Tapia-Arancibia, L., Bordonne, R., Filipowicz, W., Bertrand, E., & Rage, F. (2008). Dendrites of mammalian neurons contain specialized P-body-like structures that respond to neuronal activation. *J Neurosci*, 28(51), 13793-13804. <https://doi.org/10.1523/JNEUROSCI.4155-08.2008>
- Courel, M., Clement, Y., Bossevain, C., Foretek, D., Vidal Cruchez, O., Yi, Z., Benard, M., Benassy, M. N., Kress, M., Vindry, C., Ernoult-Lange, M., Antoniewski, C., Morillon, A., Brest, P., Hubstenberger, A., Roest Crollius, H., Standart, N., & Weil, D. (2019). GC content shapes mRNA storage and decay in human cells. *Elife*, 8. <https://doi.org/10.7554/eLife.49708>
- Darnell, J. C., Van Driesche, S. J., Zhang, C., Hung, K. Y., Mele, A., Fraser, C. E., Stone, E. F., Chen, C., Fak, J. J., Chi, S. W., Licatalosi, D. D., Richter, J. D., & Darnell, R. B. (2011). FMRP stalls ribosomal translocation on mRNAs linked to synaptic function and autism. *Cell*, 146(2), 247-261. <https://doi.org/10.1016/j.cell.2011.06.013>
- David, D. C., Ollikainen, N., Trinidad, J. C., Cary, M. P., Burlingame, A. L., & Kenyon, C. (2010). Widespread protein aggregation as an inherent part of aging in *C. elegans*. *PLoS Biol*, 8(8), e1000450. <https://doi.org/10.1371/journal.pbio.1000450>
- Davidovic, L., Jaglin, X. H., Lepagnol-Bestel, A. M., Tremblay, S., Simonneau, M., Bardoni, B., & Khandjian, E. W. (2007). The fragile X mental retardation protein is a molecular adaptor between the neurospecific KIF3C kinesin and dendritic RNA granules. *Hum Mol Genet*, 16(24), 3047-3058. <https://doi.org/10.1093/hmg/ddm263>
- Davis, R. L. (2005). Olfactory memory formation in Drosophila: from molecular to systems neuroscience. *Annu Rev Neurosci*, 28, 275-302. <https://doi.org/10.1146/annurev.neuro.28.061604.135651>
- De Graeve, F., & Besse, F. (2018). Neuronal RNP granules: from physiological to pathological assemblies. *Biol Chem*, 399(7), 623-635. <https://doi.org/10.1515/hsz-2018-0141>
- de Magalhaes, J. P. (2013). How ageing processes influence cancer. *Nat Rev Cancer*, 13(5), 357-365. <https://doi.org/10.1038/nrc3497>
- de Valoir, T., Tucker, M. A., Belikoff, E. J., Camp, L. A., Bolduc, C., & Beckingham, K. (1991). A second maternally expressed Drosophila gene encodes a putative RNA helicase of the "DEAD box" family. *Proc Natl Acad Sci U S A*, 88(6), 2113-2117. <https://doi.org/10.1073/pnas.88.6.2113>
- Degrauwe, N., Suva, M. L., Janiszewska, M., Riggi, N., & Stamenkovic, I. (2016). IMPs: an RNA-binding protein family that provides a link between stem cell maintenance in normal development and cancer. *Genes Dev*, 30(22), 2459-2474. <https://doi.org/10.1101/gad.287540.116>

- DeHaan, H., McCambridge, A., Armstrong, B., Cruse, C., Solanki, D., Trinidad, J. C., Arkov, A. L., & Gao, M. (2017). An in vivo proteomic analysis of the Me31B interactome in *Drosophila* germ granules. *FEBS Lett*, *591*(21), 3536-3547. <https://doi.org/10.1002/1873-3468.12854>
- Del Valle Rodríguez, A., Didiano, D., & Desplan, C. (2012). Power tools for gene expression and clonal analysis in *Drosophila*. *Nature Methods*, *9*(1), 47-55. <https://doi.org/10.1038/nmeth.1800>
- Demontis, F., & Perrimon, N. (2010). FOXO/4E-BP signaling in *Drosophila* muscles regulates organism-wide proteostasis during aging. *Cell*, *143*(5), 813-825. <https://doi.org/10.1016/j.cell.2010.10.007>
- Deng, H., Gao, K., & Jankovic, J. (2014). The role of FUS gene variants in neurodegenerative diseases. *Nat Rev Neurol*, *10*(6), 337-348. <https://doi.org/10.1038/nrneurol.2014.78>
- Deshler, J. O., Highett, M. I., Abramson, T., & Schnapp, B. J. (1998). A highly conserved RNA-binding protein for cytoplasmic mRNA localization in vertebrates. *Curr Biol*, *8*(9), 489-496. [https://doi.org/10.1016/s0960-9822\(98\)70200-3](https://doi.org/10.1016/s0960-9822(98)70200-3)
- DeZazzo, J., & Tully, T. (1995). Dissection of memory formation: from behavioral pharmacology to molecular genetics. *Trends Neurosci*, *18*(5), 212-218. [https://doi.org/10.1016/0166-2236\(95\)93905-d](https://doi.org/10.1016/0166-2236(95)93905-d)
- Dictenberg, J. B., Swanger, S. A., Antar, L. N., Singer, R. H., & Bassell, G. J. (2008). A direct role for FMRP in activity-dependent dendritic mRNA transport links filopodial-spine morphogenesis to fragile X syndrome. *Dev Cell*, *14*(6), 926-939. <https://doi.org/10.1016/j.devcel.2008.04.003>
- Ditlev, J. A., Case, L. B., & Rosen, M. K. (2018). Who's In and Who's Out-Compositional Control of Biomolecular Condensates. *J Mol Biol*, *430*(23), 4666-4684. <https://doi.org/10.1016/j.jmb.2018.08.003>
- Donnelly, C. J., Willis, D. E., Xu, M., Tep, C., Jiang, C., Yoo, S., Schanen, N. C., Kirn-Safran, C. B., van Minnen, J., English, A., Yoon, S. O., Bassell, G. J., & Twiss, J. L. (2011). Limited availability of ZBP1 restricts axonal mRNA localization and nerve regeneration capacity. *EMBO J*, *30*(22), 4665-4677. <https://doi.org/10.1038/emboj.2011.347>
- Dormann, D., Madl, T., Valori, C. F., Bentmann, E., Tahirovic, S., Abou-Ajram, C., Kremmer, E., Ansorge, O., Mackenzie, I. R., Neumann, M., & Haass, C. (2012). Arginine methylation next to the PY-NLS modulates Transportin binding and nuclear import of FUS. *EMBO J*, *31*(22), 4258-4275. <https://doi.org/10.1038/emboj.2012.261>
- Dormann, D., Rodde, R., Edbauer, D., Bentmann, E., Fischer, I., Hruscha, A., Than, M. E., Mackenzie, I. R., Capell, A., Schmid, B., Neumann, M., & Haass, C. (2010). ALS-associated fused in sarcoma (FUS) mutations disrupt Transportin-mediated nuclear import. *EMBO J*, *29*(16), 2841-2857. <https://doi.org/10.1038/emboj.2010.143>
- Doyle, G. A., Betz, N. A., Leeds, P. F., Fleisig, A. J., Prokipcak, R. D., & Ross, J. (1998). The c-myc coding region determinant-binding protein: a member of a family of KH domain RNA-binding proteins. *Nucleic Acids Res*, *26*(22), 5036-5044. <https://doi.org/10.1093/nar/26.22.5036>
- Drain, P., Folkers, E., & Quinn, W. G. (1991). cAMP-dependent protein kinase and the disruption of learning in transgenic flies. *Neuron*, *6*(1), 71-82. [https://doi.org/10.1016/0896-6273\(91\)90123-h](https://doi.org/10.1016/0896-6273(91)90123-h)
- Drino, A., & Schaefer, M. R. (2018). RNAs, Phase Separation, and Membrane-Less Organelles: Are Post-Transcriptional Modifications Modulating Organelle Dynamics? *Bioessays*, *40*(12), e1800085. <https://doi.org/10.1002/bies.201800085>
- Droppelmann, C. A., Campos-Melo, D., Ishtiaq, M., Volkening, K., & Strong, M. J. (2014). RNA metabolism in ALS: when normal processes become pathological. *Amyotroph Lateral Scler Frontotemporal Degener*, *15*(5-6), 321-336. <https://doi.org/10.3109/21678421.2014.881377>
- Dubnau, J. (2012). Neuroscience. Ode to the mushroom bodies. *Science*, *335*(6069), 664-665. <https://doi.org/10.1126/science.1218171>
- Dundr, M., Hebert, M. D., Karpova, T. S., Stanek, D., Xu, H., Shpargel, K. B., Meier, U. T., Neugebauer, K. M., Matera, A. G., & Misteli, T. (2004). In vivo kinetics of Cajal body components. *J Cell Biol*, *164*(6), 831-842. <https://doi.org/10.1083/jcb.200311121>
- Dynes, J. L., & Steward, O. (2012). Arc mRNA docks precisely at the base of individual dendritic spines indicating the existence of a specialized microdomain for synapse-specific mRNA translation. *J Comp Neurol*, *520*(14), 3105-3119. <https://doi.org/10.1002/cne.23073>
- Ehrenberg, L. (1946). Influence of temperature on the nucleolus and its coacervate nature. *Hereditas*, *32*(3-4), 407-418. <https://doi.org/10.1111/j.1601-5223.1946.tb02783.x>
- El Fatimy, R., Davidovic, L., Tremblay, S., Jaglin, X., Dury, A., Robert, C., De Koninck, P., & Khandjian, E. W. (2016). Tracking the Fragile X Mental Retardation Protein in a Highly Ordered Neuronal RiboNucleoParticles Population: A Link between Stalled Polyribosomes and RNA Granules. *PLoS Genet*, *12*(7), e1006192. <https://doi.org/10.1371/journal.pgen.1006192>
- Elbaum-Garfinkle, S., Kim, Y., Szczepaniak, K., Chen, C. C., Eckmann, C. R., Myong, S., & Brangwynne, C. P. (2015). The disordered P granule protein LAF-1 drives phase separation into droplets with

- tunable viscosity and dynamics. *Proc Natl Acad Sci U S A*, 112(23), 7189-7194. <https://doi.org/10.1073/pnas.1504822112>
- Ellis, R. J., & Minton, A. P. (2003). Cell biology: join the crowd. *Nature*, 425(6953), 27-28. <https://doi.org/10.1038/425027a>
- Elvira, G., Wasiak, S., Blandford, V., Tong, X. K., Serrano, A., Fan, X., del Rayo Sanchez-Carbente, M., Servant, F., Bell, A. W., Boismenu, D., Lacaille, J. C., McPherson, P. S., DesGroseillers, L., & Sossin, W. S. (2006). Characterization of an RNA granule from developing brain. *Mol Cell Proteomics*, 5(4), 635-651. <https://doi.org/10.1074/mcp.M500255-MCP200>
- Eulalio, A., Behm-Ansmant, I., Schweizer, D., & Izaurralde, E. (2007). P-body formation is a consequence, not the cause, of RNA-mediated gene silencing. *Mol Cell Biol*, 27(11), 3970-3981. <https://doi.org/10.1128/MCB.00128-07>
- Fairman, M. E., Maroney, P. A., Wang, W., Bowers, H. A., Gollnick, P., Nilsen, T. W., & Jankowsky, E. (2004). Protein displacement by DExH/D "RNA helicases" without duplex unwinding. *Science*, 304(5671), 730-734. <https://doi.org/10.1126/science.1095596>
- Falahati, H., Pelham-Webb, B., Blythe, S., & Wieschaus, E. (2016). Nucleation by rRNA Dictates the Precision of Nucleolus Assembly. *Curr Biol*, 26(3), 277-285. <https://doi.org/10.1016/j.cub.2015.11.065>
- Farina, K. L., Huttelmaier, S., Musunuru, K., Darnell, R., & Singer, R. H. (2003). Two ZBP1 KH domains facilitate beta-actin mRNA localization, granule formation, and cytoskeletal attachment. *J Cell Biol*, 160(1), 77-87. <https://doi.org/10.1083/jcb.200206003>
- Feric, M., Vaidya, N., Harmon, T. S., Mitrea, D. M., Zhu, L., Richardson, T. M., Kriwacki, R. W., Pappu, R. V., & Brangwynne, C. P. (2016). Coexisting Liquid Phases Underlie Nucleolar Subcompartments. *Cell*, 165(7), 1686-1697. <https://doi.org/10.1016/j.cell.2016.04.047>
- Flora, P., Wong-Deyrup, S. W., Martin, E. T., Palumbo, R. J., Nasrallah, M., Oligney, A., Blatt, P., Patel, D., Fuchs, G., & Rangan, P. (2018). Sequential Regulation of Maternal mRNAs through a Conserved cis-Acting Element in Their 3' UTRs. *Cell Rep*, 25(13), 3828-3843 e3829. <https://doi.org/10.1016/j.celrep.2018.12.007>
- Fontana, L., Partridge, L., & Longo, V. D. (2010). Extending healthy life span--from yeast to humans. *Science*, 328(5976), 321-326. <https://doi.org/10.1126/science.1172539>
- Formicola, N., Vijayakumar, J., & Besse, F. (2019). Neuronal ribonucleoprotein granules: Dynamic sensors of localized signals. *Traffic*, 20(9), 639-649. <https://doi.org/10.1111/tra.12672>
- Fox, A. H., Nakagawa, S., Hirose, T., & Bond, C. S. (2018). Paraspeckles: Where Long Noncoding RNA Meets Phase Separation. *Trends Biochem Sci*, 43(2), 124-135. <https://doi.org/10.1016/j.tibs.2017.12.001>
- Franzmann, T. M., & Alberti, S. (2019). Prion-like low-complexity sequences: Key regulators of protein solubility and phase behavior. *J Biol Chem*, 294(18), 7128-7136. <https://doi.org/10.1074/jbc.TM118.001190>
- Friedman, D. B., & Johnson, T. E. (1988). A mutation in the age-1 gene in *Caenorhabditis elegans* lengthens life and reduces hermaphrodite fertility. *Genetics*, 118(1), 75-86. <https://www.ncbi.nlm.nih.gov/pubmed/8608934>
- Fritzsche, R., Karra, D., Bennett, K. L., Ang, F. Y., Heraud-Farlow, J. E., Tolino, M., Doyle, M., Bauer, K. E., Thomas, S., Planyavsky, M., Arn, E., Bakosova, A., Jungwirth, K., Hormann, A., Palfi, Z., Sandholzer, J., Schwarz, M., Macchi, P., Colinge, J., Superti-Furga, G., & Kiebler, M. A. (2013). Interactome of two diverse RNA granules links mRNA localization to translational repression in neurons. *Cell Rep*, 5(6), 1749-1762. <https://doi.org/10.1016/j.celrep.2013.11.023>
- Fu, X. D. (2020). RNA helicases regulate RNA condensates. *Cell Res*, 30(4), 281-282. <https://doi.org/10.1038/s41422-020-0296-7>
- Fushimi, K., & Verkman, A. S. (1991). Low viscosity in the aqueous domain of cell cytoplasm measured by picosecond polarization microfluorimetry. *J Cell Biol*, 112(4), 719-725. <https://doi.org/10.1083/jcb.112.4.719>
- Galganski, L., Urbanek, M. O., & Krzyzosiak, W. J. (2017). Nuclear speckles: molecular organization, biological function and role in disease. *Nucleic Acids Res*, 45(18), 10350-10368. <https://doi.org/10.1093/nar/gkx759>
- Gallagher, M. (1997). Animal models of memory impairment. *Philos Trans R Soc Lond B Biol Sci*, 352(1362), 1711-1717. <https://doi.org/10.1098/rstb.1997.0153>
- Gan, L., Cookson, M. R., Petrucelli, L., & La Spada, A. R. (2018). Converging pathways in neurodegeneration, from genetics to mechanisms. *Nat Neurosci*, 21(10), 1300-1309. <https://doi.org/10.1038/s41593-018-0237-7>
- Garcia-Jove Navarro, M., Kashida, S., Chouaib, R., Souquere, S., Pierron, G., Weil, D., & Gueroui, Z. (2019). RNA is a critical element for the sizing and the composition of phase-separated RNA-

- protein condensates. *Nature Communications*, 10(1). <https://doi.org/10.1038/s41467-019-11241-6>
- Garner, C. C., Tucker, R. P., & Matus, A. (1988). Selective localization of messenger RNA for cytoskeletal protein MAP2 in dendrites. *Nature*, 336(6200), 674-677. <https://doi.org/10.1038/336674a0>
- Gems, D., & Partridge, L. (2013). Genetics of longevity in model organisms: debates and paradigm shifts. *Annu Rev Physiol*, 75, 621-644. <https://doi.org/10.1146/annurev-physiol-030212-183712>
- Gervasi, N., Tchenio, P., & Preat, T. (2010). PKA dynamics in a Drosophila learning center: coincidence detection by rutabaga adenylyl cyclase and spatial regulation by dunce phosphodiesterase. *Neuron*, 65(4), 516-529. <https://doi.org/10.1016/j.neuron.2010.01.014>
- Gilks, N., Kedersha, N., Ayodele, M., Shen, L., Stoecklin, G., Dember, L. M., & Anderson, P. (2004). Stress granule assembly is mediated by prion-like aggregation of TIA-1. *Mol Biol Cell*, 15(12), 5383-5398. <https://doi.org/10.1091/mbc.e04-08-0715>
- Gillian, A. L., & Svaren, J. (2004). The Ddx20/DP103 dead box protein represses transcriptional activation by Egr2/Krox-20. *J Biol Chem*, 279(10), 9056-9063. <https://doi.org/10.1074/jbc.M309308200>
- Gopal, P. P., Nirschl, J. J., Klinman, E., & Holzbaur, E. L. (2017). Amyotrophic lateral sclerosis-linked mutations increase the viscosity of liquid-like TDP-43 RNP granules in neurons. *Proc Natl Acad Sci U S A*, 114(12), E2466-E2475. <https://doi.org/10.1073/pnas.1614462114>
- Gotze, M., Dufourt, J., Ihling, C., Rammelt, C., Pierson, S., Sambrani, N., Temme, C., Sinz, A., Simonelig, M., & Wahle, E. (2017). Translational repression of the Drosophila nanos mRNA involves the RNA helicase Belle and RNA coating by Me31B and Trailer hitch. *RNA*, 23(10), 1552-1568. <https://doi.org/10.1261/rna.062208.117>
- Graber, T. E., Hebert-Seropian, S., Khoutorsky, A., David, A., Yewdell, J. W., Lacaille, J. C., & Sossin, W. S. (2013). Reactivation of stalled polyribosomes in synaptic plasticity. *Proc Natl Acad Sci U S A*, 110(40), 16205-16210. <https://doi.org/10.1073/pnas.1307747110>
- Green, D. R., Galluzzi, L., & Kroemer, G. (2011). Mitochondria and the autophagy-inflammation-cell death axis in organismal aging. *Science*, 333(6046), 1109-1112. <https://doi.org/10.1126/science.1201940>
- Gu, L., Shigemasa, K., & Ohama, K. (2004). Increased expression of IGF II mRNA-binding protein 1 mRNA is associated with an advanced clinical stage and poor prognosis in patients with ovarian cancer. *Int J Oncol*, 24(3), 671-678. <https://www.ncbi.nlm.nih.gov/pubmed/14767552>
- Guillen-Boixet, J., Kopach, A., Holehouse, A. S., Wittmann, S., Jahnel, M., Schlusser, R., Kim, K., Trussina, I., Wang, J., Mateju, D., Poser, I., Maharana, S., Ruer-Gruss, M., Richter, D., Zhang, X., Chang, Y. T., Guck, J., Honigsmann, A., Mahamid, J., Hyman, A. A., Pappu, R. V., Alberti, S., & Franzmann, T. M. (2020). RNA-Induced Conformational Switching and Clustering of G3BP Drive Stress Granule Assembly by Condensation. *Cell*, 181(2), 346-361 e317. <https://doi.org/10.1016/j.cell.2020.03.049>
- Guo, A., Salomoni, P., Luo, J., Shih, A., Zhong, S., Gu, W., & Pandolfi, P. P. (2000). The function of PML in p53-dependent apoptosis. *Nat Cell Biol*, 2(10), 730-736. <https://doi.org/10.1038/35036365>
- Gustafson, E. A., & Wessel, G. M. (2010). Vasa genes: emerging roles in the germ line and in multipotent cells. *Bioessays*, 32(7), 626-637. <https://doi.org/10.1002/bies.201000001>
- Guzikowski, A. R., Chen, Y. S., & Zid, B. M. (2019). Stress-induced mRNP granules: Form and function of processing bodies and stress granules. *Wiley Interdiscip Rev RNA*, 10(3), e1524. <https://doi.org/10.1002/wrna.1524>
- Haas, G., Braun, J. E., Igreja, C., Tritschler, F., Nishihara, T., & Izaurrealde, E. (2010). HPat provides a link between deadenylation and decapping in metazoa. *J Cell Biol*, 189(2), 289-302. <https://doi.org/10.1083/jcb.200910141>
- Hafner, A. S., Donlin-Asp, P. G., Leitch, B., Herzog, E., & Schuman, E. M. (2019). Local protein synthesis is a ubiquitous feature of neuronal pre- and postsynaptic compartments. *Science*, 364(6441). <https://doi.org/10.1126/science.aau3644>
- Ham, S., & Lee, S. V. (2020). Advances in transcriptome analysis of human brain aging. *Exp Mol Med*, 52(11), 1787-1797. <https://doi.org/10.1038/s12276-020-00522-6>
- Han, P. L., Levin, L. R., Reed, R. R., & Davis, R. L. (1992). Preferential expression of the Drosophila rutabaga gene in mushroom bodies, neural centers for learning in insects. *Neuron*, 9(4), 619-627. [https://doi.org/10.1016/0896-6273\(92\)90026-a](https://doi.org/10.1016/0896-6273(92)90026-a)
- Han, S., & Brunet, A. (2012). Histone methylation makes its mark on longevity. *Trends Cell Biol*, 22(1), 42-49. <https://doi.org/10.1016/j.tcb.2011.11.001>
- Handwerker, K. E., Cordero, J. A., & Gall, J. G. (2005). Cajal bodies, nucleoli, and speckles in the Xenopus oocyte nucleus have a low-density, sponge-like structure. *Mol Biol Cell*, 16(1), 202-211. <https://doi.org/10.1091/mbc.e04-08-0742>

- Handwerger, K. E., & Gall, J. G. (2006). Subnuclear organelles: new insights into form and function. *Trends Cell Biol*, 16(1), 19-26. <https://doi.org/10.1016/j.tcb.2005.11.005>
- Hansen, H. T., Rasmussen, S. H., Adolph, S. K., Plass, M., Krogh, A., Sanford, J., Nielsen, F. C., & Christiansen, J. (2015). Drosophila Imp iCLIP identifies an RNA assemblage coordinating F-actin formation. *Genome Biol*, 16, 123. <https://doi.org/10.1186/s13059-015-0687-0>
- Hara, T., Nakamura, K., Matsui, M., Yamamoto, A., Nakahara, Y., Suzuki-Migishima, R., Yokoyama, M., Mishima, K., Saito, I., Okano, H., & Mizushima, N. (2006). Suppression of basal autophagy in neural cells causes neurodegenerative disease in mice. *Nature*, 441(7095), 885-889. <https://doi.org/10.1038/nature04724>
- Havin, L., Git, A., Elisha, Z., Oberman, F., Yaniv, K., Schwartz, S. P., Standart, N., & Yisraeli, J. K. (1998). RNA-binding protein conserved in both microtubule- and microfilament-based RNA localization. *Genes Dev*, 12(11), 1593-1598. <https://doi.org/10.1101/gad.12.11.1593>
- He, X., Memczak, S., Qu, J., Belmonte, J. C. I., & Liu, G. H. (2020). Single-cell omics in ageing: a young and growing field. *Nat Metab*, 2(4), 293-302. <https://doi.org/10.1038/s42255-020-0196-7>
- Heisenberg, M. (2003). Mushroom body memoir: from maps to models. *Nat Rev Neurosci*, 4(4), 266-275. <https://doi.org/10.1038/nrn1074>
- Heisenberg, M., Borst, A., Wagner, S., & Byers, D. (1985). Drosophila mushroom body mutants are deficient in olfactory learning. *J Neurogenet*, 2(1), 1-30. <https://doi.org/10.3109/01677068509100140>
- Heraud-Farlow, J. E., Sharangdhar, T., Li, X., Pfeifer, P., Tauber, S., Orozco, D., Hormann, A., Thomas, S., Bakosova, A., Farlow, A. R., Edbauer, D., Lipshitz, H. D., Morris, Q. D., Bilban, M., Doyle, M., & Kiebler, M. A. (2013). Stauf2 regulates neuronal target RNAs. *Cell Rep*, 5(6), 1511-1518. <https://doi.org/10.1016/j.celrep.2013.11.039>
- Higashimoto, Y., Asanomi, Y., Takakusagi, S., Lewis, M. S., Uosaki, K., Durell, S. R., Anderson, C. W., Appella, E., & Sakaguchi, K. (2006). Unfolding, aggregation, and amyloid formation by the tetramerization domain from mutant p53 associated with lung cancer. *Biochemistry*, 45(6), 1608-1619. <https://doi.org/10.1021/bi051192j>
- Hillebrand, J., Pan, K., Kokaram, A., Barbee, S., Parker, R., & Ramaswami, M. (2010). The Me31B DEAD-Box Helicase Localizes to Postsynaptic Foci and Regulates Expression of a CaMKII Reporter mRNA in Dendrites of Drosophila Olfactory Projection Neurons. *Front Neural Circuits*, 4, 121. <https://doi.org/10.3389/fncir.2010.00121>
- Hilliker, A., Gao, Z., Jankowsky, E., & Parker, R. (2011). The DEAD-box protein Ded1 modulates translation by the formation and resolution of an eIF4F-mRNA complex. *Mol Cell*, 43(6), 962-972. <https://doi.org/10.1016/j.molcel.2011.08.008>
- Hofweber, M., & Dormann, D. (2019). Friend or foe-Post-translational modifications as regulators of phase separation and RNP granule dynamics. *J Biol Chem*, 294(18), 7137-7150. <https://doi.org/10.1074/jbc.TM118.001189>
- Hofweber, M., Hutten, S., Bourgeois, B., Spreitzer, E., Niedner-Boblenz, A., Schifferer, M., Ruepp, M. D., Simons, M., Niessing, D., Madl, T., & Dormann, D. (2018). Phase Separation of FUS Is Suppressed by Its Nuclear Import Receptor and Arginine Methylation. *Cell*, 173(3), 706-719 e713. <https://doi.org/10.1016/j.cell.2018.03.004>
- Holt, C. E., & Schuman, E. M. (2013). The central dogma decentralized: new perspectives on RNA function and local translation in neurons. *Neuron*, 80(3), 648-657. <https://doi.org/10.1016/j.neuron.2013.10.036>
- Holzenberger, M., Dupont, J., Ducos, B., Leneuve, P., Geloën, A., Even, P. C., Cervera, P., & Le Bouc, Y. (2003). IGF-1 receptor regulates lifespan and resistance to oxidative stress in mice. *Nature*, 421(6919), 182-187. <https://doi.org/10.1038/nature01298>
- Hondele, M., Sachdev, R., Heinrich, S., Wang, J., Vallotton, P., Fontoura, B. M. A., & Weis, K. (2019). DEAD-box ATPases are global regulators of phase-separated organelles. *Nature*, 573(7772), 144-148. <https://doi.org/10.1038/s41586-019-1502-y>
- Horvathova, I., Voigt, F., Kotrys, A. V., Zhan, Y., Artus-Revel, C. G., Eglinger, J., Stadler, M. B., Giorgetti, L., & Chao, J. A. (2017). The Dynamics of mRNA Turnover Revealed by Single-Molecule Imaging in Single Cells. *Mol Cell*, 68(3), 615-625 e619. <https://doi.org/10.1016/j.molcel.2017.09.030>
- Houseley, J., & Tollervey, D. (2009). The many pathways of RNA degradation. *Cell*, 136(4), 763-776. <https://doi.org/10.1016/j.cell.2009.01.019>
- Huang, C., Chen, Y., Dai, H., Zhang, H., Xie, M., Zhang, H., Chen, F., Kang, X., Bai, X., & Chen, Z. (2020). UBAP2L arginine methylation by PRMT1 modulates stress granule assembly. *Cell Death Differ*, 27(1), 227-241. <https://doi.org/10.1038/s41418-019-0350-5>

- Huang, H., Weng, H., Sun, W., Qin, X., Shi, H., Wu, H., Zhao, B. S., Mesquita, A., Liu, C., Yuan, C. L., Hu, Y. C., Huttelmaier, S., Skibbe, J. R., Su, R., Deng, X., Dong, L., Sun, M., Li, C., Nachtergaele, S., Wang, Y., Hu, C., Ferchen, K., Greis, K. D., Jiang, X., Wei, M., Qu, L., Guan, J. L., He, C., Yang, J., & Chen, J. (2018). Recognition of RNA N(6)-methyladenosine by IGF2BP proteins enhances mRNA stability and translation. *Nat Cell Biol*, 20(3), 285-295. <https://doi.org/10.1038/s41556-018-0045-z>
- Hubstenberger, A., Courel, M., Benard, M., Souquere, S., Ernoult-Lange, M., Chouaib, R., Yi, Z., Morlot, J. B., Munier, A., Fradet, M., Daunesse, M., Bertrand, E., Pierron, G., Mozziconacci, J., Kress, M., & Weil, D. (2017). P-Body Purification Reveals the Condensation of Repressed mRNA Regulons. *Mol Cell*, 68(1), 144-157 e145. <https://doi.org/10.1016/j.molcel.2017.09.003>
- Hubstenberger, A., Noble, S. L., Cameron, C., & Evans, T. C. (2013). Translation repressors, an RNA helicase, and developmental cues control RNP phase transitions during early development. *Dev Cell*, 27(2), 161-173. <https://doi.org/10.1016/j.devcel.2013.09.024>
- Huch, S., & Nissan, T. (2017). An mRNA decapping mutant deficient in P body assembly limits mRNA stabilization in response to osmotic stress. *Sci Rep*, 7, 44395. <https://doi.org/10.1038/srep44395>
- Huttelmaier, S., Zenklusen, D., Lederer, M., Dichtenberg, J., Lorenz, M., Meng, X., Bassell, G. J., Condeelis, J., & Singer, R. H. (2005). Spatial regulation of beta-actin translation by Src-dependent phosphorylation of ZBP1. *Nature*, 438(7067), 512-515. <https://doi.org/10.1038/nature04115>
- Ingolia, N. T., Ghaemmaghami, S., Newman, J. R., & Weissman, J. S. (2009). Genome-wide analysis in vivo of translation with nucleotide resolution using ribosome profiling. *Science*, 324(5924), 218-223. <https://doi.org/10.1126/science.1168978>
- Ishov, A. M., Sotnikov, A. G., Negorev, D., Vladimirova, O. V., Neff, N., Kamitani, T., Yeh, E. T., Strauss, J. F., 3rd, & Maul, G. G. (1999). PML is critical for ND10 formation and recruits the PML-interacting protein daxx to this nuclear structure when modified by SUMO-1. *J Cell Biol*, 147(2), 221-234. <https://doi.org/10.1083/jcb.147.2.221>
- Ito, K., & Hotta, Y. (1992). Proliferation pattern of postembryonic neuroblasts in the brain of *Drosophila melanogaster*. *Dev Biol*, 149(1), 134-148. [https://doi.org/10.1016/0012-1606\(92\)90270-q](https://doi.org/10.1016/0012-1606(92)90270-q)
- Ivanov, P., Kedersha, N., & Anderson, P. (2019). Stress Granules and Processing Bodies in Translational Control. *Cold Spring Harb Perspect Biol*, 11(5). <https://doi.org/10.1101/cshperspect.a032813>
- Jain, A., & Vale, R. D. (2017). RNA phase transitions in repeat expansion disorders. *Nature*, 546(7657), 243-247. <https://doi.org/10.1038/nature22386>
- Jain, S., Wheeler, J. R., Walters, R. W., Agrawal, A., Barsic, A., & Parker, R. (2016). ATPase-Modulated Stress Granules Contain a Diverse Proteome and Substructure. *Cell*, 164(3), 487-498. <https://doi.org/10.1016/j.cell.2015.12.038>
- Jankowsky, E. (2011). RNA helicases at work: binding and rearranging. *Trends Biochem Sci*, 36(1), 19-29. <https://doi.org/10.1016/j.tibs.2010.07.008>
- Jankowsky, E., Gross, C. H., Shuman, S., & Pyle, A. M. (2001). Active disruption of an RNA-protein interaction by a DExH/D RNA helicase. *Science*, 291(5501), 121-125. <https://doi.org/10.1126/science.291.5501.121>
- Jens Eggers, J. R. L. a. H. A. S. (1999). Coalescence of liquid drops. *Journal of Fluid Mechanics*, 401, 293-310.
- Jeong, J. H., Nam, Y. J., Kim, S. Y., Kim, E. G., Jeong, J., & Kim, H. K. (2007). The transport of Staufen2-containing ribonucleoprotein complexes involves kinesin motor protein and is modulated by mitogen-activated protein kinase pathway. *J Neurochem*, 102(6), 2073-2084. <https://doi.org/10.1111/j.1471-4159.2007.04697.x>
- Jiang, C. H., Tsien, J. Z., Schultz, P. G., & Hu, Y. (2001). The effects of aging on gene expression in the hypothalamus and cortex of mice. *Proc Natl Acad Sci U S A*, 98(4), 1930-1934. <https://doi.org/10.1073/pnas.98.4.1930>
- Jiang, S., Fagman, J. B., Chen, C., Alberti, S., & Liu, B. (2020). Protein phase separation and its role in tumorigenesis. *Elife*, 9. <https://doi.org/10.7554/eLife.60264>
- Johnson, S. C., Dong, X., Vijg, J., & Suh, Y. (2015). Genetic evidence for common pathways in human age-related diseases. *Aging Cell*, 14(5), 809-817. <https://doi.org/10.1111/accel.12362>
- Jonas, S., & Izaurralde, E. (2013). The role of disordered protein regions in the assembly of decapping complexes and RNP granules. *Genes Dev*, 27(24), 2628-2641. <https://doi.org/10.1101/gad.227843.113>
- Jones, S. G., Nixon, K. C. J., Chubak, M. C., & Kramer, J. M. (2018). Mushroom Body Specific Transcriptome Analysis Reveals Dynamic Regulation of Learning and Memory Genes After Acquisition of Long-Term Courtship Memory in *Drosophila*. *G3 (Bethesda)*, 8(11), 3433-3446. <https://doi.org/10.1534/g3.118.200560>

- Jonson, L., Christiansen, J., Hansen, T. V. O., Vikesa, J., Yamamoto, Y., & Nielsen, F. C. (2014). IMP3 RNP safe houses prevent miRNA-directed HMGA2 mRNA decay in cancer and development. *Cell Rep*, 7(2), 539-551. <https://doi.org/10.1016/j.celrep.2014.03.015>
- Jonson, L., Vikesaa, J., Krogh, A., Nielsen, L. K., Hansen, T., Borup, R., Johnsen, A. H., Christiansen, J., & Nielsen, F. C. (2007). Molecular composition of IMP1 ribonucleoprotein granules. *Mol Cell Proteomics*, 6(5), 798-811. <https://doi.org/10.1074/mcp.M600346-MCP200>
- Juhasz, G., Erdi, B., Sass, M., & Neufeld, T. P. (2007). Atg7-dependent autophagy promotes neuronal health, stress tolerance, and longevity but is dispensable for metamorphosis in *Drosophila*. *Genes Dev*, 21(23), 3061-3066. <https://doi.org/10.1101/gad.1600707>
- Jung, H., Yoon, B. C., & Holt, C. E. (2012). Axonal mRNA localization and local protein synthesis in nervous system assembly, maintenance and repair. *Nat Rev Neurosci*, 13(5), 308-324. <https://doi.org/10.1038/nrn3210>
- Kamagata, K., Kanbayashi, S., Honda, M., Itoh, Y., Takahashi, H., Kameda, T., Nagatsugi, F., & Takahashi, S. (2020). Liquid-like droplet formation by tumor suppressor p53 induced by multivalent electrostatic interactions between two disordered domains. *Sci Rep*, 10(1), 580. <https://doi.org/10.1038/s41598-020-57521-w>
- Kanai, Y., Dohmae, N., & Hirokawa, N. (2004). Kinesin transports RNA: isolation and characterization of an RNA-transporting granule. *Neuron*, 43(4), 513-525. <https://doi.org/10.1016/j.neuron.2004.07.022>
- Kandel, E. R. (2012). The molecular biology of memory: cAMP, PKA, CRE, CREB-1, CREB-2, and CPEB. *Mol Brain*, 5, 14. <https://doi.org/10.1186/1756-6606-5-14>
- Kanfi, Y., Naiman, S., Amir, G., Peshti, V., Zinman, G., Nahum, L., Bar-Joseph, Z., & Cohen, H. Y. (2012). The sirtuin SIRT6 regulates lifespan in male mice. *Nature*, 483(7388), 218-221. <https://doi.org/10.1038/nature10815>
- Kang, H., & Schuman, E. M. (1996). A requirement for local protein synthesis in neurotrophin-induced hippocampal synaptic plasticity. *Science*, 273(5280), 1402-1406. <https://doi.org/10.1126/science.273.5280.1402>
- Kapeli, K., Martinez, F. J., & Yeo, G. W. (2017). Genetic mutations in RNA-binding proteins and their roles in ALS. *Hum Genet*, 136(9), 1193-1214. <https://doi.org/10.1007/s00439-017-1830-7>
- Karpen, G. H., Schaefer, J. E., & Laird, C. D. (1988). A *Drosophila* rRNA gene located in euchromatin is active in transcription and nucleolus formation. *Genes Dev*, 2(12B), 1745-1763. <https://doi.org/10.1101/gad.2.12b.1745>
- Kato, M., Han, T. W., Xie, S., Shi, K., Du, X., Wu, L. C., Mirzaei, H., Goldsmith, E. J., Longgood, J., Pei, J., Grishin, N. V., Frantz, D. E., Schneider, J. W., Chen, S., Li, L., Sawaya, M. R., Eisenberg, D., Tycko, R., & McKnight, S. L. (2012). Cell-free formation of RNA granules: low complexity sequence domains form dynamic fibers within hydrogels. *Cell*, 149(4), 753-767. <https://doi.org/10.1016/j.cell.2012.04.017>
- Kato, Y., & Nakamura, A. (2012). Roles of cytoplasmic RNP granules in intracellular RNA localization and translational control in the *Drosophila* oocyte. *Development, Growth & Differentiation*, 54(1), 19-31. <https://doi.org/10.1111/j.1440-169x.2011.01314.x>
- Kedersha, N., Cho, M. R., Li, W., Yacono, P. W., Chen, S., Gilks, N., Golan, D. E., & Anderson, P. (2000). Dynamic shuttling of TIA-1 accompanies the recruitment of mRNA to mammalian stress granules. *J Cell Biol*, 151(6), 1257-1268. <https://doi.org/10.1083/jcb.151.6.1257>
- Kedersha, N., Panas, M. D., Achorn, C. A., Lyons, S., Tisdale, S., Hickman, T., Thomas, M., Lieberman, J., McInerney, G. M., Ivanov, P., & Anderson, P. (2016). G3BP-Caprin1-USP10 complexes mediate stress granule condensation and associate with 40S subunits. *J Cell Biol*, 212(7), 845-860. <https://doi.org/10.1083/jcb.201508028>
- Kedersha, N., Stoecklin, G., Ayodele, M., Yacono, P., Lykke-Andersen, J., Fritzler, M. J., Scheuner, D., Kaufman, R. J., Golan, D. E., & Anderson, P. (2005). Stress granules and processing bodies are dynamically linked sites of mRNP remodeling. *J Cell Biol*, 169(6), 871-884. <https://doi.org/10.1083/jcb.200502088>
- Kenyon, C. J. (2010). The genetics of ageing. *Nature*, 464(7288), 504-512. <https://doi.org/10.1038/nature08980>
- Khayachi, A., Gwizdek, C., Poupon, G., Alcor, D., Chafai, M., Casse, F., Maurin, T., Prieto, M., Folci, A., De Graeve, F., Castagnola, S., Gautier, R., Schorova, L., Loriol, C., Pronot, M., Besse, F., Brau, F., Deval, E., Bardoni, B., & Martin, S. (2018). Sumoylation regulates FMRP-mediated dendritic spine elimination and maturation. *Nat Commun*, 9(1), 757. <https://doi.org/10.1038/s41467-018-03222-y>

- Khong, A., Matheny, T., Jain, S., Mitchell, S. F., Wheeler, J. R., & Parker, R. (2017). The Stress Granule Transcriptome Reveals Principles of mRNA Accumulation in Stress Granules. *Mol Cell*, 68(4), 808-820 e805. <https://doi.org/10.1016/j.molcel.2017.10.015>
- Kiebler, M. A., & Bassell, G. J. (2006). Neuronal RNA granules: movers and makers. *Neuron*, 51(6), 685-690. <https://doi.org/10.1016/j.neuron.2006.08.021>
- Kim, H. J., Kim, N. C., Wang, Y. D., Scarborough, E. A., Moore, J., Diaz, Z., MacLea, K. S., Freibaum, B., Li, S., Molliex, A., Kanagaraj, A. P., Carter, R., Boylan, K. B., Wojtas, A. M., Rademakers, R., Pinkus, J. L., Greenberg, S. A., Trojanowski, J. Q., Traynor, B. J., Smith, B. N., Topp, S., Gkazi, A. S., Miller, J., Shaw, C. E., Kottlors, M., Kirschner, J., Pestronk, A., Li, Y. R., Ford, A. F., Gitler, A. D., Benatar, M., King, O. D., Kimonis, V. E., Ross, E. D., Weihl, C. C., Shorter, J., & Taylor, J. P. (2013). Mutations in prion-like domains in hnRNPA2B1 and hnRNPA1 cause multisystem proteinopathy and ALS. *Nature*, 495(7442), 467-473. <https://doi.org/10.1038/nature11922>
- Kim, T. H., Tsang, B., Vernon, R. M., Sonenberg, N., Kay, L. E., & Forman-Kay, J. D. (2019). Phospho-dependent phase separation of FMRP and CAPRIN1 recapitulates regulation of translation and deadenylation. *Science*, 365(6455), 825-829. <https://doi.org/10.1126/science.aax4240>
- King, O. D., Gitler, A. D., & Shorter, J. (2012). The tip of the iceberg: RNA-binding proteins with prion-like domains in neurodegenerative disease. *Brain Res*, 1462, 61-80. <https://doi.org/10.1016/j.brainres.2012.01.016>
- Kinkel, K., Veith, K., Grunwald, M., & Bono, F. (2012). Crystal structure of a minimal eIF4E-Cup complex reveals a general mechanism of eIF4E regulation in translational repression. *RNA*, 18(9), 1624-1634. <https://doi.org/10.1261/rna.033639.112>
- Kirkwood, T. B. (2005). Understanding the odd science of aging. *Cell*, 120(4), 437-447. <https://doi.org/10.1016/j.cell.2005.01.027>
- Klann, E., & Dever, T. E. (2004). Biochemical mechanisms for translational regulation in synaptic plasticity. *Nat Rev Neurosci*, 5(12), 931-942. <https://doi.org/10.1038/nrn1557>
- Klosin, A., Oltch, F., Harmon, T., Honigsmann, A., Julicher, F., Hyman, A. A., & Zechner, C. (2020). Phase separation provides a mechanism to reduce noise in cells. *Science*, 367(6476), 464-468. <https://doi.org/10.1126/science.aav6691>
- Knowles, R. B., Sabry, J. H., Martone, M. E., Deerinck, T. J., Ellisman, M. H., Bassell, G. J., & Kosik, K. S. (1996). Translocation of RNA granules in living neurons. *J Neurosci*, 16(24), 7812-7820. <https://www.ncbi.nlm.nih.gov/pubmed/8987809>
- Kohrmann, M., Luo, M., Kaether, C., DesGroseillers, L., Dotti, C. G., & Kiebler, M. A. (1999). Microtubule-dependent recruitment of Staufen-green fluorescent protein into large RNA-containing granules and subsequent dendritic transport in living hippocampal neurons. *Mol Biol Cell*, 10(9), 2945-2953. <https://doi.org/10.1091/mbc.10.9.2945>
- Komatsu, M., Waguri, S., Chiba, T., Murata, S., Iwata, J., Tanida, I., Ueno, T., Koike, M., Uchiyama, Y., Kominami, E., & Tanaka, K. (2006). Loss of autophagy in the central nervous system causes neurodegeneration in mice. *Nature*, 441(7095), 880-884. <https://doi.org/10.1038/nature04723>
- Konopacki, F. A., Wong, H. H., Dwivedy, A., Bellon, A., Blower, M. D., & Holt, C. E. (2016). ESCRT-II controls retinal axon growth by regulating DCC receptor levels and local protein synthesis. *Open Biol*, 6(4), 150218. <https://doi.org/10.1098/rsob.150218>
- Krichevsky, A. M., & Kosik, K. S. (2001). Neuronal RNA granules: a link between RNA localization and stimulation-dependent translation. *Neuron*, 32(4), 683-696. [https://doi.org/10.1016/s0896-6273\(01\)00508-6](https://doi.org/10.1016/s0896-6273(01)00508-6)
- Kroschwald, S., Maharana, S., Mateju, D., Malinowska, L., Nuske, E., Poser, I., Richter, D., & Alberti, S. (2015). Promiscuous interactions and protein disaggregases determine the material state of stress-inducible RNP granules. *Elife*, 4, e06807. <https://doi.org/10.7554/eLife.06807>
- Kwon, S., Zhang, Y., & Matthias, P. (2007). The deacetylase HDAC6 is a novel critical component of stress granules involved in the stress response. *Genes Dev*, 21(24), 3381-3394. <https://doi.org/10.1101/gad.461107>
- Lafontaine, D. L. J., Riback, J. A., Bascetin, R., & Brangwynne, C. P. (2020). The nucleolus as a multiphase liquid condensate. *Nat Rev Mol Cell Biol*. <https://doi.org/10.1038/s41580-020-0272-6>
- Lallemand-Breitenbach, V., & de The, H. (2018). PML nuclear bodies: from architecture to function. *Curr Opin Cell Biol*, 52, 154-161. <https://doi.org/10.1016/j.ceb.2018.03.011>
- Langdon, E. M., Qiu, Y., Ghanbari Niaki, A., McLaughlin, G. A., Weidmann, C. A., Gerbich, T. M., Smith, J. A., Crutchley, J. M., Termini, C. M., Weeks, K. M., Myong, S., & Gladfelter, A. S. (2018). mRNA structure determines specificity of a polyQ-driven phase separation. *Science*, 360(6391), 922-927. <https://doi.org/10.1126/science.aar7432>

- Leatherman, J. L., & Jongens, T. A. (2003). Transcriptional silencing and translational control: key features of early germline development. *Bioessays*, 25(4), 326-335. <https://doi.org/10.1002/bies.10247>
- Lechler, M. C., Crawford, E. D., Groh, N., Widmaier, K., Jung, R., Kirstein, J., Trinidad, J. C., Burlingame, A. L., & David, D. C. (2017). Reduced Insulin/IGF-1 Signaling Restores the Dynamic Properties of Key Stress Granule Proteins during Aging. *Cell Rep*, 18(2), 454-467. <https://doi.org/10.1016/j.celrep.2016.12.033>
- Lee, C., Occhipinti, P., & Gladfelter, A. S. (2015). PolyQ-dependent RNA-protein assemblies control symmetry breaking. *J Cell Biol*, 208(5), 533-544. <https://doi.org/10.1083/jcb.201407105>
- Lee, C. K., Weindruch, R., & Prolla, T. A. (2000). Gene-expression profile of the ageing brain in mice. *Nat Genet*, 25(3), 294-297. <https://doi.org/10.1038/77046>
- Lee, C. S., Dias, A. P., Jedrychowski, M., Patel, A. H., Hsu, J. L., & Reed, R. (2008). Human DDX3 functions in translation and interacts with the translation initiation factor eIF3. *Nucleic Acids Res*, 36(14), 4708-4718. <https://doi.org/10.1093/nar/gkn454>
- Lee, T., Lee, A., & Luo, L. (1999). Development of the Drosophila mushroom bodies: sequential generation of three distinct types of neurons from a neuroblast. *Development*, 126(18), 4065-4076. <https://www.ncbi.nlm.nih.gov/pubmed/10457015>
- Lehmann, R. (2016). Germ Plasm Biogenesis--An Oskar-Centric Perspective. *Curr Top Dev Biol*, 116, 679-707. <https://doi.org/10.1016/bs.ctdb.2015.11.024>
- Lemm, I., & Ross, J. (2002). Regulation of c-myc mRNA decay by translational pausing in a coding region instability determinant. *Mol Cell Biol*, 22(12), 3959-3969. <https://doi.org/10.1128/mcb.22.12.3959-3969.2002>
- Lepelletier, L., Langlois, S. D., Kent, C. B., Welshhans, K., Morin, S., Bassell, G. J., Yam, P. T., & Charron, F. (2017). Sonic Hedgehog Guides Axons via Zipcode Binding Protein 1-Mediated Local Translation. *J Neurosci*, 37(7), 1685-1695. <https://doi.org/10.1523/JNEUROSCI.3016-16.2016>
- Leung, K. M., van Horck, F. P., Lin, A. C., Allison, R., Standart, N., & Holt, C. E. (2006). Asymmetrical beta-actin mRNA translation in growth cones mediates attractive turning to netrin-1. *Nat Neurosci*, 9(10), 1247-1256. <https://doi.org/10.1038/nn1775>
- Levin, L. R., Han, P. L., Hwang, P. M., Feinstein, P. G., Davis, R. L., & Reed, R. R. (1992). The Drosophila learning and memory gene rutabaga encodes a Ca²⁺/Calmodulin-responsive adenylyl cyclase. *Cell*, 68(3), 479-489. [https://doi.org/10.1016/0092-8674\(92\)90185-f](https://doi.org/10.1016/0092-8674(92)90185-f)
- Li, P., Banjade, S., Cheng, H. C., Kim, S., Chen, B., Guo, L., Llaguno, M., Hollingsworth, J. V., King, D. S., Banani, S. F., Russo, P. S., Jiang, Q. X., Nixon, B. T., & Rosen, M. K. (2012). Phase transitions in the assembly of multivalent signalling proteins. *Nature*, 483(7389), 336-340. <https://doi.org/10.1038/nature10879>
- Li, W., Tully, T., & Kalderon, D. (1996). Effects of a conditional Drosophila PKA mutant on olfactory learning and memory. *Learn Mem*, 2(6), 320-333. <https://doi.org/10.1101/lm.2.6.320>
- Liao, Y. C., Fernandopulle, M. S., Wang, G., Choi, H., Hao, L., Drerup, C. M., Patel, R., Qamar, S., Nixon-Abell, J., Shen, Y., Meadows, W., Vendruscolo, M., Knowles, T. P. J., Nelson, M., Czekalska, M. A., Musteikyte, G., Gachechiladze, M. A., Stephens, C. A., Pasolli, H. A., Forrest, L. R., St George-Hyslop, P., Lippincott-Schwartz, J., & Ward, M. E. (2019). RNA Granules Hitchhike on Lysosomes for Long-Distance Transport, Using Annexin A11 as a Molecular Tether. *Cell*, 179(1), 147-164 e120. <https://doi.org/10.1016/j.cell.2019.08.050>
- Lin, D. Y., Huang, Y. S., Jeng, J. C., Kuo, H. Y., Chang, C. C., Chao, T. T., Ho, C. C., Chen, Y. C., Lin, T. P., Fang, H. I., Hung, C. C., Suen, C. S., Hwang, M. J., Chang, K. S., Maul, G. G., & Shih, H. M. (2006). Role of SUMO-interacting motif in Daxx SUMO modification, subnuclear localization, and repression of sumoylated transcription factors. *Mol Cell*, 24(3), 341-354. <https://doi.org/10.1016/j.molcel.2006.10.019>
- Lin, Y., Protter, D. S., Rosen, M. K., & Parker, R. (2015). Formation and Maturation of Phase-Separated Liquid Droplets by RNA-Binding Proteins. *Mol Cell*, 60(2), 208-219. <https://doi.org/10.1016/j.molcel.2015.08.018>
- Linder, P. (2006). Dead-box proteins: a family affair--active and passive players in RNP-remodeling. *Nucleic Acids Res*, 34(15), 4168-4180. <https://doi.org/10.1093/nar/gkl468>
- Linder, P., Lasko, P. F., Ashburner, M., Leroy, P., Nielsen, P. J., Nishi, K., Schnier, J., & Slonimski, P. P. (1989). Birth of the D-E-A-D box. *Nature*, 337(6203), 121-122. <https://doi.org/10.1038/337121a0>
- Lipinski, M. M., Zheng, B., Lu, T., Yan, Z., Py, B. F., Ng, A., Xavier, R. J., Li, C., Yankner, B. A., Scherzer, C. R., & Yuan, J. (2010). Genome-wide analysis reveals mechanisms modulating autophagy in normal brain aging and in Alzheimer's disease. *Proc Natl Acad Sci U S A*, 107(32), 14164-14169. <https://doi.org/10.1073/pnas.1009485107>

- Liu, G., Rogers, J., Murphy, C. T., & Rongo, C. (2011). EGF signalling activates the ubiquitin proteasome system to modulate *C. elegans* lifespan. *EMBO J*, 30(15), 2990-3003. <https://doi.org/10.1038/emboj.2011.195>
- Liu, J., Rivas, F. V., Wohlschlegel, J., Yates, J. R., 3rd, Parker, R., & Hannon, G. J. (2005). A role for the P-body component GW182 in microRNA function. *Nat Cell Biol*, 7(12), 1261-1266. <https://doi.org/10.1038/ncb1333>
- Liu, J., Valencia-Sanchez, M. A., Hannon, G. J., & Parker, R. (2005). MicroRNA-dependent localization of targeted mRNAs to mammalian P-bodies. *Nat Cell Biol*, 7(7), 719-723. <https://doi.org/10.1038/ncb1274>
- Liu, Z., Yang, C. P., Sugino, K., Fu, C. C., Liu, L. Y., Yao, X., Lee, L. P., & Lee, T. (2015). Opposing intrinsic temporal gradients guide neural stem cell production of varied neuronal fates. *Science*, 350(6258), 317-320. <https://doi.org/10.1126/science.aad1886>
- Lopez-Otin, C., Blasco, M. A., Partridge, L., Serrano, M., & Kroemer, G. (2013). The hallmarks of aging. *Cell*, 153(6), 1194-1217. <https://doi.org/10.1016/j.cell.2013.05.039>
- Ma, S., Avanesov, A. S., Porter, E., Lee, B. C., Mariotti, M., Zemskaya, N., Guigo, R., Moskalev, A. A., & Gladyshev, V. N. (2018). Comparative transcriptomics across 14 *Drosophila* species reveals signatures of longevity. *Aging Cell*, 17(4), e12740. <https://doi.org/10.1111/accel.12740>
- Mackenzie, I. R., Nicholson, A. M., Sarkar, M., Messing, J., Purice, M. D., Pottier, C., Annu, K., Baker, M., Perkerson, R. B., Kurti, A., Matchett, B. J., Mittag, T., Temirov, J., Hsiung, G. R., Krieger, C., Murray, M. E., Kato, M., Fryer, J. D., Petrucelli, L., Zinman, L., Weintraub, S., Mesulam, M., Keith, J., Zivkovic, S. A., Hirsch-Reinshagen, V., Roos, R. P., Zuchner, S., Graff-Radford, N. R., Petersen, R. C., Caselli, R. J., Wszolek, Z. K., Finger, E., Lippa, C., Lacomis, D., Stewart, H., Dickson, D. W., Kim, H. J., Rogaeva, E., Bigio, E., Boylan, K. B., Taylor, J. P., & Rademakers, R. (2017). TIA1 Mutations in Amyotrophic Lateral Sclerosis and Frontotemporal Dementia Promote Phase Separation and Alter Stress Granule Dynamics. *Neuron*, 95(4), 808-816 e809. <https://doi.org/10.1016/j.neuron.2017.07.025>
- Maharana, S., Wang, J., Papadopoulos, D. K., Richter, D., Pozniakovskiy, A., Poser, I., Bickle, M., Rizk, S., Guillen-Boixet, J., Franzmann, T. M., Jahnel, M., Marrone, L., Chang, Y. T., Sternecker, J., Tomancak, P., Hyman, A. A., & Alberti, S. (2018). RNA buffers the phase separation behavior of prion-like RNA binding proteins. *Science*, 360(6391), 918-921. <https://doi.org/10.1126/science.aar7366>
- Mahowald, A. P. (1962). Fine structure of pole cells and polar granules in *Drosophila melanogaster*. *J. exp. Zool.*, 201-216.
- Mahowald, A. P. (2001). Assembly of the *Drosophila* germ plasm. *Int Rev Cytol*, 203, 187-213. [https://doi.org/10.1016/s0074-7696\(01\)03007-8](https://doi.org/10.1016/s0074-7696(01)03007-8)
- Malinowska, L., Kroschwald, S., & Alberti, S. (2013). Protein disorder, prion propensities, and self-organizing macromolecular collectives. *Biochim Biophys Acta*, 1834(5), 918-931. <https://doi.org/10.1016/j.bbapap.2013.01.003>
- Margulies, C., Tully, T., & Dubnau, J. (2005). Deconstructing memory in *Drosophila*. *Curr Biol*, 15(17), R700-713. <https://doi.org/10.1016/j.cub.2005.08.024>
- Markmiller, S., Soltanieh, S., Server, K. L., Mak, R., Jin, W., Fang, M. Y., Luo, E. C., Krach, F., Yang, D., Sen, A., Fulzele, A., Wozniak, J. M., Gonzalez, D. J., Kankel, M. W., Gao, F. B., Bennett, E. J., Lecuyer, E., & Yeo, G. W. (2018). Context-Dependent and Disease-Specific Diversity in Protein Interactions within Stress Granules. *Cell*, 172(3), 590-604 e513. <https://doi.org/10.1016/j.cell.2017.12.032>
- Marrone, L., Drexler, H. C. A., Wang, J., Tripathi, P., Distler, T., Heisterkamp, P., Anderson, E. N., Kour, S., Moraiti, A., Maharana, S., Bhatnagar, R., Belgard, T. G., Tripathy, V., Kalmbach, N., Hosseinzadeh, Z., Crippa, V., Abo-Rady, M., Wegner, F., Poletti, A., Troost, D., Aronica, E., Busskamp, V., Weis, J., Pandey, U. B., Hyman, A. A., Alberti, S., Goswami, A., & Sternecker, J. (2019). FUS pathology in ALS is linked to alterations in multiple ALS-associated proteins and rescued by drugs stimulating autophagy. *Acta Neuropathol*, 138(1), 67-84. <https://doi.org/10.1007/s00401-019-01998-x>
- Martin, K. C., Casadio, A., Zhu, H., Yaping, E., Rose, J. C., Chen, M., Bailey, C. H., & Kandel, E. R. (1997). Synapse-specific, long-term facilitation of aplysia sensory to motor synapses: a function for local protein synthesis in memory storage. *Cell*, 91(7), 927-938. [https://doi.org/10.1016/s0092-8674\(00\)80484-5](https://doi.org/10.1016/s0092-8674(00)80484-5)
- Martins, R., Lithgow, G. J., & Link, W. (2016). Long live FOXO: unraveling the role of FOXO proteins in aging and longevity. *Aging Cell*, 15(2), 196-207. <https://doi.org/10.1111/accel.12427>

- Mateju, D., Eichenberger, B., Voigt, F., Eglinger, J., Roth, G., & Chao, J. A. (2020). Single-Molecule Imaging Reveals Translation of mRNAs Localized to Stress Granules. *Cell*, *183*(7), 1801-1812 e1813. <https://doi.org/10.1016/j.cell.2020.11.010>
- Matheny, T., Van Treeck, B., Huynh, T. N., & Parker, R. (2021). RNA partitioning into stress granules is based on the summation of multiple interactions. *RNA*, *27*(2), 174-189. <https://doi.org/10.1261/rna.078204.120>
- Matsuki, H., Takahashi, M., Higuchi, M., Makokha, G. N., Oie, M., & Fujii, M. (2013). Both G3BP1 and G3BP2 contribute to stress granule formation. *Genes Cells*, *18*(2), 135-146. <https://doi.org/10.1111/gtc.12023>
- Matsumoto, K., Nakayama, H., Yoshimura, M., Masuda, A., Dohmae, N., Matsumoto, S., & Tsujimoto, M. (2012). PRMT1 is required for RAP55 to localize to processing bodies. *RNA Biol*, *9*(5), 610-623. <https://doi.org/10.4161/rna.19527>
- McGuffee, S. R., & Elcock, A. H. (2010). Diffusion, crowding & protein stability in a dynamic molecular model of the bacterial cytoplasm. *PLoS Comput Biol*, *6*(3), e1000694. <https://doi.org/10.1371/journal.pcbi.1000694>
- McGuire, S. E., Le, P. T., & Davis, R. L. (2001). The role of Drosophila mushroom body signaling in olfactory memory. *Science*, *293*(5533), 1330-1333. <https://doi.org/10.1126/science.1062622>
- Medioni, C., Ramialison, M., Ephrussi, A., & Besse, F. (2014). Imp promotes axonal remodeling by regulating profilin mRNA during brain development. *Curr Biol*, *24*(7), 793-800. <https://doi.org/10.1016/j.cub.2014.02.038>
- Metschnikoff, E. (1865). Veber die Entwicklung der Cecidomyienlarven aus dem Pseudovum. *Arch. furr Naturg.*, *Bd 1*.
- Miller, L. C., Blandford, V., McAdam, R., Sanchez-Carbente, M. R., Badeaux, F., DesGroseillers, L., & Sossin, W. S. (2009). Combinations of DEAD box proteins distinguish distinct types of RNA: protein complexes in neurons. *Mol Cell Neurosci*, *40*(4), 485-495. <https://doi.org/10.1016/j.mcn.2009.01.007>
- Minshall, N., & Standart, N. (2004). The active form of Xp54 RNA helicase in translational repression is an RNA-mediated oligomer. *Nucleic Acids Res*, *32*(4), 1325-1334. <https://doi.org/10.1093/nar/gkh303>
- Mitsumori, K., Takei, Y., & Hirokawa, N. (2017). Components of RNA granules affect their localization and dynamics in neuronal dendrites. *Mol Biol Cell*, *28*(11), 1412-1417. <https://doi.org/10.1091/mbc.E16-07-0497>
- Molliex, A., Temirov, J., Lee, J., Coughlin, M., Kanagaraj, A. P., Kim, H. J., Mittag, T., & Taylor, J. P. (2015). Phase separation by low complexity domains promotes stress granule assembly and drives pathological fibrillization. *Cell*, *163*(1), 123-133. <https://doi.org/10.1016/j.cell.2015.09.015>
- Monahan, Z., Ryan, V. H., Janke, A. M., Burke, K. A., Rhoads, S. N., Zerze, G. H., O'Meally, R., Dignon, G. L., Conicella, A. E., Zheng, W., Best, R. B., Cole, R. N., Mittal, J., Shewmaker, F., & Fawzi, N. L. (2017). Phosphorylation of the FUS low-complexity domain disrupts phase separation, aggregation, and toxicity. *EMBO J*, *36*(20), 2951-2967. <https://doi.org/10.15252/emboj.201696394>
- Mori, F., Tanji, K., Zhang, H. X., Nishihira, Y., Tan, C. F., Takahashi, H., & Wakabayashi, K. (2008). Maturation process of TDP-43-positive neuronal cytoplasmic inclusions in amyotrophic lateral sclerosis with and without dementia. *Acta Neuropathol*, *116*(2), 193-203. <https://doi.org/10.1007/s00401-008-0396-9>
- Morrow, G., Battistini, S., Zhang, P., & Tanguay, R. M. (2004). Decreased lifespan in the absence of expression of the mitochondrial small heat shock protein Hsp22 in Drosophila. *J Biol Chem*, *279*(42), 43382-43385. <https://doi.org/10.1074/jbc.C400357200>
- Moser, J. J., & Fritzler, M. J. (2010). Cytoplasmic ribonucleoprotein (RNP) bodies and their relationship to GW/P bodies. *Int J Biochem Cell Biol*, *42*(6), 828-843. <https://doi.org/10.1016/j.biocel.2009.11.018>
- Mostoslavsky, R., Chua, K. F., Lombard, D. B., Pang, W. W., Fischer, M. R., Gellon, L., Liu, P., Mostoslavsky, G., Franco, S., Murphy, M. M., Mills, K. D., Patel, P., Hsu, J. T., Hong, A. L., Ford, E., Cheng, H. L., Kennedy, C., Nunez, N., Bronson, R., Frendewey, D., Auerbach, W., Valenzuela, D., Karow, M., Hottiger, M. O., Hursting, S., Barrett, J. C., Guarente, L., Mulligan, R., Demple, B., Yancopoulos, G. D., & Alt, F. W. (2006). Genomic instability and aging-like phenotype in the absence of mammalian SIRT6. *Cell*, *124*(2), 315-329. <https://doi.org/10.1016/j.cell.2005.11.044>
- Mugler, C. F., Hondele, M., Heinrich, S., Sachdev, R., Vallotton, P., Koek, A. Y., Chan, L. Y., & Weis, K. (2016). ATPase activity of the DEAD-box protein Dhh1 controls processing body formation. *Elife*, *5*. <https://doi.org/10.7554/eLife.18746>

- Munro, T. P., Kwon, S., Schnapp, B. J., & St Johnston, D. (2006). A repeated IMP-binding motif controls oskar mRNA translation and anchoring independently of *Drosophila melanogaster* IMP. *J Cell Biol*, 172(4), 577-588. <https://doi.org/10.1083/jcb.200510044>
- Murakami, T., Qamar, S., Lin, J. Q., Schierle, G. S., Rees, E., Miyashita, A., Costa, A. R., Dodd, R. B., Chan, F. T., Michel, C. H., Kronenberg-Versteeg, D., Li, Y., Yang, S. P., Wakutani, Y., Meadows, W., Ferry, R. R., Dong, L., Tartaglia, G. G., Favrin, G., Lin, W. L., Dickson, D. W., Zhen, M., Ron, D., Schmitt-Ulms, G., Fraser, P. E., Shneider, N. A., Holt, C., Vendruscolo, M., Kaminski, C. F., & St George-Hyslop, P. (2015). ALS/FTD Mutation-Induced Phase Transition of FUS Liquid Droplets and Reversible Hydrogels into Irreversible Hydrogels Impairs RNP Granule Function. *Neuron*, 88(4), 678-690. <https://doi.org/10.1016/j.neuron.2015.10.030>
- Nakamura, A., Amikura, R., Hanyu, K., & Kobayashi, S. (2001). Me31B silences translation of oocyte-localizing RNAs through the formation of cytoplasmic RNP complex during *Drosophila* oogenesis. *Development*, 128(17), 3233-3242. <https://www.ncbi.nlm.nih.gov/pubmed/11546740>
- Nakamura, A., Sato, K., & Hanyu-Nakamura, K. (2004). *Drosophila* cup is an eIF4E binding protein that associates with Bruno and regulates oskar mRNA translation in oogenesis. *Dev Cell*, 6(1), 69-78. [https://doi.org/10.1016/s1534-5807\(03\)00400-3](https://doi.org/10.1016/s1534-5807(03)00400-3)
- Nakayama, K., Ohashi, R., Shinoda, Y., Yamazaki, M., Abe, M., Fujikawa, A., Shigenobu, S., Futatsugi, A., Noda, M., Mikoshiba, K., Furuichi, T., Sakimura, K., & Shiina, N. (2017). RNG105/caprin1, an RNA granule protein for dendritic mRNA localization, is essential for long-term memory formation. *Elife*, 6. <https://doi.org/10.7554/eLife.29677>
- Nalavadi, V. C., Griffin, L. E., Picard-Fraser, P., Swanson, A. M., Takumi, T., & Bassell, G. J. (2012). Regulation of zipcode binding protein 1 transport dynamics in axons by myosin Va. *J Neurosci*, 32(43), 15133-15141. <https://doi.org/10.1523/JNEUROSCI.2006-12.2012>
- Namkoong, S., Ho, A., Woo, Y. M., Kwak, H., & Lee, J. H. (2018). Systematic Characterization of Stress-Induced RNA Granulation. *Mol Cell*, 70(1), 175-187 e178. <https://doi.org/10.1016/j.molcel.2018.02.025>
- Nelson, M. R., Leidal, A. M., & Smibert, C. A. (2004). *Drosophila* Cup is an eIF4E-binding protein that functions in Smaug-mediated translational repression. *EMBO J*, 23(1), 150-159. <https://doi.org/10.1038/sj.emboj.7600026>
- Niccoli, T., & Partridge, L. (2012). Ageing as a risk factor for disease. *Curr Biol*, 22(17), R741-752. <https://doi.org/10.1016/j.cub.2012.07.024>
- Nielsen, J., Christiansen, J., Lykke-Andersen, J., Johnsen, A. H., Wewer, U. M., & Nielsen, F. C. (1999). A family of insulin-like growth factor II mRNA-binding proteins represses translation in late development. *Mol Cell Biol*, 19(2), 1262-1270. <https://doi.org/10.1128/mcb.19.2.1262>
- Nielsen, J., Cilius Nielsen, F., Kragh Jakobsen, R., & Christiansen, J. (2000). The biphasic expression of IMP/Vg1-RBP is conserved between vertebrates and *Drosophila*. *Mech Dev*, 96(1), 129-132. [https://doi.org/10.1016/s0925-4773\(00\)00383-x](https://doi.org/10.1016/s0925-4773(00)00383-x)
- Nielsen, J., Kristensen, M. A., Willemoes, M., Nielsen, F. C., & Christiansen, J. (2004). Sequential dimerization of human zipcode-binding protein IMP1 on RNA: a cooperative mechanism providing RNP stability. *Nucleic Acids Res*, 32(14), 4368-4376. <https://doi.org/10.1093/nar/gkh754>
- Nighorn, A., Healy, M. J., & Davis, R. L. (1991). The cyclic AMP phosphodiesterase encoded by the *Drosophila dunce* gene is concentrated in the mushroom body neuropil. *Neuron*, 6(3), 455-467. [https://doi.org/10.1016/0896-6273\(91\)90253-v](https://doi.org/10.1016/0896-6273(91)90253-v)
- Nott, T. J., Petsalaki, E., Farber, P., Jervis, D., Fussner, E., Plochowietz, A., Craggs, T. D., Bazett-Jones, D. P., Pawson, T., Forman-Kay, J. D., & Baldwin, A. J. (2015). Phase transition of a disordered nuage protein generates environmentally responsive membraneless organelles. *Mol Cell*, 57(5), 936-947. <https://doi.org/10.1016/j.molcel.2015.01.013>
- Noubissi, F. K., Elcheva, I., Bhatia, N., Shakoori, A., Ougolkov, A., Liu, J., Minamoto, T., Ross, J., Fuchs, S. Y., & Spiegelman, V. S. (2006). CRD-BP mediates stabilization of betaTrCP1 and c-myc mRNA in response to beta-catenin signalling. *Nature*, 441(7095), 898-901. <https://doi.org/10.1038/nature04839>
- Nunes, V. S., & Moretti, N. S. (2017). Nuclear subcompartments: an overview. *Cell Biol Int*, 41(1), 2-7. <https://doi.org/10.1002/cbin.10703>
- Oakes, M. L., Johzuka, K., Vu, L., Eliason, K., & Nomura, M. (2006). Expression of rRNA genes and nucleolus formation at ectopic chromosomal sites in the yeast *Saccharomyces cerevisiae*. *Mol Cell Biol*, 26(16), 6223-6238. <https://doi.org/10.1128/MCB.02324-05>
- Oldfield, C. J., & Dunker, A. K. (2014). Intrinsically disordered proteins and intrinsically disordered protein regions. *Annu Rev Biochem*, 83, 553-584. <https://doi.org/10.1146/annurev-biochem-072711-164947>

- Ori, A., Toyama, B. H., Harris, M. S., Bock, T., Iskar, M., Bork, P., Ingolia, N. T., Hetzer, M. W., & Beck, M. (2015). Integrated Transcriptome and Proteome Analyses Reveal Organ-Specific Proteome Deterioration in Old Rats. *Cell Syst*, *1*(3), 224-237. <https://doi.org/10.1016/j.cels.2015.08.012>
- Ostareck, D. H., Naarmann-de Vries, I. S., & Ostareck-Lederer, A. (2014). DDX6 and its orthologs as modulators of cellular and viral RNA expression. *Wiley Interdiscip Rev RNA*, *5*(5), 659-678. <https://doi.org/10.1002/wrna.1237>
- Pacifico, R., MacMullen, C. M., Walkinshaw, E., Zhang, X., & Davis, R. L. (2018). Brain transcriptome changes in the aging *Drosophila melanogaster* accompany olfactory memory performance deficits. *PLoS One*, *13*(12), e0209405. <https://doi.org/10.1371/journal.pone.0209405>
- Panas, M. D., Ivanov, P., & Anderson, P. (2016). Mechanistic insights into mammalian stress granule dynamics. *J Cell Biol*, *215*(3), 313-323. <https://doi.org/10.1083/jcb.201609081>
- Parker, R., & Sheth, U. (2007). P bodies and the control of mRNA translation and degradation. *Mol Cell*, *25*(5), 635-646. <https://doi.org/10.1016/j.molcel.2007.02.011>
- Parsyan, A., Svitkin, Y., Shahbazian, D., Gkogkas, C., Lasko, P., Merrick, W. C., & Sonenberg, N. (2011). mRNA helicases: the tacticians of translational control. *Nat Rev Mol Cell Biol*, *12*(4), 235-245. <https://doi.org/10.1038/nrm3083>
- Patel, A., Lee, H. O., Jawerth, L., Maharana, S., Jahnel, M., Hein, M. Y., Stoyanov, S., Mahamid, J., Saha, S., Franzmann, T. M., Pozniakovski, A., Poser, I., Maghelli, N., Royer, L. A., Weigert, M., Myers, E. W., Grill, S., Drechsel, D., Hyman, A. A., & Alberti, S. (2015). A Liquid-to-Solid Phase Transition of the ALS Protein FUS Accelerated by Disease Mutation. *Cell*, *162*(5), 1066-1077. <https://doi.org/10.1016/j.cell.2015.07.047>
- Patel, A., Malinowska, L., Saha, S., Wang, J., Alberti, S., Krishnan, Y., & Hyman, A. A. (2017). ATP as a biological hydrotrope. *Science*, *356*(6339), 753-756. <https://doi.org/10.1126/science.aaf6846>
- Pederson, T. (2011). The nucleolus. *Cold Spring Harb Perspect Biol*, *3*(3). <https://doi.org/10.1101/cshperspect.a000638>
- Peter, D., Igreja, C., Weber, R., Wohlbold, L., Weiler, C., Ebertsch, L., Weichenrieder, O., & Izaurralde, E. (2015). Molecular architecture of 4E-BP translational inhibitors bound to eIF4E. *Mol Cell*, *57*(6), 1074-1087. <https://doi.org/10.1016/j.molcel.2015.01.017>
- Pimentel, J., & Boccaccio, G. L. (2014). Translation and silencing in RNA granules: a tale of sand grains. *Front Mol Neurosci*, *7*, 68. <https://doi.org/10.3389/fnmol.2014.00068>
- Piper, M. D. W., & Partridge, L. (2018). *Drosophila* as a model for ageing. *Biochim Biophys Acta Mol Basis Dis*, *1864*(9 Pt A), 2707-2717. <https://doi.org/10.1016/j.bbadis.2017.09.016>
- Pushpalatha, K. V., & Besse, F. (2019). Local Translation in Axons: When Membraneless RNP Granules Meet Membrane-Bound Organelles. *Front Mol Biosci*, *6*, 129. <https://doi.org/10.3389/fmolb.2019.00129>
- Putnam, A., Cassani, M., Smith, J., & Seydoux, G. (2019). A gel phase promotes condensation of liquid P granules in *Caenorhabditis elegans* embryos. *Nat Struct Mol Biol*, *26*(3), 220-226. <https://doi.org/10.1038/s41594-019-0193-2>
- Qamar, S., Wang, G., Randle, S. J., Ruggeri, F. S., Varela, J. A., Lin, J. Q., Phillips, E. C., Miyashita, A., Williams, D., Strohl, F., Meadows, W., Ferry, R., Dardov, V. J., Tartaglia, G. G., Farrer, L. A., Kaminski Schierle, G. S., Kaminski, C. F., Holt, C. E., Fraser, P. E., Schmitt-Ulms, G., Klenerman, D., Knowles, T., Vendruscolo, M., & St George-Hyslop, P. (2018). FUS Phase Separation Is Modulated by a Molecular Chaperone and Methylation of Arginine Cation-pi Interactions. *Cell*, *173*(3), 720-734 e715. <https://doi.org/10.1016/j.cell.2018.03.056>
- Raj, A., van den Bogaard, P., Rifkin, S. A., van Oudenaarden, A., & Tyagi, S. (2008). Imaging individual mRNA molecules using multiple singly labeled probes. *Nat Methods*, *5*(10), 877-879. <https://doi.org/10.1038/nmeth.1253>
- Ramaswami, M., Taylor, J. P., & Parker, R. (2013). Altered ribostasis: RNA-protein granules in degenerative disorders. *Cell*, *154*(4), 727-736. <https://doi.org/10.1016/j.cell.2013.07.038>
- Ramos, B. P., Birnbaum, S. G., Lindenmayer, I., Newton, S. S., Duman, R. S., & Arnsten, A. F. (2003). Dysregulation of protein kinase signaling in the aged prefrontal cortex: new strategy for treating age-related cognitive decline. *Neuron*, *40*(4), 835-845. [https://doi.org/10.1016/s0896-6273\(03\)00694-9](https://doi.org/10.1016/s0896-6273(03)00694-9)
- Rappsilber, J., Friesen, W. J., Paushkin, S., Dreyfuss, G., & Mann, M. (2003). Detection of arginine dimethylated peptides by parallel precursor ion scanning mass spectrometry in positive ion mode. *Anal Chem*, *75*(13), 3107-3114. <https://doi.org/10.1021/ac026283q>
- Reineke, L. C., Cheema, S. A., Dubrulle, J., & Neilson, J. R. (2018). Chronic starvation induces noncanonical pro-death stress granules. *J Cell Sci*, *131*(19). <https://doi.org/10.1242/jcs.220244>
- Reis-Rodrigues, P., Czerwieńiec, G., Peters, T. W., Evani, U. S., Alavez, S., Gaman, E. A., Vantipalli, M., Mooney, S. D., Gibson, B. W., Lithgow, G. J., & Hughes, R. E. (2012). Proteomic analysis of age-

- dependent changes in protein solubility identifies genes that modulate lifespan. *Aging Cell*, 11(1), 120-127. <https://doi.org/10.1111/j.1474-9726.2011.00765.x>
- Rhee, H. W., Zou, P., Udeshi, N. D., Martell, J. D., Mootha, V. K., Carr, S. A., & Ting, A. Y. (2013). Proteomic mapping of mitochondria in living cells via spatially restricted enzymatic tagging. *Science*, 339(6125), 1328-1331. <https://doi.org/10.1126/science.1230593>
- Rhoads, S. N., Monahan, Z. T., Yee, D. S., Leung, A. Y., Newcombe, C. G., O'Meally, R. N., Cole, R. N., & Shewmaker, F. P. (2018). The prionlike domain of FUS is multiphosphorylated following DNA damage without altering nuclear localization. *Mol Biol Cell*, 29(15), 1786-1797. <https://doi.org/10.1091/mbc.E17-12-0735>
- Rhoads, S. N., Monahan, Z. T., Yee, D. S., & Shewmaker, F. P. (2018). The Role of Post-Translational Modifications on Prion-Like Aggregation and Liquid-Phase Separation of FUS. *Int J Mol Sci*, 19(3). <https://doi.org/10.3390/ijms19030886>
- Riback, J. A., & Brangwynne, C. P. (2020). Can phase separation buffer cellular noise? *Science*, 367(6476), 364-365. <https://doi.org/10.1126/science.aba0446>
- Riback, J. A., Zhu, L., Ferrolino, M. C., Tolbert, M., Mitrea, D. M., Sanders, D. W., Wei, M. T., Kriwacki, R. W., & Brangwynne, C. P. (2020). Composition-dependent thermodynamics of intracellular phase separation. *Nature*, 581(7807), 209-214. <https://doi.org/10.1038/s41586-020-2256-2>
- Ribeiro de Almeida, C., Dhir, S., Dhir, A., Moghaddam, A. E., Sattentau, Q., Meinhart, A., & Proudfoot, N. J. (2018). RNA Helicase DDX1 Converts RNA G-Quadruplex Structures into R-Loops to Promote IgH Class Switch Recombination. *Mol Cell*, 70(4), 650-662 e658. <https://doi.org/10.1016/j.molcel.2018.04.001>
- Ries, R. J., Zaccara, S., Klein, P., Orlarerin-George, A., Namkoong, S., Pickering, B. F., Patil, D. P., Kwak, H., Lee, J. H., & Jaffrey, S. R. (2019). m(6)A enhances the phase separation potential of mRNA. *Nature*, 571(7765), 424-428. <https://doi.org/10.1038/s41586-019-1374-1>
- Rocak, S., & Linder, P. (2004). DEAD-box proteins: the driving forces behind RNA metabolism. *Nat Rev Mol Cell Biol*, 5(3), 232-241. <https://doi.org/10.1038/nrm1335>
- Ross, A. F., Oleynikov, Y., Kislauskis, E. H., Taneja, K. L., & Singer, R. H. (1997). Characterization of a beta-actin mRNA zipcode-binding protein. *Mol Cell Biol*, 17(4), 2158-2165. <https://doi.org/10.1128/mcb.17.4.2158>
- Rousakis, A., Vlanti, A., Borbolis, F., Roumelioti, F., Kapetanou, M., & Syntichaki, P. (2014). Diverse functions of mRNA metabolism factors in stress defense and aging of *Caenorhabditis elegans*. *PLoS One*, 9(7), e103365. <https://doi.org/10.1371/journal.pone.0103365>
- Rubinsztein, D. C., Marino, G., & Kroemer, G. (2011). Autophagy and aging. *Cell*, 146(5), 682-695. <https://doi.org/10.1016/j.cell.2011.07.030>
- Runge, S., Nielsen, F. C., Nielsen, J., Lykke-Andersen, J., Wewer, U. M., & Christiansen, J. (2000). H19 RNA binds four molecules of insulin-like growth factor II mRNA-binding protein. *J Biol Chem*, 275(38), 29562-29569. <https://doi.org/10.1074/jbc.M001156200>
- Saad, S., Cereghetti, G., Feng, Y., Picotti, P., Peter, M., & Dechant, R. (2017). Reversible protein aggregation is a protective mechanism to ensure cell cycle restart after stress. *Nat Cell Biol*, 19(10), 1202-1213. <https://doi.org/10.1038/ncb3600>
- Saha, S., Weber, C. A., Nusch, M., Adame-Arana, O., Hoegge, C., Hein, M. Y., Osborne-Nishimura, E., Mahamid, J., Jahnel, M., Jawerth, L., Pozniakovski, A., Eckmann, C. R., Julicher, F., & Hyman, A. A. (2016). Polar Positioning of Phase-Separated Liquid Compartments in Cells Regulated by an mRNA Competition Mechanism. *Cell*, 166(6), 1572-1584 e1516. <https://doi.org/10.1016/j.cell.2016.08.006>
- Samuels, T. J., Jarvelin, A. I., Ish-Horowicz, D., & Davis, I. (2020). Imp/IGF2BP levels modulate individual neural stem cell growth and division through myc mRNA stability. *Elife*, 9. <https://doi.org/10.7554/eLife.51529>
- Sanders, D. W., Kedersha, N., Lee, D. S. W., Strom, A. R., Drake, V., Riback, J. A., Bracha, D., Eeftens, J. M., Iwanicki, A., Wang, A., Wei, M. T., Whitney, G., Lyons, S. M., Anderson, P., Jacobs, W. M., Ivanov, P., & Brangwynne, C. P. (2020). Competing Protein-RNA Interaction Networks Control Multiphase Intracellular Organization. *Cell*, 181(2), 306-324 e328. <https://doi.org/10.1016/j.cell.2020.03.050>
- Santos, A. L., Sinha, S., & Lindner, A. B. (2018). The Good, the Bad, and the Ugly of ROS: New Insights on Aging and Aging-Related Diseases from Eukaryotic and Prokaryotic Model Organisms. *Oxid Med Cell Longev*, 2018, 1941285. <https://doi.org/10.1155/2018/1941285>
- Sawicka, K., Bushell, M., Spriggs, K. A., & Willis, A. E. (2008). Polypyrimidine-tract-binding protein: a multifunctional RNA-binding protein. *Biochem Soc Trans*, 36(Pt 4), 641-647. <https://doi.org/10.1042/BST0360641>

- Sawyer, I. A., Sturgill, D., Sung, M. H., Hager, G. L., & Dundr, M. (2016). Cajal body function in genome organization and transcriptome diversity. *Bioessays*, 38(12), 1197-1208. <https://doi.org/10.1002/bies.201600144>
- Schmidt, R. L., & Sheeley, S. L. (2015). Mating and memory: an educational primer for use with "epigenetic control of learning and memory in Drosophila by Tip60 HAT action". *Genetics*, 200(1), 21-28. <https://doi.org/10.1534/genetics.115.176313>
- Schwer, B. (2001). A new twist on RNA helicases: DExH/D box proteins as RNAPases. *Nat Struct Biol*, 8(2), 113-116. <https://doi.org/10.1038/84091>
- Sears, J. C., & Broadie, K. (2020). FMRP-PKA Activity Negative Feedback Regulates RNA Binding-Dependent Fibrillation in Brain Learning and Memory Circuitry. *Cell Rep*, 33(2), 108266. <https://doi.org/10.1016/j.celrep.2020.108266>
- Sengupta, M. S., & Boag, P. R. (2012). Germ granules and the control of mRNA translation. *IUBMB Life*, 64(7), 586-594. <https://doi.org/10.1002/iub.1039>
- Sheth, U., & Parker, R. (2003). Decapping and decay of messenger RNA occur in cytoplasmic processing bodies. *Science*, 300(5620), 805-808. <https://doi.org/10.1126/science.1082320>
- Shigeoka, T., Jung, H., Jung, J., Turner-Bridger, B., Ohk, J., Lin, J. Q., Amieux, P. S., & Holt, C. E. (2016). Dynamic Axonal Translation in Developing and Mature Visual Circuits. *Cell*, 166(1), 181-192. <https://doi.org/10.1016/j.cell.2016.05.029>
- Shigeoka, T., Lu, B., & Holt, C. E. (2013). Cell biology in neuroscience: RNA-based mechanisms underlying axon guidance. *J Cell Biol*, 202(7), 991-999. <https://doi.org/10.1083/jcb.201305139>
- Shih, J. W., Wang, W. T., Tsai, T. Y., Kuo, C. Y., Li, H. K., & Wu Lee, Y. H. (2012). Critical roles of RNA helicase DDX3 and its interactions with eIF4E/PABP1 in stress granule assembly and stress response. *Biochem J*, 441(1), 119-129. <https://doi.org/10.1042/BJ20110739>
- Shin, Y., Berry, J., Pannucci, N., Haataja, M. P., Toettcher, J. E., & Brangwynne, C. P. (2017). Spatiotemporal Control of Intracellular Phase Transitions Using Light-Activated optoDroplets. *Cell*, 168(1-2), 159-171 e114. <https://doi.org/10.1016/j.cell.2016.11.054>
- Silverman, E., Edwalds-Gilbert, G., & Lin, R. J. (2003). DExD/H-box proteins and their partners: helping RNA helicases unwind. *Gene*, 312, 1-16. [https://doi.org/10.1016/s0378-1119\(03\)00626-7](https://doi.org/10.1016/s0378-1119(03)00626-7)
- Singh, G., Pratt, G., Yeo, G. W., & Moore, M. J. (2015). The Clothes Make the mRNA: Past and Present Trends in mRNP Fashion. *Annu Rev Biochem*, 84, 325-354. <https://doi.org/10.1146/annurev-biochem-080111-092106>
- Skoulakis, E. M., Kalderon, D., & Davis, R. L. (1993). Preferential expression in mushroom bodies of the catalytic subunit of protein kinase A and its role in learning and memory. *Neuron*, 11(2), 197-208. [https://doi.org/10.1016/0896-6273\(93\)90178-t](https://doi.org/10.1016/0896-6273(93)90178-t)
- Smith, J., Calidas, D., Schmidt, H., Lu, T., Rasoloson, D., & Seydoux, G. (2016). Spatial patterning of P granules by RNA-induced phase separation of the intrinsically-disordered protein MEG-3. *Elife*, 5. <https://doi.org/10.7554/eLife.21337>
- Snead, W. T., & Gladfelter, A. S. (2019). The Control Centers of Biomolecular Phase Separation: How Membrane Surfaces, PTMs, and Active Processes Regulate Condensation. *Mol Cell*, 76(2), 295-305. <https://doi.org/10.1016/j.molcel.2019.09.016>
- Sonenberg, N., & Hinnebusch, A. G. (2009). Regulation of translation initiation in eukaryotes: mechanisms and biological targets. *Cell*, 136(4), 731-745. <https://doi.org/10.1016/j.cell.2009.01.042>
- Sparanese, D., & Lee, C. H. (2007). CRD-BP shields c-myc and MDR-1 RNA from endonucleolytic attack by a mammalian endoribonuclease. *Nucleic Acids Res*, 35(4), 1209-1221. <https://doi.org/10.1093/nar/gkl1148>
- Spector, D. L. (2006). SnapShot: Cellular bodies. *Cell*, 127(5), 1071. <https://doi.org/10.1016/j.cell.2006.11.026>
- St-Denis, N., & Gingras, A. C. (2012). Mass spectrometric tools for systematic analysis of protein phosphorylation. *Prog Mol Biol Transl Sci*, 106, 3-32. <https://doi.org/10.1016/B978-0-12-396456-4.00014-6>
- Stanton, P. K., & Sarvey, J. M. (1984). Blockade of long-term potentiation in rat hippocampal CA1 region by inhibitors of protein synthesis. *J Neurosci*, 4(12), 3080-3088. <https://www.ncbi.nlm.nih.gov/pubmed/6502226>
- Stegeman, R., & Weake, V. M. (2017). Transcriptional Signatures of Aging. *J Mol Biol*, 429(16), 2427-2437. <https://doi.org/10.1016/j.jmb.2017.06.019>
- Stoecklin, G., & Kedersha, N. (2013). Relationship of GW/P-bodies with stress granules. *Adv Exp Med Biol*, 768, 197-211. https://doi.org/10.1007/978-1-4614-5107-5_12
- Stoeger, T., Battich, N., & Pelkmans, L. (2016). Passive Noise Filtering by Cellular Compartmentalization. *Cell*, 164(6), 1151-1161. <https://doi.org/10.1016/j.cell.2016.02.005>

- Stroberg, W., & Schnell, S. (2018). Do Cellular Condensates Accelerate Biochemical Reactions? Lessons from Microdroplet Chemistry. *Biophys J*, *115*(1), 3-8. <https://doi.org/10.1016/j.bpj.2018.05.023>
- Strom, A. R., & Brangwynne, C. P. (2019). The liquid nucleome - phase transitions in the nucleus at a glance. *J Cell Sci*, *132*(22). <https://doi.org/10.1242/jcs.235093>
- Suarez-Calvet, M., Neumann, M., Arzberger, T., Abou-Ajram, C., Funk, E., Hartmann, H., Edbauer, D., Kremmer, E., Gobl, C., Resch, M., Bourgeois, B., Madl, T., Reber, S., Jutzi, D., Ruepp, M. D., Mackenzie, I. R., Ansorge, O., Dormann, D., & Haass, C. (2016). Monomethylated and unmethylated FUS exhibit increased binding to Transportin and distinguish FTLD-FUS from ALS-FUS. *Acta Neuropathol*, *131*(4), 587-604. <https://doi.org/10.1007/s00401-016-1544-2>
- Sudhakaran, I. P., & Ramaswami, M. (2017). Long-term memory consolidation: The role of RNA-binding proteins with prion-like domains. *RNA Biol*, *14*(5), 568-586. <https://doi.org/10.1080/15476286.2016.1244588>
- Sutton, M. A., & Schuman, E. M. (2006). Dendritic protein synthesis, synaptic plasticity, and memory. *Cell*, *127*(1), 49-58. <https://doi.org/10.1016/j.cell.2006.09.014>
- Symmons, O., & Raj, A. (2016). What's Luck Got to Do with It: Single Cells, Multiple Fates, and Biological Nondeterminism. *Mol Cell*, *62*(5), 788-802. <https://doi.org/10.1016/j.molcel.2016.05.023>
- Takahara, T., & Maeda, T. (2012). Transient sequestration of TORC1 into stress granules during heat stress. *Mol Cell*, *47*(2), 242-252. <https://doi.org/10.1016/j.molcel.2012.05.019>
- Taliaferro, J. M., Vidaki, M., Oliveira, R., Olson, S., Zhan, L., Saxena, T., Wang, E. T., Graveley, B. R., Gertler, F. B., Swanson, M. S., & Burge, C. B. (2016). Distal Alternative Last Exons Localize mRNAs to Neural Projections. *Mol Cell*, *61*(6), 821-833. <https://doi.org/10.1016/j.molcel.2016.01.020>
- Tamura, T., Chiang, A. S., Ito, N., Liu, H. P., Horiuchi, J., Tully, T., & Saitoe, M. (2003). Aging specifically impairs amnesiac-dependent memory in *Drosophila*. *Neuron*, *40*(5), 1003-1011. [https://doi.org/10.1016/s0896-6273\(03\)00732-3](https://doi.org/10.1016/s0896-6273(03)00732-3)
- Tanner, N. K., Cordin, O., Banroques, J., Doere, M., & Linder, P. (2003). The Q motif: a newly identified motif in DEAD box helicases may regulate ATP binding and hydrolysis. *Mol Cell*, *11*(1), 127-138. [https://doi.org/10.1016/s1097-2765\(03\)00006-6](https://doi.org/10.1016/s1097-2765(03)00006-6)
- Tatar, M., Kopelman, A., Epstein, D., Tu, M. P., Yin, C. M., & Garofalo, R. S. (2001). A mutant *Drosophila* insulin receptor homolog that extends life-span and impairs neuroendocrine function. *Science*, *292*(5514), 107-110. <https://doi.org/10.1126/science.1057987>
- Tauber, D., Tauber, G., Khong, A., Van Treeck, B., Pelletier, J., & Parker, R. (2020). Modulation of RNA Condensation by the DEAD-Box Protein eIF4A. *Cell*, *180*(3), 411-426 e416. <https://doi.org/10.1016/j.cell.2019.12.031>
- Taylor, J. P., Brown, R. H., Jr., & Cleveland, D. W. (2016). Decoding ALS: from genes to mechanism. *Nature*, *539*(7628), 197-206. <https://doi.org/10.1038/nature20413>
- Taylor, J. P., Hardy, J., & Fischbeck, K. H. (2002). Toxic proteins in neurodegenerative disease. *Science*, *296*(5575), 1991-1995. <https://doi.org/10.1126/science.1067122>
- Teixeira, D., Sheth, U., Valencia-Sanchez, M. A., Brengues, M., & Parker, R. (2005). Processing bodies require RNA for assembly and contain nontranslating mRNAs. *RNA*, *11*(4), 371-382. <https://doi.org/10.1261/rna.7258505>
- Tiruchinapalli, D. M., Oleynikov, Y., Kelic, S., Shenoy, S. M., Hartley, A., Stanton, P. K., Singer, R. H., & Bassell, G. J. (2003). Activity-dependent trafficking and dynamic localization of zipcode binding protein 1 and beta-actin mRNA in dendrites and spines of hippocampal neurons. *J Neurosci*, *23*(8), 3251-3261. <https://www.ncbi.nlm.nih.gov/pubmed/12716932>
- Tomaru, U., Takahashi, S., Ishizu, A., Miyatake, Y., Gohda, A., Suzuki, S., Ono, A., Ohara, J., Baba, T., Murata, S., Tanaka, K., & Kasahara, M. (2012). Decreased proteasomal activity causes age-related phenotypes and promotes the development of metabolic abnormalities. *Am J Pathol*, *180*(3), 963-972. <https://doi.org/10.1016/j.ajpath.2011.11.012>
- Tourriere, H., Chebli, K., Zekri, L., Courselaud, B., Blanchard, J. M., Bertrand, E., & Tazi, J. (2003). The RasGAP-associated endoribonuclease G3BP assembles stress granules. *J Cell Biol*, *160*(6), 823-831. <https://doi.org/10.1083/jcb.200212128>
- Trifunovic, A., Wredenberg, A., Falkenberg, M., Spelbrink, J. N., Rovio, A. T., Bruder, C. E., Bohlooly, Y. M., Gidlof, S., Oldfors, A., Wibom, R., Tornell, J., Jacobs, H. T., & Larsson, N. G. (2004). Premature ageing in mice expressing defective mitochondrial DNA polymerase. *Nature*, *429*(6990), 417-423. <https://doi.org/10.1038/nature02517>
- Tritschler, F., Braun, J. E., Eulalio, A., Truffault, V., Izaurralde, E., & Weichenrieder, O. (2009). Structural basis for the mutually exclusive anchoring of P body components EDC3 and Tral to the DEAD box protein DDX6/Me31B. *Mol Cell*, *33*(5), 661-668. <https://doi.org/10.1016/j.molcel.2009.02.014>

- Tritschler, F., Eulalio, A., Helms, S., Schmidt, S., Coles, M., Weichenrieder, O., Izaurralde, E., & Truffault, V. (2008). Similar modes of interaction enable Trailer Hitch and EDC3 to associate with DCPI and Me31B in distinct protein complexes. *Mol Cell Biol*, 28(21), 6695-6708. <https://doi.org/10.1128/MCB.00759-08>
- Tsai, W. C., Gayatri, S., Reineke, L. C., Sbardella, G., Bedford, M. T., & Lloyd, R. E. (2016). Arginine Demethylation of G3BP1 Promotes Stress Granule Assembly. *J Biol Chem*, 291(43), 22671-22685. <https://doi.org/10.1074/jbc.M116.739573>
- Tsai, W. C., Reineke, L. C., Jain, A., Jung, S. Y., & Lloyd, R. E. (2017). Histone arginine demethylase JMJD6 is linked to stress granule assembly through demethylation of the stress granule-nucleating protein G3BP1. *J Biol Chem*, 292(46), 18886-18896. <https://doi.org/10.1074/jbc.M117.800706>
- Tseng-Rogenski, S. S., Chong, J. L., Thomas, C. B., Enomoto, S., Berman, J., & Chang, T. H. (2003). Functional conservation of Dhh1p, a cytoplasmic DExD/H-box protein present in large complexes. *Nucleic Acids Res*, 31(17), 4995-5002. <https://doi.org/10.1093/nar/gkg712>
- Turrel, O., Rabah, Y., Placais, P. Y., Goguel, V., & Preat, T. (2020). Drosophila Middle-Term Memory: Amnesiac is Required for PKA Activation in the Mushroom Bodies, a Function Modulated by Neprilysin 1. *J Neurosci*, 40(21), 4219-4229. <https://doi.org/10.1523/JNEUROSCI.2311-19.2020>
- Updike, D. L., & Strome, S. (2009). A genomewide RNAi screen for genes that affect the stability, distribution and function of P granules in *Caenorhabditis elegans*. *Genetics*, 183(4), 1397-1419. <https://doi.org/10.1534/genetics.109.110171>
- Urbanska, A. S., Janusz-Kaminska, A., Switon, K., Hawthorne, A. L., Perycz, M., Urbanska, M., Bassell, G. J., & Jaworski, J. (2017). ZBP1 phosphorylation at serine 181 regulates its dendritic transport and the development of dendritic trees of hippocampal neurons. *Sci Rep*, 7(1), 1876. <https://doi.org/10.1038/s41598-017-01963-2>
- Van Treeck, B., & Parker, R. (2018). Emerging Roles for Intermolecular RNA-RNA Interactions in RNP Assemblies. *Cell*, 174(4), 791-802. <https://doi.org/10.1016/j.cell.2018.07.023>
- Van Treeck, B., Protter, D. S. W., Matheny, T., Khong, A., Link, C. D., & Parker, R. (2018). RNA self-assembly contributes to stress granule formation and defining the stress granule transcriptome. *Proc Natl Acad Sci U S A*, 115(11), 2734-2739. <https://doi.org/10.1073/pnas.1800038115>
- Vermulst, M., Wanagat, J., Kujoth, G. C., Bielas, J. H., Rabinovitch, P. S., Prolla, T. A., & Loeb, L. A. (2008). DNA deletions and clonal mutations drive premature aging in mitochondrial mutator mice. *Nat Genet*, 40(4), 392-394. <https://doi.org/10.1038/ng.95>
- Vijayakumar, J., Perrois, C., Heim, M., Bousset, L., Alberti, S., & Besse, F. (2019). The prion-like domain of Drosophila Imp promotes axonal transport of RNP granules in vivo. *Nat Commun*, 10(1), 2593. <https://doi.org/10.1038/s41467-019-10554-w>
- Vikesaa, J., Hansen, T. V., Jonson, L., Borup, R., Wewer, U. M., Christiansen, J., & Nielsen, F. C. (2006). RNA-binding IMPs promote cell adhesion and invadopodia formation. *EMBO J*, 25(7), 1456-1468. <https://doi.org/10.1038/sj.emboj.7601039>
- Wachter, K., Kohn, M., Stohr, N., & Huttelmaier, S. (2013). Subcellular localization and RNP formation of IGF2BPs (IGF2 mRNA-binding proteins) is modulated by distinct RNA-binding domains. *Biol Chem*, 394(8), 1077-1090. <https://doi.org/10.1515/hsz-2013-0111>
- Walker, G. A., & Lithgow, G. J. (2003). Lifespan extension in *C. elegans* by a molecular chaperone dependent upon insulin-like signals. *Aging Cell*, 2(2), 131-139. <https://doi.org/10.1046/j.1474-9728.2003.00045.x>
- Walther, D. M., Kasturi, P., Zheng, M., Pinkert, S., Vecchi, G., Ciryam, P., Morimoto, R. I., Dobson, C. M., Vendruscolo, M., Mann, M., & Hartl, F. U. (2015). Widespread Proteome Remodeling and Aggregation in Aging *C. elegans*. *Cell*, 161(4), 919-932. <https://doi.org/10.1016/j.cell.2015.03.032>
- Wang, A. C., Jensen, E. H., Rexach, J. E., Vinters, H. V., & Hsieh-Wilson, L. C. (2016). Loss of O-GlcNAc glycosylation in forebrain excitatory neurons induces neurodegeneration. *Proc Natl Acad Sci U S A*, 113(52), 15120-15125. <https://doi.org/10.1073/pnas.1606899113>
- Wang, C., Schmich, F., Srivatsa, S., Weidner, J., Beerenwinkel, N., & Spang, A. (2018). Context-dependent deposition and regulation of mRNAs in P-bodies. *Elife*, 7. <https://doi.org/10.7554/eLife.29815>
- Wang, I. F., Wu, L. S., Chang, H. Y., & Shen, C. K. (2008). TDP-43, the signature protein of FTL-D-U, is a neuronal activity-responsive factor. *J Neurochem*, 105(3), 797-806. <https://doi.org/10.1111/j.1471-4159.2007.05190.x>
- Wang, J., Choi, J. M., Holehouse, A. S., Lee, H. O., Zhang, X., Jahnel, M., Maharana, S., Lemaitre, R., Pozniakovskiy, A., Drechsel, D., Poser, I., Pappu, R. V., Alberti, S., & Hyman, A. A. (2018). A Molecular Grammar Governing the Driving Forces for Phase Separation of Prion-like RNA Binding Proteins. *Cell*, 174(3), 688-699 e616. <https://doi.org/10.1016/j.cell.2018.06.006>

- Wang, J., Li, T., Deng, S., Ma, E., Zhang, J., & Xing, S. (2021). DDX6 Is Essential for Oocyte Development and Maturation in *Locusta migratoria*. *Insects*, *12*(1). <https://doi.org/10.3390/insects12010070>
- Wang, M., Ly, M., Lugowski, A., Laver, J. D., Lipshitz, H. D., Smibert, C. A., & Rissland, O. S. (2017). ME31B globally represses maternal mRNAs by two distinct mechanisms during the *Drosophila* maternal-to-zygotic transition. *Elife*, *6*. <https://doi.org/10.7554/eLife.27891>
- Wang, W. Y., Pan, L., Su, S. C., Quinn, E. J., Sasaki, M., Jimenez, J. C., Mackenzie, I. R., Huang, E. J., & Tsai, L. H. (2013). Interaction of FUS and HDAC1 regulates DNA damage response and repair in neurons. *Nat Neurosci*, *16*(10), 1383-1391. <https://doi.org/10.1038/nn.3514>
- Weber, S. C., & Brangwynne, C. P. (2015). Inverse size scaling of the nucleolus by a concentration-dependent phase transition. *Curr Biol*, *25*(5), 641-646. <https://doi.org/10.1016/j.cub.2015.01.012>
- Weidtkamp-Peters, S., Lenser, T., Negorev, D., Gerstner, N., Hofmann, T. G., Schwanitz, G., Hoischen, C., Maul, G., Dittrich, P., & Hemmerich, P. (2008). Dynamics of component exchange at PML nuclear bodies. *J Cell Sci*, *121*(Pt 16), 2731-2743. <https://doi.org/10.1242/jcs.031922>
- Wheeler, J. R., Matheny, T., Jain, S., Abrisch, R., & Parker, R. (2016). Distinct stages in stress granule assembly and disassembly. *Elife*, *5*. <https://doi.org/10.7554/eLife.18413>
- Wilcken, R., Wang, G., Boeckler, F. M., & Fersht, A. R. (2012). Kinetic mechanism of p53 oncogenic mutant aggregation and its inhibition. *Proc Natl Acad Sci U S A*, *109*(34), 13584-13589. <https://doi.org/10.1073/pnas.1211550109>
- Wippich, F., Bodenmiller, B., Trajkovska, M. G., Wanka, S., Aebersold, R., & Pelkmans, L. (2013). Dual specificity kinase DYRK3 couples stress granule condensation/dissolution to mTORC1 signaling. *Cell*, *152*(4), 791-805. <https://doi.org/10.1016/j.cell.2013.01.033>
- Wolozin, B., & Ivanov, P. (2019). Stress granules and neurodegeneration. *Nat Rev Neurosci*, *20*(11), 649-666. <https://doi.org/10.1038/s41583-019-0222-5>
- Wong, H. H., Lin, J. Q., Strohl, F., Roque, C. G., Cioni, J. M., Cagnetta, R., Turner-Bridger, B., Laine, R. F., Harris, W. A., Kaminski, C. F., & Holt, C. E. (2017). RNA Docking and Local Translation Regulate Site-Specific Axon Remodeling In Vivo. *Neuron*, *95*(4), 852-868 e858. <https://doi.org/10.1016/j.neuron.2017.07.016>
- Woulfe, J., Gray, D. A., & Mackenzie, I. R. (2010). FUS-immunoreactive intranuclear inclusions in neurodegenerative disease. *Brain Pathol*, *20*(3), 589-597. <https://doi.org/10.1111/j.1750-3639.2009.00337.x>
- Wu, B., Eliscovich, C., Yoon, Y. J., & Singer, R. H. (2016). Translation dynamics of single mRNAs in live cells and neurons. *Science*, *352*(6292), 1430-1435. <https://doi.org/10.1126/science.aaf1084>
- Xiang, S., Kato, M., Wu, L. C., Lin, Y., Ding, M., Zhang, Y., Yu, Y., & McKnight, S. L. (2015). The LC Domain of hnRNP A2 Adopts Similar Conformations in Hydrogel Polymers, Liquid-like Droplets, and Nuclei. *Cell*, *163*(4), 829-839. <https://doi.org/10.1016/j.cell.2015.10.040>
- Xing, W., Muhrlad, D., Parker, R., & Rosen, M. K. (2020). A quantitative inventory of yeast P body proteins reveals principles of composition and specificity. *Elife*, *9*. <https://doi.org/10.7554/eLife.56525>
- Xue, S., Gong, R., He, F., Li, Y., Wang, Y., Tan, T., & Luo, S. Z. (2019). Low-complexity domain of U1-70K modulates phase separation and aggregation through distinctive basic-acidic motifs. *Sci Adv*, *5*(11), eaax5349. <https://doi.org/10.1126/sciadv.aax5349>
- Yamazaki, D., Horiuchi, J., Miyashita, T., & Saitoe, M. (2010). Acute inhibition of PKA activity at old ages ameliorates age-related memory impairment in *Drosophila*. *J Neurosci*, *30*(46), 15573-15577. <https://doi.org/10.1523/JNEUROSCI.3229-10.2010>
- Yamazaki, D., Horiuchi, J., Nakagami, Y., Nagano, S., Tamura, T., & Saitoe, M. (2007). The *Drosophila* DCO mutation suppresses age-related memory impairment without affecting lifespan. *Nat Neurosci*, *10*(4), 478-484. <https://doi.org/10.1038/nn1863>
- Yamazaki, D., & Saitoe, M. (2008). [cAMP/PKA signaling underlies age-related memory impairment]. *Brain Nerve*, *60*(7), 717-724. <https://www.ncbi.nlm.nih.gov/pubmed/18646611>
- Yan, X., Hoek, T. A., Vale, R. D., & Tanenbaum, M. E. (2016). Dynamics of Translation of Single mRNA Molecules In Vivo. *Cell*, *165*(4), 976-989. <https://doi.org/10.1016/j.cell.2016.04.034>
- Yan, X., Mouillet, J. F., Ou, Q., & Sadosky, Y. (2003). A novel domain within the DEAD-box protein DP103 is essential for transcriptional repression and helicase activity. *Mol Cell Biol*, *23*(1), 414-423. <https://doi.org/10.1128/mcb.23.1.414-423.2003>
- Yang, C. P., Samuels, T. J., Huang, Y., Yang, L., Ish-Horowicz, D., Davis, I., & Lee, T. (2017). Imp and Syp RNA-binding proteins govern decommissioning of *Drosophila* neural stem cells. *Development*, *144*(19), 3454-3464. <https://doi.org/10.1242/dev.149500>
- Yang, L., Cao, Y., Zhao, J., Fang, Y., Liu, N., & Zhang, Y. (2019). Multidimensional Proteomics Identifies Declines in Protein Homeostasis and Mitochondria as Early Signals for Normal Aging and Age-associated Disease in *Drosophila*. *Mol Cell Proteomics*, *18*(10), 2078-2088. <https://doi.org/10.1074/mcp.RA119.001621>

- Yaniv, K., Fainsod, A., Kalcheim, C., & Yisraeli, J. K. (2003). The RNA-binding protein Vg1 RBP is required for cell migration during early neural development. *Development*, *130*(23), 5649-5661. <https://doi.org/10.1242/dev.00810>
- Youn, J. Y., Dunham, W. H., Hong, S. J., Knight, J. D. R., Bashkurov, M., Chen, G. I., Bagci, H., Rathod, B., MacLeod, G., Eng, S. W. M., Angers, S., Morris, Q., Fabian, M., Cote, J. F., & Gingras, A. C. (2018). High-Density Proximity Mapping Reveals the Subcellular Organization of mRNA-Associated Granules and Bodies. *Mol Cell*, *69*(3), 517-532 e511. <https://doi.org/10.1016/j.molcel.2017.12.020>
- Yu, F., & Schuldiner, O. (2014). Axon and dendrite pruning in Drosophila. *Curr Opin Neurobiol*, *27*, 192-198. <https://doi.org/10.1016/j.conb.2014.04.005>
- Zappulo, A., van den Bruck, D., Ciolli Mattioli, C., Franke, V., Imami, K., McShane, E., Moreno-Estelles, M., Calviello, L., Filipchuk, A., Peguero-Sanchez, E., Muller, T., Woehler, A., Birchmeier, C., Merino, E., Rajewsky, N., Ohler, U., Mazzoni, E. O., Selbach, M., Akalin, A., & Chekulaeva, M. (2017). RNA localization is a key determinant of neurite-enriched proteome. *Nat Commun*, *8*(1), 583. <https://doi.org/10.1038/s41467-017-00690-6>
- Zeitelhofer, M., Karra, D., Macchi, P., Tolino, M., Thomas, S., Schwarz, M., Kiebler, M., & Dahm, R. (2008). Dynamic interaction between P-bodies and transport ribonucleoprotein particles in dendrites of mature hippocampal neurons. *J Neurosci*, *28*(30), 7555-7562. <https://doi.org/10.1523/JNEUROSCI.0104-08.2008>
- Zhang, C., & Cuervo, A. M. (2008). Restoration of chaperone-mediated autophagy in aging liver improves cellular maintenance and hepatic function. *Nat Med*, *14*(9), 959-965. <https://doi.org/10.1038/nm.1851>
- Zhang, H., Elbaum-Garfinkle, S., Langdon, E. M., Taylor, N., Occhipinti, P., Bridges, A. A., Brangwynne, C. P., & Gladfelter, A. S. (2015). RNA Controls PolyQ Protein Phase Transitions. *Mol Cell*, *60*(2), 220-230. <https://doi.org/10.1016/j.molcel.2015.09.017>
- Zhang, H. L., Eom, T., Oleynikov, Y., Shenoy, S. M., Liebelt, D. A., Dichtenberg, J. B., Singer, R. H., & Bassell, G. J. (2001). Neurotrophin-induced transport of a beta-actin mRNP complex increases beta-actin levels and stimulates growth cone motility. *Neuron*, *31*(2), 261-275. [https://doi.org/10.1016/s0896-6273\(01\)00357-9](https://doi.org/10.1016/s0896-6273(01)00357-9)
- Zhang, P., Fan, B., Yang, P., Temirov, J., Messing, J., Kim, H. J., & Taylor, J. P. (2019). Chronic optogenetic induction of stress granules is cytotoxic and reveals the evolution of ALS-FTD pathology. *Elife*, *8*. <https://doi.org/10.7554/eLife.39578>
- Zhang, Q., Chen, C. Y., Yedavalli, V. S., & Jeang, K. T. (2013). NEAT1 long noncoding RNA and paraspeckle bodies modulate HIV-1 posttranscriptional expression. *mBio*, *4*(1), e00596-00512. <https://doi.org/10.1128/mBio.00596-12>
- Zhong, S., Muller, S., Ronchetti, S., Freemont, P. S., Dejean, A., & Pandolfi, P. P. (2000). Role of SUMO-1-modified PML in nuclear body formation. *Blood*, *95*(9), 2748-2752. <https://www.ncbi.nlm.nih.gov/pubmed/10779416>

Appendix

- 1) Review- Local Translation in Axons: When Membraneless RNP Granules Meet Membrane-Bound Organelles
- 2) Method chapter- Detecting Stress Granules in Drosophila neurons



Local Translation in Axons: When Membraneless RNP Granules Meet Membrane-Bound Organelles

Kavya Vinayan Pushpalatha and Florence Besse*

Université Côte d'Azur, CNRS, Inserm, Institut de Biologie Valrose, Nice, France

OPEN ACCESS

Edited by:

Florence Rage,
Délégation Languedoc Roussillon
(CNRS), France

Reviewed by:

Michael A. Kiebler,
Ludwig Maximilian University of
Munich, Germany
Maria Paola Paronetto,
Foro Italico University of Rome, Italy

*Correspondence:

Florence Besse
florence.besse@univ-cotedazur.fr

Specialty section:

This article was submitted to
Protein and RNA Networks,
a section of the journal
Frontiers in Molecular Biosciences

Received: 23 September 2019

Accepted: 06 November 2019

Published: 22 November 2019

Citation:

Pushpalatha KV and Besse F (2019)
Local Translation in Axons: When
Membraneless RNP Granules Meet
Membrane-Bound Organelles.
Front. Mol. Biosci. 6:129.
doi: 10.3389/fmolb.2019.00129

Eukaryotic cell compartmentalization relies on long-known membrane-delimited organelles, as well as on more recently discovered membraneless macromolecular condensates. How these two types of organelles interact to regulate cellular functions is still largely unclear. In this review, we highlight how membraneless ribonucleoprotein (RNP) organelles, enriched in RNAs and associated regulatory proteins, cooperate with membrane-bound organelles for tight spatio-temporal control of gene expression in the axons of neuronal cells. Specifically, we present recent evidence that motile membrane-bound organelles are used as vehicles by RNP cargoes, promoting the long-range transport of mRNA molecules to distal axons. As demonstrated by recent work, membrane-bound organelles also promote local protein synthesis, by serving as platforms for the local translation of mRNAs recruited to their outer surface. Furthermore, dynamic and specific association between RNP cargoes and membrane-bound organelles is mediated by bi-partite adapter molecules that interact with both types of organelles selectively, in a regulated-manner. Maintaining such a dynamic interplay is critical, as alterations in this process are linked to neurodegenerative diseases. Together, emerging studies thus point to the coordination of membrane-bound and membraneless organelles as an organizing principle underlying local cellular responses.

Keywords: RNA transport, local translation, RNP granules, axon, vesicular trafficking, mitochondria

INTRODUCTION

Neurons are highly polarized cells that establish long-distance contacts with numerous other cells by extending cellular processes specialized in information transfer, processing and storage. During nervous system development, neurons in particular extend growing axons that navigate toward specific targets and branch in response to chemical and mechanical cues. Axonal processes then mature into presynaptic terminals that are actively maintained in response to neurotrophic factors and locally remodeled upon neuronal activity. Thus, both immature and mature axons must dynamically adjust their molecular content to respond rapidly to localized extracellular cues. Local translation of mRNAs targeted to axonal compartments has proven to be a very efficient means employed by neuronal cells to regulate their axonal proteome with high spatio-temporal resolution (Jung et al., 2012; Sahoo et al., 2018; Holt et al., 2019). Indeed, recent *in vitro* and *in vivo* transcriptome-wide studies have revealed that up to hundreds of transcripts are found in axons and translated in response to specific cues (Zivraj et al., 2010; Gumy et al., 2011; Shigeoka et al., 2016; Cagnetta et al., 2018; Pouloupoulos et al., 2019). Furthermore, functionally relevant changes in the axonal transcriptome are observed during nervous system maturation, upon switching from

axonal elongation to neurotransmission (Shigeoka et al., 2016). Both specific targeting of mRNAs and tight translational regulation are controlled by RNA binding proteins (RBPs) that recognize distinct sets of transcripts and assemble with their targets into macromolecular ribonucleoprotein (RNP) assemblies termed RNP granules (Muller-McNicoll and Neugebauer, 2013; De Graeve and Besse, 2018; Gallagher and Ramos, 2018; Formicola et al., 2019). These granules are actively transported along axons and contribute to translational control dually, on one hand by participating to the repression of their associated mRNAs during transport, and on the other hand by fuelling local protein synthesis upon cue-induced remodeling (De Graeve and Besse, 2018; Formicola et al., 2019). As revealed by recent *in vitro* and *in vivo* work, neuronal RNP granules result from a self-assembly process that generates phase-separated condensates selectively concentrating RNA and protein molecules (Murakami et al., 2015; Patel et al., 2015; Gopal et al., 2017; Shin and Brangwynne, 2017; Tsang et al., 2019). While this discovery nicely explains the dynamic behavior of these membraneless organelles, it does not shed light onto how RNP granules are hooked to the transport machinery for long-distance transport, or how they are linked to the translational machinery.

In this review, we first present recent work describing the material properties of RNP condensates. We then discuss recent evidence suggesting that RNP condensates tightly interact with membrane-bound organelles undergoing active, motor-driven motion for their transport to axons. Tight connections between membraneless RNP granules and axonally-localized membrane-bound organelles are also crucial for translation, as both mitochondria and endosomes were shown to serve as platforms supporting local protein synthesis. Understanding how these connections are regulated is key, and we highlight here the major role played by adapter molecules that bridge the two types of organelles specifically, in response to local signals. In the last part of this review, we present a model whereby targeting of RNP granules to distinct membrane-bound organelles or sub-cellular compartments may lead to stimuli-specific translation activation patterns. Finally, evidence linking altered interactions between RNP granule and membrane-bound organelles with the progression of neurodegenerative diseases is discussed.

NEURONAL RNP GRANULES ARE MEMBRANELESS PHASE-SEPARATED ORGANELLES

Cellular and biochemical studies have defined neuronal RNP granules as macromolecular entities enriched in RNA and associated RNA binding proteins, and detected as punctate structures by light microscopy (De Graeve and Besse, 2018; Formicola et al., 2019). Characterization of RNP granule content, on one hand, revealed that neuronal RNP granules are not all identical, but rather contain heterogeneous sets of regulatory proteins and target RNAs (De Graeve and Besse, 2018). For example, a minimal overlap was observed in both the protein and the RNA content of RNP granules purified from rat brain using two established RBP markers: Staufen2

and Barentsz (Fritzsche et al., 2013; Heraud-Farlow et al., 2013). Furthermore, differences in granule composition were observed when comparing dendritically- and axonally-localized FMRP-positive granules (Christie et al., 2009). Ultra-structural analyses, on the other hand, demonstrated that RNP granules are not bound by a membrane, defining them as *bona fide* membraneless organelles (Knowles et al., 1996; Krichevsky and Kosik, 2001; Elvira et al., 2006; El Fatimy et al., 2016). If neuronal RNP granules are not delimited by a membrane, how are their constituent molecules then assembling into coherent and delimited entities? Extensive recent work performed in cells and in reconstituted systems has demonstrated that RNP granules in fact behave as liquid-like condensates that form through liquid-liquid phase separation, i.e., by demixing of their components from the cytoplasm (Weber and Brangwynne, 2012; Alberti, 2017; Banani et al., 2017; Mittag and Parker, 2018; Van Treeck and Parker, 2018). Such a self-assembly mechanism relies on the establishment of dense and dynamic networks of RNA-RNA, RNA-protein and protein-protein interactions (Mittag and Parker, 2018; Van Treeck and Parker, 2018). It involves multivalent molecular interactions mediated by repeated domains as well as low-complexity domains that are prone to interact with both RNA and protein and frequently found in neuronal RBPs (Formicola et al., 2019; Franzmann and Alberti, 2019). Consistent with surface tension dictating their morphology, neuronal RNP granules are spherical at rest and deform under the shear stress induced by fast axonal transport (Gopal et al., 2017; Andrusiak et al., 2019). Furthermore, combining high resolution imaging with FRAP experiments revealed that neuronal RNP granules behave as droplets, undergoing fusion with characteristic relaxation times together with rapid internal rearrangements and constant exchange with the surrounding cytoplasm (Cougot et al., 2008; Park et al., 2014; El Fatimy et al., 2016; Gopal et al., 2017; Andrusiak et al., 2019).

A remarkable feature of phase-separated organelles is their capacity to rapidly and reversibly disassemble, or modulate their dynamic properties and composition in response to changes in the phase behavior of their constituent molecules (Banani et al., 2017). In the axons of cultured neurons, for example, TDP-43-containing granules with different properties are observed: while rather static granules with a low turnover rate are observed proximally, highly dynamic granules, strongly dependent on weak hydrophobic interactions, are observed more distally (Gopal et al., 2017). Although the origin of such differences is still unclear, they likely reflect subcellular heterogeneities in the concentrations of granule components, cations, or biological hydrotropes along neuronal processes (Buxbaum et al., 2014; Patel et al., 2017; Onuchic et al., 2019). More acute changes in granule properties are also observed in response to external stimuli. In *C. elegans* mechanosensory neurons, for example, axotomy induces within minutes an increase in the number of TIAR-2-containing axonal granules together with a change in their material properties manifested by a reduction in granule fusion events and circularity (Andrusiak et al., 2019). Point mutations preventing these changes inhibit the function of TIAR-2 in axon regeneration, highlighting the functional importance of controlling phase behavior. Understanding the nature and

precise impact of the molecular determinants modulating phase separation has been the subject of intensive research, and it has become clear that modifications of both proteins and RNAs play a very important role in this process. By altering charge or steric properties, post-translational modifications (PTMs) of RNA binding proteins, including phosphorylation, SUMOylation or methylation, were indeed shown to positively or negatively modulate *cis*- and *trans*-interactions, thus altering phase separation and molecule partitioning in reconstituted systems (Hofweber and Dormann, 2019). In neuronal cells, preventing PTMs of granule-associated proteins was shown to alter granule component oligomerization, as well as granule dynamics, nucleation and/or growth (Majumdar et al., 2012; Khayachi et al., 2018; Qamar et al., 2018; Andrusiak et al., 2019; Ford et al., 2019). Such changes in granule properties were associated with impaired axonal translation (Qamar et al., 2018), regenerative capacities (Andrusiak et al., 2019), synaptic properties (Khayachi et al., 2018), or long-term memory (Majumdar et al., 2012; White-Grindley et al., 2014), highlighting that PTMs of neuronal RBPs are essential for the tight regulation of RNP granule function. More recently, chemical modification of RNA molecules, in particular m6A methylation, was also shown to regulate phase behavior *in vitro* and to impact on the recruitment of RNP components in cells (Ries et al., 2019), although evidence for a role of m6A in the assembly and regulation of constitutive neuronal RNP granules is still lacking. Together, these studies have provided a conceptual framework explaining the dynamic regulatory properties of membraneless RNP organelles. To date, a few studies have started investigating how phase behavior impacts on the translation repressor function of RNP granule components (Khan et al., 2015; Kim et al., 2019; Tsang et al., 2019). However, we still lack a precise understanding of how individual activities might be coordinated in the context of these macromolecular complexes. Furthermore, how such dynamic assemblies connect to the transport machinery and travel over long distances along axons remains unclear.

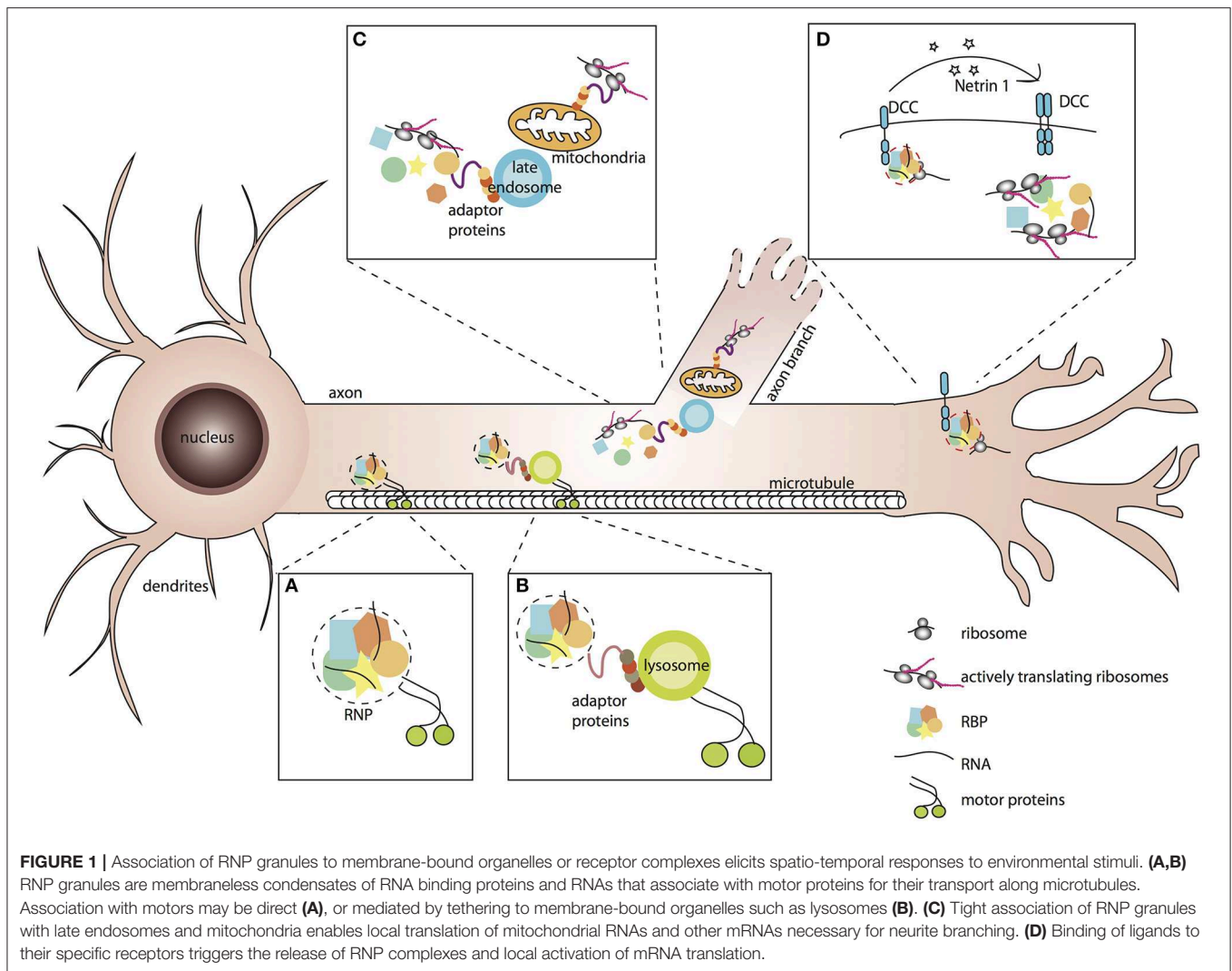
MEMBRANE-BOUND ORGANELLES AS VEHICLES FOR AXONAL TRANSPORT OF RNAs

In vitro and *ex vivo* live-imaging of fluorescently-tagged mRNAs or their associated RBPs has revealed that RNP assemblies are transported to distal axons through active, bi-directional motion characterized by the presence of both anterograde and retrograde processive events interspaced by long stationary phases (Knowles et al., 1996; Tiruchinapalli et al., 2003; Leung et al., 2006, 2018; Nalavadi et al., 2012; Alami et al., 2014; Medioni et al., 2014; Gopal et al., 2017; Wong et al., 2017; De Graeve and Besse, 2018; Turner-Bridger et al., 2018; Vijayakumar et al., 2019). Long-range transport of RNP granules along the axon shaft relies on the integrity of the microtubule cytoskeleton (Knowles et al., 1996; Medioni et al., 2014; Leung et al., 2018) and likely requires the combined activity of kinesin and dynein motors, although direct evidence is still scarce (Das et al., 2019). How are molecular motors recruited to RNP assemblies for their transport to axons?

Physical interactions between neuronal RBPs and molecular motors have been described (Figure 1A; Kanai et al., 2004; Davidovic et al., 2007; Dichtenberg et al., 2008; Bianco et al., 2010; Urbanska et al., 2017), suggesting that RBPs may engage motor proteins through direct or adaptor-mediated binding. Recent lines of evidence, however, have challenged this classical view and proposed that RNP cargoes may hitchhike on motile membrane-bound organelles for their subcellular trafficking (Jansen et al., 2014; Salogiannis and Reck-Peterson, 2017).

Intimate connections between localizing mRNAs and ER-related endomembranes have long been described in non-neuronal cells (e.g., vertebrate and invertebrate oocytes, yeast), where ER tubules were shown to promote the targeting of mRNAs encoding membrane and secreted proteins, possibly facilitating their local translation (Trautwein et al., 2004; Cohen, 2005; Schmid et al., 2006). In motor neurons, evidence for axonal co-trafficking of golgi-derived coat protein I (COPI) vesicles and the RNP chaperone SMN, together with the demonstration that COPI subunits physically and functionally interact with axonally-localized mRNAs, had also suggested that RNP trafficking may be facilitated by membrane-bound components (Bi et al., 2007; Peter et al., 2011; Todd et al., 2013).

Direct evidence that membrane-bound organelles undergoing bi-directional, microtubule-dependent motion may serve as vehicles for the transport of mRNA molecules arose more recently, first through elegant work performed in the filamentous fungus *Ustilago maydis*. In this model, Kinesin and dynein-dependent co-transport of Rab5a-positive endosomes and RNP components was observed along the elongating hyphal processes (Baumann et al., 2012, 2014). Furthermore, molecularly uncoupling mRNAs from endosomes prevented mRNA localization without interfering with endosome shuttling, demonstrating that RNP assemblies indeed behave as cargoes and endosomes as vehicles (Baumann et al., 2014; Pohlmann et al., 2015). Together, this work supported an emerging model in which endosomes are not purely dedicated to the sorting or recycling of internalized components, but also serve as versatile multipurpose platforms that recruit and localize signaling molecules (Gould and Lippincott-Schwartz, 2009). Strikingly, extensive colocalization was also recently observed between axonal mRNAs and Rab5-positive early endosomes or Rab7-positive late endosomes in vertebrate Retinal Ganglion neurons (Konopacki et al., 2016; Cioni et al., 2019). As shown by expression of dominant negative versions of Rab5 and 7, however, endosomes appear to be dispensable for the transport of RNP granules in this system (Cioni et al., 2019). Alternative membrane-bound organelles actively transported along axonal microtubules (Farias et al., 2017) may however be used as vehicles in neuronal cells. In a recent study, indeed, Ward and colleagues proposed that RNP granules may hitch a ride on lysosomes for their long-distance transport to axons (Figure 1B; Liao et al., 2019), based on the following lines of evidence: (i) most motile RNP granules co-localized with LAMP1-positive lysosomes, (ii) a tight association of the two organelles was observed by correlative light-electron microscopy, suggestive of a docking mechanism, and (iii) inhibition of motor-dependent lysosomal movement blocked RNP granule transport. Arguing



against an indirect effect of lysosomal trafficking impairment, specific disruption of RNP granule hitchhiking on lysosomes reduced the number of RNP granules actively trafficking along axons *in vitro* and *in vivo*. Whether these lysosomal vesicles correspond to mature degradative lysosomes, or rather to the less acidic lysosome-related vesicles recently shown to mediate the transport of presynaptic components (Vukoja et al., 2018), remains to be addressed.

An outstanding question arising from these discoveries is how the tethering of phase-separated RNP condensates on membrane-bound organelles is molecularly achieved. Work performed in *Saccharomyces cerevisiae* first demonstrated that the RNA binding protein She2p possesses lipid-binding properties and specifically recognized membrane structures with a high curvature typical of tubular ER, suggesting that RBPs can directly and specifically bridge the two organelles (Genz et al., 2013). Association between membraneless and membrane-bound organelles may also be mediated by bipartite adapter proteins containing both a membrane binding domain and

an RNP association domain. In *Ustilago*, for example, the adapter molecule Upa1 directly couples RNP and endosomes by binding directly to endosomes, through its C-terminal FYVE domains, and to the main RBP involved in mRNA transport, through its PALM2 domains (Pohlmann et al., 2015). Notably, mutating either the FYVE domains or the PALM2 domain of Upa1 prevented association of mRNAs with endosomes and transport, without affecting general endosome functions. Similarly, Annexin A11 was recently proposed to act as an adaptor between RNP granules and lysosomes in mammalian neurons. Annexin A11, indeed, was identified as both a lysosome and an RNP granule interactor by proximity labeling proteomics (Markmiller et al., 2018; Liao et al., 2019). Furthermore, it contains both an N-terminal low-complexity domain mediating phase separation into granule-like droplets *in vitro* and incorporation into stress-induced RNP granules in cells, and C-terminal Annexin domains that bind membranes containing PI(3,5)P₂ lysosomal lipids (Liao et al., 2019). Remarkably, downregulating Annexin A11 drastically reduced the number of

axonal RNP granules trafficking on lysosomes without altering axonal lysosome transport itself. Altered hitchhiking of RNP granules was associated with a decreased accumulation of β -actin mRNA in distal axons, indicating the functional relevance of this process in axonal mRNA localization.

Interestingly, docking of RNP assemblies on shuttling membrane-bound organelles is very dynamic, as frequent on and off-loading events were observed by live-imaging in different systems (Higuchi et al., 2014; Cioni et al., 2019; Liao et al., 2019). To date, how the docking process is regulated physiologically largely remains unclear, although work on the Annexin A11 protein has revealed that its interaction with lysosomes is both calcium- and phospholipid-sensitive (Liao et al., 2019). As measured using a FRET sensor monitoring the association between Annexin A11 and the lysosomal protein LAMP1, indeed, chelating free cytoplasmic Ca^{2+} , or inhibiting the formation of $\text{PI}(3,5)\text{P}_2$, decreased Annexin A11/lysosome interaction. Such regulatory mechanisms thus provide neurons with flexible means to regulate with high spatial and temporal resolution the trafficking of RNP assemblies.

MEMBRANE-BOUND ORGANELLES AS PLATFORMS FOR LOCAL TRANSLATION

For proteins to be produced in axons, mRNA localization must be tightly coupled to translation. Although the capacity of axons to support local translation has been debated over years, combinations of metabolic labeling and proteomic studies have unambiguously demonstrated that both cytosolic and transmembrane proteins can be translated in distal axons (Sahoo et al., 2018; Holt et al., 2019). How the translation machinery is trafficked to axons is still an open question, but the detection of both ribosomal proteins and translation factors in Mass-Spectrometry analyses of RNP granule content has suggested that it may at least partly be co-transported with neuronal RNP granules (Kanai et al., 2004; Elvira et al., 2006; El Fatimy et al., 2016). Importantly, recent studies demonstrating the importance of organelle-coupled translation completed this view (Bethune et al., 2019), indicating that membrane-bound organelles including mitochondria and endosomes may serve as sites for the local translation of a significant fraction of axonal mRNAs.

Nuclear-encoded mitochondrial RNAs (mtRNAs) have long and reproducibly been identified in transcriptomic analyses of axonally localized mRNAs (Taylor et al., 2009; Andreassi et al., 2010; Gumy et al., 2011; Aschrafi et al., 2016), and were more recently shown to be translated in axons (Yoon et al., 2012; Shigeoka et al., 2016; Cagnetta et al., 2018). These observations, together with the discovery that mtRNAs are targeted and translated at the mitochondrial surface (Lesnik et al., 2015), suggest a speculative model whereby mtRNAs might hitchhike on mitochondria for their transport and get translated on axonally localized mitochondria. Consistent with such a model, mitochondria are dynamically transported to axons and enriched distally (Smith and Gallo, 2018). Second, hundreds of nuclear-encoded mtRNAs were shown to accumulate at

the mitochondrial outer membrane, a fraction of them being targeted via 3'UTR-located *cis*-regulatory sequences (Marc et al., 2002; Sylvestre et al., 2003; Fazal et al., 2019). Furthermore, as demonstrated for the axonally-localized *cytochrome c oxidase IV* mRNA, the distal region of the transcript's 3'UTR is both required for mitochondrial targeting and for axon localization (Aschrafi et al., 2010). Third, proximity-specific ribosome profiling analysis revealed that hundreds of transcripts encoding mitochondrial proteins are translated at the vicinity of mitochondria, a discovery consistent with the identification of translating ribosomes at mitochondrial outer membranes (Zhang et al., 2016; Gold et al., 2017). Notably, mitochondria were also shown to be required more indirectly, through mitochondrial respiration, for the local translation of axonal mRNAs such as *β -actin*, *Arp2*, or *cortactin*, as well as for protein synthesis-dependent axon branching (Spillane et al., 2013). During this process, preferential association of mitochondria with sites of active axonal translation was observed, further suggesting a tight coupling of energy supply to RNA translation.

A tight coupling was also observed between mitochondria and late endosomes (Figure 1C), other membrane-bound organelles recently proposed to behave as hot spots for intra-axonal protein synthesis (Cioni et al., 2019). As demonstrated by high resolution imaging of *Xenopus* Retinal Ganglion Cell axons, both RNP components and ribosomes were frequently found in close proximity to Rab7a-positive late endosomes. Furthermore, translation of axonal mRNAs was detected on endosomes, corroborating previous work suggesting endosome-sited translation in heterologous systems (Baumann et al., 2014; Higuchi et al., 2014). Finally, inhibiting late endosomes through downregulation of Rab7 activity, or pharmacological blockage of late endosome maturation, decreased the translation of axonal *laminB2* mRNAs as well as global axonal translation, indicating that late endosomes significantly contribute to local translation (Cioni et al., 2019). Intriguingly, while extensive coupling of RNP granules to early endosomes was also observed in axons, inhibiting early endosome function did not impair axonal translation, indicating the existence of yet unknown specificity mechanism(s). Another important open question concerns the nature and properties of the molecular linker(s) tethering both mRNAs and the translation machinery to endosomes. Identifying such linker(s) will be key to perform more targeted manipulation and should open the door to a mechanistic and functional understanding of endosome-sited translation regulation.

SUBCELLULAR COMPARTMENTALIZATION AS A MEANS TO GENERATE SPECIFIC TRANSLATIONAL PATTERNS?

During development, local translation is required for cue-induced axon outgrowth, branching, as well as for the chemotropic response of growth cones to guidance molecules (Campbell and Holt, 2001; Wu et al., 2005; Hengst et al., 2009; Jung et al., 2012; Medioni et al., 2012; Spillane et al., 2012; Wong et al., 2017). Strikingly, seminal studies performed in cultured

Retinal Ganglion Cell axons revealed that Netrin-1-induced axon turning is associated with the translation of β -actin, while Slit2-induced growth cone collapse is associated with the translation of *cofilin* (Leung et al., 2006; Piper et al., 2006; Lin and Holt, 2008). These results suggested first that different cues trigger translation of different mRNAs, and second that attractive and repulsive cues may stimulate the translation of proteins with opposite functions in the assembly/disassembly of the F-actin cytoskeleton. By providing a more comprehensive view on the nascent proteomes induced by different cues in somaless retinal axons, recent work performed using highly sensitive sample preparation and metabolic labeling both confirmed and completed this view (Cagnetta et al., 2018). Indeed, while the translation of some axonal mRNAs was commonly activated in response to different cues, cue-specific up- and down-regulation of dozens of nascent proteins was also observed. Furthermore, opposite changes in translation patterns were observed upon switching from repulsive to attractive chemotropic responses, suggesting that guidance molecules induce distinct and functionally relevant proteomic signatures.

These observations raise the question of how specificity of translational patterns is achieved (Besse and Ephrussi, 2008). One way to selectively regulate the translation of subgroups of localized mRNAs is to organize them into so-called post-transcriptional operons, or regulons (Keene, 2007), composed of functionally-related RNAs recognized by specific RNA binding protein(s). By targeting their bound RNAs to specialized organelles or subcellular micro-domains, RBPs may thus favor stimuli-specific spatio-temporal responses. Although a systematic profiling of organelle-associated transcriptomes has not been performed in neuronal cells, distinct RBPs and mRNA populations were found associated with different types of membrane-bound organelles, consistent with such a model (Peter et al., 2011; Todd et al., 2013; Debaisieux et al., 2016; Yarmishyn et al., 2016; Liao et al., 2019). Analysis of mRNAs co-precipitating with COPIa, for example, revealed the presence of more than a thousand of mRNAs, 8 to 10% overlapping with the axonal transcriptome and about the same percentage encoding cytoskeletal components and/or regulators (Todd et al., 2013). Furthermore, RNP complexes with specific protein and RNA signatures were recently found in the immunoprecipitates of different guidance cue receptors in neuronal cells (Koppers et al., 2019). The RBP Staufen 1, for example, was found significantly associated with the Neuropilin receptor Nrp1, whereas hnRNPA2/B1 was found interacting with the Netrin-1 DCC receptor. Interestingly, Nrp1 and DCC also bound distinct subsets of mRNAs, the translation of which was exclusively induced by their specific ligand. As demonstrated in *Xenopus* Retinal Ganglion neurons, translation of β -catenin (*ctnmb1*) mRNA was for example activated in response to the DCC ligand Netrin-1, but not in response to Sema3A (Koppers et al., 2019). Translation activation correlated with a release of both RNAs and associated ribosomes from the receptor complex, suggesting (i) that mRNAs tethered to receptors are kept in a translationally repressed state and (ii) that cue-induced release may represent a rapid and direct means to trigger selective translation activation (Figure 1D; Tcherkezian

et al., 2010; Koppers et al., 2019). How such release is achieved remains to be understood, but a possibility is that cue-induced signaling triggers the phosphorylation of RBPs associated with transmembrane receptors. Signal-specific phosphorylation of neuronal RBPs has already been documented in different contexts and linked to decreased affinity for target mRNAs (Huang et al., 2002; Huttmelmaier et al., 2005; Lee, 2012), consistent with the idea that cue-induced signaling may lead to the release of mRNAs from their local anchor. Whether such a model of regulated association/dissociation holds true for mRNAs associated with other sub-cellular organelles or compartments is unclear, and would be worth investigating in the future.

ALTERATIONS IN RNP GRANULE TRANSPORT AND THEIR MEMBRANE-BOUND VEHICLES ARE LINKED TO NEURODEGENERATIVE DISEASES

Alterations in axonal mRNA transport and local translation impact various aspects of axon function, including axon survival (Jung et al., 2012; Sahoo et al., 2018). Consistent with this, an increasing number of neurodegenerative disease-causing mutations have been mapped to proteins, either RNA binding or adapter molecules, present in axonal RNP granules (Table 1) (Costa and Willis, 2018; Khalil et al., 2018). Interestingly, functional studies of pathogenic mutations have suggested that they may impair RNP cargo transport by at least two different means: (i) by perturbing the assembly or material properties of RNP condensates, or (ii) by altering the tethering of RNP cargoes to motile membrane-bound organelles.

A prominent example of neurodegenerative disease linked to altered axonal RNP cargo transport is amyotrophic lateral sclerosis (ALS), a disease characterized by the loss of upper and lower motor neurons (Taylor et al., 2016). Remarkably, while the vast majority of ALS cases are sporadic, about 10% are familial and largely caused by mutations in genes coding for RNA binding proteins (Zhao et al., 2018). Mutations in two components of axonally-localized RNP granules, FUS/TLS and TDP-43, have been particularly studied and their impact on axonal mRNA transport and translation investigated (Yasuda and Mili, 2016). ALS mutations in FUS were shown to inhibit general intra-axonal protein synthesis in cultures of *Xenopus* retinal neurons (Murakami et al., 2015), as well as in mouse sciatic nerve axons *in vivo* (Lopez-Erauskin et al., 2018). Furthermore, mutant TDP-43 proteins, when expressed in cultured neurons, exhibit defective axonal transport characterized by a decreased anterograde movement and a depletion of TDP-43-containing granules from the distal axonal compartment (Alami et al., 2014; Gopal et al., 2017). This phenotype is accompanied by a defective anterograde trafficking of the TDP-43 target mRNA *Neurofilament-L*, both in cultured cortical neurons and in IPS cell-derived human motor neurons carrying ALS-causing mutations, indicating that disrupting the delivery of mRNAs to axons may underlie axonal degeneration (Alami et al., 2014). How the disease mutations molecularly impair

TABLE 1 | List of neurodegenerative disease-associated proteins and mutations mentioned in the main text.

Disease	Protein	Category of protein	Functional domains	Molecular function	Alterations in RNP regulation upon mutation	Examples of disease-associated mutations in the corresponding domains
Spinal muscular atrophy (SMA)	SMN	RNP chaperone	Protein-protein interaction domain	Mediates interaction with α -COP (K76 and K82)	nd	nd
	α -COP	Subunit of the COPI vesicle	C-terminal domain	Mediates interaction with SMN (Y1090 residue)	nd	nd
Amyotrophic lateral sclerosis (ALS)/Fronto-temporal dementia (FTD)	TDP-43	RNA binding protein	Low complexity domain	Promotes phase separation	Decreased RNP component exchange rate and axonal transport of RNP granules	G298S, M637V
	FUS	RNA binding protein	Low complexity domain	Promotes phase separation	Decreased RNP component exchange rate, impaired axonal translation	G156E
	Annexin A11	Adaptor protein	NLS domain Low-complexity domain	Promotes nuclear localization Promotes phase separation	Decreased RNP component exchange rate, impaired axonal translation Decreased RNP component exchange rate	R521C, R521H D40G
Charcot-Marie-Tooth disease type 2B (CMT2B)	Rab7	Small GTPase	Annexin domains GTP binding and hydrolysis domain	Association with lysosomes GTPase activity	Decreased RNP component exchange rate, RNP granule trafficking and axonal mRNA localization	R235Q, R346C
Huntington's disease (HD)	Htt	Scaffolding protein	na	Binding to molecular motors	Decreased endosome sited axonal mRNA translation Decreased dendritic mRNA transport*	L129F, K157N, N161T/I, V162M (in Σ 3 and Σ 4 motifs) na

*Domains involved and their molecular functions are summarized. nd, not determined; na, not applicable. *Studies performed by downregulating (not mutating) Htt.*

mRNA transport and translation remains to be understood, but mutations found in the low-complexity domains of FUS and TDP-43 were shown to alter granule material properties, promoting a liquid-to-solid phase transition (Johnson et al., 2009; Murakami et al., 2015; Patel et al., 2015). The increased viscosity and aggregated state of RNP granules observed in mutant contexts may then directly impact on granule motility and cue-induced remodeling, or more indirectly affect local RNA homeostasis, by sequestration of essential RNA or protein molecules (Ramaswami et al., 2013; Bowden and Dormann, 2016; Alberti and Dormann, 2019). Further emphasizing the importance of RNP granule homeostasis in the etiology of the disease, numerous ALS-associated mutations were found in the Annexin A11 protein (Table 1; Smith et al., 2017). These mutations, found either in the N-terminal low complexity domain, or in the C-terminal lysosome association domains, were shown to induce a solidification of associated RNP granules (Liao et al., 2019). C-terminal mutations also specifically impair the association of Annexin A11 to lysosomes, and, when expressed in primary cultured neurons or *in vivo* in zebrafish neurons, disrupt both hitchhiking of RNP cargoes to motile lysosomes and targeting of mRNAs to the distal end of axons (Liao et al., 2019). Together, these results illustrate how different ALS mutations converge on factors controlling axonal RNP motility and dynamic interaction with membrane-bound organelles, highlighting the likely involvement of this process in disease pathogenesis or progression.

Another example of axonal RNP-associated protein linked to disease is SMN, whose deficiency causes spinal muscular atrophy (SMA), a neurodegenerative disease characterized by a progressive loss of spinal motor neurons and skeletal muscle atrophy (Fallini et al., 2012; Beattie and Kolb, 2018). SMN is an RNP chaperone molecule shown to interact with several RBPs and to be transported within axonal RNP granules undergoing active bi-directional motion. In the absence of SMN, loss of axonal RNP granules and significant decrease in axonal mRNA levels are observed (Rage et al., 2013; Fallini et al., 2014, 2016; Saal et al., 2014), indicating that defective RNP assembly and subsequent axonal transport defects may at least partially lead to SMA. Interestingly, specifically altering the COPI/SMN interaction impairs the developmental function of SMN in axons (Custer et al., 2013, 2019; Li et al., 2015), suggesting that loosing the tight interactions between axonal RNP granules and membrane-bound organelles might also play a role in disease progression. Further supporting the importance of such interactions, mutations in the late endosome protein Rab7 known to be causally linked to the Charcot-Marie-Tooth disease type 2B (CMT2B), disrupted axonal mRNA translation when expressed in cultured retinal neurons (Cioni et al., 2019). Notably, the above-described examples likely reflect only the tip of the iceberg, as defective regulation of axon ribostasis and membrane-bound organelle trafficking is emerging as a general feature of neurodegenerative diseases, including Alzheimer disease or Huntington disease (De Vos et al., 2008; Ma et al., 2011; Ramaswami et al., 2013; Schrej et al., 2016; Khalil et al., 2018; Lie and Nixon, 2019). The Huntingtin (Htt) protein, in particular, was shown to (i) undergo active, bi-directional transport in

axons (Gunawardena et al., 2003) and (ii) to associate and co-traffic with both RNP granule components (Savas et al., 2010; Ma et al., 2011) and membrane-bound organelles such as BDNF vesicles or Rab-positive recycling endosomes (Gauthier et al., 2004; White et al., 2015; Saudou and Humbert, 2016). Inactivating Htt impaired the localization of its associated RNAs and membranous organelles (Table 1; Gauthier et al., 2004; Trushina et al., 2004; White et al., 2015), indicating its functional role in connecting these cargoes to the transport machinery. Although Htt was reported to physically interact with the dynein molecular motor (Li et al., 1998; Gauthier et al., 2004; Caviston et al., 2007), its specific normal and pathological functions in cargo recruitment and hitchhiking remain to be clarified, thus emphasizing the need to better understand the molecular bases of RNP granule/membrane-bound organelle co-trafficking.

CONCLUSIONS AND PERSPECTIVES

Extensive anterograde and retrograde trafficking of both membrane-bound and membraneless cargoes has long been observed along axons and shown to supply the distal ends of these long processes with a source of membranes, proteins and RNAs. While different types of cargoes have largely been studied independent of each other, recent work summarized in this review has demonstrated the dependency of phase-separated RNP granules on membrane-bound vesicles or organelles, both for long-distance transport of RNP cargoes and for local translation of their associated mRNAs. A number of challenging questions still remain to be addressed regarding the specificity of these interactions. For example, it will be very important to characterize the transcriptomes of the different membrane-bound organelles trafficked to axons and thus understand if and how different RNP complexes are specifically targeted to distinct membrane-bound organelles. Furthermore, identifying the adapter molecules tethering RNP granules to their membrane-bound vehicles or anchors will be key to functionally dissect the role and physiological regulation of this

interaction. Transcriptomic and proteomic studies required to address these questions will be possible with the advent of technologies providing both high sensitivity and high spatial resolution (Markmiller et al., 2018; Medioni and Besse, 2018; Fazal et al., 2019). Last, it will be interesting to investigate the contribution of specialized ribosomes to the specific translation activation patterns observed in response to different extracellular cues. As suggested by recent work, indeed, ribosomes of different compositions and functional properties may co-exist and exhibit preferential selectivity for subsets of mRNAs (Shi and Barna, 2015; Segev and Gerst, 2018). In axons, remarkable differences in the stoichiometry of defined ribosomal proteins were found when comparing the composition of ribosomes associated with distinct guidance molecule receptors (Koppers et al., 2019). Furthermore, on-site incorporation of axonally-synthesized ribosomal proteins and subsequent remodeling of ribosomes was observed (Shigeoka et al., 2019), thus opening the door for functional dissection of this additional layer of spatio-temporal regulation.

AUTHOR CONTRIBUTIONS

KP and FB contributed to manuscript preparation, read, and approved the submitted version.

FUNDING

Work in FB's group was supported by the ANR (through the RNAGRIMP and MASTERMOD research grants and the Investments for the Future LABEX SIGNALIFE program # ANR-11-LABX-0028-01) and the Fondation pour la Recherche Médicale (Equipe FRM DEQ20180339161).

ACKNOWLEDGMENTS

We apologize to those whose work could not be cited owing to space constraints. We thank F. De Graeve and C. Medioni for critical reading of the manuscript.

REFERENCES

- Alami, N. H., Smith, R. B., Carrasco, M. A., Williams, L. A., Winborn, C. S., Han, S. S. W., et al. (2014). Axonal transport of TDP-43 mRNA granules is impaired by ALS-causing mutations. *Neuron* 81, 536–543. doi: 10.1016/j.neuron.2013.12.018
- Alberti, S. (2017). The wisdom of crowds: regulating cell function through condensed states of living matter. *J. Cell Sci.* 130, 2789–2796. doi: 10.1242/jcs.200295
- Alberti, S., and Dormann, D. (2019). Liquid-liquid phase separation in disease. *Annu. Rev. Genet.* 53, 3.1–3.24 doi: 10.1146/annurev-genet-112618-043527
- Andreassi, C., Zimmermann, C., Mitter, R., Fusco, S., De Vita, S., Saiardi, A., et al. (2010). An NGF-responsive element targets myo-inositol monophosphatase-1 mRNA to sympathetic neuron axons. *Nat. Neurosci.* 13, 291–301. doi: 10.1038/nn.2486
- Andrusiak, M. G., Sharifnia, P., Lyu, X., Wang, Z., Dickey, A. M., Wu, Z., et al. (2019). Inhibition of axon regeneration by liquid-like TIAR-2 granules. *Neuron*. doi: 10.1016/j.neuron.2019.07.004
- Aschrafi, A., Kar, A. N., Gale, J. R., Elkahlon, A. G., Vargas, J. N., Sales, N., et al. (2016). A heterogeneous population of nuclear-encoded mitochondrial mRNAs is present in the axons of primary sympathetic neurons. *Mitochondrion* 30, 18–23. doi: 10.1016/j.mito.2016.06.002
- Aschrafi, A., Natera-Naranjo, O., Gioio, A. E., and Kaplan, B. B. (2010). Regulation of axonal trafficking of cytochrome c oxidase IV mRNA. *Mol. Cell. Neurosci.* 43, 422–430. doi: 10.1016/j.mcn.2010.01.009
- Banani, S. F., Lee, H. O., Hyman, A. A., and Rosen, M. K. (2017). Biomolecular condensates: organizers of cellular biochemistry. *Nat. Rev. Mol. Cell Biol.* 18, 285–298. doi: 10.1038/nrm.2017.7
- Baumann, S., König, J., Koepke, J., and Feldbrugge, M. (2014). Endosomal transport of septin mRNA and protein indicates local translation on endosomes and is required for correct septin filamentation. *EMBO Rep.* 15, 94–102. doi: 10.1002/embr.201338037
- Baumann, S., Pohlmann, T., Jungbluth, M., Brachmann, A., and Feldbrugge, M. (2012). Kinesin-3 and dynein mediate microtubule-dependent co-transport of mRNPs and endosomes. *J. Cell Sci.* 125(Pt 11), 2740–2752. doi: 10.1242/jcs.101212

- Beattie, C. E., and Kolb, S. J. (2018). Spinal muscular atrophy: Selective motor neuron loss and global defect in the assembly of ribonucleoproteins. *Brain Res.* 1693(Pt A), 92–97. doi: 10.1016/j.brainres.2018.02.022
- Besse, F., and Ephrussi, A. (2008). Translational control of localized mRNAs: restricting protein synthesis in space and time. *Nat. Rev. Mol. Cell Biol.* 9, 971–980. doi: 10.1038/nrm2548
- Bethune, J., Jansen, R. P., Feldbrugge, M., and Zarnack, K. (2019). Membrane-associated RNA-binding proteins orchestrate organelle-coupled translation. *Trends Cell Biol.* 29, 178–188. doi: 10.1016/j.tcb.2018.10.005
- Bi, J., Tsai, N. P., Lu, H. Y., Loh, H. H., and Wei, L. N. (2007). Copb1-facilitated axonal transport and translation of kappa opioid-receptor mRNA. *Proc. Natl. Acad. Sci. U.S.A.* 104, 13810–13815. doi: 10.1073/pnas.0703805104
- Bianco, A., Dienstbier, M., Salter, H. K., Gatto, G., and Bullock, S. L. (2010). Bicaudal-D regulates fragile X mental retardation protein levels, motility, and function during neuronal morphogenesis. *Curr. Biol.* 20, 1487–1492. doi: 10.1016/j.cub.2010.07.016
- Bowden, H. A., and Dormann, D. (2016). Altered mRNP granule dynamics in FTLD pathogenesis. *J. Neurochem.* 138(Suppl. 1), 112–133. doi: 10.1111/jnc.13601
- Buxbaum, A. R., Wu, B., and Singer, R. H. (2014). Single beta-actin mRNA detection in neurons reveals a mechanism for regulating its translatability. *Science* 343, 419–422. doi: 10.1126/science.1242939
- Cagnetta, R., Frese, C. K., Shigeoka, T., Krijgsvelde, J., and Holt, C. E. (2018). Rapid cue-specific remodeling of the nascent axonal proteome. *Neuron* 99, 29–46.e4. doi: 10.1016/j.neuron.2018.06.004
- Campbell, D. S., and Holt, C. E. (2001). Chemotropic responses of retinal growth cones mediated by rapid local protein synthesis and degradation. *Neuron* 32, 1013–1026. doi: 10.1016/s0896-6273(01)00551-7
- Caviston, J. P., Ross, J. L., Antony, S. M., Tokito, M., and Holzbaur, E. L. (2007). Huntingtin facilitates dynein/dynactin-mediated vesicle transport. *Proc. Natl. Acad. Sci. U.S.A.* 104, 10045–10050. doi: 10.1073/pnas.0610628104
- Christie, S. B., Akins, M. R., Schwob, J. E., and Fallon, J. R. (2009). The FXG: a presynaptic fragile X granule expressed in a subset of developing brain circuits. *J. Neurosci.* 29, 1514–1524. doi: 10.1523/JNEUROSCI.3937-08.2009
- Cioni, J. M., Lin, J. Q., Holtermann, A. V., Koppers, M., Jakobs, M. A. H., Azizi, A., et al. (2019). Late endosomes act as mRNA translation platforms and sustain mitochondria in axons. *Cell* 176, 56–72.e15. doi: 10.1016/j.cell.2018.11.030
- Cohen, R. S. (2005). The role of membranes and membrane trafficking in RNA localization. *Biol. Cell* 97, 5–18. doi: 10.1042/BC20040056
- Costa, C. J., and Willis, D. E. (2018). To the end of the line: axonal mRNA transport and local translation in health and neurodegenerative disease. *Dev. Neurobiol.* 78, 209–220. doi: 10.1002/dneu.22555
- Cougot, N., Bhattacharyya, S. N., Tapia-Arancibia, L., Bordonne, R., Filipowicz, W., Bertrand, E., et al. (2008). Dendrites of mammalian neurons contain specialized P-body-like structures that respond to neuronal activation. *J. Neurosci.* 28, 13793–13804. doi: 10.1523/JNEUROSCI.4155-08.2008
- Custer, S. K., Astroski, J. W., Li, H. X., and Androphy, E. J. (2019). Interaction between alpha-COP and SMN ameliorates disease phenotype in a mouse model of spinal muscular atrophy. *Biochem. Biophys. Res. Commun.* 514, 530–537. doi: 10.1016/j.bbrc.2019.04.176
- Custer, S. K., Todd, A. G., Singh, N. N., and Androphy, E. J. (2013). Dilysine motifs in exon 2b of SMN protein mediate binding to the COPI vesicle protein alpha-COP and neurite outgrowth in a cell culture model of spinal muscular atrophy. *Hum. Mol. Genet.* 22, 4043–4052. doi: 10.1093/hmg/ddt254
- Das, S., Singer, R. H., and Yoon, Y. J. (2019). The travels of mRNAs in neurons: do they know where they are going? *Curr. Opin. Neurobiol.* 57, 110–116. doi: 10.1016/j.conb.2019.01.016
- Davidovic, L., Jaglin, X. H., Lepagnol-Bestel, A. M., Tremblay, S., Simonneau, M., Bardoni, B., et al. (2007). The fragile X mental retardation protein is a molecular adaptor between the neurospecific KIF3C kinesin and dendritic RNA granules. *Hum. Mol. Genet.* 16, 3047–3058. doi: 10.1093/hmg/ddm263
- De Graeve, F., and Besse, F. (2018). Neuronal RNP granules: from physiological to pathological assemblies. *Biol. Chem.* 399, 623–635. doi: 10.1515/hsz-2018-0141
- De Vos, K. J., Grierson, A. J., Ackerley, S., and Miller, C. C. (2008). Role of axonal transport in neurodegenerative diseases. *Annu. Rev. Neurosci.* 31, 151–173. doi: 10.1146/annurev.neuro.31.061307.090711
- Debaisieux, S., Encheva, V., Chakravarty, P., Snijders, A. P., and Schiavo, G. (2016). Analysis of signaling endosome composition and dynamics using SILAC in embryonic stem cell-derived neurons. *Mol. Cell. Proteomics* 15, 542–557. doi: 10.1074/mcp.M115.051649
- Dicthenberg, J. B., Swanger, S. A., Antar, L. N., Singer, R. H., and Bassell, G. J. (2008). A direct role for FMRP in activity-dependent dendritic mRNA transport links filopodial-spine morphogenesis to fragile X syndrome. *Dev. Cell* 14, 926–939. doi: 10.1016/j.devcel.2008.04.003
- El Fatimy, R., Davidovic, L., Tremblay, S., Jaglin, X., Dury, A., Robert, C., et al. (2016). Tracking the fragile X mental retardation protein in a highly ordered neuronal ribonucleoproteins population: a link between stalled polyribosomes and RNA granules. *PLoS Genet.* 12, e1006192. doi: 10.1371/journal.pgen.1006192
- Elvira, G., Wasiak, S., Blandford, V., Tong, X. K., Serrano, A., Fan, X., et al. (2006). Characterization of an RNA granule from developing brain. *Mol. Cell. Proteomics* 5, 635–651. doi: 10.1074/mcp.M500255-MCP200
- Fallini, C., Bassell, G. J., and Rossoll, W. (2012). Spinal muscular atrophy: the role of SMN in axonal mRNA regulation. *Brain Res.* 1462, 81–92. doi: 10.1016/j.brainres.2012.01.044
- Fallini, C., Donlin-Asp, P. G., Rouanet, J. P., Bassell, G. J., and Rossoll, W. (2016). Deficiency of the survival of motor neuron protein impairs mRNA localization and local translation in the growth cone of motor neurons. *J. Neurosci.* 36, 3811–3820. doi: 10.1523/JNEUROSCI.2396-15.2016
- Fallini, C., Rouanet, J. P., Donlin-Asp, P. G., Guo, P., Zhang, H., Singer, R. H., et al. (2014). Dynamics of survival of motor neuron (SMN) protein interaction with the mRNA-binding protein IMP1 facilitates its trafficking into motor neuron axons. *Dev. Neurobiol.* 74, 319–332. doi: 10.1002/dneu.22111
- Farias, G. G., Guardia, C. M., De Pace, R., Britt, D. J., and Bonifacino, J. S. (2017). BORC/kinesin-1 ensemble drives polarized transport of lysosomes into the axon. *Proc. Natl. Acad. Sci. U.S.A.* 114, E2955–E2964. doi: 10.1073/pnas.1616363114
- Fazal, F. M., Han, S., Parker, K. R., Kaewwapsak, P., Xu, J., Boettiger, A. N., et al. (2019). Atlas of subcellular RNA localization revealed by APEX-Seq. *Cell* 178, 473–490.e26. doi: 10.1016/j.cell.2019.05.027
- Ford, L., Ling, E., Kandel, E. R., and Fioriti, L. (2019). CPEB3 inhibits translation of mRNA targets by localizing them to P bodies. *Proc. Natl. Acad. Sci. U.S.A.* 116, 18078–18087. doi: 10.1073/pnas.1815275116
- Formicola, N., Vijayakumar, J., and Besse, F. (2019). Neuronal ribonucleoprotein granules: dynamic sensors of localized signals. *Traffic* 20, 639–649. doi: 10.1111/tra.12672
- Franzmann, T. M., and Alberti, S. (2019). Prion-like low-complexity sequences: key regulators of protein solubility and phase behavior. *J. Biol. Chem.* 294, 7128–7136. doi: 10.1074/jbc.TM118.001190
- Fritzsche, R., Karra, D., Bennett, K. L., Ang, F. Y., Heraud-Farlow, J. E., Tolino, M., et al. (2013). Interactome of two diverse RNA granules links mRNA localization to translational repression in neurons. *Cell Rep.* 5, 1749–1762. doi: 10.1016/j.celrep.2013.11.023
- Gallagher, C., and Ramos, A. (2018). Joining the dots - protein-RNA interactions mediating local mRNA translation in neurons. *FEBS Lett.* 592, 2932–2947. doi: 10.1002/1873-3468.13121
- Gauthier, L. R., Charrin, B. C., Borrell-Pages, M., Dompierre, J. P., Rangone, H., Cordelieres, F. P., et al. (2004). Huntingtin controls neurotrophic support and survival of neurons by enhancing BDNF vesicular transport along microtubules. *Cell* 118, 127–138. doi: 10.1016/j.cell.2004.06.018
- Genz, C., Fundakowski, J., Hermesh, O., Schmid, M., and Jansen, R. P. (2013). Association of the yeast RNA-binding protein She2p with the tubular endoplasmic reticulum depends on membrane curvature. *J. Biol. Chem.* 288, 32384–32393. doi: 10.1074/jbc.M113.486431
- Gold, V. A., Chrosicki, P., Bragoszewski, P., and Chacinska, A. (2017). Visualization of cytosolic ribosomes on the surface of mitochondria by electron cryo-tomography. *EMBO Rep.* 18, 1786–1800. doi: 10.15252/embr.201744261
- Gopal, P. P., Nirschl, J. J., Klinman, E., and Holzbaur, E. L. (2017). Amyotrophic lateral sclerosis-linked mutations increase the viscosity of liquid-like TDP-43 RNP granules in neurons. *Proc. Natl. Acad. Sci. U.S.A.* 114, E2466–E2475. doi: 10.1073/pnas.1614462114
- Gould, G. W., and Lippincott-Schwartz, J. (2009). New roles for endosomes: from vesicular carriers to multi-purpose platforms. *Nat. Rev. Mol. Cell Biol.* 10, 287–292. doi: 10.1038/nrm2652

- Gumy, L. F., Yeo, G. S., Tung, Y. C., Zivraj, K. H., Willis, D., Coppola, G., et al. (2011). Transcriptome analysis of embryonic and adult sensory axons reveals changes in mRNA repertoire localization. *RNA* 17, 85–98. doi: 10.1261/rna.2386111
- Gunawardena, S., Her, L. S., Bruschi, R. G., Laymon, R. A., Niesman, I. R., Gordesky-Gold, B., et al. (2003). Disruption of axonal transport by loss of huntingtin or expression of pathogenic polyQ proteins in *Drosophila*. *Neuron* 40, 25–40. doi: 10.1016/s0896-6273(03)00594-4
- Hengst, U., Deglincerti, A., Kim, H. J., Jeon, N. L., and Jaffrey, S. R. (2009). Axonal elongation triggered by stimulus-induced local translation of a polarity complex protein. *Nat. Cell Biol.* 11, 1024–1030. doi: 10.1038/ncb1916
- Heraud-Farlow, J. E., Sharangdhar, T., Li, X., Pfeifer, P., Tauber, S., Orozco, D., et al. (2013). Staufen2 regulates neuronal target RNAs. *Cell Rep.* 5, 1511–1518. doi: 10.1016/j.celrep.2013.11.039
- Higuchi, Y., Ashwin, P., Roger, Y., and Steinberg, G. (2014). Early endosome motility spatially organizes polysome distribution. *J. Cell Biol.* 204, 343–357. doi: 10.1083/jcb.201307164
- Hofweber, M., and Dormann, D. (2019). Friend or foe—post-translational modifications as regulators of phase separation and RNP granule dynamics. *J. Biol. Chem.* 294, 7137–7150. doi: 10.1074/jbc.TM118.001189
- Holt, C. E., Martin, K. C., and Schuman, E. M. (2019). Local translation in neurons: visualization and function. *Nat. Struct. Mol. Biol.* 26, 557–566. doi: 10.1038/s41594-019-0263-5
- Huang, Y. S., Jung, M. Y., Sarkissian, M., and Richter, J. D. (2002). N-methyl-D-aspartate receptor signaling results in Aurora kinase-catalyzed CPEB phosphorylation and alpha CaMKII mRNA polyadenylation at synapses. *EMBO J.* 21, 2139–2148. doi: 10.1093/emboj/21.9.2139
- Huttelmaier, S., Zenklusen, D., Lederer, M., Dichtenberg, J., Lorenz, M., Meng, X., et al. (2005). Spatial regulation of beta-actin translation by Src-dependent phosphorylation of ZBP1. *Nature* 438, 512–515. doi: 10.1038/nature04115
- Jansen, R. P., Niessing, D., Baumann, S., and Feldbrugge, M. (2014). mRNA transport meets membrane traffic. *Trends Genet.* 30, 408–417. doi: 10.1016/j.tig.2014.07.002
- Johnson, B. S., Sneed, D., Lee, J. J., McCaffery, J. M., Shorter, J., and Gitler, A. D. (2009). TDP-43 is intrinsically aggregation-prone, and amyotrophic lateral sclerosis-linked mutations accelerate aggregation and increase toxicity. *J. Biol. Chem.* 284, 20329–20339. doi: 10.1074/jbc.M109.010264
- Jung, H., Yoon, B. C., and Holt, C. E. (2012). Axonal mRNA localization and local protein synthesis in nervous system assembly, maintenance and repair. *Nat. Rev. Neurosci.* 13, 308–324. doi: 10.1038/nrn3210
- Kanai, Y., Dohmae, N., and Hirokawa, N. (2004). Kinesin transports RNA: isolation and characterization of an RNA-transporting granule. *Neuron* 43, 513–525. doi: 10.1016/j.neuron.2004.07.022
- Keene, J. D. (2007). RNA regulons: coordination of post-transcriptional events. *Nat. Rev. Genet.* 8, 533–543. doi: 10.1038/nrg2111
- Khalil, B., Morderer, D., Price, P. L., Liu, F., and Rossoll, W. (2018). mRNP assembly, axonal transport, and local translation in neurodegenerative diseases. *Brain Res.* 1693(Pt A), 75–91. doi: 10.1016/j.brainres.2018.02.018
- Khan, M. R., Li, L., Perez-Sanchez, C., Saraf, A., Florens, L., Slaughter, B. D., et al. (2015). Amyloidogenic oligomerization transforms *Drosophila* Orb2 from a translation repressor to an activator. *Cell* 163, 1468–1483. doi: 10.1016/j.cell.2015.11.020
- Khayachi, A., Gwizdek, C., Poupon, G., Alcor, D., Chafai, M., Casse, F., et al. (2018). Sumoylation regulates FMRP-mediated dendritic spine elimination and maturation. *Nat. Commun.* 9:757. doi: 10.1038/s41467-018-03222-y
- Kim, T. H., Tsang, B., Vernon, R. M., Sonenberg, N., Kay, L. E., and Forman-Kay, J. D. (2019). Phospho-dependent phase separation of FMRP and CAPRIN1 recapitulates regulation of translation and deadenylation. *Science* 365, 825–829. doi: 10.1126/science.aax4240
- Knowles, R. B., Sabry, J. H., Martone, M. E., Deerinck, T. J., Ellisman, M. H., Bassell, G. J., et al. (1996). Translocation of RNA granules in living neurons. *J. Neurosci.* 16, 7812–7820
- Konopacki, F. A., Wong, H. H., Dwivedy, A., Bellon, A., Blower, M. D., and Holt, C. E. (2016). ESCRT-II controls retinal axon growth by regulating DCC receptor levels and local protein synthesis. *Open Biol.* 6:150218. doi: 10.1098/rsob.150218
- Koppers, M., Cagnetta, R., Shigeoka, T., Wunderlich, L., Zhao, S., Minett, M., et al. (2019). Receptor-specific interactome as a hub for rapid cue-induced selective translation in axons. *bioRxiv [Preprint]*. doi: 10.1101/673798
- Krichevsky, A. M., and Kosik, K. S. (2001). Neuronal RNA granules: a link between RNA localization and stimulation-dependent translation. *Neuron* 32, 683–696. doi: 10.1016/s0896-6273(01)00508-6
- Lee, E. K. (2012). Post-translational modifications of RNA-binding proteins and their roles in RNA granules. *Curr. Protein Pept. Sci.* 13, 331–336. doi: 10.2174/138920312801619411
- Lesnik, C., Golani-Armon, A., and Arava, Y. (2015). Localized translation near the mitochondrial outer membrane: an update. *RNA Biol.* 12, 801–809. doi: 10.1080/15476286.2015.1058686
- Leung, K. M., Lu, B., Wong, H. H., Lin, J. Q., Turner-Bridger, B., and Holt, C. E. (2018). Cue-polarized transport of beta-actin mRNA depends on 3'UTR and microtubules in live growth cones. *Front. Cell. Neurosci.* 12:300. doi: 10.3389/fncel.2018.00300
- Leung, K. M., van Horck, F. P., Lin, A. C., Allison, R., Standart, N., and Holt, C. E. (2006). Asymmetrical beta-actin mRNA translation in growth cones mediates attractive turning to netrin-1. *Nat. Neurosci.* 9, 1247–1256. doi: 10.1038/nn1775
- Li, H., Custer, S. K., Gilson, T., Hao, L. T., Beattie, C. E., and Androphy, E. J. (2015). alpha-COP binding to the survival motor neuron protein SMN is required for neuronal process outgrowth. *Hum. Mol. Genet.* 24, 7295–7307. doi: 10.1093/hmg/ddv428
- Li, S. H., Gutekunst, C. A., Hersch, S. M., and Li, X. J. (1998). Interaction of huntingtin-associated protein with dynactin P150Glued. *J. Neurosci.* 18, 1261–1269.
- Liao, Y. C., Fernandopulle, M. S., Wang, G., Choi, H., Hao, L., Drerup, C. M., et al. (2019). RNA granules hitchhike on lysosomes for long-distance transport, using annexin A11 as a molecular tether. *Cell* 179, 147–164.e20. doi: 10.1016/j.cell.2019.08.050
- Lie, P. P. Y., and Nixon, R. A. (2019). Lysosome trafficking and signaling in health and neurodegenerative diseases. *Neurobiol. Dis.* 122, 94–105. doi: 10.1016/j.nbd.2018.05.015
- Lin, A. C., and Holt, C. E. (2008). Function and regulation of local axonal translation. *Curr. Opin. Neurobiol.* 18, 60–68. doi: 10.1016/j.conb.2008.05.004
- Lopez-Erauskin, J., Tadokoro, T., Baughn, M. W., Myers, B., McAlonis-Downes, M., Chillón-Marinas, C., et al. (2018). ALS/FTD-linked mutation in FUS suppresses intra-axonal protein synthesis and drives disease without nuclear loss-of-function of FUS. *Neuron* 100, 816–830.e17. doi: 10.1016/j.neuron.2018.09.044
- Ma, B., Savas, J., Yu, M., Culver, B., Chao, M., and Tanese, N. (2011). Huntingtin mediates dendritic transport of beta-actin mRNA in rat neurons. *Sci. Rep.* 1:140. doi: 10.1038/srep00140
- Majumdar, A., Cesario, W. C., White-Grindley, E., Jiang, H., Ren, F., Khan, M. R., et al. (2012). Critical role of amyloid-like oligomers of *Drosophila* Orb2 in the persistence of memory. *Cell* 148, 515–529. doi: 10.1016/j.cell.2012.01.004
- Marc, P., Margeot, A., Devaux, F., Blugeon, C., Corral-Debrinski, M., and Jacq, C. (2002). Genome-wide analysis of mRNAs targeted to yeast mitochondria. *EMBO Rep.* 3, 159–164. doi: 10.1093/embo-reports/kvf025
- Markmiller, S., Soltanieh, S., Server, K. L., Mak, R., Jin, W., Fang, M. Y., et al. (2018). Context-dependent and disease-specific diversity in protein interactions within stress granules. *Cell* 172, 590–604.e13. doi: 10.1016/j.cell.2017.12.032
- Medioni, C., and Besse, F. (2018). The secret life of RNA: lessons from emerging methodologies. *Methods Mol. Biol.* 1649, 1–28. doi: 10.1007/978-1-4939-7213-5_1
- Medioni, C., Mowry, K., and Besse, F. (2012). Principles and roles of mRNA localization in animal development. *Development* 139, 3263–3276. doi: 10.1242/dev.078626
- Medioni, C., Ramalison, M., Ephrussi, A., and Besse, F. (2014). Imp promotes axonal remodeling by regulating profilin mRNA during brain development. *Curr. Biol.* 24, 793–800. doi: 10.1016/j.cub.2014.02.038
- Mittag, T., and Parker, R. (2018). Multiple modes of protein-protein interactions promote RNP granule assembly. *J. Mol. Biol.* 430, 4636–4649. doi: 10.1016/j.jmb.2018.08.005
- Muller-McNicol, M., and Neugebauer, K. M. (2013). How cells get the message: dynamic assembly and function of mRNA-protein complexes. *Nat. Rev. Genet.* 14, 275–287. doi: 10.1038/nrg3434

- Murakami, T., Qamar, S., Lin, J. Q., Schierle, G. S., Rees, E., Miyashita, A., et al. (2015). ALS/FTD mutation-induced phase transition of FUS liquid droplets and reversible hydrogels into irreversible hydrogels impairs RNP granule function. *Neuron* 88, 678–690. doi: 10.1016/j.neuron.2015.10.030
- Nalavadi, V. C., Griffin, L. E., Picard-Fraser, P., Swanson, A. M., Takumi, T., and Bassell, G. J. (2012). Regulation of zipcode binding protein 1 transport dynamics in axons by myosin Va. *J. Neurosci.* 32, 15133–15141. doi: 10.1523/JNEUROSCI.2006-12.2012
- Onuchic, P. L., Milin, A. N., Alshareedah, I., Deniz, A. A., and Banerjee, P. R. (2019). Divalent cations can control a switch-like behavior in heterotypic and homotypic RNA coacervates. *Sci. Rep.* 9:12161. doi: 10.1038/s41598-019-48457-x
- Park, H. Y., Lim, H., Yoon, Y. J., Follenzi, A., Nwokafor, C., Lopez-Jones, M., et al. (2014). Visualization of dynamics of single endogenous mRNA labeled in live mouse. *Science* 343, 422–424. doi: 10.1126/science.1239200
- Patel, A., Lee, H. O., Jawerth, L., Maharana, S., Jahnel, M., Hein, M. Y., et al. (2015). A liquid-to-solid phase transition of the ALS protein FUS accelerated by disease mutation. *Cell* 162, 1066–1077. doi: 10.1016/j.cell.2015.07.047
- Patel, A., Malinowska, L., Saha, S., Wang, J., Alberti, S., Krishnan, Y., et al. (2017). ATP as a biological hydrotrope. *Science* 356, 753–756. doi: 10.1126/science.aaf6846
- Peter, C. J., Evans, M., Thayani, V., Taniguchi-Ishigaki, N., Bach, I., Kolpak, A., et al. (2011). The COPI vesicle complex binds and moves with survival motor neuron within axons. *Hum. Mol. Genet.* 20, 1701–1711. doi: 10.1093/hmg/ddr046
- Piper, M., Anderson, R., Dwivedy, A., Weinl, C., van Horck, F., Leung, K. M., et al. (2006). Signaling mechanisms underlying Slit2-induced collapse of Xenopus retinal growth cones. *Neuron* 49, 215–228. doi: 10.1016/j.neuron.2005.12.008
- Pohlmann, T., Baumann, S., Haag, C., Albrecht, M., and Feldbrugge, M. (2015). A FYVE zinc finger domain protein specifically links mRNA transport to endosome trafficking. *Elife* 4:e06041. doi: 10.7554/eLife.06041
- Pouloupoulos, A., Murphy, A. J., Ozkan, A., Davis, P., Hatch, J., Kirchner, R., et al. (2019). Subcellular transcriptomes and proteomes of developing axon projections in the cerebral cortex. *Nature* 565, 356–360. doi: 10.1038/s41586-018-0847-y
- Qamar, S., Wang, G., Randle, S. J., Ruggeri, F. S., Varela, J. A., Lin, J. Q., et al. (2018). FUS phase separation is modulated by a molecular chaperone and methylation of arginine cation-pi interactions. *Cell* 173, 720–734. doi: 10.1016/j.cell.2018.03.056
- Rage, F., Boulisfane, N., Rihan, K., Neel, H., Gostan, T., Bertrand, E., et al. (2013). Genome-wide identification of mRNAs associated with the protein SMN whose depletion decreases their axonal localization. *RNA* 19, 1755–1766. doi: 10.1261/rna.040204.113
- Ramaswami, M., Taylor, J. P., and Parker, R. (2013). Altered ribostasis: RNA-protein granules in degenerative disorders. *Cell* 154, 727–736. doi: 10.1016/j.cell.2013.07.038
- Ries, R. J., Zaccara, S., Klein, P., Orlarier-George, A., Namkoong, S., Pickering, B. F., et al. (2019). m(6)A enhances the phase separation potential of mRNA. *Nature* 571, 424–428. doi: 10.1038/s41586-019-1374-1
- Saal, L., Briese, M., Kneitz, S., Glinka, M., and Sendtner, M. (2014). Subcellular transcriptome alterations in a cell culture model of spinal muscular atrophy point to widespread defects in axonal growth and presynaptic differentiation. *RNA* 20, 1789–1802. doi: 10.1261/rna.047373.114
- Sahoo, P. K., Smith, D. S., Perrone-Bizzozero, N., and Twiss, J. L. (2018). Axonal mRNA transport and translation at a glance. *J. Cell Sci.* 131:jcs196808. doi: 10.1242/jcs.196808
- Salogiannis, J., and Reck-Peterson, S. L. (2017). Hitchhiking: a non-canonical mode of microtubule-based transport. *Trends Cell Biol.* 27, 141–150. doi: 10.1016/j.tcb.2016.09.005
- Saudou, F., and Humbert, S. (2016). The biology of huntingtin. *Neuron* 89, 910–926. doi: 10.1016/j.neuron.2016.02.003
- Savas, J. N., Ma, B., Deinhardt, K., Culver, B. P., Restituito, S., Wu, L., et al. (2010). A role for huntingtin disease protein in dendritic RNA granules. *J. Biol. Chem.* 285, 13142–13153. doi: 10.1074/jbc.M110.114561
- Schmid, M., Jaedicke, A., Du, T. G., and Jansen, R. P. (2006). Coordination of endoplasmic reticulum and mRNA localization to the yeast bud. *Curr. Biol.* 16, 1538–1543. doi: 10.1016/j.cub.2006.06.025
- Schreij, A. M., Fon, E. A., and McPherson, P. S. (2016). Endocytic membrane trafficking and neurodegenerative disease. *Cell. Mol. Life Sci.* 73, 1529–1545. doi: 10.1007/s00018-015-2105-x
- Segev, N., and Gerst, J. E. (2018). Specialized ribosomes and specific ribosomal protein paralogs control translation of mitochondrial proteins. *J. Cell Biol.* 217, 117–126. doi: 10.1083/jcb.201706059
- Shi, Z., and Barna, M. (2015). Translating the genome in time and space: specialized ribosomes, RNA regulons, and RNA-binding proteins. *Annu. Rev. Cell Dev. Biol.* 31, 31–54. doi: 10.1146/annurev-cellbio-100814-125346
- Shigeoka, T., Jung, H., Jung, J., Turner-Bridger, B., Ohk, J., Lin, J. Q., et al. (2016). Dynamic axonal translation in developing and mature visual circuits. *Cell* 166, 181–192. doi: 10.1016/j.cell.2016.05.029
- Shigeoka, T., Koppers, M., Wong, H. H. W., Lin, J. Q., Dwivedy, A., de Freitas Nascimento, J., et al. (2019). On-site ribosome remodeling by locally synthesized ribosomal proteins in axons. *bioRxiv [Preprint]*. doi: 10.1101/500033
- Shin, Y., and Brangwynne, C. P. (2017). Liquid phase condensation in cell physiology and disease. *Science* 357:eaaf4382. doi: 10.1126/science.aaf4382
- Smith, B. N., Topp, S. D., Fallini, C., Shibata, H., Chen, H. J., Troakes, C., et al. (2017). Mutations in the vesicular trafficking protein annexin A11 are associated with amyotrophic lateral sclerosis. *Sci. Transl. Med.* 9:eaad9157. doi: 10.1126/scitranslmed.aad9157
- Smith, G. M., and Gallo, G. (2018). The role of mitochondria in axon development and regeneration. *Dev. Neurobiol.* 78, 221–237. doi: 10.1002/dneu.22546
- Spillane, M., Ketschek, A., Donnelly, C. J., Pacheco, A., Twiss, J. L., and Gallo, G. (2012). Nerve growth factor-induced formation of axonal filopodia and collateral branches involves the intra-axonal synthesis of regulators of the actin-nucleating Arp2/3 complex. *J. Neurosci.* 32, 17671–17689. doi: 10.1523/JNEUROSCI.1079-12.2012
- Spillane, M., Ketschek, A., Merianda, T. T., Twiss, J. L., and Gallo, G. (2013). Mitochondria coordinate sites of axon branching through localized intra-axonal protein synthesis. *Cell Rep.* 5, 1564–1575. doi: 10.1016/j.celrep.2013.11.022
- Sylvestre, J., Margeot, A., Jacq, C., Dujardin, G., and Corral-Debrinski, M. (2003). The role of the 3' untranslated region in mRNA sorting to the vicinity of mitochondria is conserved from yeast to human cells. *Mol. Biol. Cell* 14, 3848–3856. doi: 10.1091/mbc.e03-02-0074
- Taylor, A. M., Berchtold, N. C., Perreau, V. M., Tu, C. H., Li Jeon, N., and Cotman, C. W. (2009). Axonal mRNA in uninjured and regenerating cortical mammalian axons. *J. Neurosci.* 29, 4697–4707. doi: 10.1523/JNEUROSCI.6130-08.2009
- Taylor, J. P., Brown, R. H. Jr., and Cleveland, D. W. (2016). Decoding ALS: from genes to mechanism. *Nature* 539, 197–206. doi: 10.1038/nature20413
- Tcherkezian, J., Britts, P. A., Thomas, F., Roux, P. P., and Flanagan, J. G. (2010). Transmembrane receptor DCC associates with protein synthesis machinery and regulates translation. *Cell* 141, 632–644. doi: 10.1016/j.cell.2010.04.008
- Tiruchinapalli, D. M., Oleynikov, Y., Kelic, S., Shenoy, S. M., Hartley, A., Stanton, P. K., et al. (2003). Activity-dependent trafficking and dynamic localization of zipcode binding protein 1 and beta-actin mRNA in dendrites and spines of hippocampal neurons. *J. Neurosci.* 23, 3251–3261. doi: 10.1523/JNEUROSCI.23-08-03251.2003
- Todd, A. G., Lin, H., Ebert, A. D., Liu, Y., and Androphy, E. J. (2013). COPI transport complexes bind to specific RNAs in neuronal cells. *Hum. Mol. Genet.* 22, 729–736. doi: 10.1093/hmg/ddt480
- Trautwein, M., Dengjel, J., Schirle, M., and Spang, A. (2004). Arf1p provides an unexpected link between COPI vesicles and mRNA in *Saccharomyces cerevisiae*. *Mol. Cell Biol.* 24, 5021–5037. doi: 10.1091/mbc.e04-05-0411
- Trushina, E., Dyer, R. B., Badger, J. D. 2nd, Ure, D., Eide, L., Tran, D. D., et al. (2004). Mutant huntingtin impairs axonal trafficking in mammalian neurons *in vivo* and *in vitro*. *Mol. Cell Biol.* 24, 8195–8209. doi: 10.1128/MCB.24.18.8195-8209.2004
- Tsang, B., Arsenault, J., Vernon, R. M., Lin, H., Sonenberg, N., Wang, L. Y., et al. (2019). Phosphoregulated FMRP phase separation models activity-dependent translation through bidirectional control of mRNA granule formation. *Proc. Natl. Acad. Sci. U.S.A.* 116:4218–4227. doi: 10.1073/pnas.1814385116
- Turner-Bridger, B., Jakobs, M., Muresan, L., Wong, H. H., Franze, K., Harris, W. A., et al. (2018). Single-molecule analysis of endogenous beta-actin

- mRNA trafficking reveals a mechanism for compartmentalized mRNA localization in axons. *Proc. Natl. Acad. Sci. U.S.A.* 115, E9697–E9706. doi: 10.1073/pnas.1806189115
- Urbanska, A. S., Janusz-Kaminska, A., Switon, K., Hawthorne, A. L., Perycz, M., Urbanska, M., et al. (2017). ZBP1 phosphorylation at serine 181 regulates its dendritic transport and the development of dendritic trees of hippocampal neurons. *Sci. Rep.* 7:1876. doi: 10.1038/s41598-017-01963-2
- Van Treeck, B., and Parker, R. (2018). Emerging roles for intermolecular RNA-RNA interactions in RNP assemblies. *Cell* 174, 791–802. doi: 10.1016/j.cell.2018.07.023
- Vijayakumar, J., Perrois, C., Heim, M., Bousset, L., Alberti, S., and Besse, F. (2019). The prion-like domain of *Drosophila* Imp promotes axonal transport of RNP granules *in vivo*. *Nat. Commun.* 10:2593. doi: 10.1038/s41467-019-10554-w
- Vukoja, A., Rey, U., Petzoldt, A. G., Ott, C., Vollweiler, D., Quentin, C., et al. (2018). Presynaptic biogenesis requires axonal transport of lysosome-related vesicles. *Neuron* 99, 1216–1232.e7. doi: 10.1016/j.neuron.2018.08.004
- Weber, S. C., and Brangwynne, C. P. (2012). Getting RNA and protein in phase. *Cell* 149, 1188–1191. doi: 10.1016/j.cell.2012.05.022
- White, J. A. 2nd, Anderson, E., Zimmerman, K., Zheng, K. H., Rouhani, R., and Gunawardena, S. (2015). Huntingtin differentially regulates the axonal transport of a sub-set of Rab-containing vesicles *in vivo*. *Hum. Mol. Genet.* 24, 7182–7195. doi: 10.1093/hmg/ddv415
- White-Grindley, E., Li, L., Mohammad Khan, R., Ren, F., Saraf, A., Florens, L., et al. (2014). Contribution of Orb2A stability in regulated amyloid-like oligomerization of *Drosophila* Orb2. *PLoS Biol.* 12:e1001786. doi: 10.1371/journal.pbio.1001786
- Wong, H. H., Lin, J. Q., Strohl, F., Roque, C. G., Cioni, J. M., Cagnetta, R., et al. (2017). RNA docking and local translation regulate site-specific axon remodeling *in vivo*. *Neuron* 95, 852–868.e8. doi: 10.1016/j.neuron.2017.07.016
- Wu, K. Y., Hengst, U., Cox, L. J., Macosko, E. Z., Jeromin, A., Urquhart, E. R., et al. (2005). Local translation of RhoA regulates growth cone collapse. *Nature* 436, 1020–1024. doi: 10.1038/nature03885
- Yarmishyn, A. A., Kremenskoy, M., Batagov, A. O., Preuss, A., Wong, J. H., and Kurochkin, I. V. (2016). Genome-wide analysis of mRNAs associated with mouse peroxisomes. *BMC Genomics* 17(Suppl. 13):1028. doi: 10.1186/s12864-016-3330-x
- Yasuda, K., and Mili, S. (2016). Dysregulated axonal RNA translation in amyotrophic lateral sclerosis. *Wiley Interdiscip. Rev. RNA* 7, 589–603. doi: 10.1002/wrna.1352
- Yoon, B. C., Jung, H., Dwivedy, A., O'Hare, C. M., Zivraj, K. H., and Holt, C. E. (2012). Local translation of extranuclear lamin B promotes axon maintenance. *Cell* 148, 752–764. doi: 10.1016/j.cell.2011.11.064
- Zhang, Y., Chen, Y., Gucek, M., and Xu, H. (2016). The mitochondrial outer membrane protein MDI promotes local protein synthesis and mtDNA replication. *EMBO J.* 35, 1045–1057. doi: 10.15252/embj.201592994
- Zhao, M., Kim, J. R., van Bruggen, R., and Park, J. (2018). RNA-binding proteins in amyotrophic lateral sclerosis. *Mol. Cells* 41, 818–829. doi: 10.14348/molcells.2018.0243
- Zivraj, K. H., Tung, Y. C., Piper, M., Gumy, L., Fawcett, J. W., Yeo, G. S., et al. (2010). Subcellular profiling reveals distinct and developmentally regulated repertoire of growth cone mRNAs. *J. Neurosci.* 30, 15464–15478. doi: 10.1523/JNEUROSCI.1800-10.2010

Conflict of Interest: The authors declare that the research was conducted in the absence of any commercial or financial relationships that could be construed as a potential conflict of interest.

Copyright © 2019 Pushpalatha and Besse. This is an open-access article distributed under the terms of the Creative Commons Attribution License (CC BY). The use, distribution or reproduction in other forums is permitted, provided the original author(s) and the copyright owner(s) are credited and that the original publication in this journal is cited, in accordance with accepted academic practice. No use, distribution or reproduction is permitted which does not comply with these terms.

Detecting Stress Granules in *Drosophila* neurons

Fabienne De Graeve^{1,#}, Nadia Formicola^{1,#}, Kavya Vinayan Pushpalatha^{1,#}, Akira Nakamura², Eric Debreuve³, Xavier Descombes⁴ and Florence Besse^{1,*}

1- Université Côte d'Azur, CNRS, Inserm, Institut de Biologie Valrose, Nice, France

2- Department of Germline Development, Institute of Molecular Embryology and Genetics, and Graduate School of Pharmaceutical Sciences, Kumamoto University, Kumamoto, Japan

3- Université Côte d'Azur, CNRS, Inria, Laboratoire I3S, France

4- Université Côte d'Azur, Inria, CNRS, Laboratoire I3S, France

contributed equally to the work

* corresponding author: besse@unice.fr

Abstract

Stress granules (SGs) are cytoplasmic ribonucleoprotein condensates that dynamically and reversibly assemble in response to stress. They are thought to contribute to the adaptive stress response by storing translationally inactive mRNAs as well as signaling molecules. Recent work has shown that SG composition and properties depend on both stress and cell types, and that neurons exhibit a complex SG proteome and a strong vulnerability to mutations in SG proteins. *Drosophila* has emerged as a powerful genetically tractable organism where to study the physiological regulation and functions of SGs in normal and pathological contexts. In this chapter, we describe a protocol enabling quantitative analysis of SG properties in both larval and adult *Drosophila* CNS samples. In this protocol, fluorescently-tagged SGs are induced upon acute *ex vivo* stress or chronic *in vivo* stress, imaged at high-resolution *via* confocal microscopy and detected automatically, using a dedicated software.

Keywords: central nervous system, confocal imaging, fluorescent stress granule proteins, automated detection, *Drosophila melanogaster*

1. Introduction

Cellular stress induces a translational shutdown within minutes, characterized by inhibition of translation initiation and polysome disassembly. Cytoplasmic release of translationally inactive mRNAs in turn triggers the assembly of hundreds of nanometer-sized membraneless compartments enriched in stalled housekeeping transcripts and associated proteins, and referred to as stress granules (SGs) [1,2]. These higher order ribonucleoprotein (RNP) assemblies behave as dynamic condensates: they form through the self-association of their constituents into dense networks of transient RNA-RNA, RNA-protein and protein-protein interactions and get actively disassembled upon stress release [3-5]. The rapid and reversible mode of SG assembly is thought to play important roles in the adaptive stress response, first by promoting translational reprogramming through transient sequestration of unnecessary RNAs, and second by rewiring cellular pathways through recruitment of signaling molecules [6,7]. Consistent with the functional importance of SG dynamics, extensive links have recently been established between alterations of SG material properties and neurodegenerative diseases [8-10]. Abnormally stable inclusions enriched in SG components, for example, have been observed in pathological contexts and defined as a characteristic signature of amyotrophic lateral sclerosis (ALS) or frontotemporal dementia (FTD) patient samples [11,10]. Furthermore, mutations in an increasing number of SG components, including the RNA binding proteins TDP-43, FUS or TIA1, have been causally linked to disease progression and shown to promote the transition of RNP assemblies into irreversible solid-like condensates [12-14,9,10,15]. As revealed by a recent systematic study, the pathological entities formed upon expression of ALS mutant proteins also have a composition distinct from their dynamic and reversible counterparts [16], highlighting their capacity to recruit, and potentially titrate molecules involved in RNA homeostasis. More work is now required to decipher if and how pathological SGs induce toxicity in neuronal cells, which, as long-lived non-dividing cells, appear to be particularly vulnerable to the chronic stress induced by mutant SG proteins [9]. Importantly, proteomic studies have uncovered that variations in the composition of SGs are also observed in normal contexts in function of cell types and nature of the stress [17,16]. While a core set of obligatory components, including factors essential for SG nucleation (*e.g.* G3BP1, TIA-1), has been found in the different cell types analyzed, a significant fraction of the SG proteome was shown to be

recruited exclusively in certain cell types, particularly in neurons [17,16]. Together, these studies have uncovered an unexpected diversity of SG composition and highlighted the limits of working with standard immortalized cell lines. They have raised the need to develop alternative biological models in which SG regulation and function can be studied under physiological conditions, in differentiated tissues.

Drosophila represents an excellent model organism in which advanced genetics can be combined with high-resolution imaging to unravel the mechanisms underlying SG assembly, as well as SG function in adaptation to environmental stress or disease-associated chronic stress. Fly orthologs of mammalian SG components, indeed, were shown to accumulate within cytoplasmic condensates in response to different acute stresses including oxidative stress, Endoplasmic Reticulum (ER) stress or hypoxia [18-23]. Furthermore, various *Drosophila* ALS models have been developed, in which SG proteins with disease-causing mutations are chronically expressed in the nervous system [24-27]. These models were shown to recapitulate many aspects of the disease, among which cytoplasmic accumulation of pathological SG-like assemblies [28,25,29,27]. Here, we describe a protocol that enables induction of SGs in the nervous system of *Drosophila*, either chronically in response to *in vivo* expression of pathological SG proteins, or acutely upon treatment of explants with stress inducers (*e.g.* arsenite). This protocol includes the procedure to perform high-resolution confocal imaging of fluorescently-tagged SG markers and to accurately and automatically detect SGs using the *Obj.MPP* software [28]. The described method is compatible with analysis of both larval and adult central nervous system (CNS) samples, and is particularly adapted to the quantitative analysis of SG properties in complex tissues.

2. Materials

2.1- Fly lines for expression of fluorescent SG proteins

1. Gal4 and UAS transgenic flies for conditional ectopic expression of fluorescent pathological SG proteins in the nervous system (*e.g.* OK371-Gal4 and UAS-TDP-43 fly lines; see Table 1).
2. Knock-in lines expressing fluorescent SG proteins from the endogenous locus (*e.g.* GFP-Rasputin (Rin; the fly ortholog of G3BP); see Table 1).

2.2- Arsenite treatment

- 1- Chambered slide, four wells (see **Note 1**).
- 2- Preparation of arsenite stock solution: weigh sodium (meta)arsenite powder and dissolve in freshly prepared HL3 (see 2.3.2) to obtain a 40 mM stock solution that can be stored at room temperature (see **Note 2**). Alternatively, purchase commercially available aqueous solution.

2.3- Dissection and fixation of *Drosophila* CNS samples

2.3.1- Dissection and fixation of larval CNS

1. A pair of dissection forceps.
2. 60 mm dissection petri dishes.
3. 1X Phosphate-Buffered Saline (PBS) (see **Note 3**).
4. Fixing solution: 4% formaldehyde in 1X PBS (see **Note 3**).

2.3.2- Dissection and fixation of adult brains

1. A pair of dissection forceps.
2. Minutien pins.
3. 60 mm dissection petri dishes covered with 2% agarose.
4. HL3 buffer (70 mM NaCl, 5 mM KCl, 4 mM MgCl₂, 5 mM trehalose, 115 mM sucrose, 5 mM HEPES, 10 mM NaHCO₃, pH 7.20-7.25) (see **Note 4**).
5. Fixing solution: 4% formaldehyde in HL3.
6. Wash buffer: PBS; 0.5% Triton-X.

2.4- Mounting of *Drosophila* CNS samples

1. Antifade mounting medium with DAPI (Vectashield).
2. 10-well glass slides (black teflon coating).
3. 1.5, 24X60 mm coverslips.

2.5- Image acquisition

1. Scanning confocal microscope with highly sensitive detectors.
2. 63X 1.4 NA oil objective.
3. Immersion oil.

2.6- Image analysis

1. ImageJ/Fiji (<https://imagej.net/Fiji>).
2. *Obj.MPP* software [28] (<https://gitlab.inria.fr/edebreuv/Obj.MPP>).

3. Methods

In this protocol, stress can either be applied endogenously (3.1.1) or exogenously (3.1.2) (**Fig. 1**). Note that dissection of *Drosophila* nervous system (3.2) is performed after stress induction in case of endogenous stress and before stress in case of exogenous stress (**Fig. 1**).

3.1- Induction of stress

3.1.1- Ectopic in vivo expression of pathological proteins

1. Cross transgenic flies expressing a fluorescently-tagged pathological SG protein under UAS control (*e.g.* UAS-Venus::TDP-43 M337V; see Table 1) with flies expressing a neuronal Gal4 driver (*e.g.* motorneuron OK371-Gal4; see Table 1) (**Fig. 1, upper left**).
2. Maintain the flies at 25°C and transfer them in a new vial every 3-4 days (*see Note 5*).

3.1.2- Ex vivo treatment with arsenite

- 1- Freshly prepare the working arsenite solution (0.4 mM) by diluting the stock solution in HL3 (*see Note 2*).
- 2- Transfer dissected samples in a multi-well chambered slide (**Fig. 1, upper right**). At least 15 samples should be treated per condition.
- 3- Incubate in 500 μ L of HL3 or arsenite solution for one hour at 25°C, covered from light.

3.2- Dissection of Drosophila CNS samples

3.2.1- Dissection of larval CNS

1. Collect wandering third instar larvae expressing normal or pathological fluorescent SG proteins.
2. Transfer them into a 60 mm petri dish filled with PBS (*see Note 3*).
3. Tear the larvae in two using a pair of forceps.
4. Turn the anterior half of larvae inside out, remove the fat tissue while keeping the CNS attached to the cuticle. Collect samples with forceps in microtubes containing PBS (*see Note 3*).

3.2.2- Dissection of adult brains

1. Collect 7-10 day-old flies expressing normal or pathological SG proteins and anesthetize them with CO₂.
2. Dissect brains in HL3 buffer, as described in [30,31]. Briefly, immobilize the flies ventral side up by pinning them in a dissecting dish filled with HL3. Pull the proboscis upwards with one forceps and insert the tips of the other forceps underneath, in a closed position. Slowly open the forceps so as to tear apart the head cuticle. Carefully remove the cuticle and the retina, without damaging the underlying optic lobes and central brain.
3. Complete the dissection by thoroughly removing the air sacs (*see Note 6*).
4. Separate the brains from the rest of the body. Collect the dissected brains using a glass pipette or a filter tip (*see Note 7*).

3.3- Fixation of Drosophila CNS samples

This step comes right after dissection in case of endogenous stress induction or after treatment of brain explants in case of *ex vivo* arsenite treatment.

3.3.1- Fixation of larval CNS

1. Remove 1X PBS.
2. Add 500 μ L of fixing solution and gently rock the samples for 20 minutes at room temperature (RT).
3. Replace the fixing solution with 1 mL of 1X PBS and gently rock the samples for 30 minutes at RT.

4. Repeat step 3 twice.
5. Remove 1X PBS and add a drop of antifade mounting medium supplemented with DAPI.
6. Keep at 4°C for a minimum of 2 hours (preferentially overnight).

3.3.2- Fixation of adult brains

1. Remove HL3.
2. Add 300 µL of fixing solution and gently rock the samples for 25 minutes at room temperature (RT).
3. Remove the fixing solution, replace with 800 µL of wash buffer and gently rock the samples for 30 minutes at RT.
4. Repeat step 3 twice.
5. Remove the wash buffer and add a drop of antifade mounting medium supplemented with DAPI.
6. Keep at 4°C for a minimum of 2 hours (preferentially overnight).

3.4- Mounting of *Drosophila* CNS samples

3.4.1- Mounting of larval CNS

1. Transfer the samples onto a dissection dish using a 1 mL end-cut tip and dissect the samples further by detaching the CNS from the cuticle and removing eye-antenna imaginal discs. Recover the brain lobes and ventral nerve cord.
2. Transfer the clean CNS to a multi-well slide (~ 5 CNS per well) (*see* **Notes 8, 9**).
3. Orient the larval CNS with forceps, such that the dorsal side of the ventral cord is up.
4. Carefully place a 24X60 mm coverslip on top of the slide and seal the coverslip with clear nail varnish.

3.4.2- Mounting of adult brains

1. Transfer the brains to a multi-well slide using a 1 mL end-cut tip (~ 5 CNS per well) (*see* **Notes 8, 9**).
2. Orient the brains with forceps, such that their dorsal side is up.

3. Carefully place a 24X60 mm coverslip on top of the slide and seal the coverslip with clear nail varnish.

3.5- Imaging of Drosophila CNS samples

1. Acquire images from larval CNS or adult brains with a confocal microscope equipped with high-sensitivity detectors, and appropriate laser lines (*see Note 10*).
2. Image with optimal resolution (*see Note 11*), using a 63X 1.4 NA oil objective.
3. SGs appear as discrete, bright cytoplasmic foci with a typical diameter of hundreds of nanometers (**Figs. 2 and 3**).

3.6- Image analysis: detection of Stress Granules

1. Using ImageJ/Fiji, select single optical sections and crop to generate stereotypic regions of interest. Save images in .tif format, in a single dedicated folder.
2. Launch the *Obj.MPP* software (*see Note 12*).
3. Select images to be analyzed in the first tab of the GUI.
4. Select the detection parameters in the second tab of the GUI (**Fig. 4**). These parameters include object types and expected size range (*see Note 13*), as well as object radiometric properties (defined by the quality function; *see Note 14*).
5. Set the number of iterations in the third tab of the GUI (*see Note 15*).
6. Select output files (*see Note 16*) and output path in the fourth tab of the GUI.

4. Notes

1. The multi-well chambered slides can be rigorously washed with ethanol 80% and re-used up to three times.
2. Sodium Arsenite is a hazardous substance classified as carcinogen, mutagen and teratogen; it should be handled safely, under a chemical hood. When solubilized, sodium arsenite should be stored as sealed aliquots covered from light to avoid oxidation.
3. Prefer HL3 in case long incubations are required (if applying *ex vivo* stress).

4. HL3 buffer contains sugars (sucrose and trehalose) and can easily get contaminated. Store at 4°C in aliquots sealed with parafilm. Opened aliquots should not be kept for more than 2 months.
5. Temperature should be adapted so as to permit high expression level while preventing toxicity.
6. If air sacs are not removed, brains will float, making it difficult to not pipet them away.
7. Pre-wetting the pipette tip or the glass pipette with HL3 prevents the brains from sticking to the plastic/glass wall.
8. Do not place samples in wells close to the edge of the slide; they will not be accessible on regular microscope stages.
9. Transfer samples in a drop of mounting medium only, as excess medium can make brains float over the edge of the wells.
10. We used a confocal microscope equipped with ultrasensitive detectors (Zeiss LSM 880 with gallium arsenide phosphide (GaAsP) detectors).
11. Imaging with a xy pixel size of less than 80 nm is recommended. We imaged larval CNS with a xy pixel size of 74 nm (regular confocal microscopy), and adult brains with a xy pixel size of 45 nm (Airy scan confocal microscopy).
12. *Obj.MPP* can be used either through the graphical user interface (GUI) or through a terminal console (Command-Line Interface (CLI)). More parameters can be adjusted when using the latter mode (see <https://edebreuv.gitlabpages.inria.fr/Obj.MPP/>).
13. Object types and their corresponding parameters (notably size and orientation) are described under: <https://edebreuv.gitlabpages.inria.fr/Obj.MPP/contents/users/object-types.html>). Superquadrics are typically recommended for detection of objects with potentially complex shapes such as SGs. We used the following parameter ranges for detection of SGs from larval CNS: `semi_minor_axis_range` (2, 4, 0.25), `major_minor_ratio_range` (1, 1.5, 0.025), `exponent_range` (1.5, 2.5, 0.1), `angle_degree_range` (0.0, 179.9, 5.0) and the following parameters for detection of SGs in adult brains: `semi_minor_axis_range` (3, 4, 0.25), `major_minor_ratio_range` (1, 2, 0.025), `exponent_range` (1, 2, 0.1), `angle_degree_range` (0, 179.9, 5.0) (*see Note 14* about `mpp_quality_chooser.py`).
14. Available quality functions and associated signal transformations are described under: <https://edebreuv.gitlabpages.inria.fr/Obj.MPP/contents/users/quality-measures.html>. Note that

mpp_quality_chooser.py (<https://edebreuv.gitlabpages.inria.fr/Obj.MPP/contents/users/mpp-quality-chooser.html>) can be used to identify the best quality function and parameter ranges to detect objects of interest. We used the bright-on-dark gradient quality function with a min_quality of 1.5 for larval CNS and 2.5 for adult brains.

15. The number of iterations and the number of births per iteration should be set so that best objects are all reproducibly retained at the end of the process. We used 1.500 iterations with 50 births per iteration for larval CNS and 1.000 iterations with 550 births per iteration for adult brains.

16. Different outputs can be selected in the last tab of the GUI, including: CSV files containing the characteristics of the detected granules (geometrical parameters, intensity), raw images with granule contours highlighted, or masks of the detected granules, each having its own label (**Fig. 2D-F and Fig. 3D-F**).

Acknowledgements

Development of this protocol was supported by the CNRS, as well as grants from the ANR (ANR-15-CE12-0016 and ANR-20-CE16-) and the Fondation pour la Recherche Médicale (Equipe FRM; grant #DEQ20180339161) to F.B. Part of this work was also supported by the Joint Usage/Research Center for Developmental Medicine, IMEG, Kumamoto University. N.F. and K.P. were supported by fellowships from the LABEX SIGNALIFE program (#ANR – 11 – LABX – 0028 – 01). K.P. was in addition supported by a one year- La Ligue contre le cancer fellowship. We thank the iBV PRISM Imaging facility for use of their microscopes and support (especially B. Monterroso), and L. Palin for excellent technical assistance.

References

1. Protter DSW, Parker R (2016) Principles and Properties of Stress Granules. *Trends in cell biology* 26 (9):668-679. doi:10.1016/j.tcb.2016.05.004
2. Riggs CL, Kedersha N, Ivanov P, Anderson P (2020) Mammalian stress granules and P bodies at a glance. *Journal of cell science* 133 (16). doi:10.1242/jcs.242487
3. Mittag T, Parker R (2018) Multiple Modes of Protein-Protein Interactions Promote RNP Granule Assembly. *J Mol Biol* 430 (23):4636-4649. doi:10.1016/j.jmb.2018.08.005

4. Hofmann S, Kedersha N, Anderson P, Ivanov P (2020) Molecular mechanisms of stress granule assembly and disassembly. *Biochimica et biophysica acta Molecular cell research* 1868 (1):118876. doi:10.1016/j.bbamcr.2020.118876
5. Protter DSW, Rao BS, Van Treeck B, Lin Y, Mizoue L, Rosen MK, Parker R (2018) Intrinsically Disordered Regions Can Contribute Promiscuous Interactions to RNP Granule Assembly. *Cell Rep* 22 (6):1401-1412. doi:10.1016/j.celrep.2018.01.036
6. Buchan JR, Parker R (2009) Eukaryotic stress granules: the ins and outs of translation. *Molecular cell* 36 (6):932-941. doi:10.1016/j.molcel.2009.11.020
7. Kedersha N, Ivanov P, Anderson P (2013) Stress granules and cell signaling: more than just a passing phase? *Trends in biochemical sciences* 38 (10):494-506. doi:10.1016/j.tibs.2013.07.004
8. Formicola N, Vijayakumar J, Besse F (2019) Neuronal ribonucleoprotein granules: Dynamic sensors of localized signals. *Traffic (Copenhagen, Denmark)* 20 (9):639-649. doi:10.1111/tra.12672
9. Li YR, King OD, Shorter J, Gitler AD (2013) Stress granules as crucibles of ALS pathogenesis. *The Journal of cell biology* 201 (3):361-372. doi:10.1083/jcb.201302044
10. Wolozin B, Ivanov P (2019) Stress granules and neurodegeneration. *Nature reviews Neuroscience* 20 (11):649-666. doi:10.1038/s41583-019-0222-5
11. Neumann M, Sampathu DM, Kwong LK, Truax AC, Micsenyi MC, Chou TT, Bruce J, Schuck T, Grossman M, Clark CM, McCluskey LF, Miller BL, Masliah E, Mackenzie IR, Feldman H, Feiden W, Kretzschmar HA, Trojanowski JQ, Lee VM (2006) Ubiquitinated TDP-43 in frontotemporal lobar degeneration and amyotrophic lateral sclerosis. *Science* 314 (5796):130-133. doi:10.1126/science.1134108
12. Vance C, Rogelj B, Hortobagyi T, De Vos KJ, Nishimura AL, Sreedharan J, Hu X, Smith B, Ruddy D, Wright P, Ganesalingam J, Williams KL, Tripathi V, Al-Saraj S, Al-Chalabi A, Leigh PN, Blair IP, Nicholson G, de Belleruche J, Gallo JM, Miller CC, Shaw CE (2009) Mutations in FUS, an RNA processing protein, cause familial amyotrophic lateral sclerosis type 6. *Science* 323 (5918):1208-1211. doi:10.1126/science.1165942
13. Mackenzie IR, Nicholson AM, Sarkar M, Messing J, Purice MD, Pottier C, Annu K, Baker M, Perkerson RB, Kurti A, Matchett BJ, Mittag T, Temirov J, Hsiung GR, Krieger C, Murray ME, Kato M, Fryer JD, Petrucelli L, Zinman L, Weintraub S, Mesulam M, Keith J, Zivkovic SA, Hirsch-Reinshagen V, Roos RP, Züchner S, Graff-Radford NR, Petersen RC, Caselli RJ, Wszolek ZK, Finger E, Lippa C, Lacomis D, Stewart H, Dickson DW, Kim HJ, Rogaeva E, Bigio E, Boylan KB, Taylor JP, Rademakers R (2017) TIA1 Mutations in Amyotrophic Lateral Sclerosis and Frontotemporal Dementia Promote Phase Separation and Alter Stress Granule Dynamics. *Neuron* 95 (4):808-816.e809. doi:10.1016/j.neuron.2017.07.025
14. Sreedharan J, Blair IP, Tripathi VB, Hu X, Vance C, Rogelj B, Ackerley S, Durnall JC, Williams KL, Buratti E, Baralle F, de Belleruche J, Mitchell JD, Leigh PN, Al-Chalabi A, Miller CC, Nicholson

- G, Shaw CE (2008) TDP-43 mutations in familial and sporadic amyotrophic lateral sclerosis. *Science* 319 (5870):1668-1672. doi:10.1126/science.1154584
15. Patel A, Lee HO, Jawerth L, Maharana S, Jahnel M, Hein MY, Stoyanov S, Mahamid J, Saha S, Franzmann TM, Pozniakovski A, Poser I, Maghelli N, Royer LA, Weigert M, Myers EW, Grill S, Drechsel D, Hyman AA, Alberti S (2015) A Liquid-to-Solid Phase Transition of the ALS Protein FUS Accelerated by Disease Mutation. *Cell* 162 (5):1066-1077. doi:10.1016/j.cell.2015.07.047
16. Markmiller S, Soltanieh S, Server KL, Mak R, Jin W, Fang MY, Luo EC, Krach F, Yang D, Sen A, Fulzele A, Wozniak JM, Gonzalez DJ, Kankel MW, Gao FB, Bennett EJ, Lécuyer E, Yeo GW (2018) Context-Dependent and Disease-Specific Diversity in Protein Interactions within Stress Granules. *Cell* 172 (3):590-604.e513. doi:10.1016/j.cell.2017.12.032
17. Advani VM, Ivanov P (2020) Stress granule subtypes: an emerging link to neurodegeneration. *Cellular and molecular life sciences : CMLS* 77 (23):4827-4845. doi:10.1007/s00018-020-03565-0
18. Jevtov I, Zacharogianni M, van Oorschot MM, van Zadelhoff G, Aguilera-Gomez A, Vuillez I, Braakman I, Hafen E, Stocker H, Rabouille C (2015) TORC2 mediates the heat stress response in *Drosophila* by promoting the formation of stress granules. *Journal of cell science* 128 (14):2497-2508. doi:10.1242/jcs.168724
19. Gareau C, Houssin E, Martel D, Coudert L, Mellaoui S, Huot ME, Laprise P, Mazroui R (2013) Characterization of fragile X mental retardation protein recruitment and dynamics in *Drosophila* stress granules. *PloS one* 8 (2):e55342. doi:10.1371/journal.pone.0055342
20. Farny NG, Kedersha NL, Silver PA (2009) Metazoan stress granule assembly is mediated by P-eIF2alpha-dependent and -independent mechanisms. *RNA (New York, NY)* 15 (10):1814-1821. doi:10.1261/rna.1684009
21. Buddika K, Ariyapala IS, Hazuga MA, Riffert D, Sokol NS (2020) Canonical nucleators are dispensable for stress granule assembly in *Drosophila* intestinal progenitors. *Journal of cell science* 133 (10). doi:10.1242/jcs.243451
22. van der Laan AM, van Gemert AM, Dirks RW, Noordermeer JN, Fradkin LG, Tanke HJ, Jost CR (2012) mRNA cycles through hypoxia-induced stress granules in live *Drosophila* embryonic muscles. *The International journal of developmental biology* 56 (9):701-709. doi:10.1387/ijdb.103172a1
23. Bakthavachalu B, Huelsmeier J, Sudhakaran IP, Hillebrand J, Singh A, Petrauskas A, Thiagarajan D, Sankaranarayanan M, Mizoue L, Anderson EN, Pandey UB, Ross E, VijayRaghavan K, Parker R, Ramaswami M (2018) RNP-Granule Assembly via Ataxin-2 Disordered Domains Is Required for Long-Term Memory and Neurodegeneration. *Neuron* 98 (4):754-766.e754. doi:10.1016/j.neuron.2018.04.032
24. McGurk L, Berson A, Bonini NM (2015) *Drosophila* as an In Vivo Model for Human Neurodegenerative Disease. *Genetics* 201 (2):377-402. doi:10.1534/genetics.115.179457

25. Estes PS, Boehringer A, Zwick R, Tang JE, Grigsby B, Zarnescu DC (2011) Wild-type and A315T mutant TDP-43 exert differential neurotoxicity in a *Drosophila* model of ALS. *Human molecular genetics* 20 (12):2308-2321. doi:10.1093/hmg/ddr124
26. Lanson NA, Jr., Maltare A, King H, Smith R, Kim JH, Taylor JP, Lloyd TE, Pandey UB (2011) A *Drosophila* model of FUS-related neurodegeneration reveals genetic interaction between FUS and TDP-43. *Human molecular genetics* 20 (13):2510-2523. doi:10.1093/hmg/ddr150
27. Chen Y, Yang M, Deng J, Chen X, Ye Y, Zhu L, Liu J, Ye H, Shen Y, Li Y, Rao EJ, Fushimi K, Zhou X, Bigio EH, Mesulam M, Xu Q, Wu JY (2011) Expression of human FUS protein in *Drosophila* leads to progressive neurodegeneration. *Protein & cell* 2 (6):477-486. doi:10.1007/s13238-011-1065-7
28. De Graeve F, Debreuve E, Rahmoun S, Ecsedi S, Bahri A, Hubstenberger A, Descombes X, Besse F (2019) Detecting and quantifying stress granules in tissues of multicellular organisms with the Obj.MPP analysis tool. *Traffic (Copenhagen, Denmark)* 20 (9):697-711. doi:10.1111/tra.12678
29. Alami NH, Smith RB, Carrasco MA, Williams LA, Winborn CS, Han SSW, Kiskinis E, Winborn B, Freibaum BD, Kanagaraj A, Clare AJ, Badders NM, Bilican B, Chaum E, Chandran S, Shaw CE, Eggan KC, Maniatis T, Taylor JP (2014) Axonal transport of TDP-43 mRNA granules is impaired by ALS-causing mutations. *Neuron* 81 (3):536-543. doi:10.1016/j.neuron.2013.12.018
30. Tito AJ, Cheema S, Jiang M, Zhang S (2016) A Simple One-step Dissection Protocol for Whole-mount Preparation of Adult *Drosophila* Brains. *Journal of visualized experiments : JoVE* (118). doi:10.3791/55128
31. Williamson WR, Hiesinger PR (2010) Preparation of developing and adult *Drosophila* brains and retinæ for live imaging. *Journal of visualized experiments : JoVE* (37). doi:10.3791/1936

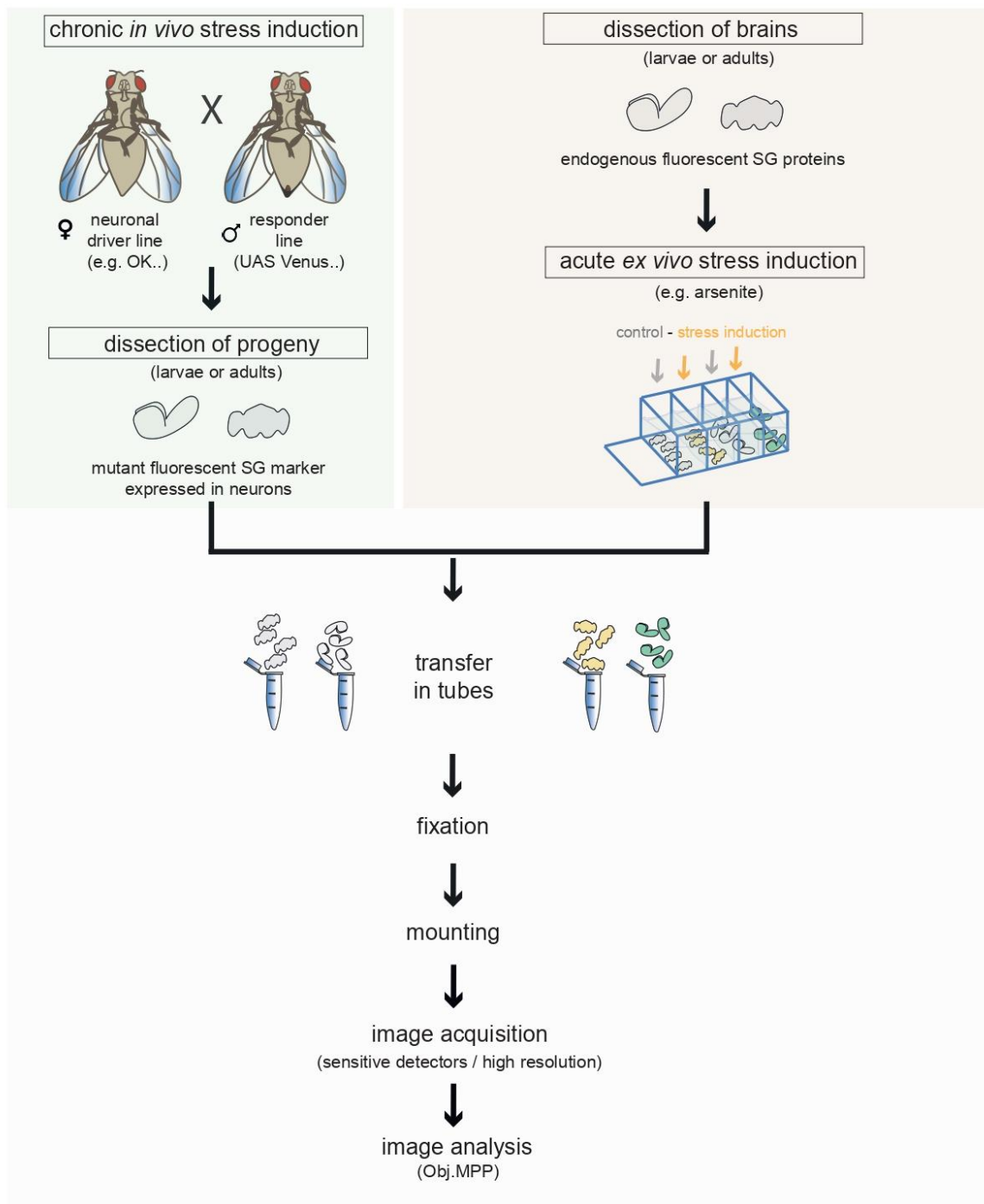


Figure 1. Method workflow.

Induction of stress in *Drosophila* nervous system was performed either endogenously (left) or exogenously (right). For the endogenous strategy, expression of fluorescent pathological SG proteins is induced chronically *in vivo* using the Gal4/UAS system. Larval or adult progenies expressing the mutant fluorescent SG markers in neurons are dissected and their CNS/brain collected. *Ex vivo* stress induction is achieved through acute arsenite treatment of larval CNS/brain explants previously dissected from larvae or adults expressing endogenous fluorescent SG proteins. In both procedures, stress induction and dissection are followed by sample fixation, mounting and confocal imaging (lower panel). Automated detection of SGs is performed *via* the *Obj.MPP* software.

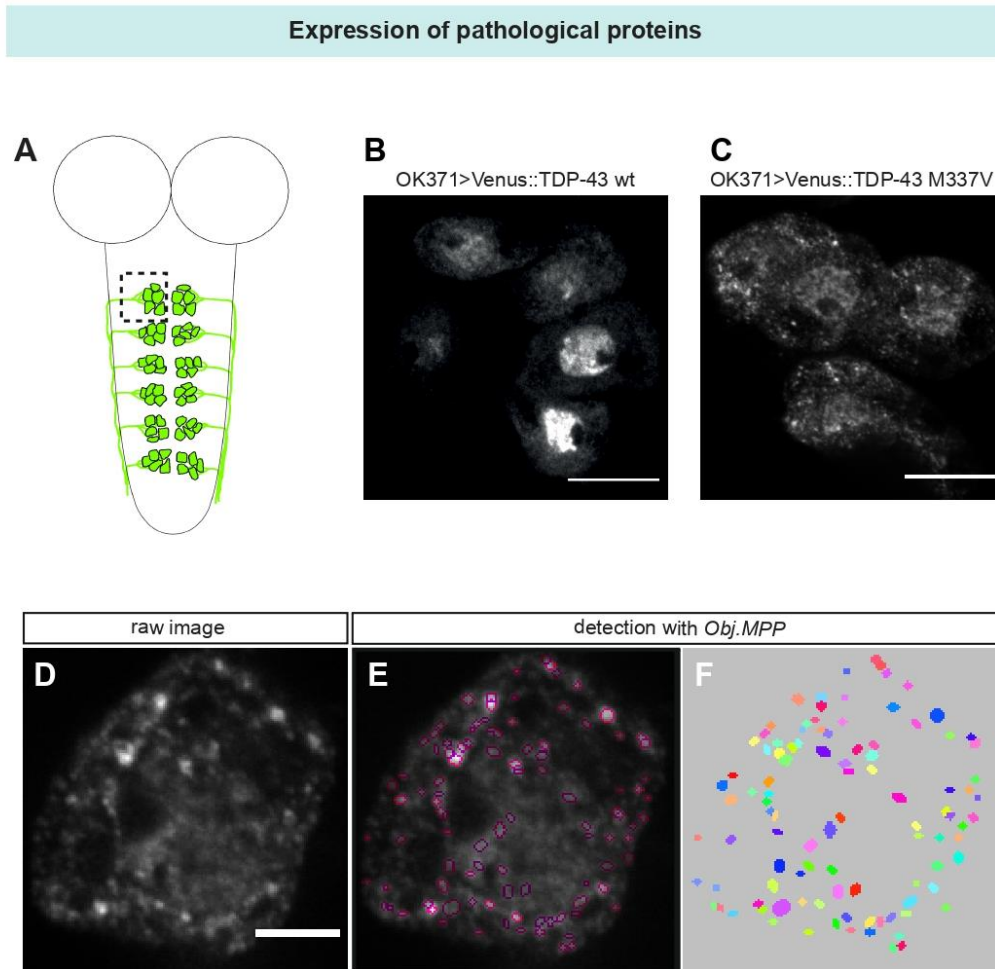


Figure 2. Imaging and automated detection of pathological SGs in larval CNS.

(A) Schematic representation of a third instar larva ventral nerve cord with the soma of a subset of OK371-Gal4-expressing motorneuron highlighted in green. The box delimits the region imaged in B,C. (B-D) Single confocal section of motorneuron cell bodies chronically expressing wild-type Venus::TDP-43 (B) or Venus::TDP-43 M337V (C,D) in motorneurons (OK371-Gal4/+; UAS-Venus::TDP43 M337V/+). Scale bar: 10 μm in B,C and 3 μm in D. Note the presence of pathological aggregates in motorneuron cytoplasm in C,D. (E) Overlay of the raw confocal image and the *Obj.MPP* detections. (F) Mask of the detected objects.

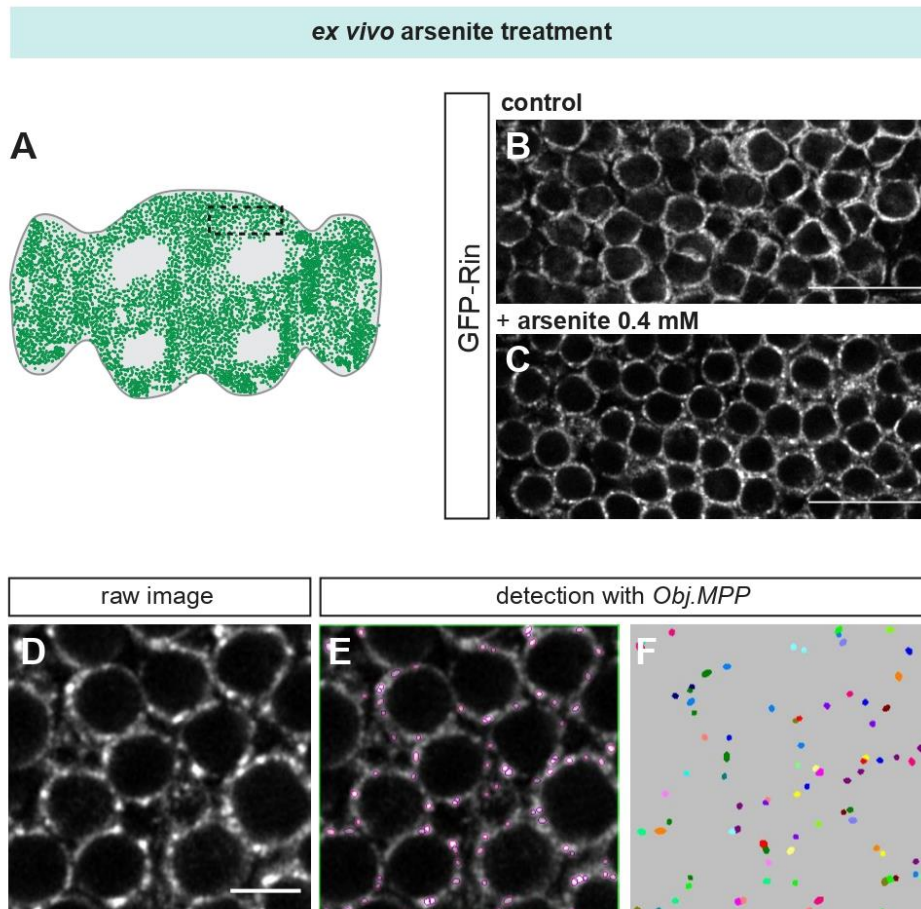


Figure 3. Imaging and automated detection of arsenite-induced SGs in adult *Drosophila* brain.

(A) Schematic representation of an adult brain expressing GFP-Rasputin (Rin) proteins from the endogenous locus (green). The box delimits the region imaged in B,C. (B-D) Single confocal section of Mushroom Body neurons expressing GFP-Rin, treated (C,D) or not (B) with arsenite. Scale bar: 10 μm in B,C and 3 μm in D. While GFP-Rin exhibits diffuse cytoplasmic distribution in the absence of stress, it localizes to SGs upon arsenite treatment. (E) Overlay of the raw confocal image and the *Obj.MPP* detections. (F) Mask of the detected objects.

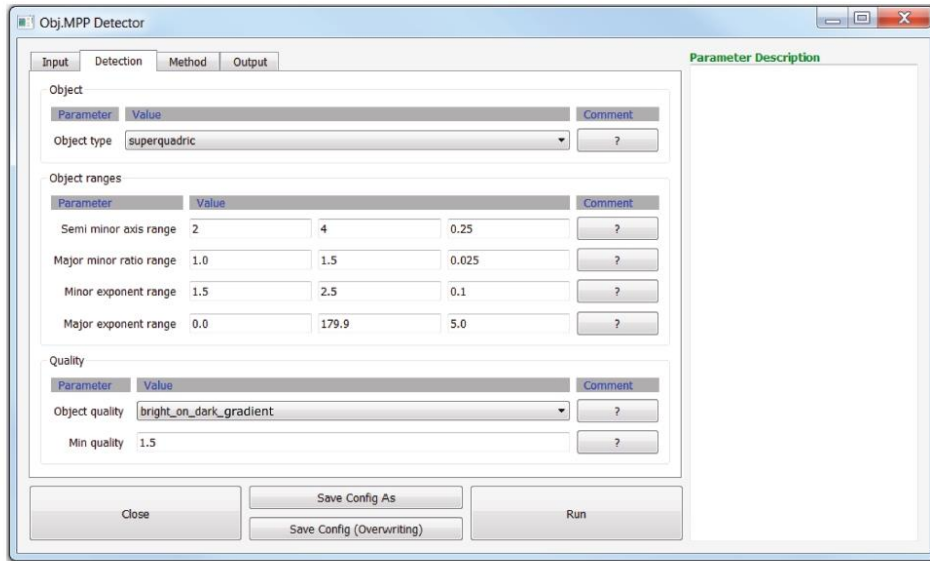


Figure 4. *Obj.MPP* graphical user interface (GUI).

The second tab of the *Obj.MPP* GUI is shown, in which detection parameters including type and size ranges of objects, as well as threshold for the quality function, must be selected. Parameter values adapted to the detection of SGs in larval motorneurons are displayed.

Table 1 - List of fly lines enabling expression of fluorescently-tagged Stress Granule components

Genotype	Chromosome	Fluorophore	Description	Functionality	Generation	Fly line Source
w;EGFP::Rin	3	EGFP	EGFP inserted in the endogenous <i>rasputin (rin)</i> locus, right after the ATG	homozygous viable	CRISPR/Cas9 editing, as described in [33]	Akira Nakamura
UAS-Venus::TDP-43 wild type	3	Venus	Venus fused N-terminally to human TDP-43; construct cloned downstream of UAS sequences	rescues the lethality of <i>tbph</i> null mutant flies	transgenesis, random insertion	Paul Taylor [29]
UAS-Venus::TDP-43M337V	3	Venus	Venus fused N-terminally to an ALS-causing form of the human TDP-43; cloned downstream of UAS sequences	does not rescue the lethality of <i>tbph</i> null mutant flies	transgenesis, random insertion	Paul Taylor [29]
OK371-Gal4	2	NA	expresses Gal4 in approximately 40 glutamatergic neurons (5 dorsal neurons identified as aCC and RP1-4 and 35 lateral and ventral neurons) and 6 glutamatergic interneurons per hemisegment.	homozygous viable	enhancer-trap screen	Serge Birman; [33]

Table 1. Useful *Drosophila* lines for detection of wild-type or pathological fluorescent SG proteins.

